Middle Rio Grande Bernalillo Report:

Morpho-dynamic Processes and Hydraulic Modeling to Assess Silvery Minnow Habitat from Hwy 550 Bridge to Montaño Road Bridge

Prepared By:
Chelsey Radobenko

Prepared For:
Dr. Pierre Julien
Dr. Aditi Bhaskar
Dr. Yoichiro Kanno

March 2023
Master of Science
Plan B Technical Report

Colorado State University
Engineering Research Center
Department of Civil and
Environmental Engineering
Fort Collins, Colorado 80523

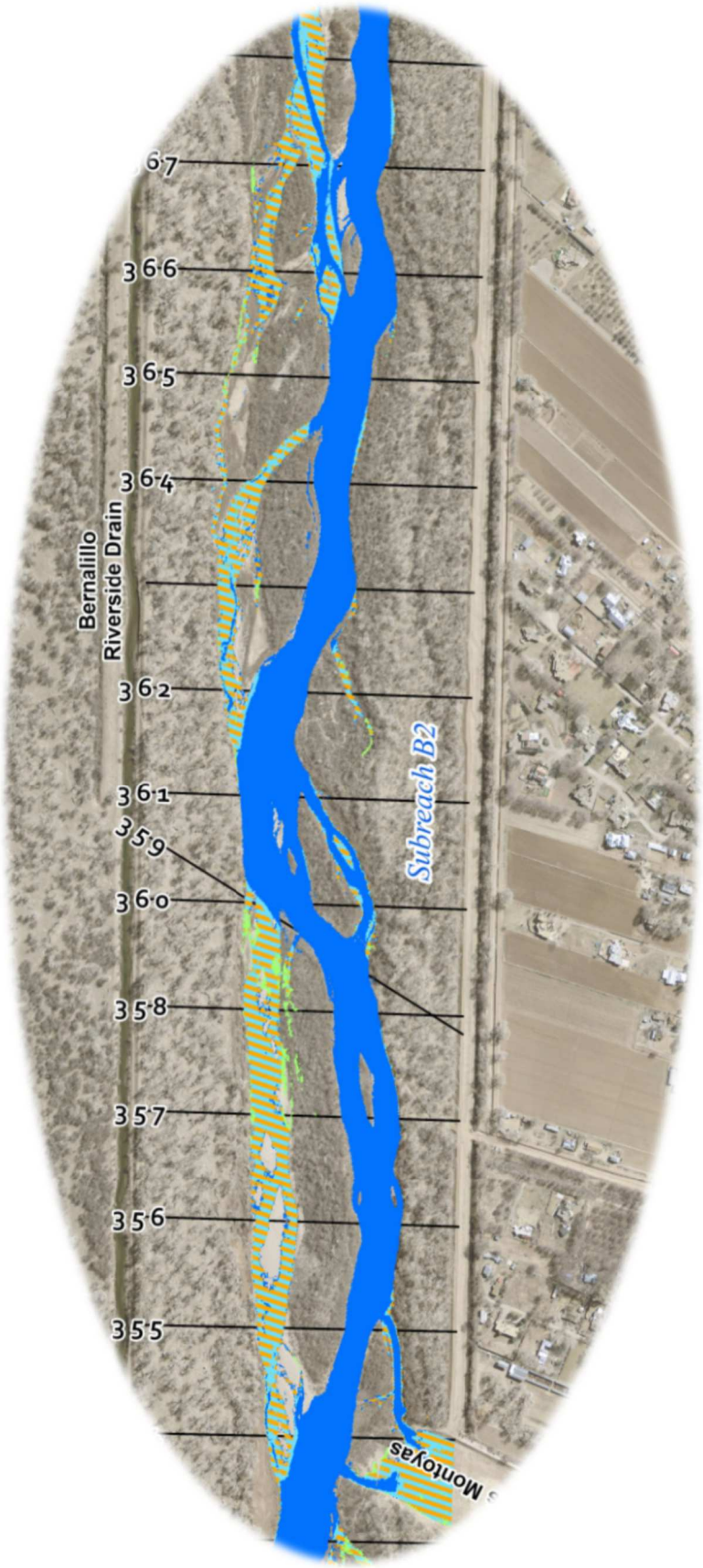

Abstract

The Bernalillo Reach spans approximately 16 miles of the Middle Rio Grande (MRG), from the Highway 550 Bridge to the Montaño Bridge crossing in Albuquerque, New Mexico. This reach report was done in conjunction with a larger Bernalillo Reach Report (Radobenko and Corsi, 2023) that was prepared for the United States Bureau of Reclamation (USBR). This report presents a summary of the morpho-dynamic processes within the Bernalillo Reach. The MRG is a dynamic river that is still responding to anthropogenic impacts over the last century. The Bernalillo Reach is split into four subreaches (B1, B2, B3, and B4). Analysis of these four subreaches illustrates spatial and temporal trends of the channel geometry and morphology.

Discharge and sediment data from the United States Geological Survey are used to identify the time and magnitude of peak discharge and sediment load in the reach. Spring snowmelt typically supplies the greatest water and sediment discharge volumes, and the monsoonal thunderstorms often transport the greatest concentration of suspended sediment for shorter periods of time.

Changes to bed elevation were observed using cross-section geometry files provided by the USBR. The Bernalillo Reach has shown cycles of degradation and aggradation. Between 1962 and 1972, the Bernalillo reach was in the process of aggrading, with the greatest degree of aggradation (~1 to 2 feet) occurring in Subreaches B1 and B2. This aggradation led to an increase in bed elevation and steepening in channel slope during this decade. The channel began to incise following the completion of the Cochiti dam in 1973, with the most significant channel bed degradation (~3 to 8 feet) occurring in Subreaches B1 and B2. In 2005, the Albuquerque Bernalillo County Water Utility Authority (ABCWUA) Adjustable Height Dam was constructed at the end of the B3 reach, causing aggradation to occur immediately upstream and degradation to occur immediately downstream.

One-dimensional hydraulic models, developed with Hydrologic Engineering Center's River Analysis System (HEC-RAS) software, estimated habitat availability for the endangered Rio Grande Silvery Minnow (RGSM) within the Bernalillo Reach. A previously developed width-slice method in HEC-RAS was applied to calculate the hydraulically suitable RGSM habitat based on flow velocity and depth criteria for the larval, juvenile, and adult stages at various discharges. Calculations for a wide range of discharges were conducted for five historical river conditions (1962, 1972, 1992, 2002, and 2012) over a span of 50 years. Subreaches B2 and B3 show more potential habitat for the juvenile and adult life stages, while Subreaches B1 and B2 may be slightly more suitable for larvae.

Detailed mapping for year 2012 was performed based on detailed LiDAR data at a 10-foot resolution to illustrate the RGSM habitat areas within the Bernalillo Reach. Due to the nature of procedure used to create these "pseudo" 2D habitat maps, several sections of the floodplain show areas that meet the RGSM velocity and depth criteria but remained disconnected from the main channel. A 2D hydraulic model using SRH-2D was used to compare the accuracy the disconnected areas and the assumptions made in the 1D model. When quantifying the silvery minnow habitat availability, the pseudo 2D mapping created by the 1D HEC-RAS model resulted in an underestimation of the habitat availability for all life stages. However, the relative increases and general locations of availably habitat followed similar trends between the 1D and 2D models for all of the life stages. These generalized locations of habitat availability could help river managers and biologists identify locations of future river restoration efforts.

Acknowledgement

This final report was done in conjunction with a larger reach study prepared for the United States Bureau of Reclamation (USBR) under Award Number R17AC00064. Thank you to my graduate research partners on this project, Brianna Corsi and Tristen Anderson, for all of their contributions and support. I would like to thank the USBR for providing the one-dimensional hydraulic model, sediment data, and terrain files used in this study and for reviewing the draft version of the larger reach study report. I would also like to that the biologists with the University of New Mexico (UNM) and the American Southwest Ichthyological Researchers (ASIR) for providing their aquatic habitat expertise on the Rio Grande Silvery Minnow (RGSM). I would also like to thank Dr. Pierre Julien for his support and guidance throughout my time at Colorado State University.

Table of Contents

List of Tables

List of Figures

List of Appendix A Figures and Tables

List of Appendix B Figures and Tables

List of Appendix C Figures and Tables

List of Appendix D Figures and Tables

List of Appendix E Figures and Tables

List of Appendix F Figures and Tables

1 Introduction

1.1 Purpose of Report

The purpose of this reach report is to evaluate the morpho-dynamic processes within the Bernalillo Reach on the Middle Rio Grande. The Bernalillo Reach spans approximately 16 miles of the Middle Rio Grande (MRG), from the Highway 550 Bridge to the Montaño Bridge crossing in Albuquerque, New Mexico. This reach report was done in conjunction with a larger Bernalillo Reach Report (Radobenko and Corsi, 2023) that was prepared for the United States Bureau of Reclamation (USBR) as part of a series of reach reports that support USBR's mission to improve habitat for endangered species on the MRG.

The MRG has been affected by continual human development/agriculture. Levees and channelization efforts have been constructed through the reach for flood control. These efforts have impacted the habitat quality and quantity that is available for the endangered Rio Grande Silvery Minnow (RGSM or silvery minnow). The RGSM is an endangered fish species that is native to the Middle Rio Grande. Currently, it occupies only about seven percent of its historical range (U.S. Fish and Wildlife Service, 2010). It was listed on the Endangered Species List by the US Fish and Wildlife Service in 1994. The goal of this reach report is to evaluate the spatial and temporal changes in morpho-dynamic processes in the Bernalillo and to utilize hydraulic modeling to identify areas of habitat availability for the different life stages of the RGSM. The specific objectives and methods of this report include:

- Summarize the trends of the historical precipitation events and flow and sediment discharges that the Bernalillo Reach experiences using precipitation data from the Bosque Ecosystem Monitoring Program from University of New Mexico (BEMP Data, 2017) and flow and sediment data from United States Geological Survey (USGS) Gages.
- Analyze the change in geomorphic characteristic trends over time at the subreach level using USBR provided HEC-RAS models from 1962, 1972, 1992, 2002 and 2012.
- Characterize available RGSM habitats for the larvae, juvenile, and adult life stages using one-dimensional (1D) hydraulic modeling.
- Determine accuracy of using a 1D hydraulic model by comparing the results to a two-dimensional (2D) hydraulic model using HEC-RAS with RAS-MAPPER and SHRH-2D.

1.2 Site Description

The Rio Grande begins in the San Juan Mountain Range of Colorado and continues into New Mexico. It travels along the Texas-Mexico border before reaching the Gulf of Mexico. The Middle Rio Grande (MRG) stretches from Cochiti Dam to Elephant Butte Reservoir. The MRG has historically been affected by periods of drought and large spring flooding events due to snowmelt. Monsoons have caused some of the largest peak flows the river has seen. These floods often caused large scale shifts in the course of the river and rapid aggradation (Massong et al., 2010). Floods helped maintain aquatic ecosystems by enabling connection of water between the main channel and the floodplains (Scurlock, 1998), but consequently threatened human establishments that were built near the Rio Grande. Beginning in the 1930s, levees were installed to prevent flooding. Beginning in the 1950s, the USBR undertook a significant channelization effort involving jetty jacks, river straightening, and other techniques. The low flow conveyance channel was in operation from the 1950s to the 1980s that diverted a portion of the water from the main channel, reducing the water available in the river. Upstream dams built in the 1950s were used to store and regulate flow in the river.

While these efforts enabled agriculture and large-scale human developments to thrive along the MRG, they also fundamentally changed the river, which led to reduced peak flows and sediment supply while altering the channel geometry and vegetation (Makar, 2006). In parts of the MRG, narrowing of the river continues, with channel degradation due to limited sediment supply and the formation of vegetated bars that encroach into the channel (Varyu, 2013; Massong et al., 2010). Farther downstream, closer to Elephant Butte Reservoir, aggradation and sediment plugs have been observed. The San Marcial plug, is an example of one of these sediment plugs that formed near the San Marcial railroad crossing (located close to agg/deg line 1702). These factors have created an ecologically stressed environment, as seen in the decline of species such as the Rio Grande Silvery Minnow (Mortensen et al., 2019).

The Bernalillo Reach of the Middle Rio Grande in New Mexico is a 16-mile stretch that begins at the Hwy 550 bridge crossing in Bernalillo and ends at the Montaño Bridge crossing in Albuquerque. **Figure 1-1** shows a timeline of hydraulically significant events that have occurred between 1870 and 2010 (Makar 2006).

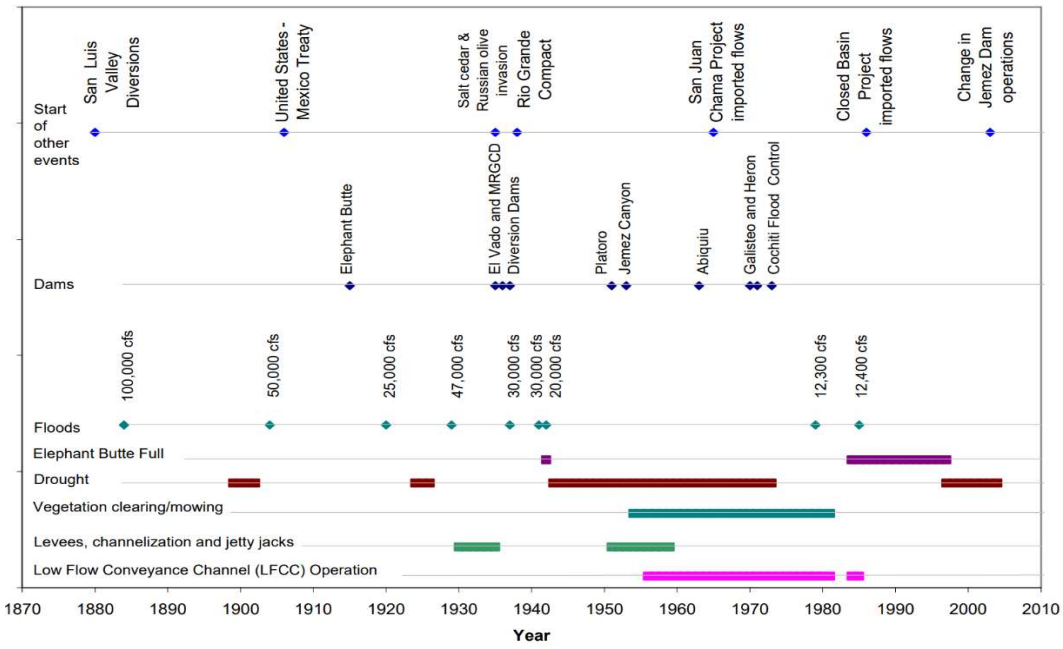

Figure 1-1 Timeline of Significant Events for the Middle Rio Grande River (Makar 2006)

1.3 Aggradation/Degradation Lines and Rangelines

Aggradation/degradation lines (agg/deg lines), spaced at 500-foot intervals along the entire MRG, were established in 1962 and are used as baselines to estimate changes in sedimentation and morphological characteristics in the river channel and floodplain over time (Posner 2017). Repeat ground surveys are implemented along these cross-section lines as well as the collection of bed material samples. Each agg/deg line has been surveyed approximately every 10 years and are available for 1962, 1972, 1992, 2002 and 2012. The cross-sectional geometry at each agg/deg line for all 5 years are available with-in HEC-RAS models that were developed for the MRG by the Technical Service Center (Varyu, 2013). The most recent 2012 survey was performed using LiDAR acquisition, while surveys prior to 2012 were developed using photogrammetry techniques. All GIS data and models use the North American Vertical Datum of 1988 (NAVD88).

LiDAR and photogrammetric survey techniques do not deliver accurate ground elevation measurements underwater. For modeling purposes, it is necessary to appropriately characterize bathymetry of the channel for an accurate representation of channel conveyance. To accomplish this, an underwater prism was estimated using the measured water surface elevation and the flow on the date of survey and has been incorporated within the HEC-RAS geometry files (Baird, pers. comm.).

In addition to agg/deg lines, rangelines are used as location identifiers in this analysis. The rangelines, created at the same time as agg/deg lines, were determined in association with geomorphic factors, such as migrating bends, incision, or river maintenance issues.

1.4 Subreach Delineation

The Bernalillo Reach spans approximately 16 miles beginning at Agg/Deg Line 298 (Hwy 550) and ending at Agg/Deg Line 463 (just upstream of the Montaño Bridge). This reach is located within an urban river corridor. For the purposes of hydraulic and geomorphic analysis, this reach was split into multiple subreaches based on notable urban and geomorphic features.

The Bernalillo Reach was delineated into four subreaches based on notable features such as the Highway 550 and Montano Bridge crossings, the Corrales Siphon crossing, the Albuquerque Metropolitan Area Flood Control Authority (AMAFCA) North Diversion Channel, and the Albuquerque Bernalillo County Water Utility Authority (ABCWUA) Adjustable Height Dam. **Table 1-1** below summarizes each subreach. **Figure 1-2** shows an overview map of the reach delineation. Close-up views of the subreach delineation with agg/deg lines and aerial imagery is given by **Figure 1-3, Figure 1-4**, **Figure 1-5**, **Figure 1-6**, and **Figure 1-7**.

The full subreach delineation report for the Bernalillo reach is provided in **Appendix A**. An analysis of the flood widths at a discharge of 3,000 cfs as well as channel widths identified by the bank stationing were considered. Other analyses preformed as part of the subreach delineation report include the longitudinal profile of the reach and the particle distribution through the reach. All analyses preformed identified boundaries consistent with the subreach delineation.

Table 1-1: Bernalillo Subreach Delineation

Subreach Name	Agg/Deg Lines	Approximate Distance	Description
B-1	298 – 339	4.0 miles	Highway 550 Bridge to Rio Rancho Bosque Preserve (Corrales Siphon crossing)
B-2	339 - 398	5.6 miles	Rio Rancho Bosque Preserve (Corrales Siphon) to AMAFCA North Diversion Channel (tributary)
B-3	398 - 422	2.4 miles	AMAFCA North Diversion Channel (tributary) to ABCWUA Adjustable Height Dam
B-4	422 - 463	4.0 miles	ABCWUA Adjustable Height Dam to Montaño Bridge

Figure 1-2 Bernalillo Subreach Delineation Overview Map

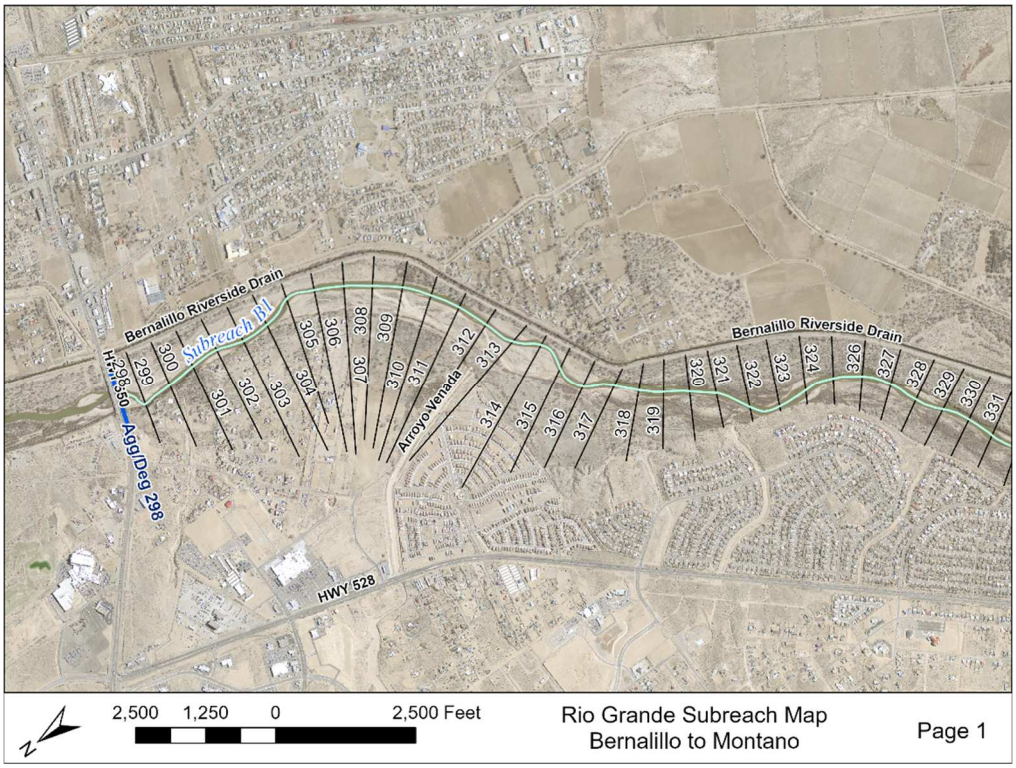

Figure 1-3 Subreach delineation with aerial imagery of the Bernalillo Reach (B1)

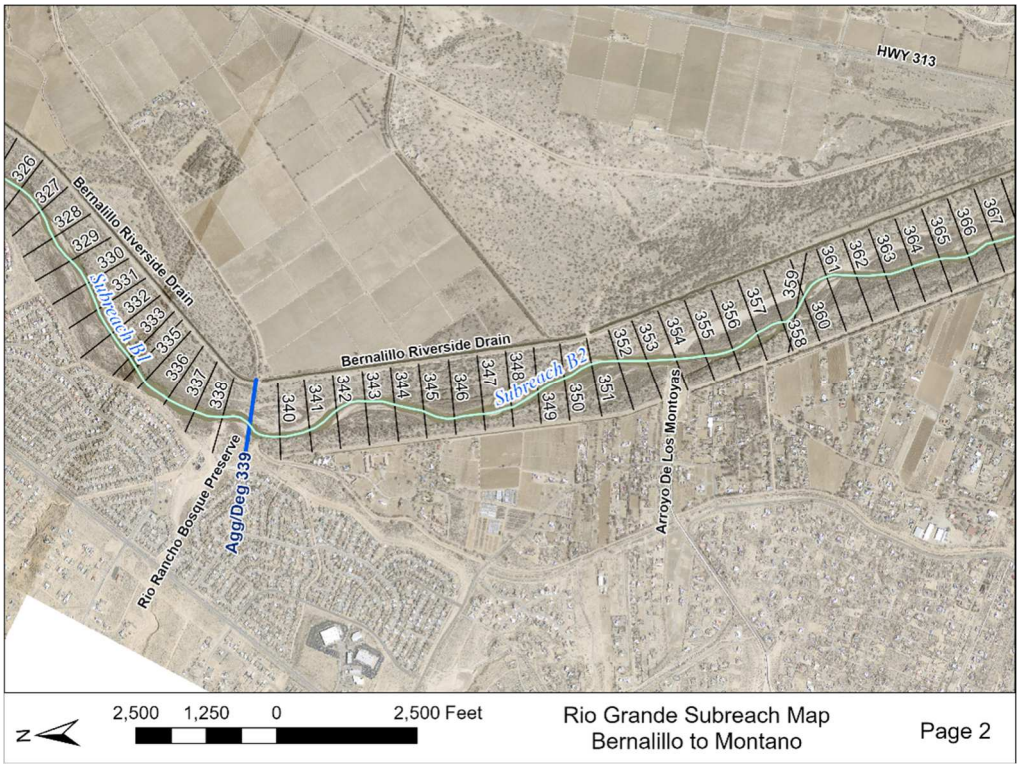

Figure 1-4 Subreach delineation with aerial imagery of the Bernalillo Reach (B1 & B2)

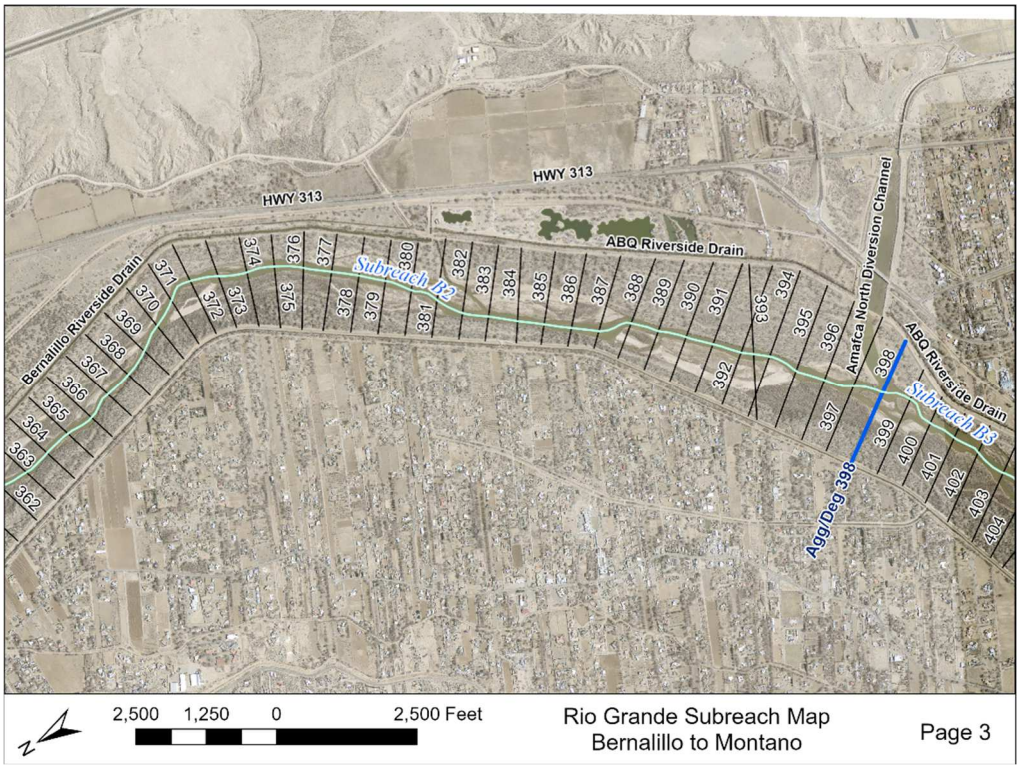

Figure 1-5 Subreach delineation with aerial imagery of the Bernalillo Reach (B2 & B3)

Figure 1-6 Subreach delineation with aerial imagery of the Bernalillo Reach (B3 & B4)

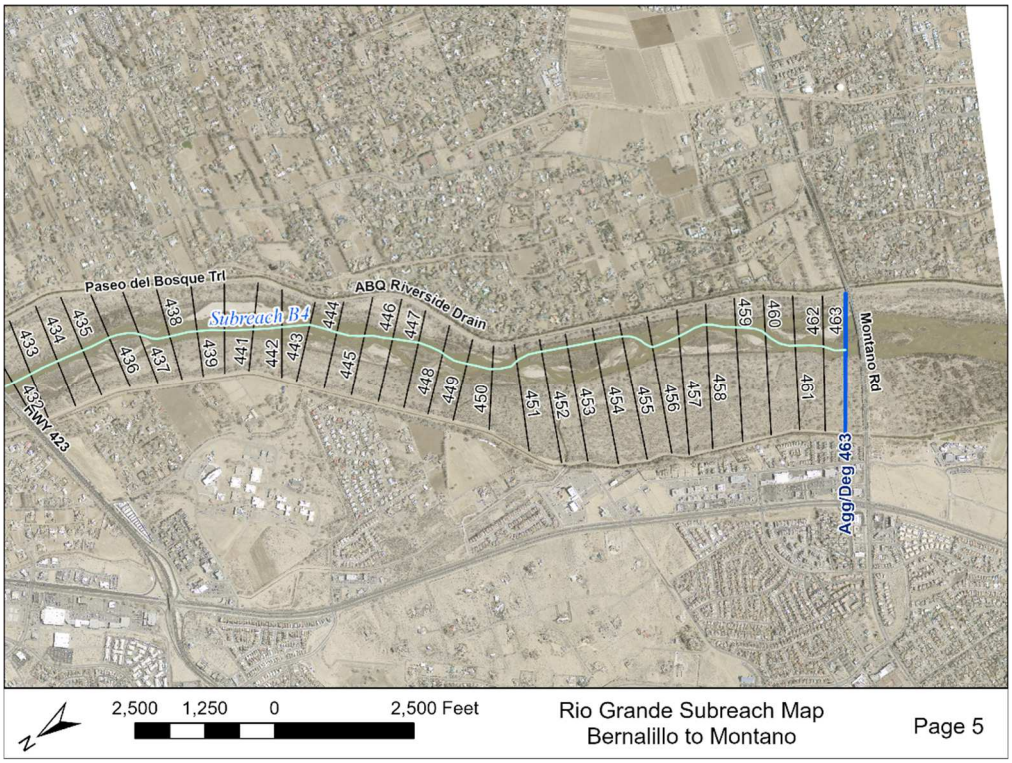

Figure 1-7 Subreach delineation with aerial imagery of the Bernalillo Reach (B4)

2 Precipitation, Flow, and Sediment Discharge Analysis

For the larger USBR reach report study, the next reach downstream of the Bernalillo Reach (subject of this report) is the Montano Reach. Due to the proximity of the reaches and the timing of the USBR reach reports, a combined evaluation of precipitation, flow, and sediment characteristics was conducted for the Bernalillo and Montaño reaches and is included in this section.

2.1 Precipitation

Precipitation data was collected along the MRG by the Bosque Ecosystem Monitoring Program from University of New Mexico (BEMP Data, 2017). The locations of the data collection sites are shown in **Figure 2-1**. The four gage sites used in the precipitation analysis, from north to south, include Santa Ana, Alameda, Rio Grande Nature Center (RGNC), and Harrison. These sites were highlighted in the following analyses based on their proximity to the relevant river reaches and period of record. The Santa Ana gage site is just north of the upstream boundary of the Bernalillo Reach and the Harrison site is near the downstream boundary of the Montaño reach.

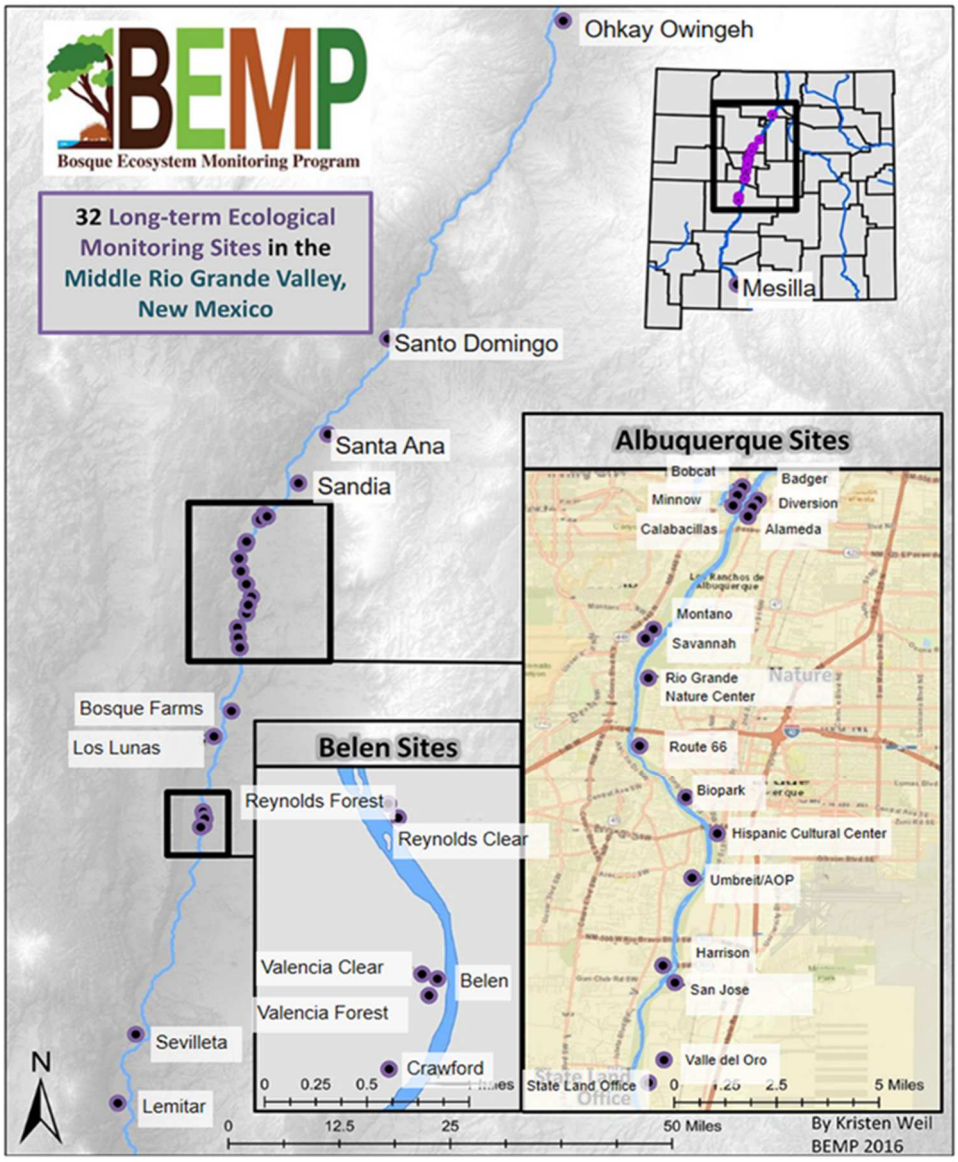

Figure 2-1 BEMP data collection sites (figures source: http://bemp.org)

The monthly precipitation data is shown in **Figure 2-2**. The highest precipitation peak, 5.7 inches of rainfall, occurred in August of 2006 at the Alameda gage. A general trend was observed with the highest precipitation values occurring during the monsoon season (late July through early September). A cumulative rainfall plot of the monthly precipitation data, **Figure 2-3**, shows that individual rain events can greatly affect the overall trend of the data. It further highlights the monsoonal rains, which create a "stepping" pattern with higher rainfall in August and September and lower levels throughout the rest of the year. The same pattern is observed across all the gages indicating rain patterns around the Bernalillo and Montaño reaches are spatially consistent. From the two gages with the longest period of record, Alameda, and RGNC, the cumulative rainfall pattern is similar until 2006. Since then, the Alameda gage has received slightly more precipitation (10 inches) than the RGNC gage.

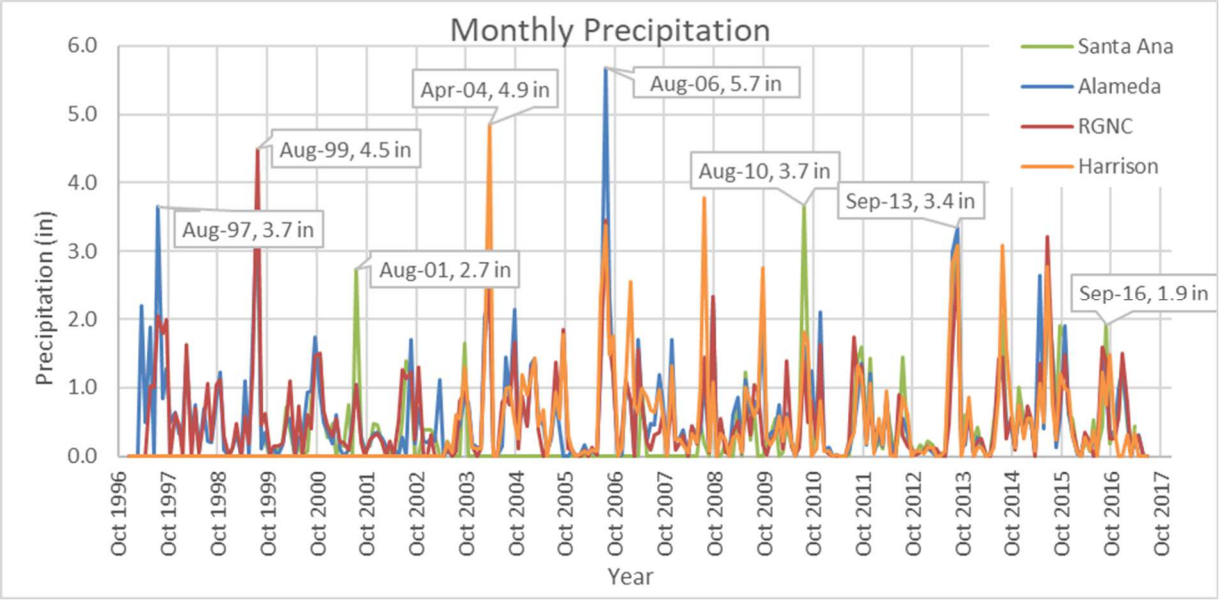

Figure 2-2 Monthly precipitation at four gages near the Bernalillo and Montaño reaches

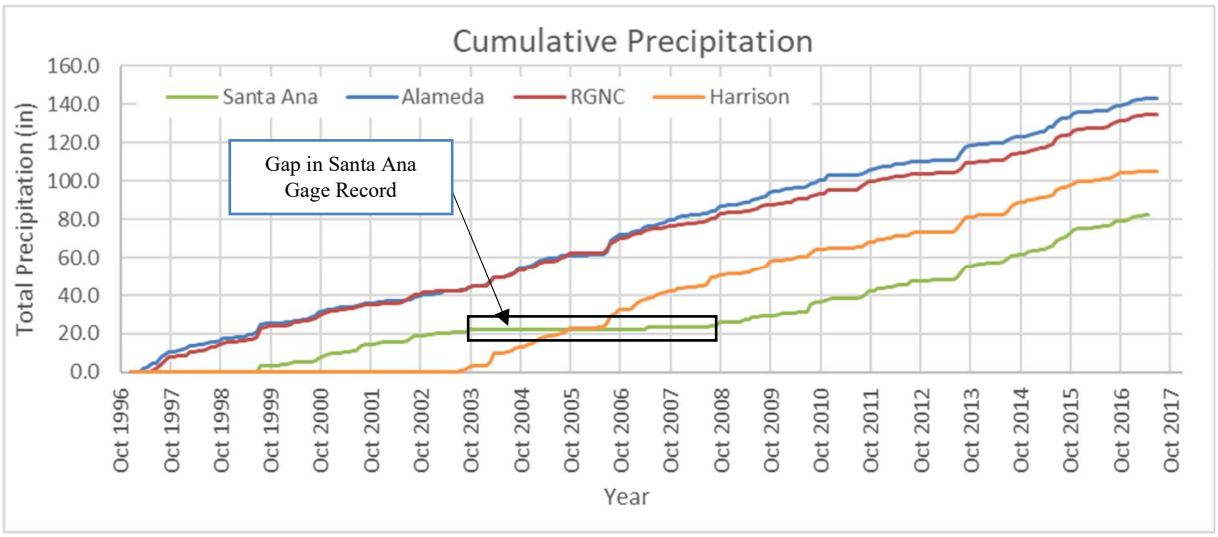

Figure 2-3 Cumulative precipitation at four gages near the Bernalillo and Montaño reaches

2.2 River Flow

2.2.1 USGS Gage Data

Information regarding river flow was gathered from the United States Geological Survey (USGS) National Water Information System. The gages relevant to the study area are included in

Table 2-1, and gage locations are shown in **Figure 2-4**. The gages highlighted in purple were chosen for closer analysis due to their location, longer period of record, and/or sediment data record.

Table 2-1. List of Relevant Gages

Reach	Station Name	Station #	Mean Daily Discharge	Suspended Sediment
Upstream	Rio Grande at Otowi Bridge, NM	08313000	February 2, 1895 to September 10, 2022	October 1, 1955 to September 30, 2021
	Rio Grande at Cochiti, NM (Historical)	08314500	June 1, 1926 to October 30, 1970	No Data
	Rio Grande Below Cochiti Dam, NM	08317400	October 1, 1970 to Present	July 1, 1974 to September 29, 1988
	Rio Grande At San Felipe, NM	08319000	January 1, 1927 to Present	No Data
	Jemez River Below Jemez Canyon Dam (Historical)	08329000	April 1, 1936 to September 29, 2009	November 15, 1955 to September 30, 2021
	Jemez River Outlet Below Jemez Dam, NM	08328950	September 30, 2009 to Present	No Data
Bernalillo Reach	Rio Grande Near Bernalillo, NM (Historical)	08329500	October 1, 1941 to September 29, 1969	October 1, 1955 to September 29, 1969
	Rio Grande at Alameda Bridge at Alameda, NM	08329918	July 4, 2003 to October 12-2020	No Data
	Rio Grande Nr. Alameda, NM	08329928	March 1, 1989 to October 12-2021	No Data
Montaño Reach	Rio Grande At Albuquerque, NM	08330000	October 1, 1965 to Present	October 1, 1969 to September 29, 2020
	Rio Grande At Isleta Lakes Nr. Isleta, NM	08330875	October 1, 2002 to September 18, 2021	No Data
Down-Stream	Rio Grande Near Bosque Farms, NM	08331160	March 16, 2006 to Present	No Data

**Note: Gages highlighted in purple were chosen for closer analysis due to their location, longer period of record, and/or sediment data record*

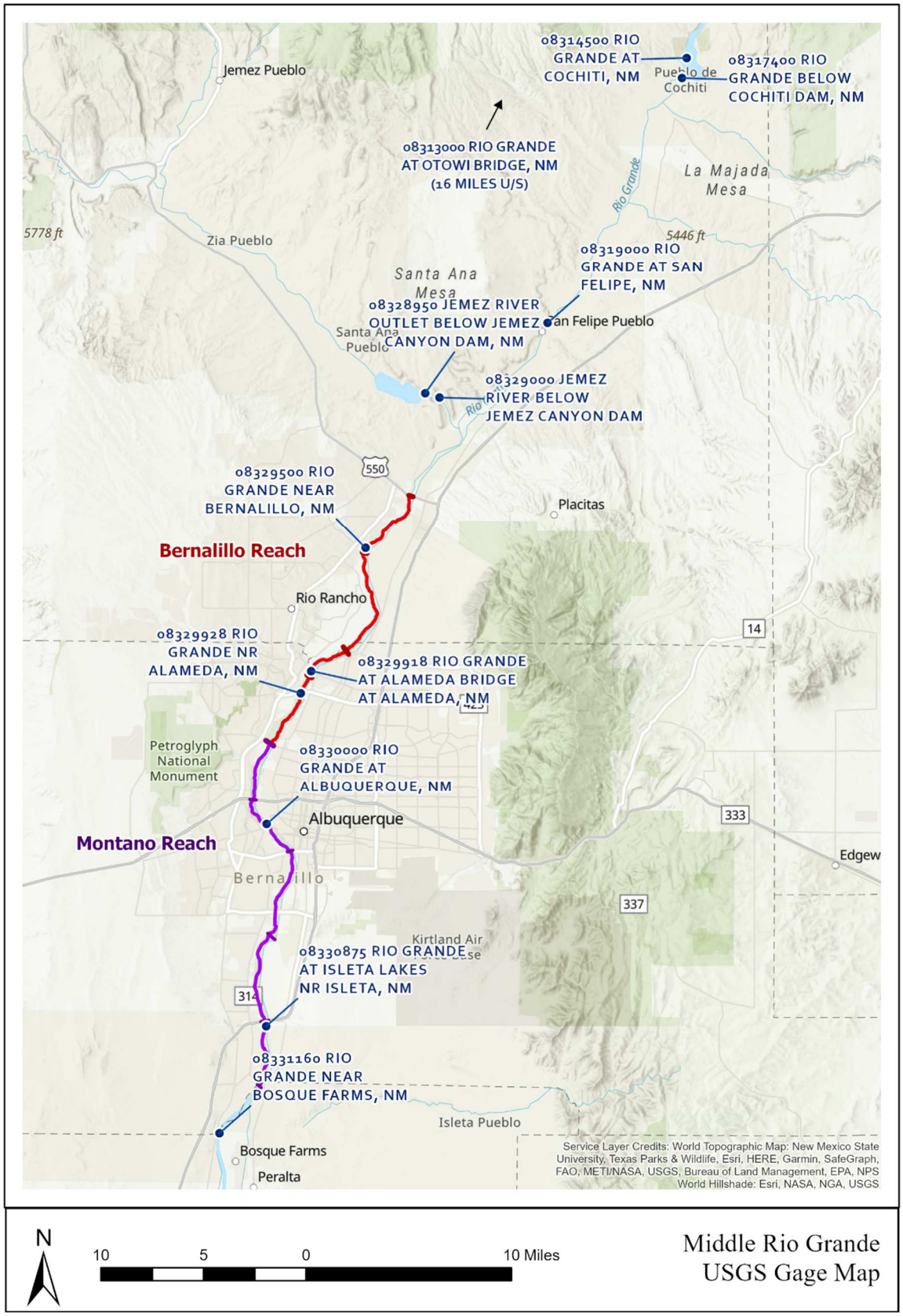

Figure 2-4. USGS gage data overview map

Construction of the Cochiti Dam commenced in 1965 and was completed in 1973. A USGS gage (08317400) was installed in 1970 during construction of the dam. Prior to dam completion, a historical gage (08314500) with a period of record between 1926 and 1970 was located 1 mile upstream of the current operating gage. The current operating gage at Cochiti Dam has sediment data for a 66-year period of record between 1974 and 2021. Given the location of this gage directly downstream of the dam, it serves as a baseline for the sediment loading prior to any sediment input from tributaries or from bank and bed erosion along the Rio Grande.

Construction of the Jemez Dam was completed in 1953. A historical gage (08329000) was installed upstream of the Jemez River and Rio Grande confluence in 1936, 17 years prior to Jemez Dam construction, and has a period of record of 73-years of flow data between 1936 and 2009. This gage also has a 71-year sediment record extending between 1955 and 2021; however, the record shows 0 tons/day of suspended sediment load between 1958 and 2014, indicating that sediment was not sampled during this time. In 2009, a new gage (08328950) that is currently operational was installed 0.7 miles upstream of the historical gage. This gage only records flow data. Due to the proximity of the gages, the flow records for USGS Gage 08329000 and 08328950 were combined for this analysis. In 2014, a pass-through channel was constructed through the Jemez Dam to allow for sediment passage through the dam. At the time of this study, 7 years of sediment data are available to evaluate any effects that the additional sediment loading has had on the Bernalillo and Montaño reaches. See **Section 2.3** for additional information on the sediment loading through the Bernalillo and Montaño reaches.

The San Felipe gage (08319000) is located 10 miles upstream of the Bernalillo Reach and 7 miles upstream of the Rio Grande confluence with the Jemez River. This gage is still operational today and has a period of record of 95 years, between 1927 and 2022. This gage has a significant period of record both before and after the construction of Cochiti Dam in 1973 and was used to evaluate the effects of the dam on flow characteristics within the Bernalillo and Montaño reaches. This gage does not include sediment data.

The historical gage near Bernalillo (08329500), located in Subreach B1 near Agg/Deg 337 and has 28 years of flow data between 1941 and 1969 as well as 14 years of sediment data between 1955 and 1969. Combined with the Albuquerque gage (below), this gage was useful in evaluating sediment loading within the Bernalillo and Montaño reaches.

The Albuquerque gage (08330000) has been operational from 1965 to present and has a sediment record between 1969 and 2020. It is located in Subreach M2 of the Montaño reach at Central Ave. in Albuquerque. The data from this gage was helpful in evaluating sediment loading within the Bernalillo and Montaño reaches of the MRG.

2.2.2 Raster Hydrographs

The raster hydrographs of daily discharge at the gages at San Felipe (left) and Albuquerque (right) are shown in **Figure 2-5**. Both gages are operational today, with a period of record of 95 years for the San Felipe gage and 57 years for the Albuquerque gage. These raster hydrographs show seasonal flow patterns, with peak flows often occurring from snowmelt runoff in April through June, low flow throughout the rest of the summer (except for strong summer thunderstorms), and medium flow from November onwards representing the end of the irrigation season. These raster hydrographs also highlight differences in flood magnitude before and after the Cochiti dam construction in 1970. Prior to 1970, the San Felipe gage shows long duration spring flood events that are sometimes on the order of magnitude between 8,000 cfs and 20,000 cfs. Conversely, the Albuquerque gage after 1970 shows these longer duration spring floods on an order of magnitude between 4,000 cfs and 6,000 cfs.

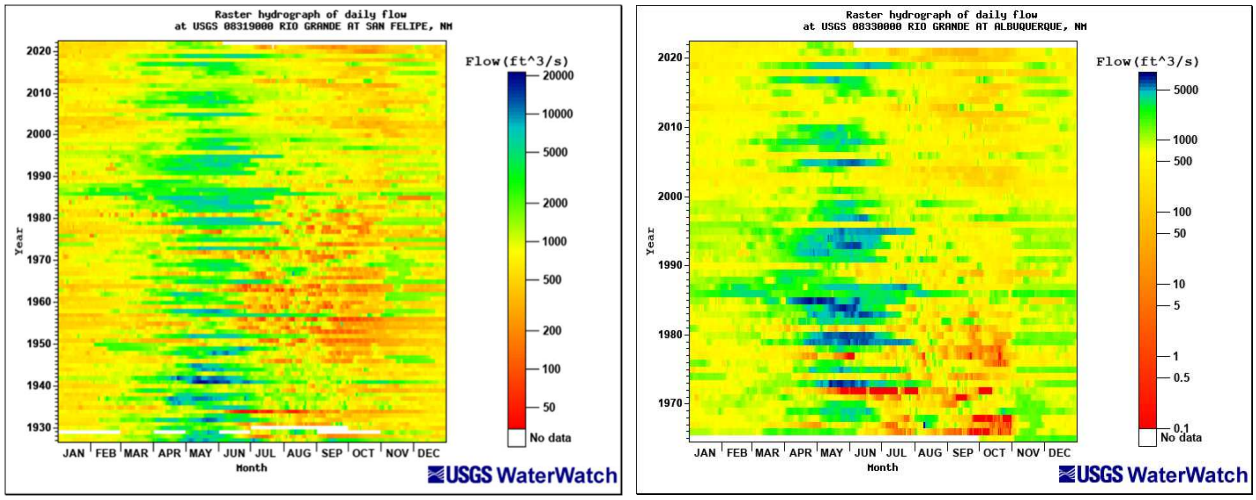

Figure 2-5 Raster hydrograph of daily discharge at USGS Station 08319000 at San Felipe (left) and USGS Station 08330000 at Albuquerque (right). (Source: https://waterwatch.usgs.gov)

The raster hydrographs of daily discharge at the gages located directly downstream of the Jemez Dam are shown in **Figure 2-6**. The combined period of record for these gages is 86 years between 1936 and present. The figures show seasonal flow patterns, with peak flows often occurring from snowmelt runoff in April through June, low flow throughout the rest of the summer (except for strong summer thunderstorms), and medium flow from November onwards representing the end of the irrigation season. The Jemez River regularly experiences very low flows (below 1 cfs) or no flow during long periods of the summer season.

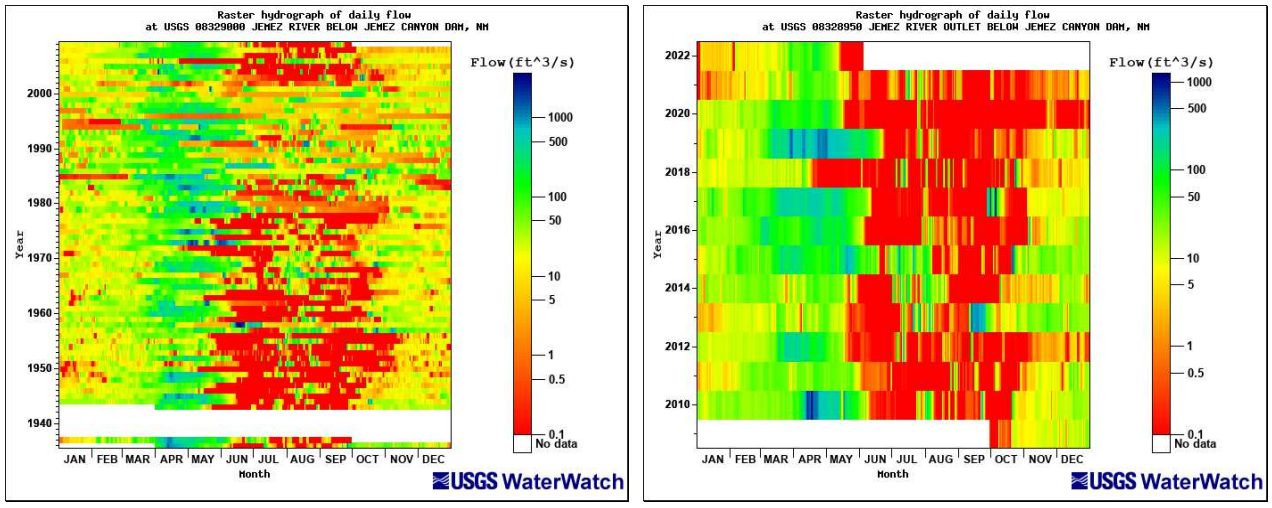

Figure 2-6 Raster hydrograph of daily discharge at historical USGS Station 08329000 (left) and USGS Station 0832950 (right) below the Jemez Dam. (Source: https://waterwatch.usgs.gov).

2.2.3 Yearly Peak Flow Events

Yearly peak flow events for the Cochiti, San Felipe, and Albuquerque gages are shown in **Figure 2-7** and **Figure 2-8**. These peak flow events were determined from average daily flow data. **Figure 2-7** shows the yearly peak flow events prior to the Cochiti Dam completion in 1970, while **Figure 2-8** shows the peak events after dam completion to present day. Like the raster hydrographs shown above, these graphs show a clear distinction between pre- and post-dam conditions. In the 44 years of gage record prior to Cochiti Dam

completion there were 11 flood events with peak daily flows larger than 10,000 cfs. In the 52 years of gage record after dam completion, peak flows became less variable and have not peaked above 9,000 cfs.

The flood of record at these gages occurred in May of 1941, with a peak of 21,300 cfs at the San Felipe gage. The following April of 1942 had the second largest recorded flood, with a peak of 17,200 cfs at the San Felipe gage. The 3 years between 1983 and 1985 show larger than normal spring flood events, with a peak flood at 8,100 cfs in May 1985 at the San Felipe gage. The more recent larger flood events occurred in May of 2017 and June of 2019, with daily peak flows of 5,800 cfs and 6,200 cfs, respectively.

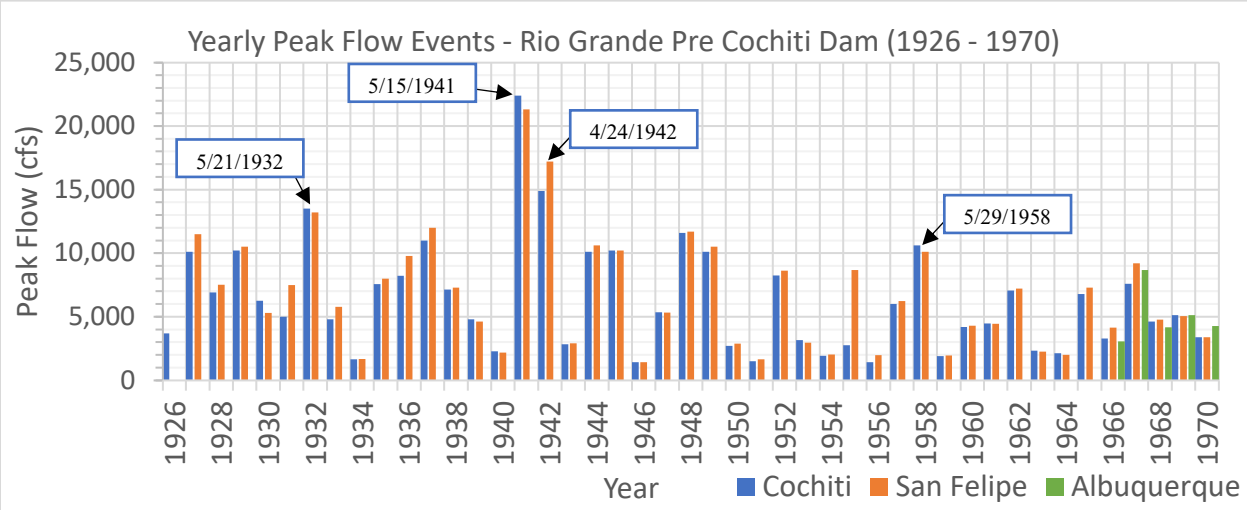

Figure 2-7 Yearly peak flow events for the Rio Grande before Cochiti Dam at Historical USGS Gage 08314500 (1926-1970) and USGS Gage 08317400 (1970-present).

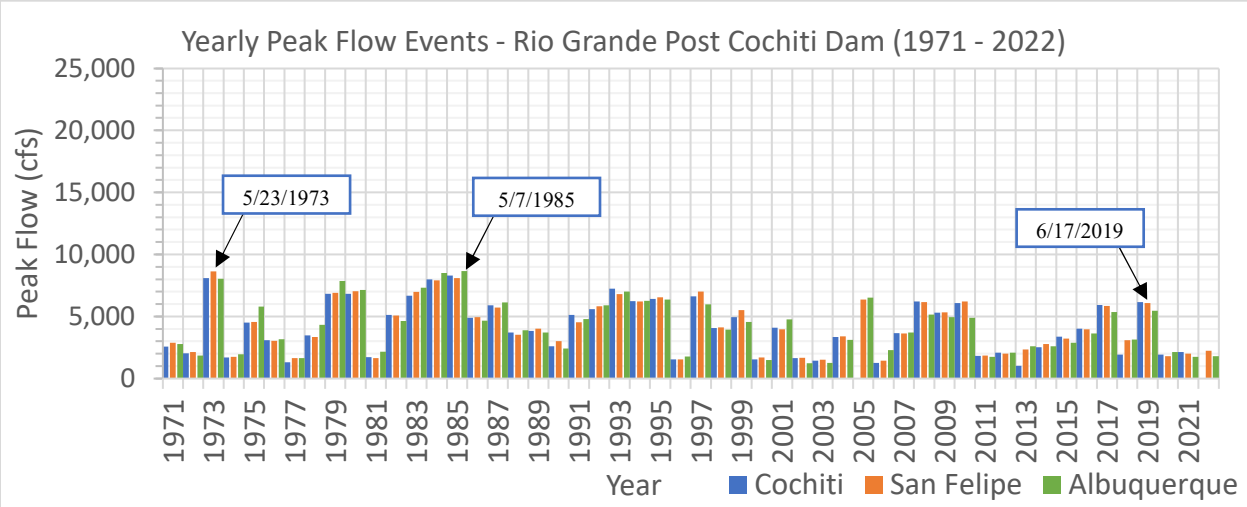

Figure 2-8 Yearly peak flow events for the Rio Grande after Cochiti Dam at USGS Gage 08317400 (1970-present).

Yearly peak flow events for the Jemez River gages are shown in **Figure 2-9**. The flow record does not show a clear influence on peak flow rates for the Jemez River caused by completion of the Jemez Dam in 1953, although this may be due to an insufficient length of gage record prior to 1953. The largest flood event for the period of record occurred in June of 1958, with a daily peak flow rate of 3,640 cfs. This timing corresponds to a large flood event along the Rio Grande that occurred in May of 1958 and had a peak flow rate of 10,100 cfs. A large flood event with a peak flow rate of 2,410 cfs, occurring in May of 1973, also corresponds with flooding along the Rio Grande in May of 1973.

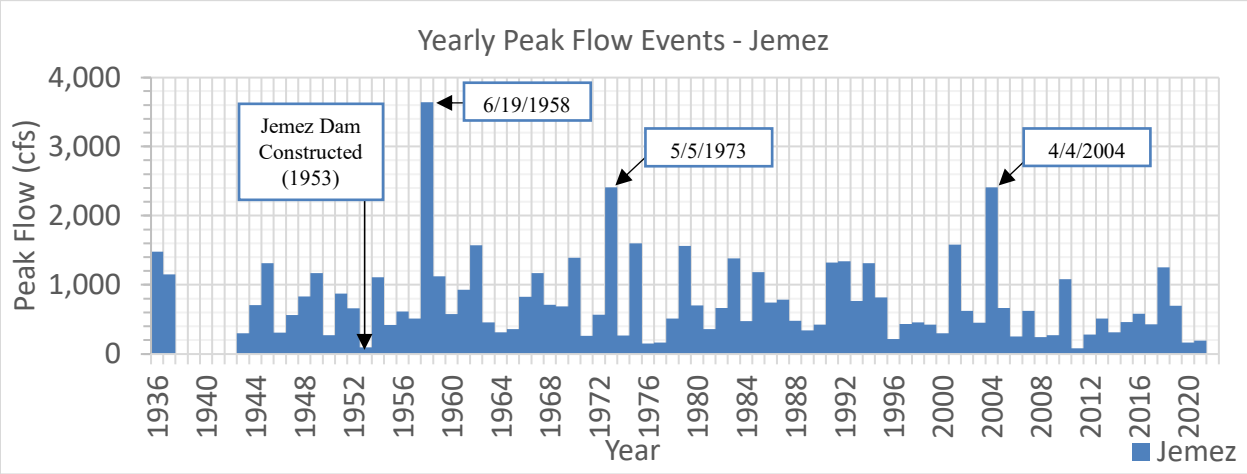

Figure 2-9 Yearly peak flow events for the Jemez River

2.2.4 Cumulative Discharge Curves

Cumulative discharge curves show changes in annual flow volume over a given time period. The slope of the line of the mass curve gives the mean annual discharge, while breaks in the slope show changes in flow volume trends. **Figure 2-10** through **Figure 2-14** shows the single mass curves at Cochiti, San Felipe, and Albuquerque. The gage records for Cochiti and San Felipe were split into pre- and post-dam construction, with October of 1970 chosen as the break point, because there was sufficient record before and after dam construction to compare differences in flow trends. The gage record at Albuquerque only begins 8 years before completion of the dam, and so the full gage record was shown in one graph. The single mass curves were divided into time periods of similar slopes to analyze long term patterns in discharge. While cumulative discharge plots are particularly useful for analyzing long-term trends in flows, occasionally, large flow-altering events can be identified from spikes in the curve.

The pre- and post- dam mass curves for Cochiti are shown by **Figure 2-10** and **Figure 2-11**, respectively. Between 1926 and 1941, the mean discharge was 1,375 cfs. The curve becomes steeper for a short time between spring of 1941 and fall of 1942, which corresponds to the two large flood events that occurred, as described above in **Section 2.2.3**. Between 1943 and 1970 the trend flattens out, with an average flow rate of 1,113 cfs.

In the years following dam completion until 1979 the slope of the curve flattens, giving an average flow rate of 966. Between 1979 and 1995 the slope of the curve steepens to an average flow rate of 1,714 cfs, indicating that this is a wetter than normal period. This trend can also be seen in the yearly peak flood events shown by **Figure 2-8** (previous page). Between 1995 and present day the slope of the curve again flattens, giving an average flow rate for this period of 974 cfs. Similar trends can be seen in the San Felipe and Albuquerque mass curves shown in **Figure 2-12** through **Figure 2-14**.

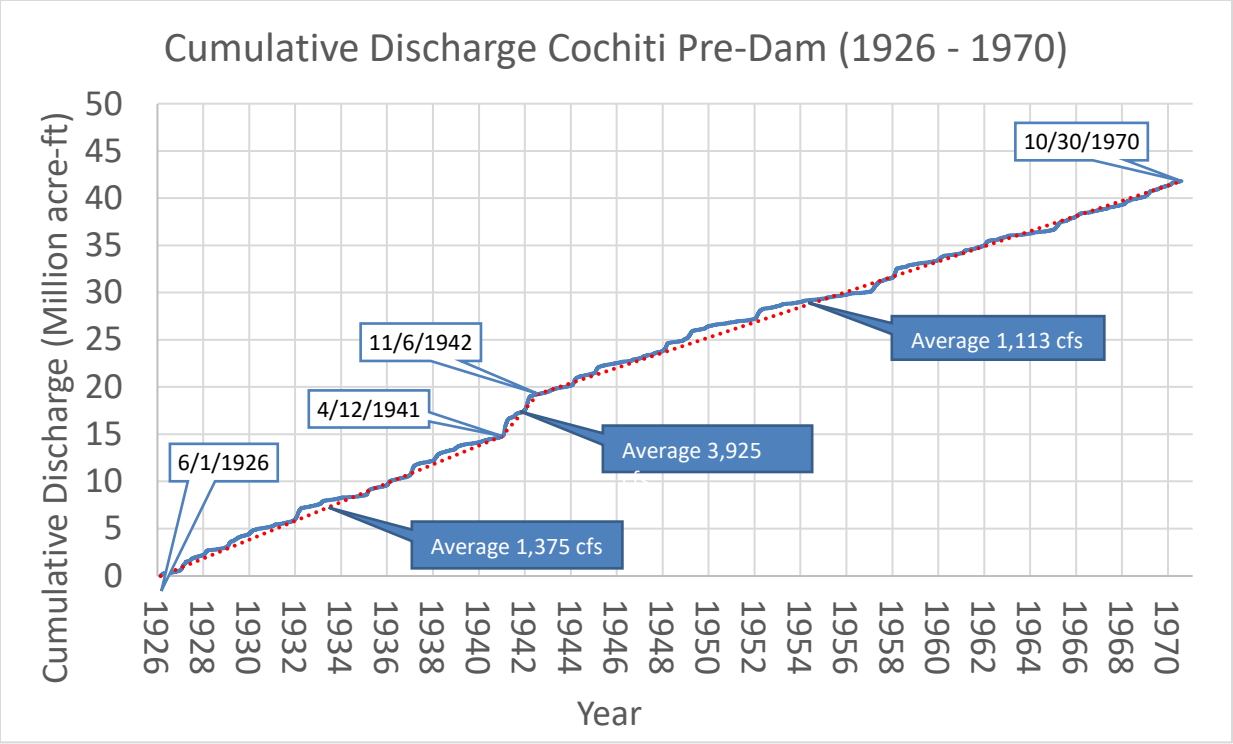

Figure 2-10 Discharge single mass curve at historical USGS gage 8314500 (Cochiti) before dam construction.

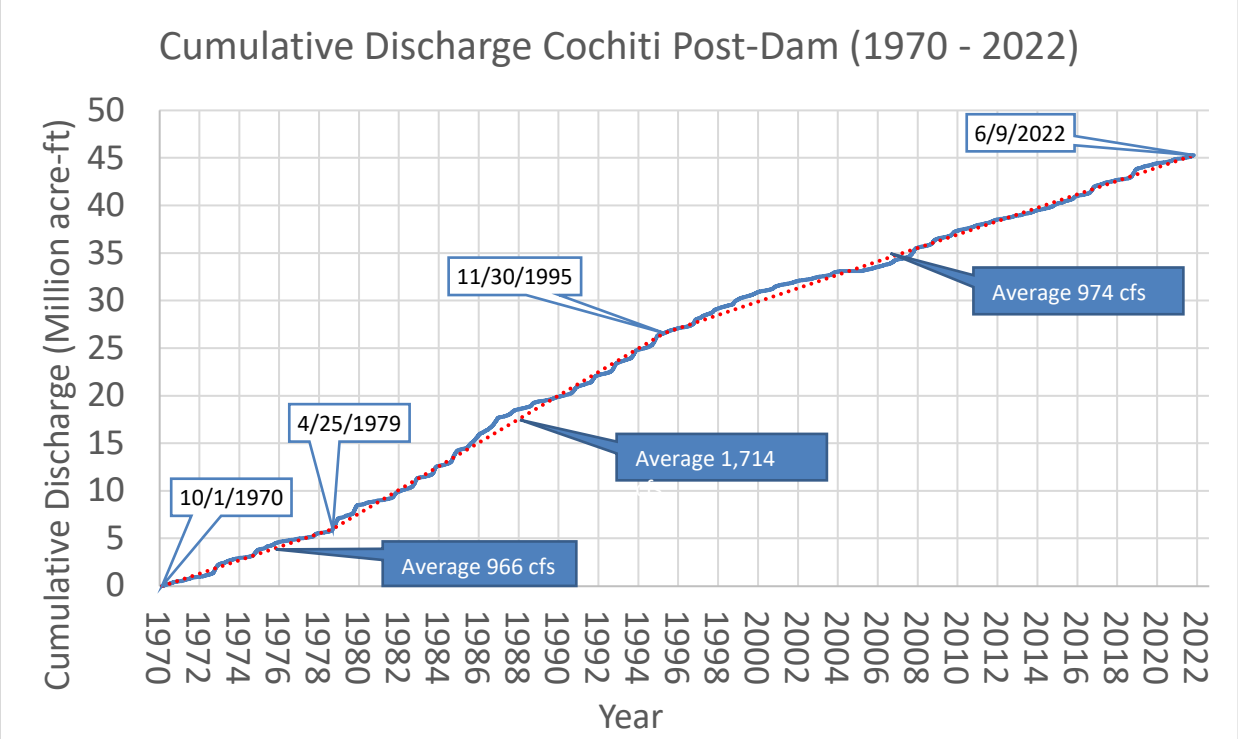

Figure 2-11 Discharge single mass curve at USGS gage 08317400 (below Cochiti Dam) after dam construction

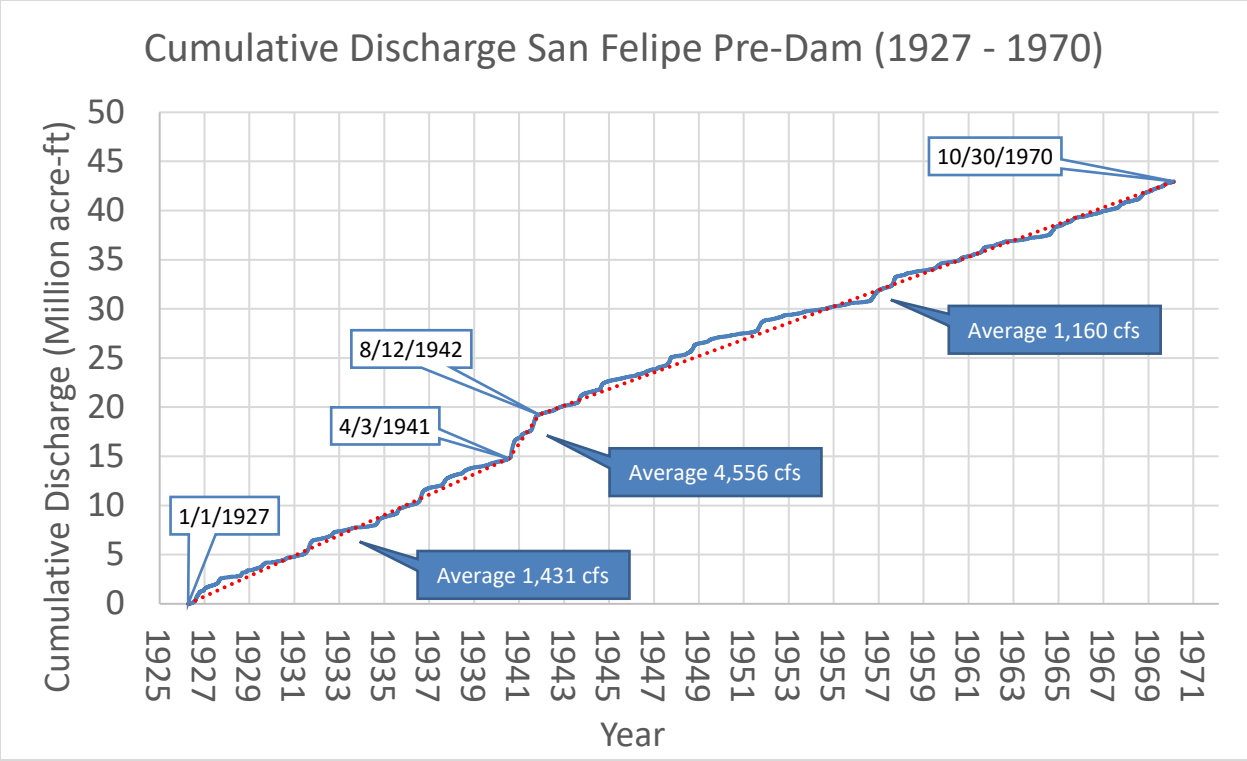

Figure 2-12 Discharge single mass curve at USGS gage 08319000 (San Felipe) before dam construction.

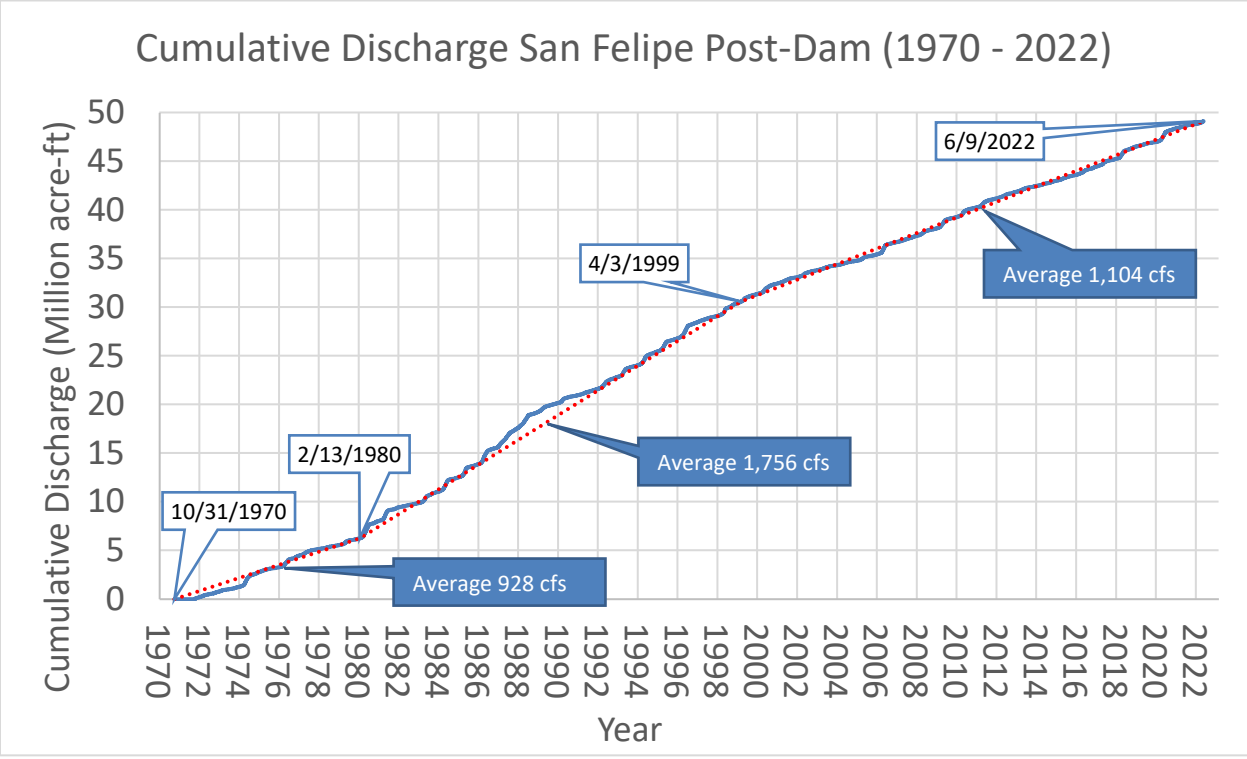

Figure 2-13 Discharge single mass curve at USGS gage 08319000 (San Felipe) after dam construction.

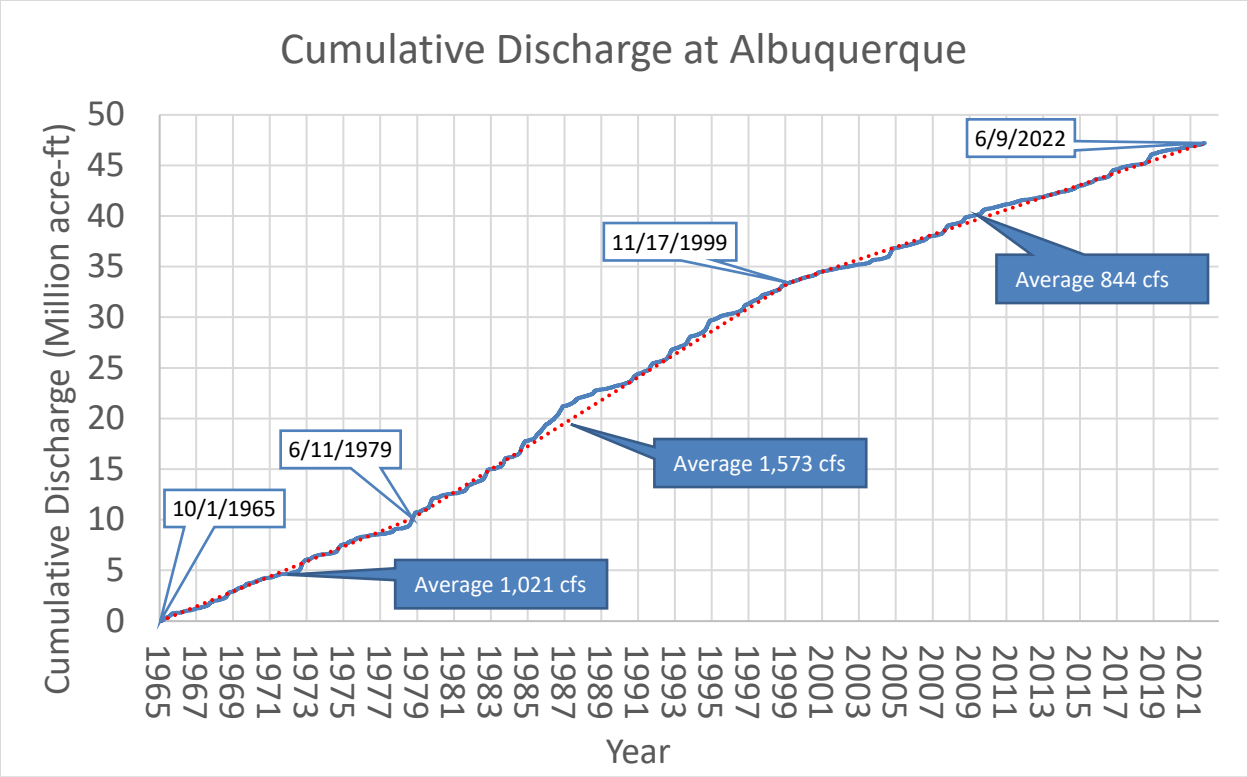

Figure 2-14 Discharge single mass curve at USGS gage 08330000 (Albuquerque).

Figure 2-15 and **Figure 2-16** show the single mass curves at the Jemez River gages. These gage records were also split into pre- and post-dam construction to compare differences in flow trends. No flow record is available between September of 1937 and March of 1943. In the two years before this gap, the average flow rate was 123 cfs. In the 10 years between 1943 and dam completion in 1953, the average flow rate was 47 cfs.

In the 26 years following completion of the dam between 1953 and 1979, the average flow rate is 54 cfs. The time period between 1979 and 1995 show a similar trend of wetter than normal years as the Rio Grande gages, with an average flow rate increasing to 89 cfs. Between 1995 and present day the slope of the curve flattens, giving an average flow rate of 42 cfs.

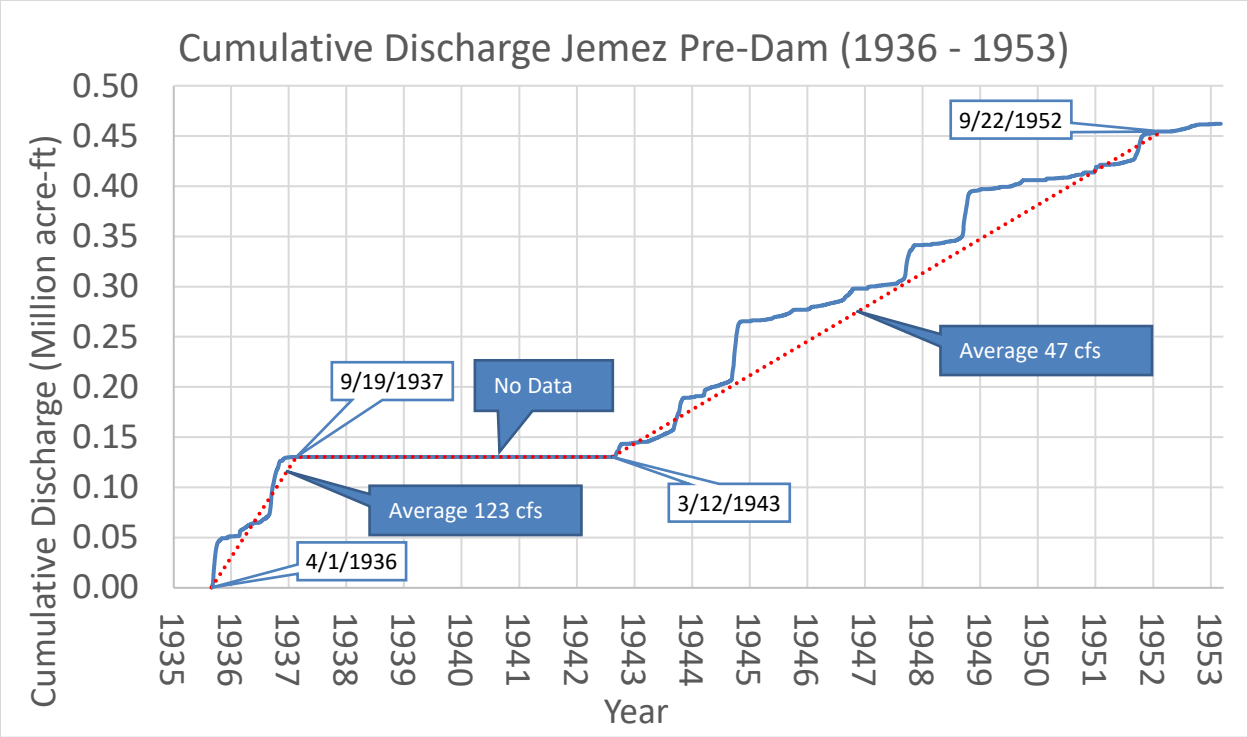

Figure 2-15 Discharge single mass curve at historical USGS gage 08329000 (Jemez) before dam construction in 1953.

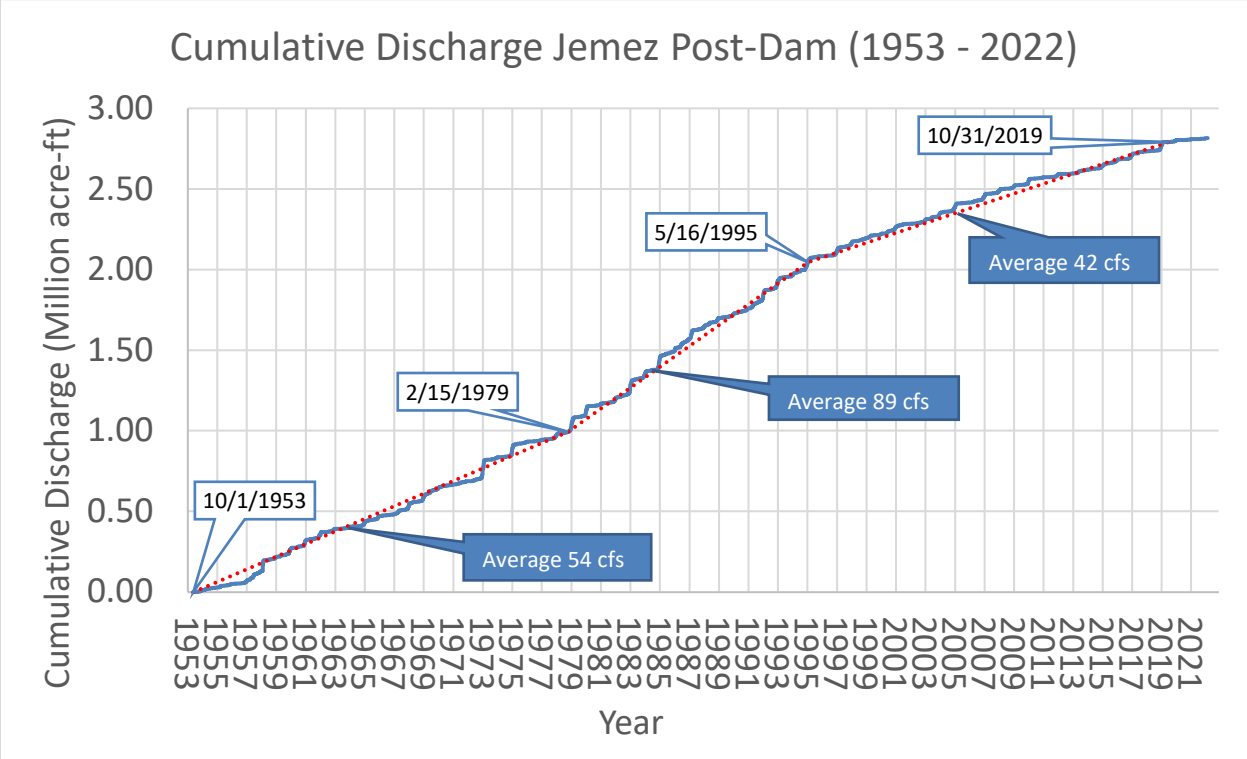

Figure 2-16 Discharge single mass curve at historical USGS gage 08329000 and USGS gage 08328950 (Jemez) after dam construction in 1953.

2.2.5 Flow Duration

Flow duration curves were developed using the mean daily flow discharge values for the Cochiti, San Felipe, Albuquerque, and Jemez River gages. **Table 2-2** shows the probabilities of daily exceedance values calculated from the flow duration curves for a range of exceedance probabilities. The gage records were split between pre- and post- construction of the Cochiti Dam for the Rio Grande gages. Gage records were similarly split for the Jemez River gages to account for any differences in flow conditions before and after the completion of the Jemez Dam. The curves for the Rio Grande gages are shown in **Figure 2-17**, and the curves for the Jemez River gages are shown in **Figure 2-18**.

While more frequent flood events with daily exceedance probabilities greater than 10% do not appear to be significantly impacted by the Cochiti Dam, the less frequent flood events less than 10% exceedance probability show a clear divergence between pre and post Cochiti Dam construction (**Figure 2-17**). The 1% daily exceedance probability shows a 3,000 cfs reduction in flow magnitude after completion of the dam. This does not appear to be the case for the Jemez Dam for the period of record. **Figure 2-18** shows a similar pattern in flows before and after the completion of the Jemez Dam in 1953.

Table 2-2 Probabilities of daily exceedance

	Discharge (cfs)						
	Pre Cochiti Dam (1926 to 1970)		Post Cochiti Dam (1970 – Present)			Pre Jemez Dam (1936 to 1953)	Post Jemez Dam (1953 to Present)
Daily Probability of Exceedance	8314500 Rio Grande at Cochiti, NM June 1, 1926 to October 30, 1970	8319000 Rio Grande at San Felipe, NM January 1, 1927 to September 30, 1970	8317400 Rio Grande Below Cochiti Dam, NM October 1, 1970 to Present	8319000 Rio Grande at San Felipe, NM October 1, 1970 to Present	[1] 8330000 Rio Grande at Albuquerque, NM October 1, 1970 to Present	[2] 8329000 Jemez River Below Jemez Canyon Dam April 1, 1936 to September 30, 1953	[3] 8329000 & 08328950 Jemez River Below Jemez Dam October 1, 1953 to Present
1%	9,280	9,560	6,190	6,320	6,160	750	650
10%	2,860	3,010	2,980	3,100	2,940	110	143
25%	1,320	1,410	1,250	1,330	1,220	36	45
50%	726	780	808	895	704	11	16
75%	487	529	573	651	467	0	2
90%	277	325	383	461	268	0	0

Notes:
[1] The pre-Cochiti Dam gage record between 1965 and 1970 for USGS gage 8330000 at Albuquerque were omitted from this analysis for consistency.
[2] Six years of missing data between 1938 and 1943 for the USGS 8329000 Jemez River gage.
[3] USGS gage 8328950 below Jemez Dam is located approximately 0.7 miles upstream of historical USGS gage 8329000. Gage records were combined for this analysis.

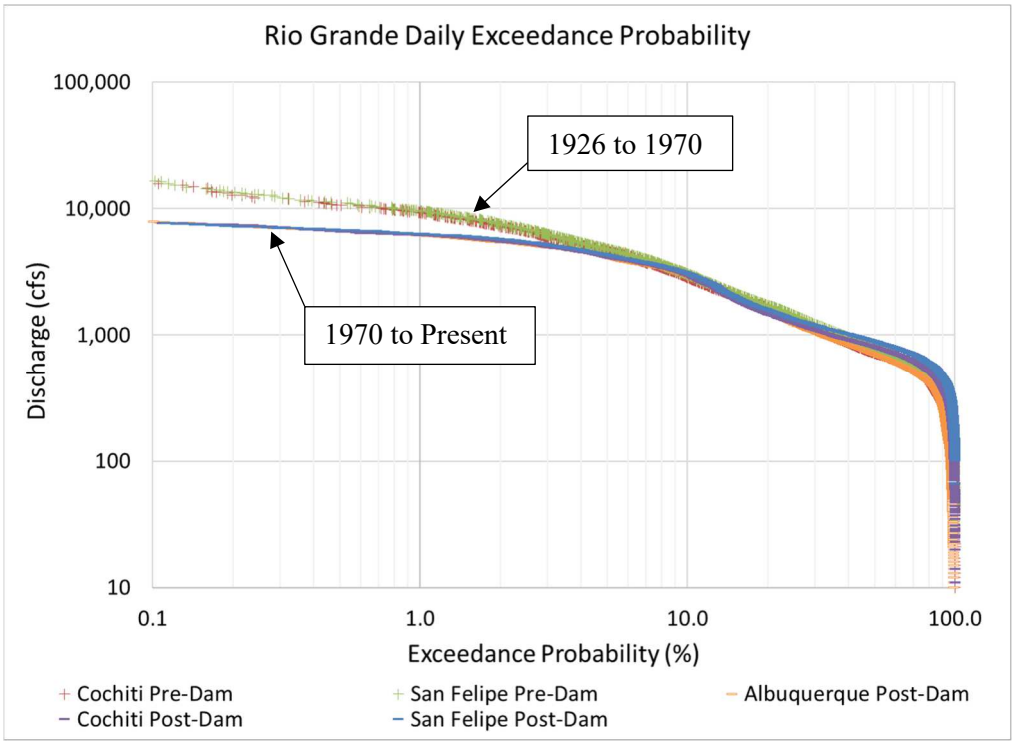

Figure 2-17 Flow duration curves for the Rio Grande gages before and after dam construction.

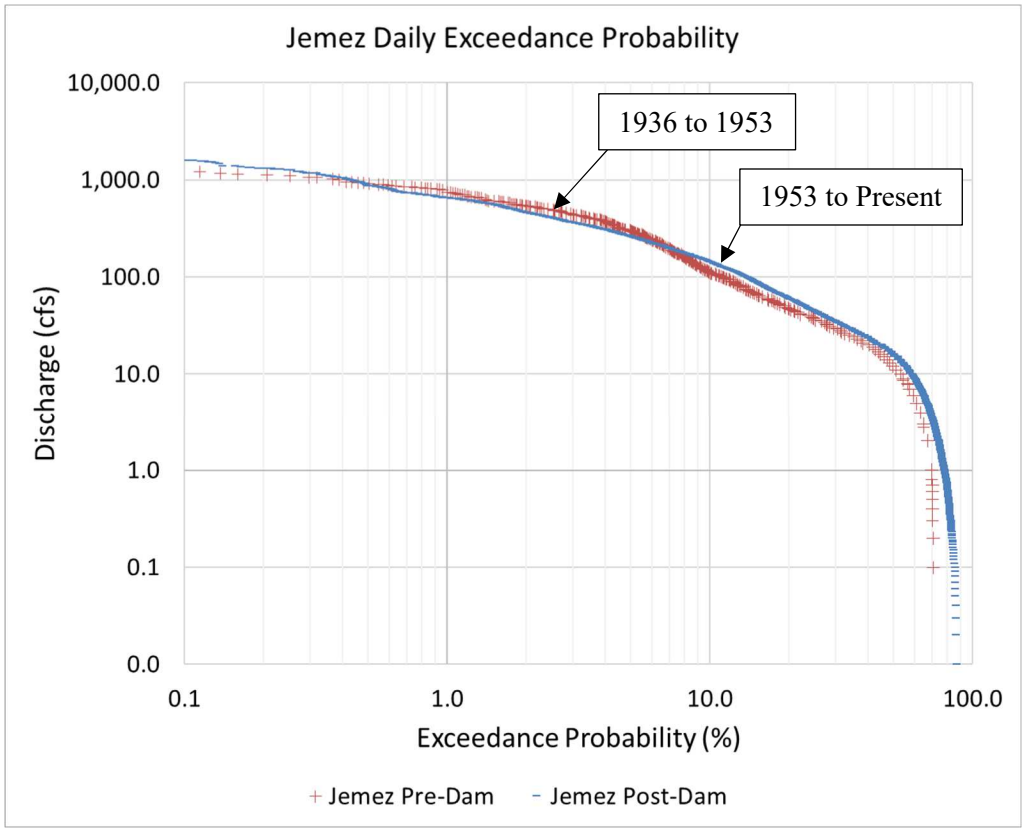

Figure 2-18 Flow duration curves for the Jemez River gages before and after dam construction in 1953.

2.2.6 Days of Flow

In addition to flow duration curves, the number of days in the water year exceeding the identified flow values at each gage were analyzed. This is purely a count of days and does not consider consecutive days. This analysis was performed for the entire record at the Cochiti, San Felipe, and Jemez River gages shown by **Figure 2-19**, **Figure 2-20**, and **Figure 2-21**, respectively. Like previous analyses, the gage records were split between pre and post dam construction for the purposes of comparison.

The Cochiti graphs have a very similar pattern to the San Felipe graphs, which is an indication that these two gages see very similar magnitude of flows. The most notable difference between the Cochiti and San Felipe graphs before and after Cochiti Dam construction is that pre-dam flow conditions saw a greater number of days above 6,000 cfs. The graphs also seem to indicate that the years between 1979 and 1999 show a greater number of days (around half of the year, on average) above 1,000 cfs. These graphs also give a good indication of dry years. For example, between 2003 and 2006, fewer than 50 days of the year saw flows greater than 1000 cfs. In general, the larger flows become less frequent after 2001.

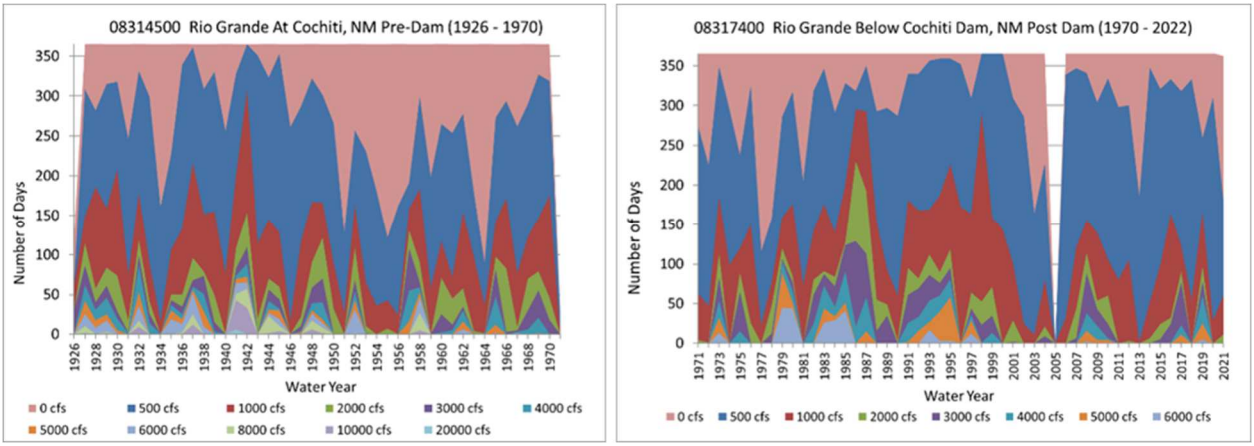

Figure 2-19 Number of days greater than an identified discharge at the Cochiti gages before (left) and after (right) dam construction.

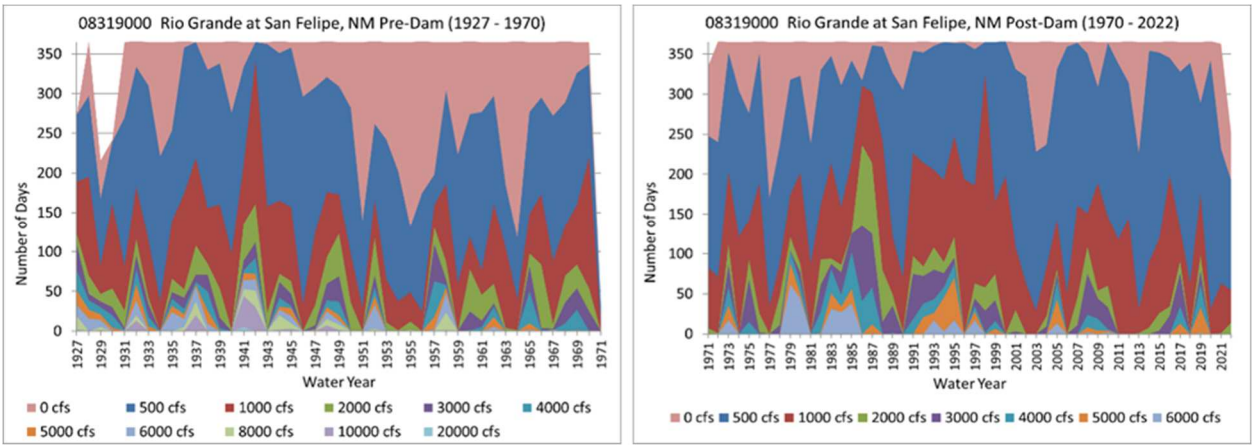

Figure 2-20 Number of days greater than an identified discharge at the San Felipe gage before (left) and after (right) dam construction.

The Jemez River is much more likely to see days with no flow. Before dam construction, the river appears to have had more frequent days with no flow than after dam construction. In the years between 1999 and present day, the Jemez River has generally seen fewer than 100 days of the year with flows greater than 50 cfs.

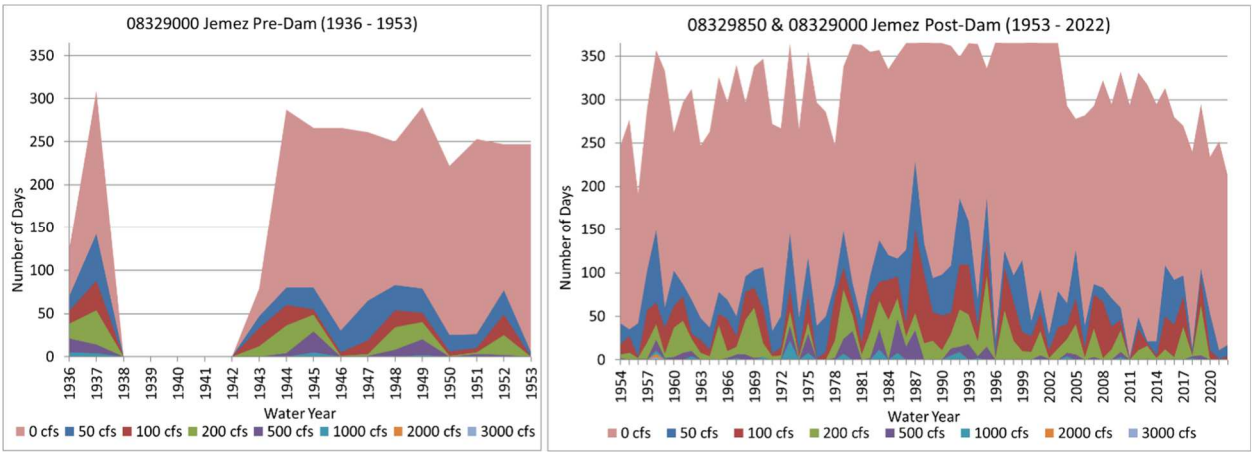

Figure 2-21 Number of days over an identified discharge at the Jemez gages before (left) and after (right) dam construction in 1953.

2.3 Suspended Sediment Load

2.3.1 Single Mass Curve

Single mass curves of cumulative suspended sediment (in millions of tons) at the Jemez River (USGS 08329000), Rio Grande Below Cochiti (USGS 08317400), Rio Grande Near Bernalillo (USGS 08329500), and Rio Grande at Albuquerque (USGS 08330000) gages are shown in **Figure 2-22** to **Figure 2-25**, respectively. These curves were created from the average daily sediment data. Additional single mass curves that show greater detail of the sediment load in the Jemez River before and after the Jemez Dam modification are found in **Section 2.3.4**.

The single mass curves show changes in daily sediment volume over a given time period. The slope of the line of the mass curve gives the mean sediment discharge, while breaks in the slope along the single mass curve show the changes in sediment flux. The Cochiti Dam was constructed in 1973. Downstream of Cochiti, at the Albuquerque gage, there is a large decrease in the mean sediment discharge after 1973 and the historical Bernalillo gage data showed large mean sediment discharges before 1973. The correlation shows that the construction of Cochiti Dam had a dramatic impact on the sediment discharge going through the MRG. The mean sediment discharge at the Cochiti gage after construction is relatively low and consistent compared to other inputs to the system, which indicates that a majority of the sediment upstream of Cochiti is getting stopped at the dam. There are no major tributaries that enter the MRG below Cochiti, however there are several small arroyos that enter the river and two flood controlled channels (Towne 2007). As mentioned in **Section 1.2**, the ephemeral tributaries are the primary source of sediment input into to MRG (Fitzner 2018). Other sources of sediment include bed erosion as the channel degrades and bank erosion during channel migration.

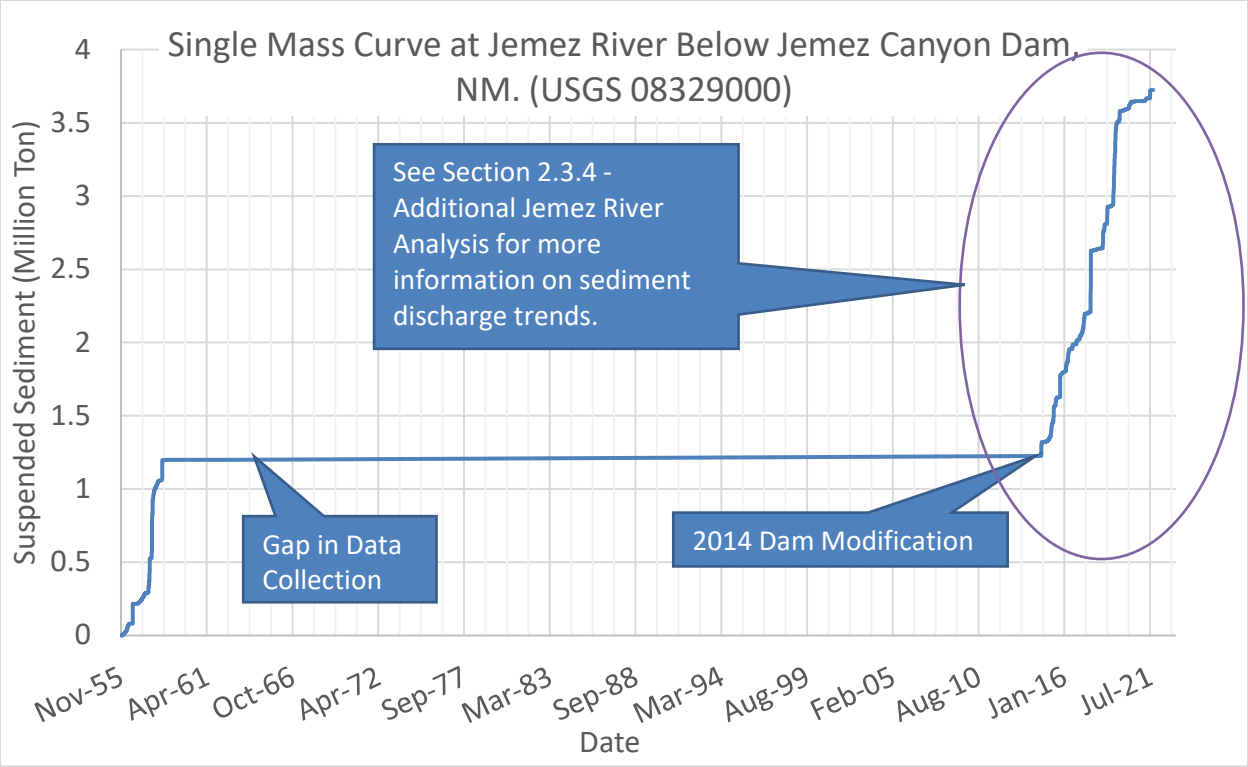

Figure 2-22 Suspended sediment discharge single mass curve for USGS gage 08329000 at Jemez River Below Jemez Canyon Dam, NM

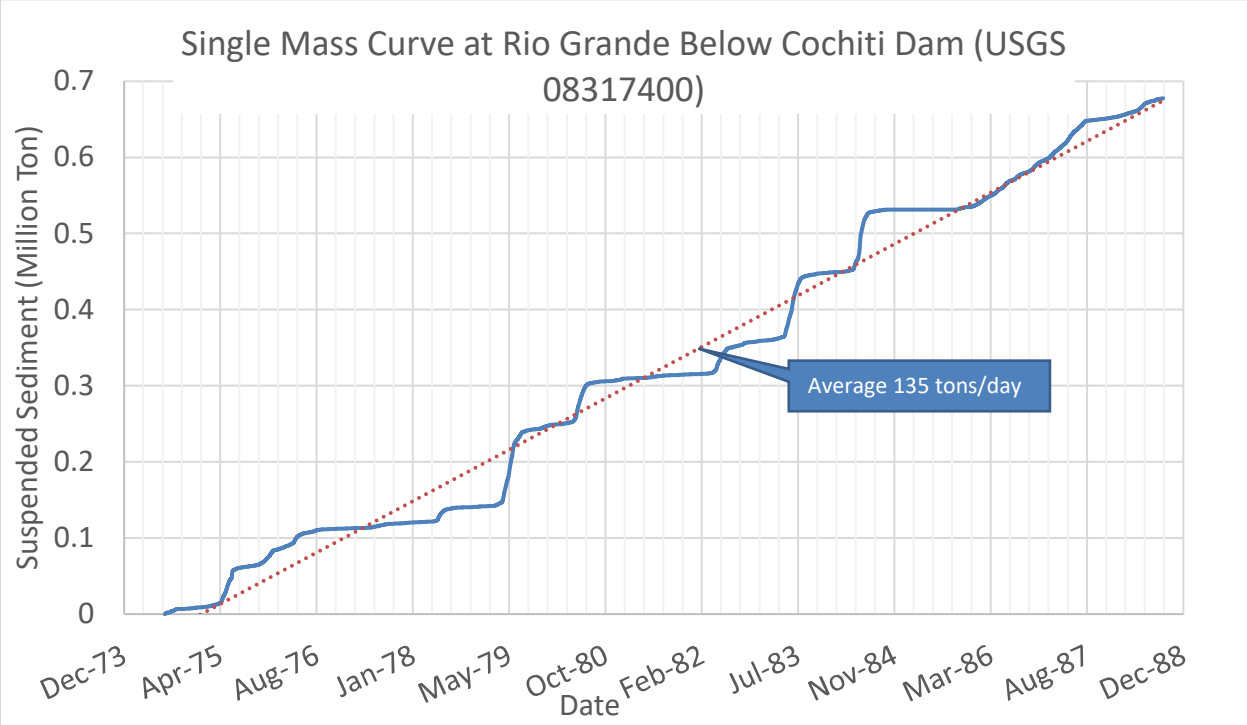

Figure 2-23 Suspended sediment discharge single mass curve for USGS gage 08317400 at Rio Grande Below Cochiti Dam, NM

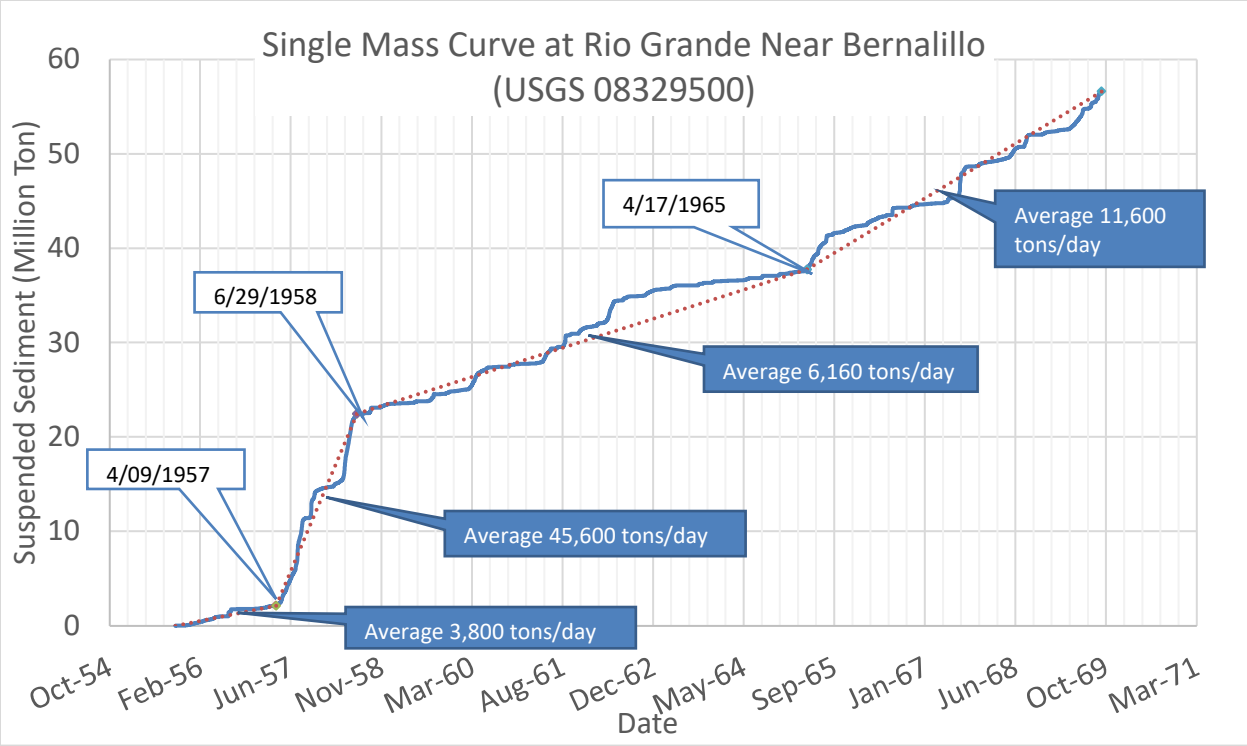

Figure 2-24 Suspended sediment discharge single mass curve for USGS gage 08329500 at Rio Grande Near Bernalillo, NM

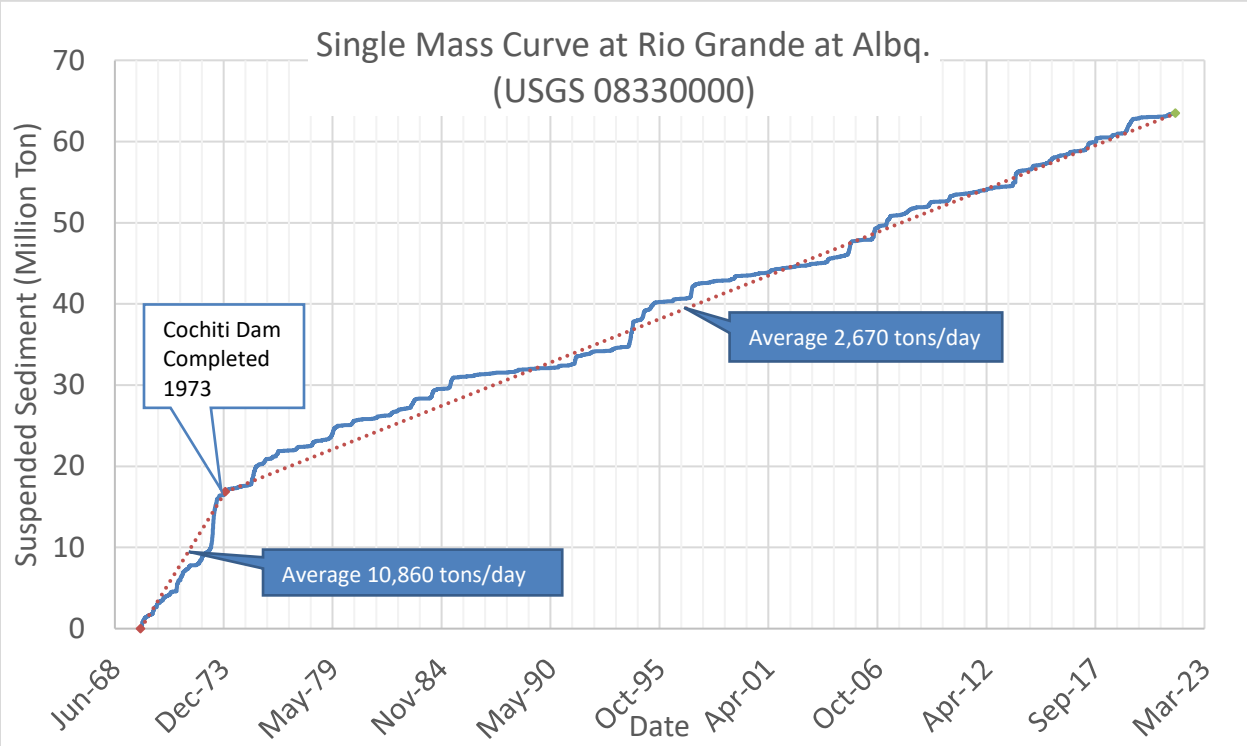

Figure 2-25 Suspended sediment discharge single mass curve for USGS gage 08330000 at Rio Grande at Albq, NM

2.3.2 Double Mass Curve

Double mass curves show how suspended sediment volume relates to the daily discharge volume. The slope of the double mass curve represents the mean sediment concentration. The double mass curve in **Figure 2-26** is for USGS gage Rio Grande at Albuquerque (USGS 08330000).

Figure 2-27 relates the cumulative average monthly suspended sediment at the Rio Grande at Albuquerque (USGS 08330000) gage (located just downstream of Montaño Bridge) to the cumulative precipitation at the Alameda Precipitation gage. The vertical steps show an increase in suspended sediment occurring without an increase in precipitation. The horizontal steps show an increase in precipitation without an increase in suspended sediment. This stair-step trend shows that at most times, there is not a significant correlation between precipitation and suspended sediment. However, there are monsoonal events that impact the suspended sediment in the Bernalillo and Montaño Reaches. The sections of steep slopes between the stair-step pattern indicate an increase in suspended sediment that is correlated with an increase in precipitation. These represent monsoonal events, such as the monsoonal events that occurred in August 2006 and September 2013.

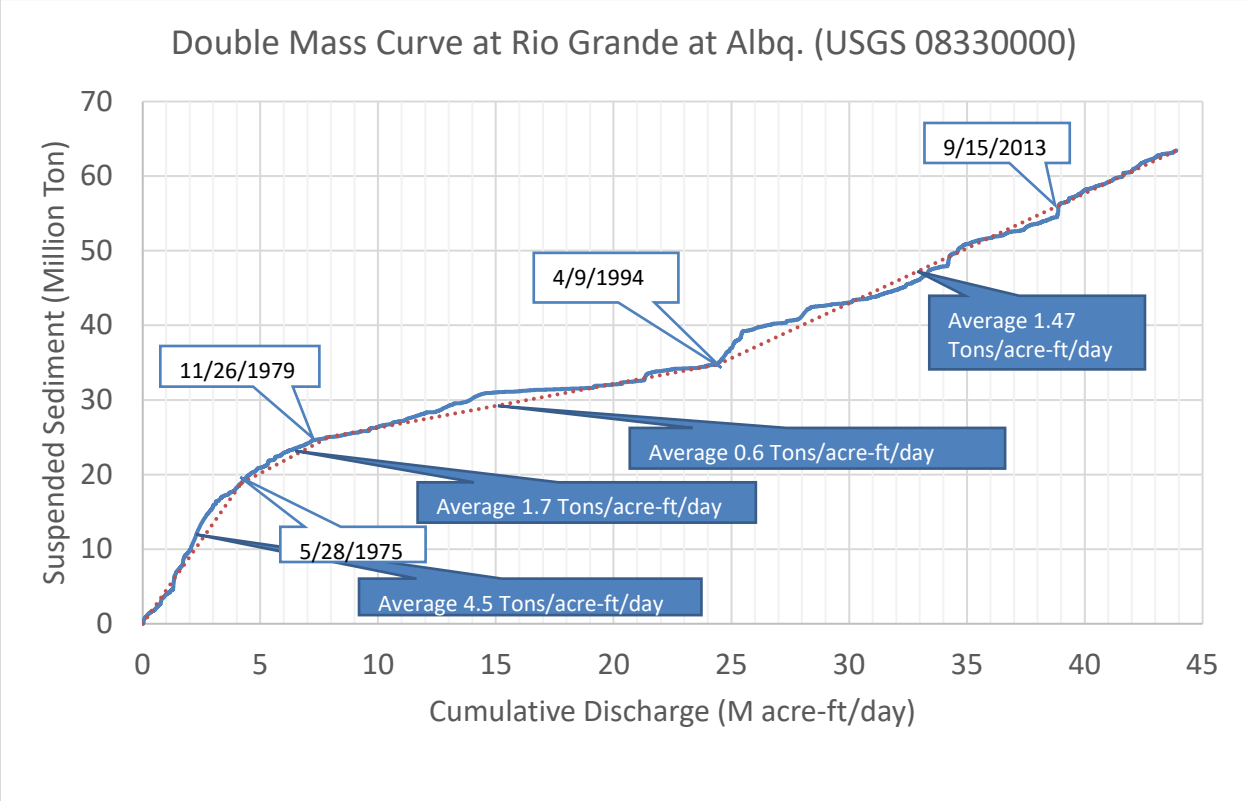

Figure 2-26 Double mass curve for USGS gage 08329500 at Rio Grande Near Bernalillo, NM

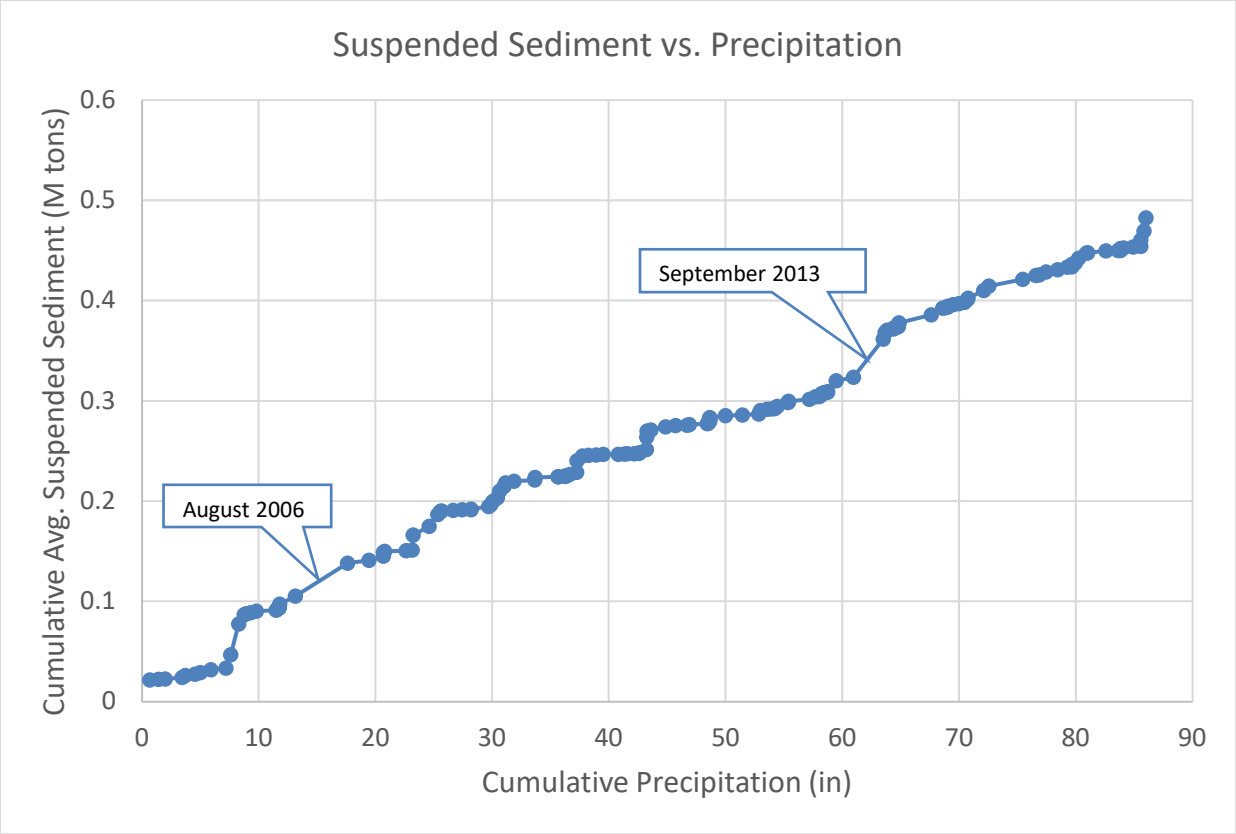

Figure 2-27 Cumulative suspended sediment (data from the Rio Grande at Albuquerque (USGS 08330000) gage) versus cumulative precipitation at the Alameda gage.

2.3.3 Monthly Sediment Variation

Plots of monthly average discharge and suspended sediment was created for the Jemez River (USGS 08329000), Rio Grande Below Cochiti (USGS 08317400), Rio Grande Near Bernalillo (USGS 08329500), and Rio Grande at Albuquerque (USGS 08330000) gages are shown in **Figure 2-28** to **Figure 2-35**, to help reveal any important seasonal trends. These figures show the seasonal trends of suspended sediment load and concentration, respectively, along with the discharges that correspond with the years. The spring snowmelt brings some of the larger flow rates associated with the larger quantities of sediment. However, the increased flows from the monsoonal storm events in the summer months were associated with the higher spikes in sediment concentration. There also peaks in suspended sediment from flood events that occurred prior to the construction of Cochiti Dam and from the 2013 flood. As shown in the figures below, a majority of the sediment flux is occurring during spring runoff associated with seasonal snowmelt in the region. Monsoonal events affect the sediment flux but are not the driving force for sediment movement in the Bernalillo and Montano Reaches of the MRG.

The primary sediment input into the MRG through the Bernalillo and Montano reaches is due to ephemeral tributaries (Fitzner 2018). The spring runoff brings sediment from these tributaries into the MRG. However, the sediment load at the Rio Grande Below Cochiti (USGS 08317400) shows the sediment being in phase with the flow and relatively lower sediment discharges and concentrations compared to the other gages. There are no uncontrolled ephemeral tributaries upstream of Cochiti, so the sediment and flow from Cochiti are both controlled by dam releases.

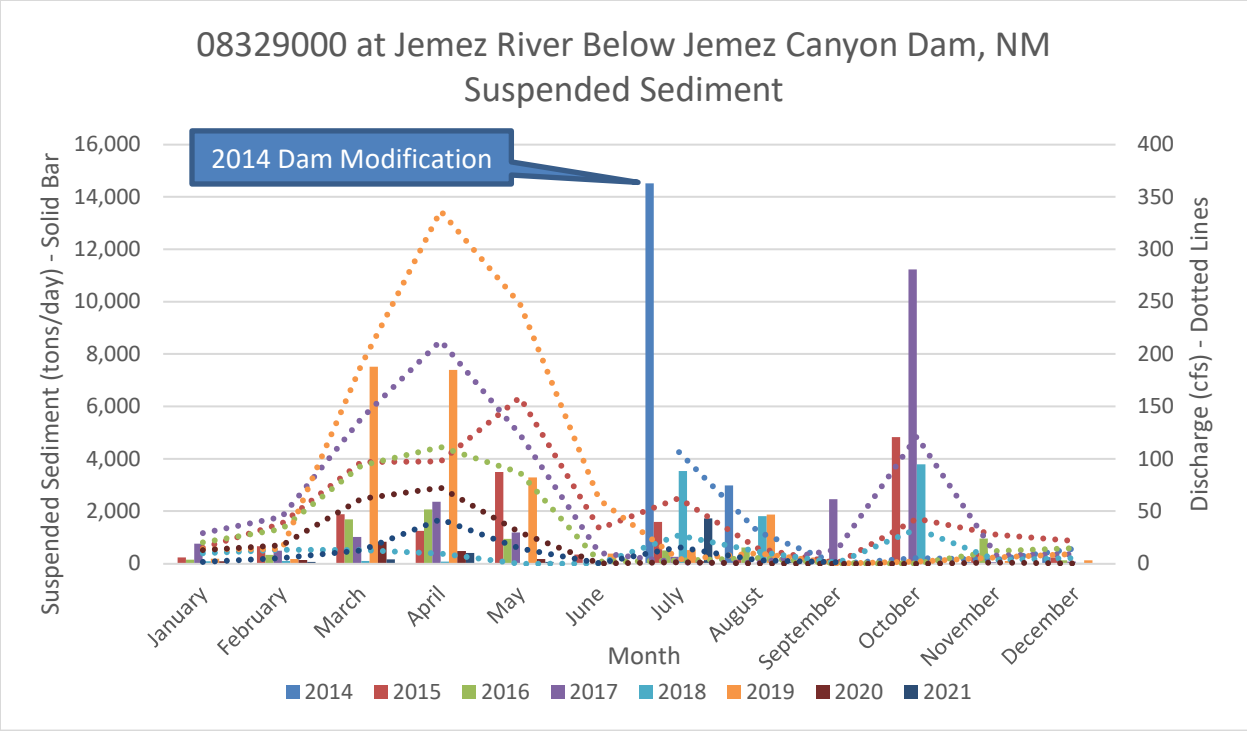

Figure 2-28 Monthly average suspended sediment and water discharge at USGS gage 08329000 at Jemez River Below Jemez Canyon Dam, NM

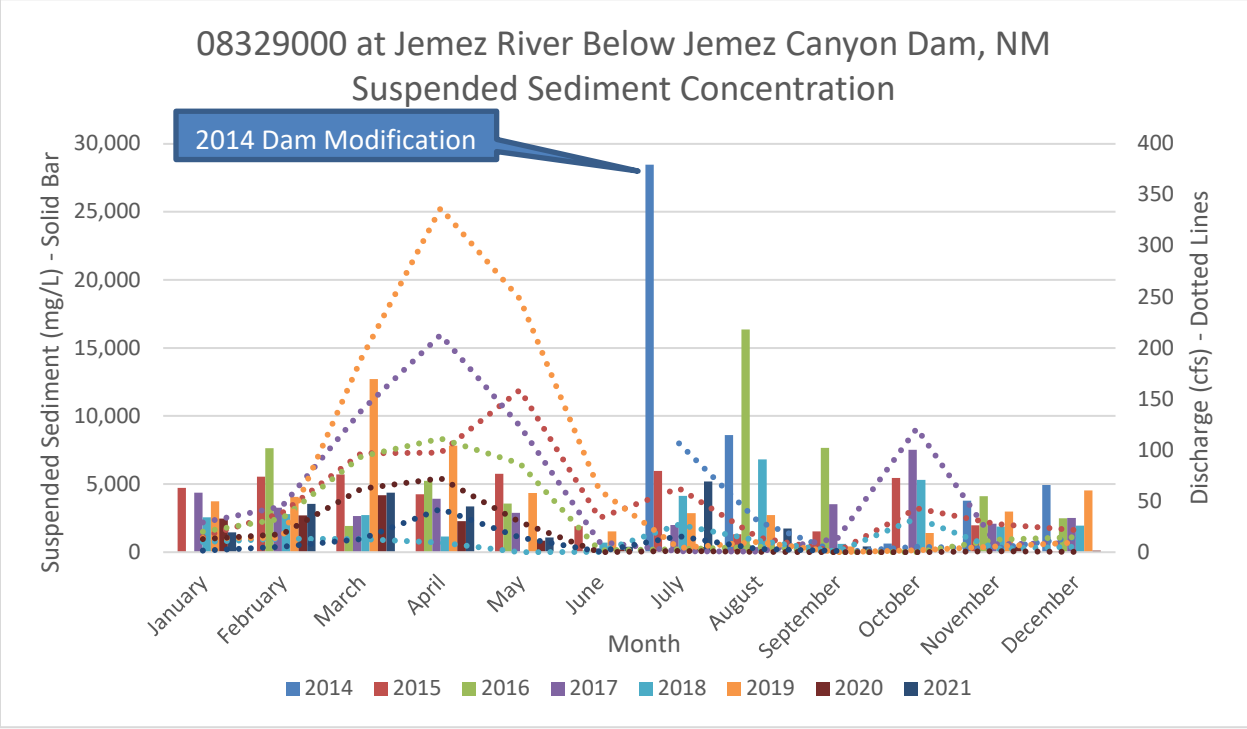

Figure 2-29 Monthly average suspended sediment concentration and water discharge at USGS gage 08329000 at Jemez River Below Jemez Canyon Dam, NM

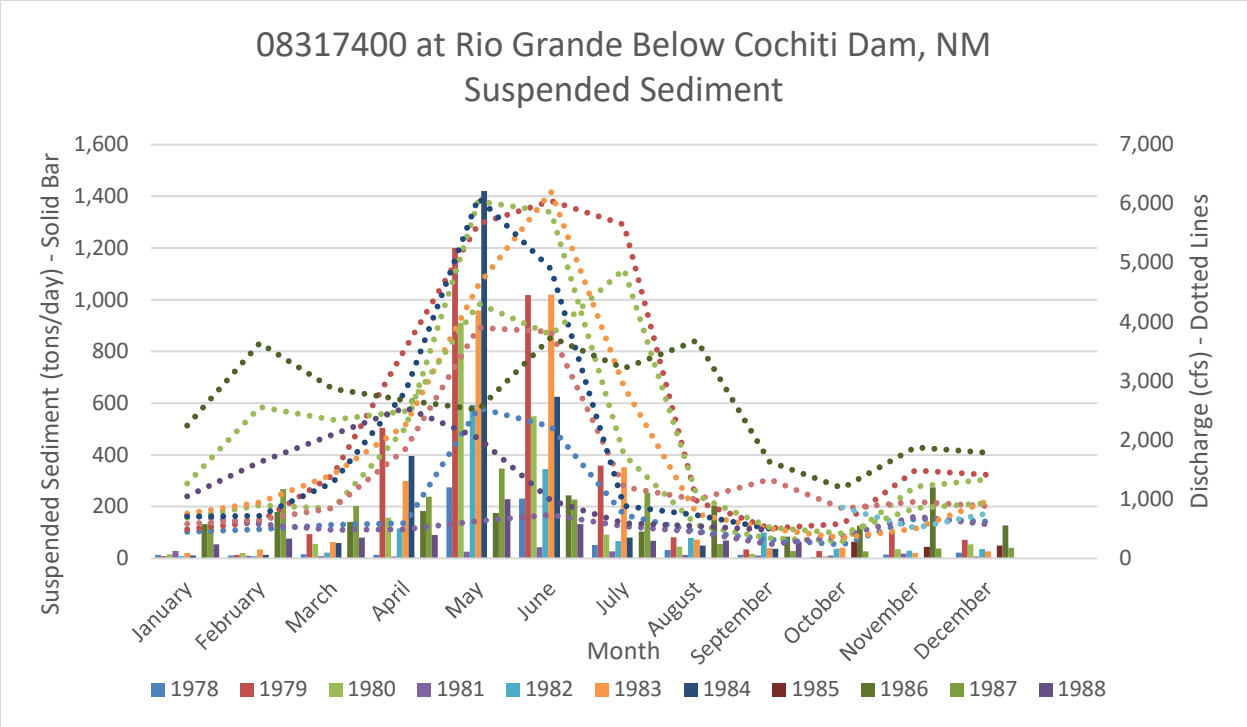

Figure 2-30 Monthly average suspended sediment and water discharge at USGS gage 08317400 at Rio Grande Below Cochiti Dam, NM

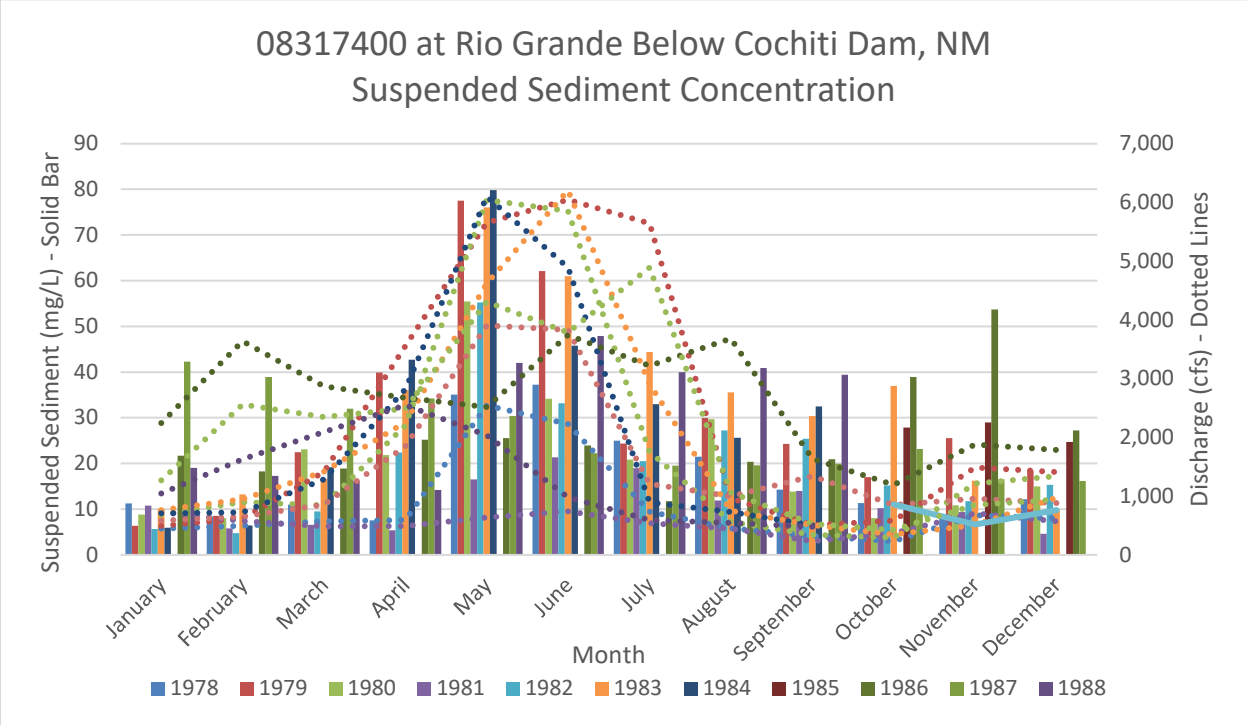

Figure 2-31 Monthly average suspended sediment concentration and water discharge at USGS gage 08317400 at Rio Grande Below Cochiti Dam, NM

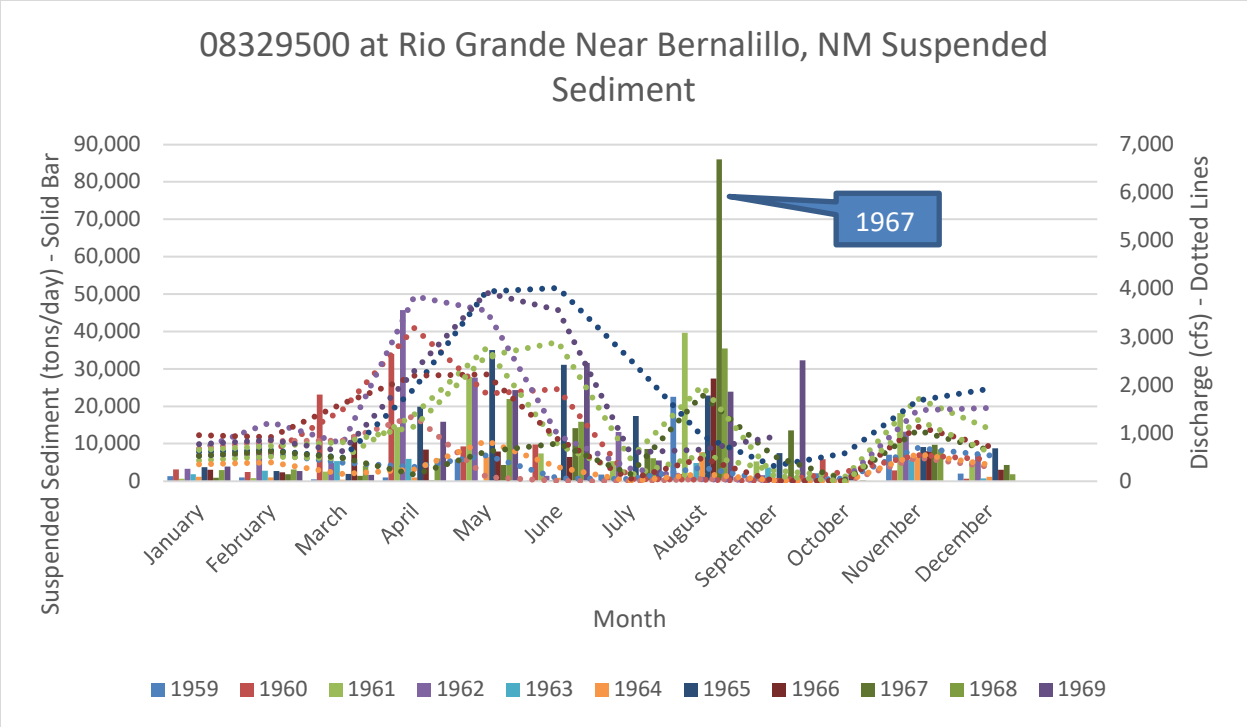

Figure 2-32 Monthly average suspended sediment and water discharge at USGS gage 08329500 at Rio Grande Near Bernalillo, NM

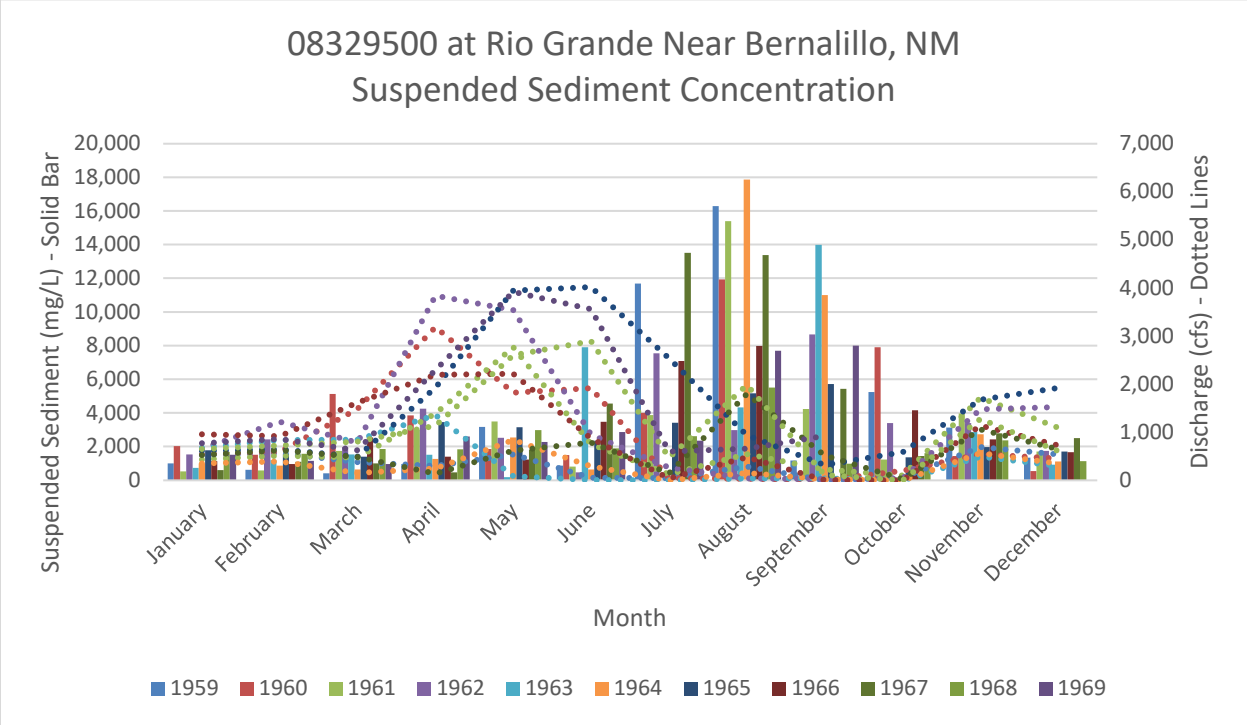

Figure 2-33 Monthly average suspended sediment concentration and water discharge at USGS gage 08329500 at Rio Grande Near Bernalillo, NM

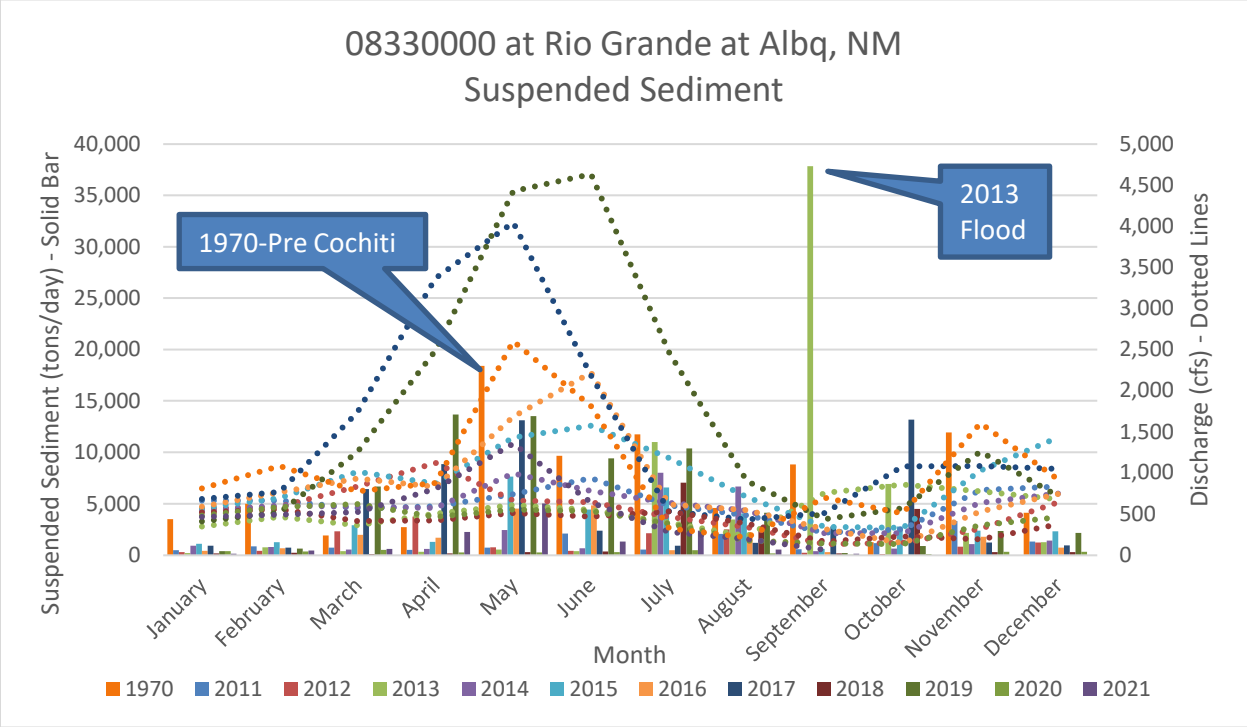

Figure 2-34 Monthly average suspended sediment and water discharge at USGS gage 08330000 at Rio Grande at Albq, NM

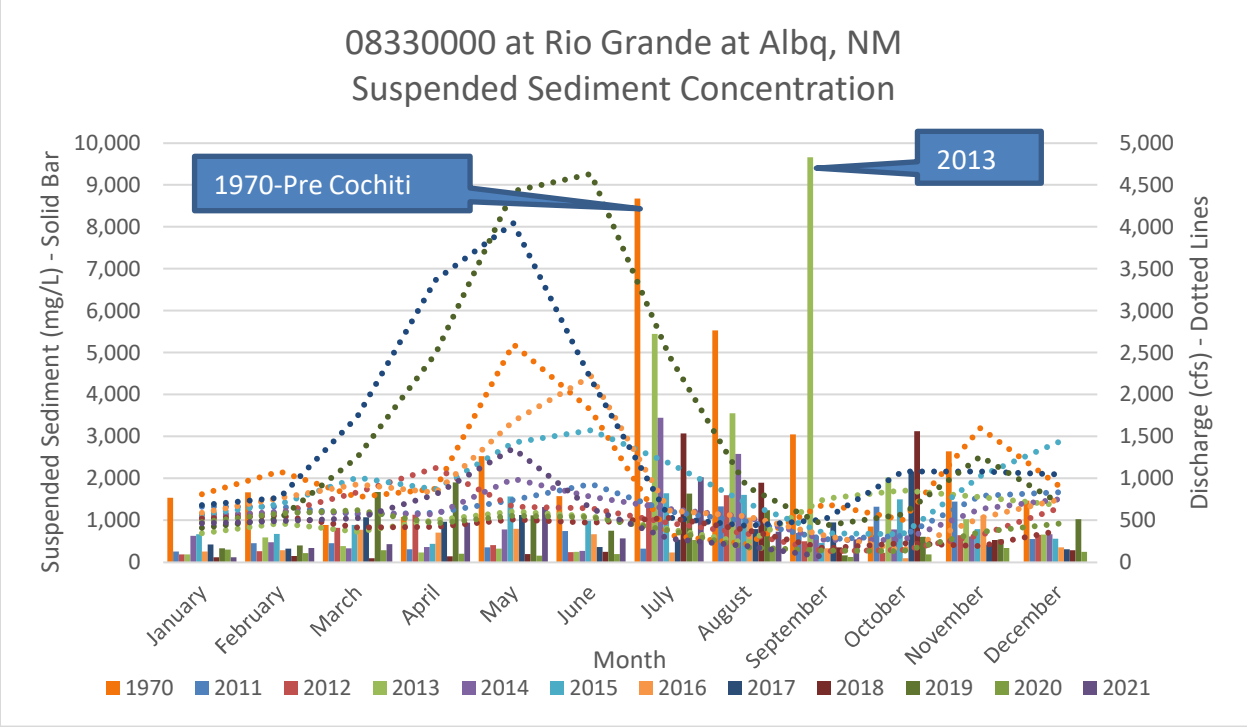

Figure 2-35 Monthly average suspended sediment concentration and water discharge at USGS gage 08330000 at Rio Grande at Albq, NM

2.3.4 Additional Jemez River Analysis

The Jemez River is a major tributary of the Bernalillo and Montaño reaches. The Jemez Dam was constructed in 1953. Sediment data was not collected prior to the construction of the dam. In 2014, the Jemez Dam underwent a modification that included a low flow channel. This modification and the subsequent effects on the suspended sediment were analyzed. **Figure 2-36** and **Figure 2-37** below show the single mass curves before and after the dam modification. It is important to note that there was a gap in sediment data collection between the years 1958-2014. It should be noted that while this analysis provides some insight into the sediment and flow characteristics for the Jemez River, the gaps in sediment data and the limited 7 years of record following modification of the Jemez Dam make it difficult to draw any definitive conclusions regarding impacts of the modification at this time.

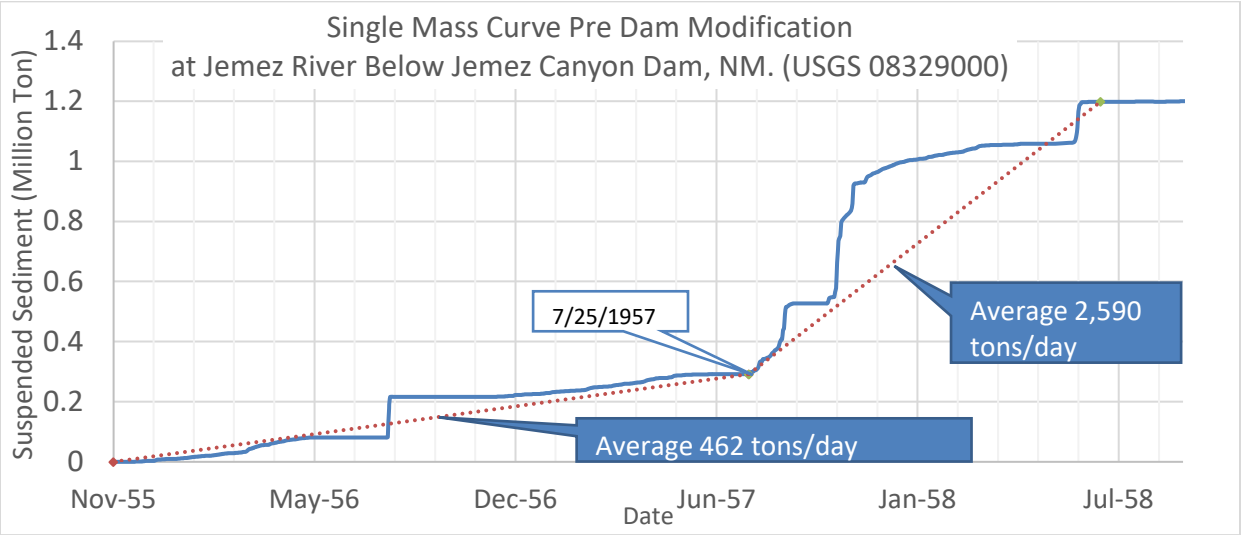

Figure 2-36 Suspended sediment discharge single mass curve for USGS gage 08329000 at Jemez River Below Jemez Canyon Dam, NM – Pre-Dam Modification

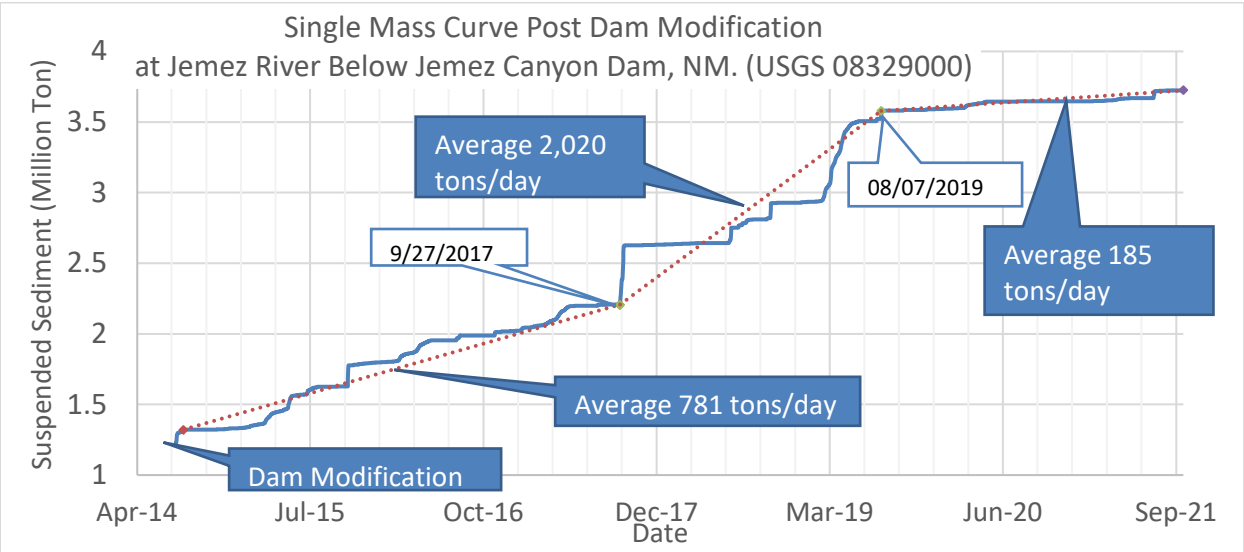

Figure 2-37 Suspended sediment discharge single mass curve for USGS gage 08329000 at Jemez River Below Jemez Canyon Dam, NM – Post-Dam Modification

The flow and sediment budget for the Middle Rio Grande through the Bernalillo and Montaño Reaches is dependent on the flow and suspended sediment coming from the Jemez River, from downstream of the Cochiti Dam, and from other sources such as ephemeral tributaries and channel erosion.

A flow budget, shown in **Figure 2-38** was determined using the gages at the outlet of the Jemez River (historical USGS Gage 08329000 and USGS Gage 08328950) along with either the Bernalillo (USGS Gage 08329500) or the Albuquerque (USGS Gage 08330000) gages located downstream of the outlet, depending on the year and data availability. The gage record was analyzed for the years of overlapping gage record between the Jemez River and the Rio Grande gages between 1944 and 2021. The Jemez contributed a total of 4% of the flow to the Bernalillo and Montaño reaches each year. The Jemez River flow contribution varied between 1.7% and 10.5%, depending on the year. The year 2021 saw the lowest contribution of flow, at 1.7%, while 1961 saw the highest contribution to flow of 10.5%.

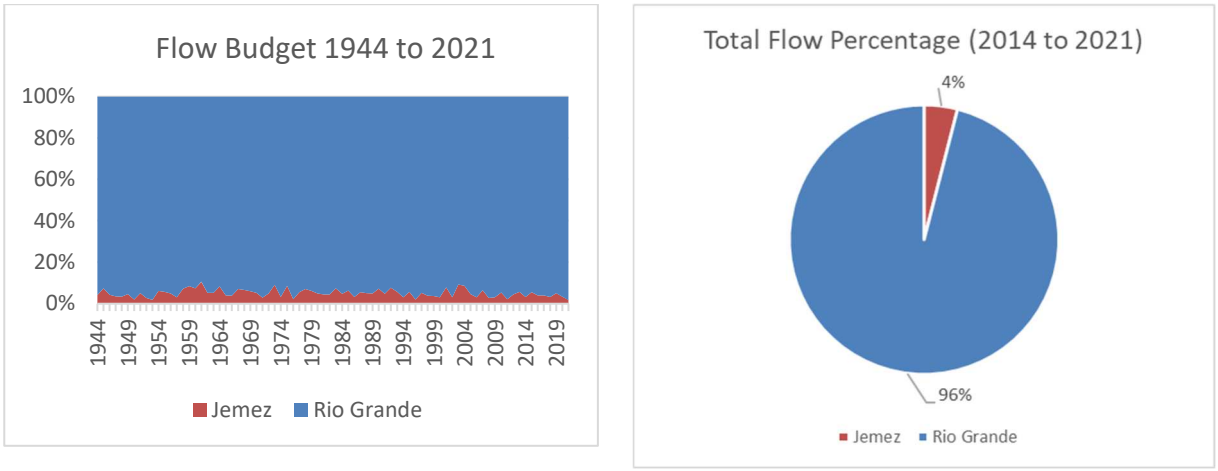

Figure 2-38 Flow Budget through the years between 1944 and 2021 (left) and total flow percentage between 2014 and 2021 (right) for the Jemez River at the Outlet and Rio Grande at Bernalillo and Albuquerque.

The slope of the single mass curves presented in this section and **Section 2.3.1**, provide average sediment discharges in tons/day for certain periods of time. The sediment budget was calculated for each year by using the average sediment discharges. The total sediment budget was approximated from either USGS Gage 08329500 at Rio Grande Near Bernalillo, NM or USGS Gage 08330000 at Rio Grande at Albuquerque, NM, since the two gages do not overlap available data and represent the furthest downstream gage, depending on the year and available data. An average sediment discharge rate from the Jemez and Cochiti gages was calculated from the slopes of the single mass curves. For the time period*s* past the available gage data at Cochiti, the same rate from the single mass curve of available data was used because the suspended sediment was consistent over time. **Figure 2-39** below shows sediment budgets for 1958 (pre-Jemez Dam modification), 2014 (the year the Jemez Dam modification was completed), and 2021 (post-Jemez Dam modification). The 1958 sediment budget does not include sediment from downstream of the Cochiti because the Cochiti Dam was not constructed then.

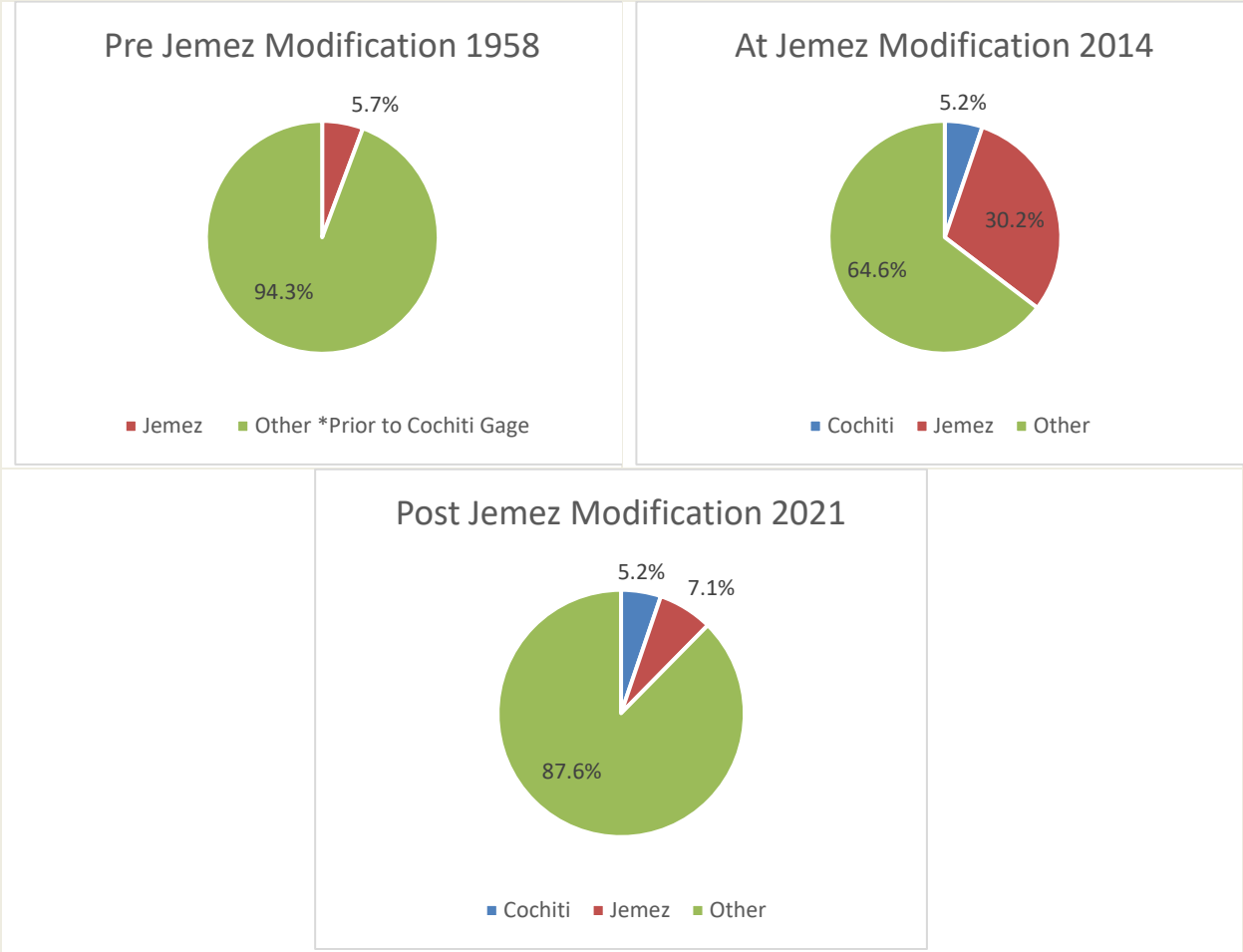

Figure 2-39 Sediment budgets pre-, at-, and post- Jemez Dam modification

Figure 2-40 below shows the average sediment budget for each year from 2014 to 2021 compared to the average sediment budget before the Cochiti Dam was construction (1955 to 1973). The results showed that the percentage of sediment coming from the Jemez was significant in between 2014 and 2017, spiked in 2018 and 2019, and receded significantly in 2020 and 2021. The spike in sediment contribution between 2014 and 2019 may have been from release of sediment that had been held behind the dam that now can now move downstream. In general, the Jemez dam provided less sediment to the overall budget seen in Albuquerque before Cochiti Dam construction. This further illustrates that the construction of Cochiti Dam lowered the amount of sediment going through the reach between the Cochiti Dam location and the Jemez River tributary. **Figure 2-40** above also shows a spike in the Jemez River average sediment budget in 2018 and 2019 which could be due to some peak flow events that occurred during those times.

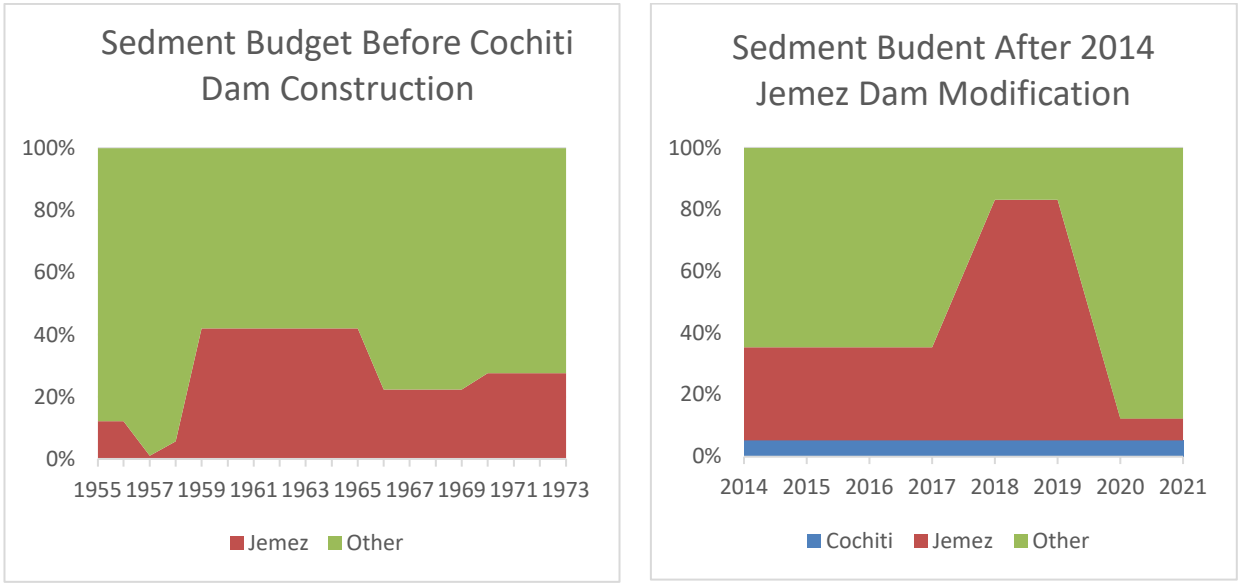

Figure 2-40 Average sediment budget comparison – before Cochiti Dam construction (left) and after Jemez Dam modification (right)

To better understand the sediment sources for the years since the Jemez Dam Modification, a total sediment budget by volume for the years 2014 through 2021 was created. Based on available data, the average daily sediment volume in tons was summed from July 30th, 2014 to September 30th, 2021. Similar to the average sediment budget analysis above, there was not sediment data for USGS Gage 08317400 at Rio Grande Below Cochiti Dam for the years 2014 to 2021. However, the average sediment budget of 135 tons/day (taken from the slope of the single mass curve) was used over the time period analyzed. **Figure 2-41** below shows the results. The Jemez River accounts for nearly 40% of the total volume during 2014 to 2021.

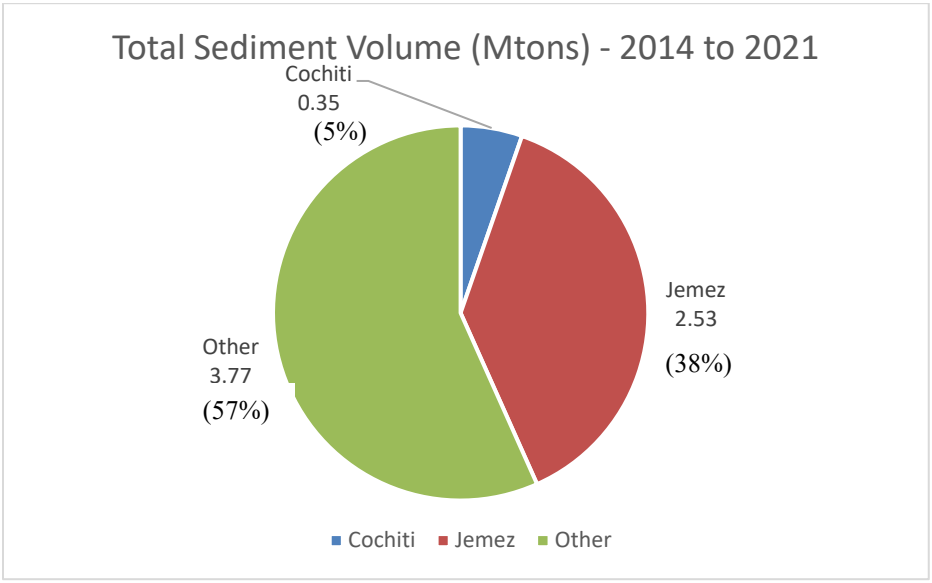

Figure 2-41 Total sediment volume2.53 budget in million tons at the USGS Gage 08330000 at Rio Grande at Albuquerque, NM from 2014 to 2021.

3 River Geomorphology

3.1 Wetted Top Width

Wetted top width can provide significant insight into hydraulic geometry. Typically, wetted top width in a compound trapezoidal channel would slowly increase as discharge values increase until there is a connection with the floodplain. At this point, the top wetted width would quickly increase as the water spills onto the floodplains. Then, a gradual increase in width would continue after this point. Analysis of the wetted top width can be used to help understand bankfull conditions and how they vary spatially and temporally in the Bernalillo Reach. A HEC-RAS model was created to analyze a variety of top width metrics. As discussed in **Section 4.1.1**, computational levees were used in HEC-RAS geometries for 1962 and 1972 and ineffective flow areas were used in the 2012 geometry to keep the water contained in the channel until bankfull is reached. An increment of 500 cfs up to 10,000 cfs was used in the top width analysis for the years with available data: 1962, 1972, 1992, 2002 and 2012.

Figure 3-1 shows the moving cross sectional averaged top wetted width at 1,000 from the HEC-RAS model results. The top width shown at each agg/deg line comes from the moving average from five consecutive cross sections: the identified agg/deg line, two upstream agg/deg lines, and two downstream agg/deg lines. Based on the analysis, Subreaches B1, B2, and B3 have experienced the most dramatic change in top width. Majority of the B1, B2, and B3 subreaches have shown a trend of narrowing since 1972. Subreach B4 has also shown a trend of narrowing over time, but at a smaller scale. Widening of the channel occurred throughout most of the Bernalillo Reach between 1962 and 1972. This widening could be a result of the large sediment discharge events that occurred post-1962 that caused aggradation of the channel. See **Section 2.3** for more detail on the sediment trends see in the Bernalillo Reach. The aggradation caused the channel invert to rise and the active top width to increase. Post 1972, the sediment discharge events were smaller in magnitude and the channel generally experienced degradation and narrowed active top widths. See **Section 3.2** for the aggradation/degradation analysis of the Bernalillo Reach. Additional figures from this analysis can be found in **Appendix C**, including plots with the corresponding top width for each agg/deg line rather than the moving average.

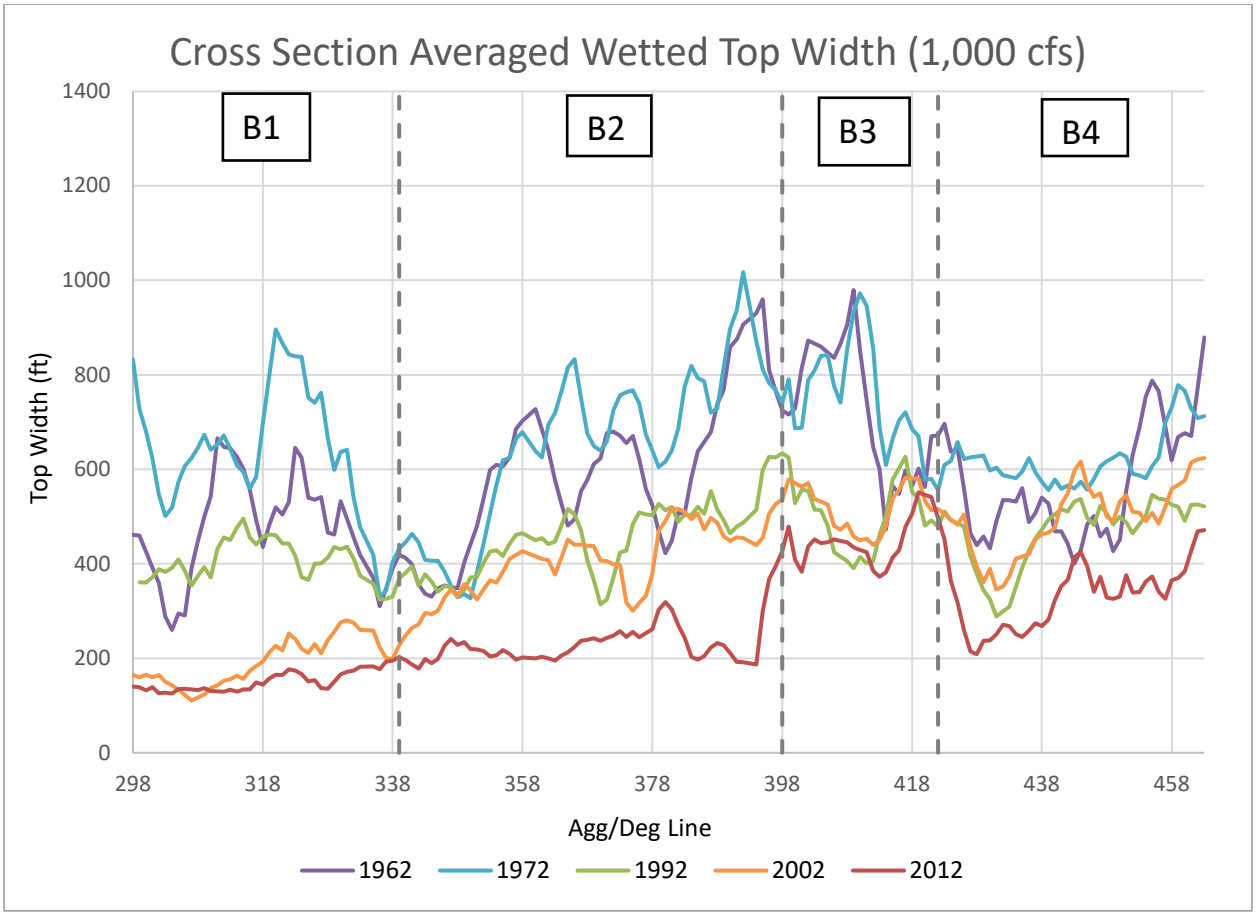

Figure 3-1 Moving cross-sectional average of the wetted top width at a discharge of 1,000 cfs.

Figure 3-2 shows the moving cross sectional averaged top wetted width at 3,000 cfs from the HEC-RAS model results. The channel width decreased dramatically in 1992 compared to 1962 and 1972. In the subsequent years at flow of 3,000 cfs, there is a steady decrease in top width in Subreaches B1 and B2. Subreaches B3 and B4 show a small decrease in top width. This is a similar trend when compared to the 1,000 cfs flow. This indicates that the floodplain might not be utilized and filled at 3,000 cfs.

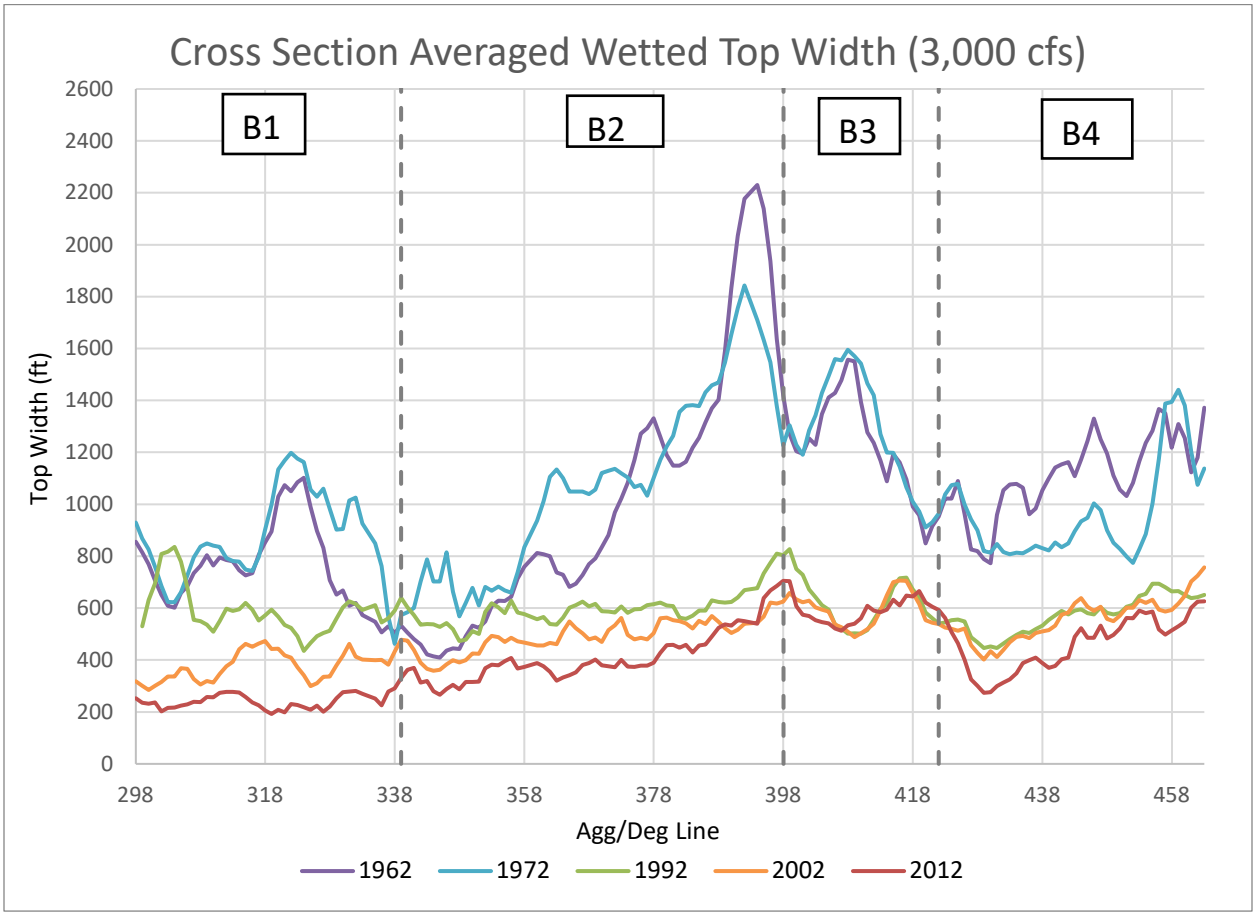

Figure 3-2 Moving cross-sectional average of the wetted top width at a discharge of 3,000 cfs.

Figure 3-3 shows the moving cross sectional averaged wetted top width at 5,000 cfs. The top width is fairly consistent from 1962 and 1972 in all of the subreaches. The top width generally decreases from 1972 to 2012, however, there are some locations within the reaches that have seen spikes in the top width. These spikes could indications sections of the channel are transiting from bankfull to the floodplain at 5,000 cfs.

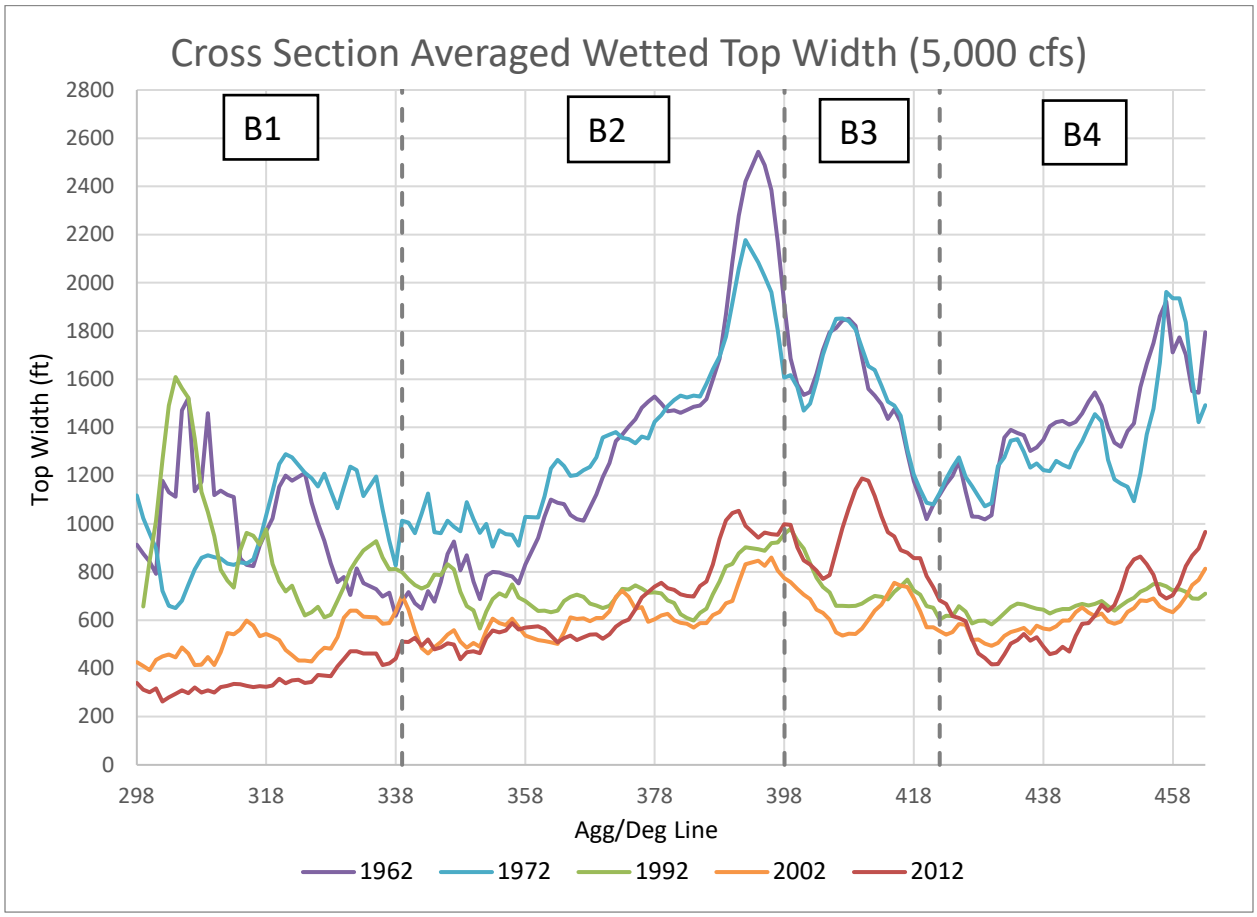

Figure 3-3 Moving cross-sectional average of the wetted top width at a discharge of 5,000 cfs.

Figure 3-4 to Figure 3-6 show the cumulative top width of the wetted cross sections. The cumulative width shows how the width through time varies within each subreach. In general, 1972 had the greatest widths with the steepest cumulative width slope in Subreach B1. As previously discussed, the increase in channel widths from 1962 to 1972 is due to aggradation potentially from large sediment discharge events. Then in 1992 the channel is significantly narrower and has a less steep cumulative width slope in Subreach B1. Subreaches B2 through B4 all have similar cumulative width slopes for all years. The significant changes in slope in Subreach B1 could be due to the channel aggrading from 1962 to 1972, and then degrading from 1972 to 2012. The discussed channel characteristics are further corroborated in **Section 1.1 and 3.2**.

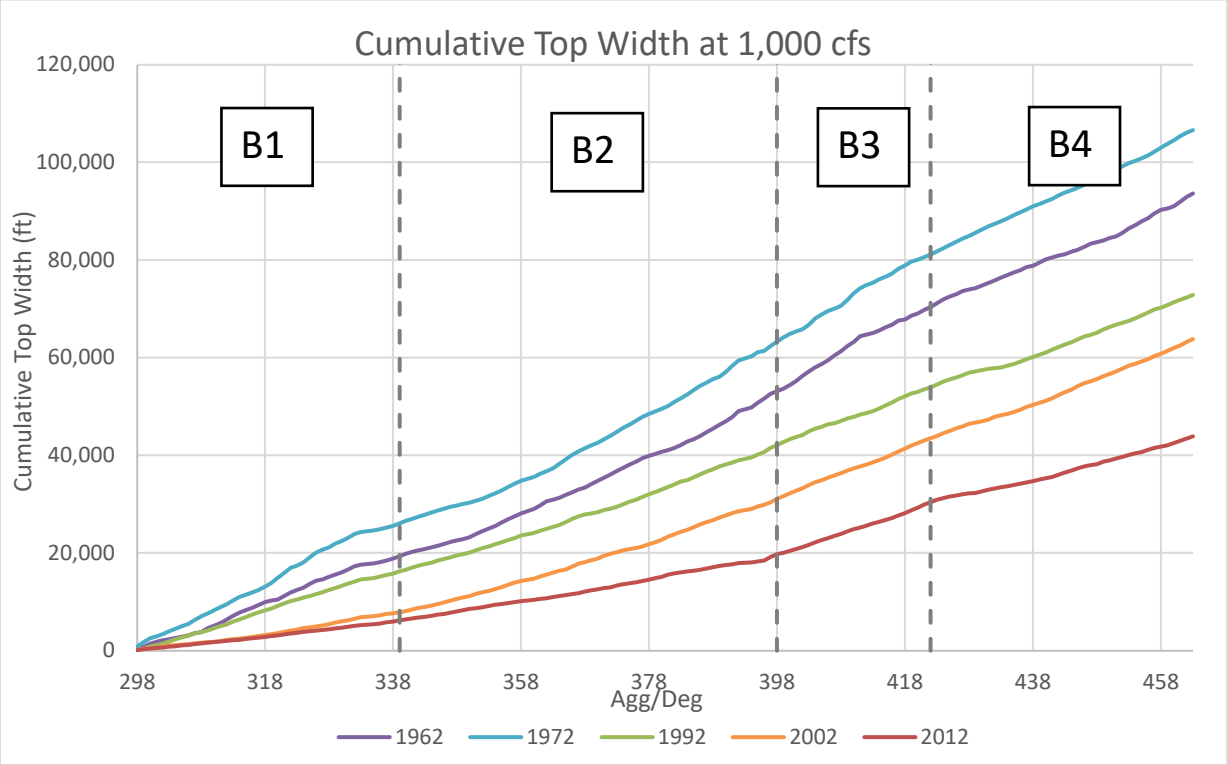

Figure 3-4 Cumulative top width at a discharge of 1,000 cfs.

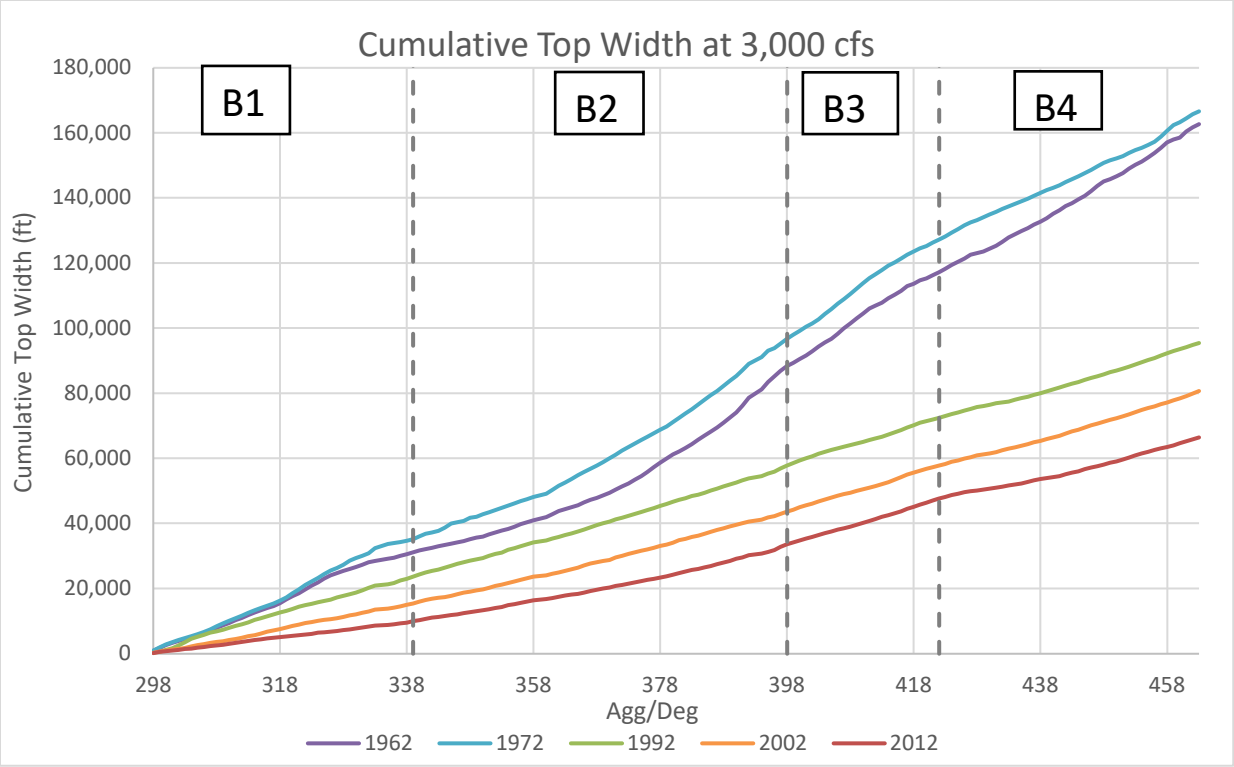

Figure 3-5 Cumulative top width at a discharge of 3,000 cfs.

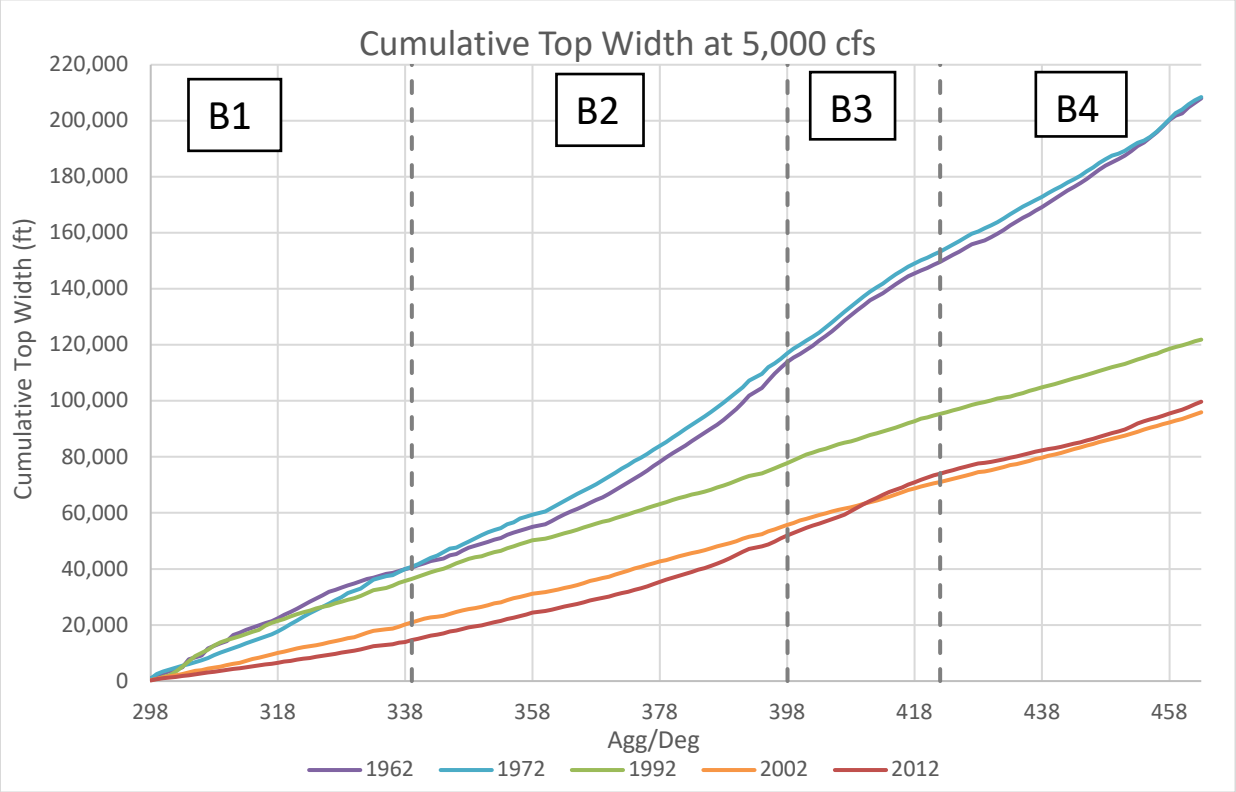

Figure 3-6 Cumulative top width at a discharge of 5,000 cfs.

The average top width for each subreach was also plotted for the years analyzed in **Figure 3-7** for discharges up to 5,000 cfs. From 1962 to 1972, the average top width for almost all of the subreaches increased. Then, from 1972 to 1992, there was a dramatic decrease in top width generally for all subreaches. The average top width for all reaches generally decreased between 1992 and 2012 showing narrowing of the channel. B1, B2, B3 and B4 show a large range of top width changes throughout the years of widening then narrowing of the channel.

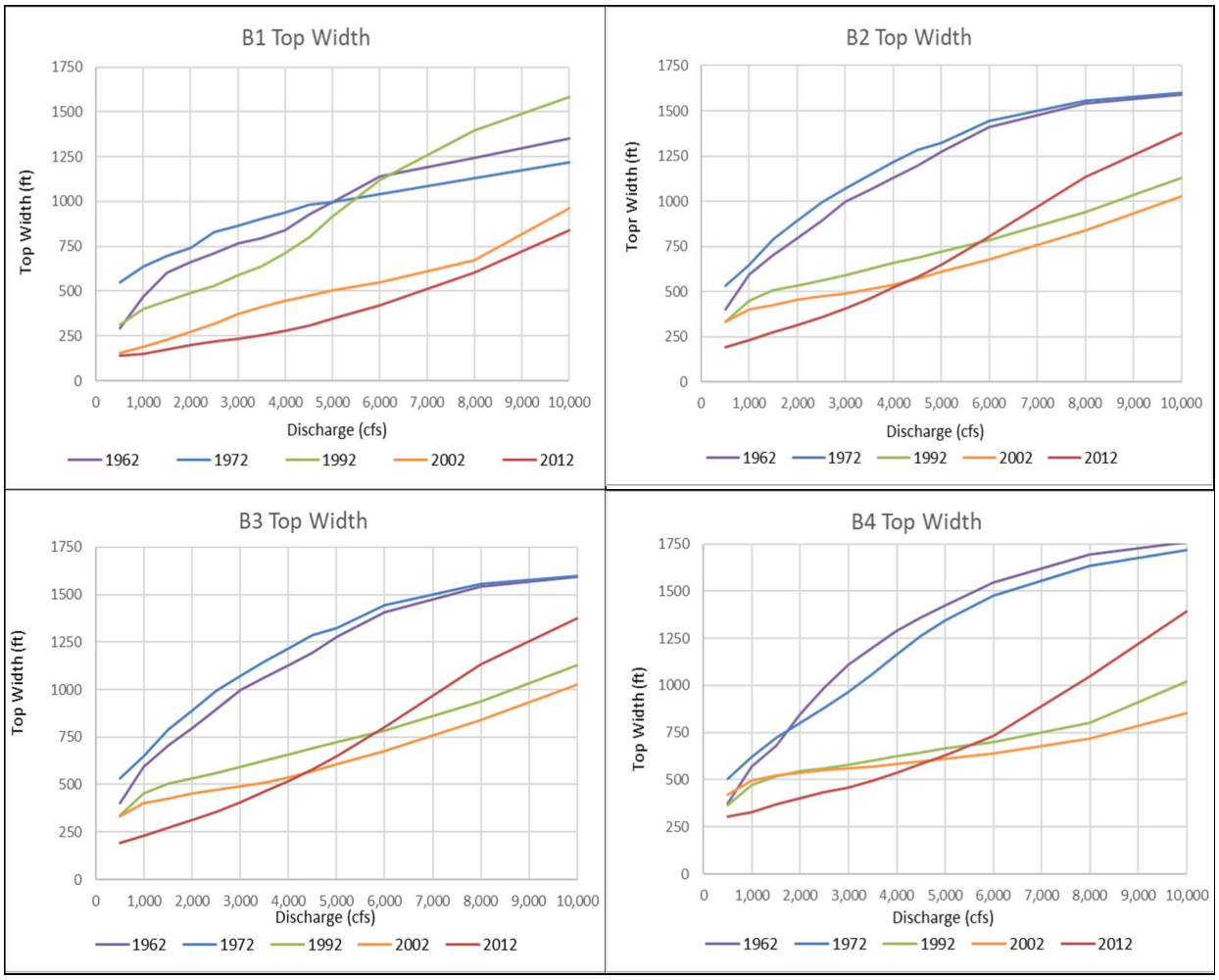

Figure 3-7 Average top width for B1 (top left), B2 (top right), B3 (bottom left), and B4 (bottom right) at discharges 500 to 5,000 cfs.

3.2 Bed Elevation

3.2.1 Channel Bed Slope

The minimum channel bed elevation is used to evaluate the change in the longitudinal profile of the Bernalillo Reach. The bed elevation of the channel comes from an estimate generated by HEC-RAS, which is based on the discharge and the water surface elevation on the day of the aerial photography. While the minimum channel elevation points may not be exact, the overall trends can still be identified throughout the Bernalillo Reach. The minimum channel elevation was obtained at each cross-section from the HEC-RAS geometry files to generate a plot of the bed elevation throughout the reach, as seen in **Figure 3-8**.

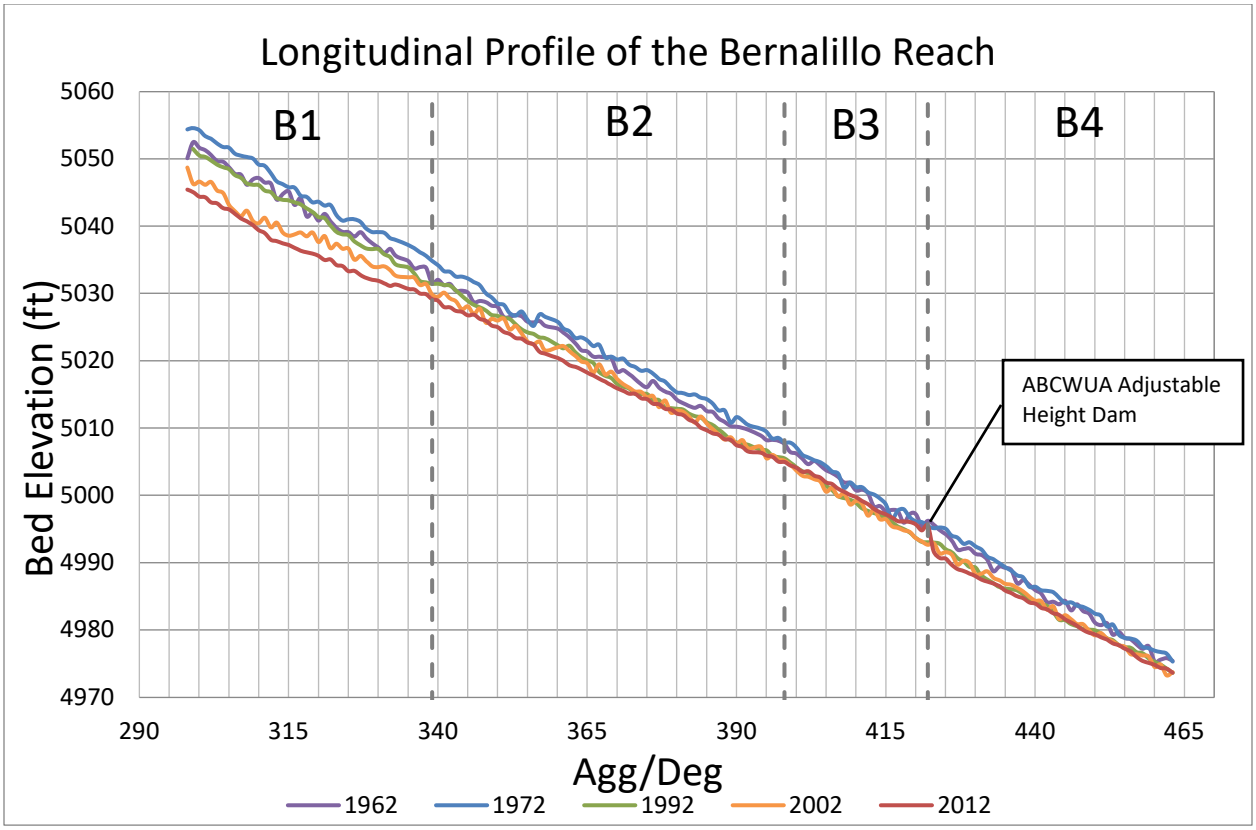

Figure 3-8 Longitudinal bed elevation profile.

The reach-averaged slope for the Bernalillo Reach has adjusted through-out the years as a result of incision, particularly in the upstream-most subreach (B1). Between 1962 and 1992 the slope for B1 remained relatively stable, ranging between 0.00091 and 0.00095. However, by 2002, the channel slope had flattened significantly to a slope of 0.00075. The slope for Subreach B3 remained consistent between 1962 and 2002, but experienced a significant drop between 2002 and 2012, from 0.00095 to 0.00082. This can be attributed to the ABCWUA Adjustable Height Dam that was constructed in 2005, which led to aggradation and a subsequent flattening of the slope behind the sill that primarily occurred in the B3 subreach. Other reaches generally saw a less significant changes in slope between 1962 and 2012, though they all show a downward trend. Refer to **Table 3-1** below for more detailed values of bed slope over the years for each subreach.

Table 3-1. Channel bed slope by subreach

Subreach	1962	1972	1992	2002	2012
B1	0.00091	0.00094	0.00095	0.00075	0.00076
B2	0.00086	0.00089	0.00092	0.00087	0.00084
B3	0.00094	0.00100	0.00097	0.00095	0.00082
B4	0.00099	0.00099	0.00093	0.00093	0.00090

3.2.2 Aggradation and Degradation by Subreach

In Subreaches B1, B2, and B4, a similar pattern of aggradation and degradation occurs throughout all years. Between the years 1962 to 1972, aggradation occurs through all subreaches. From 1972 to 2002, the river sees degradation in all subreaches. In 2005, the ABCWUA Adjustable Height Dam was constructed at the end of the B3 reach. The adjustable height dam raised the bed elevation and caused aggradation to occur upstream and degradation to occur downstream. It appears that the upstream aggradation is contained within the Subreach B3 and does not affect B1 and B2 subreaches. Upstream and downstream of B3, in Subreaches B1, B2, and B4, the degradation seen in the previous years has continued.

These trends can be observed and are analyzed in **Figure 3-9**, which shows the main channel aggradation and degradation of each subreach. The aggradation and degradation were found by first finding the average minimum channel elevation for each subreach and then subtracting the average bed elevation of the earlier year from the later year. A positive number indicates aggradation, and a negative number indicates degradation. This figure visualizes a direct comparison of trends in bed elevation between time intervals within individual subreaches. The period of 1962 to 1972 was the only period where there was aggradation throughout the entire Bernalillo Reach. This period was following by two periods, 1972 to 1992 and 1992 to 2002, of general degradation throughout the entire reach. There was some aggradation seen in B4 during the period of 1992 to 2002, but it is minor. The period of 2002 to 2012 were generally periods of degradation in all subreaches with exceptions in B3. The aggradation and degradation described in this section defines the channel slopes. For more detailed information on the channel slopes and how they have influenced the change in planform over time, see **Section 0**.

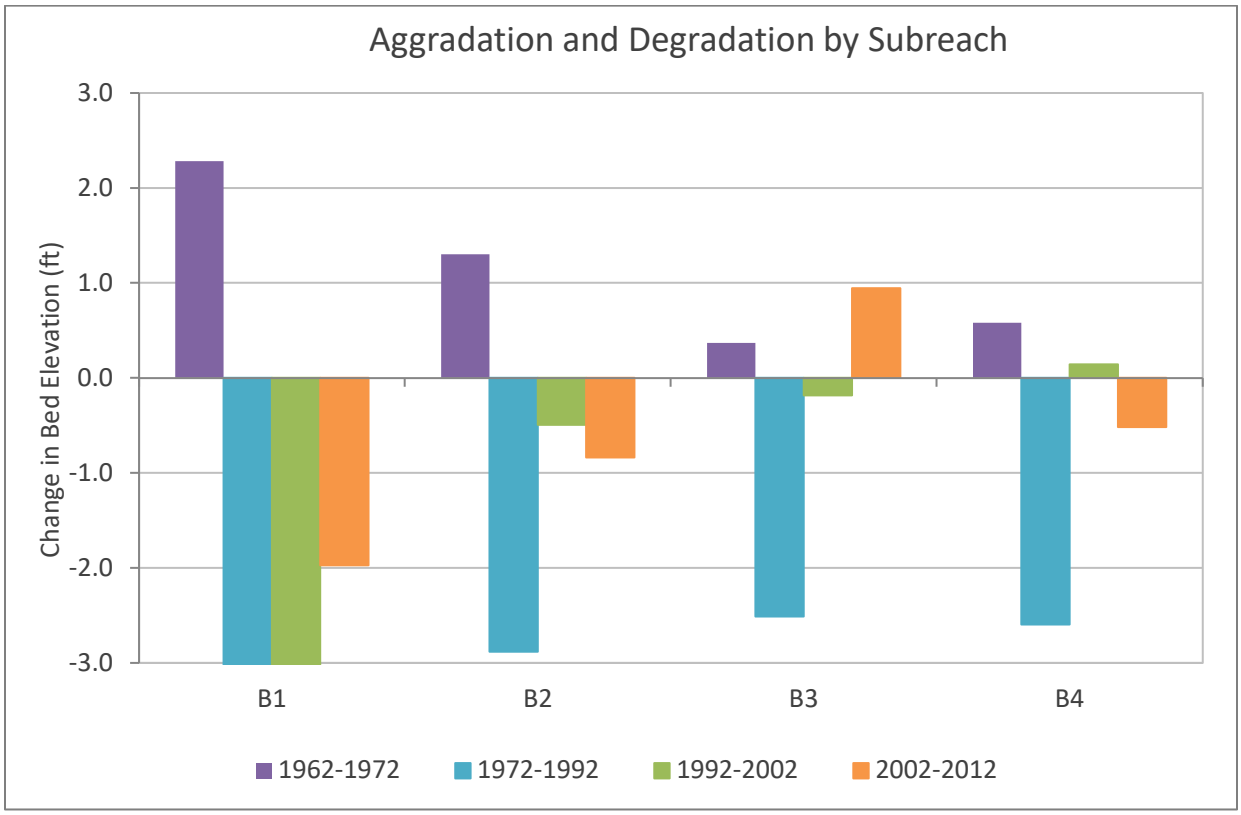

Figure 3-9 Aggradation and degradation by subreach

Figure 3-10 shows the evolution of the channel in the upstream-most subreach using a representative cross section at Agg/Deg 318 for the years 1962, 1972, 1992, 2002, and 2012.

In Subreach B1, the channel aggraded between 1962 and 1972. The 1962 cross-section shows a more clearly defined low flow channel that is approximately 150 feet wide and 2 foot deep. In contrast, the 1972 cross-section shows no clearly defined low flow channel. Between 1972 and 2012, the channel gradually degraded, narrowed, and became more clearly distinguishable from the floodplain. The channel dropped by 2 feet in the 20-year period between 1972 and 1992, by 4 feet in the 10-year period between 1992 and 2002, and another 3 feet in the 10-year period between 2002 and 2012, for a total of around 9 feet of degradation in 40 years at this cross-section. Subreach B1 shows the greatest drop in channel bed of the four subreaches within the Bernalillo Reach.

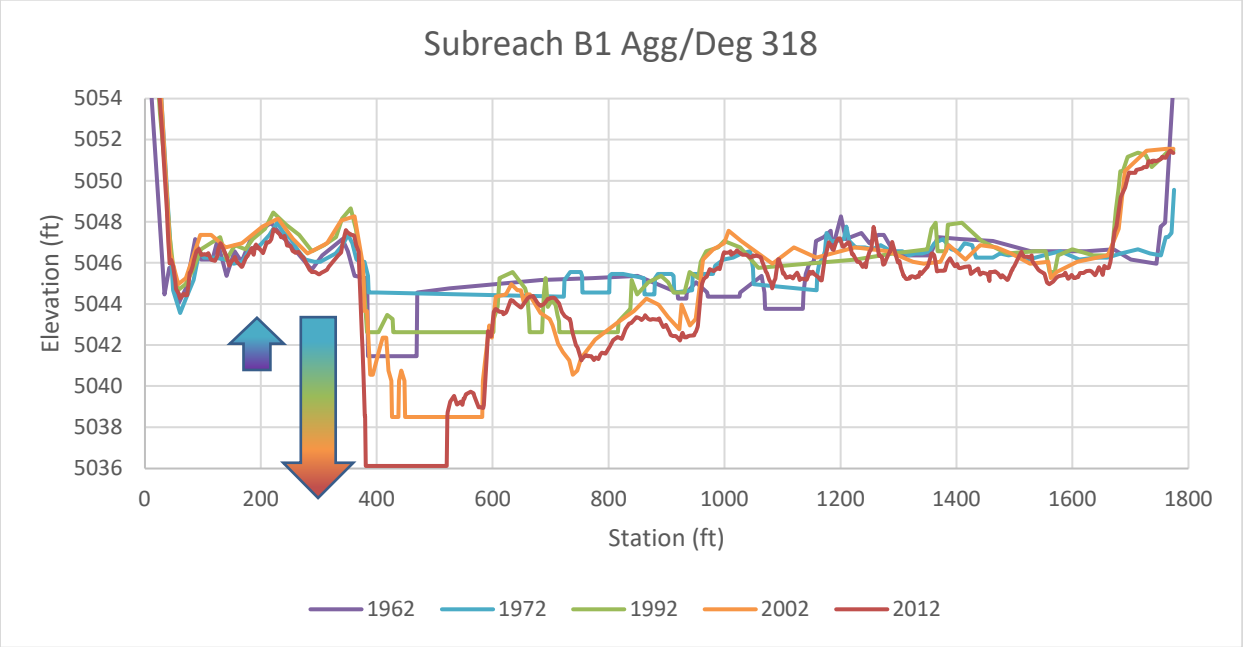

Figure 3-10 Subreach B1: Channel evolution of representative cross section Agg/Deg 318. Significant channel degradation and narrowing occurred between 1972 and 2012.

Figure 3-11 shows the evolution of the channel in Subreach B2 using a representative cross section at Agg/Deg 368 for the evaluated years.

In Subreach B2, the channel neither aggraded nor degraded between 1962 and 1972 at Agg/Deg 368. Between 1972 and 2012, the channel gradually degraded, narrowed, and became more clearly distinguishable from the floodplain. Approximately 3 feet of degradation occurred between 1972 and 1992. The channel and floodplain remain relatively static between 1992 and 2002, with approximately 2 feet aggradation filling a side-channel within the left floodplain (between stations 400 ft and 600 ft). Between 2002 and 2012, the right channel degrades by 1 foot and becomes more dominant, while the left channel (between stations 650 ft and 850 ft) begins to shrink. A total of 5 feet of degradation occurred in the 40 years between 1972 and 2012.

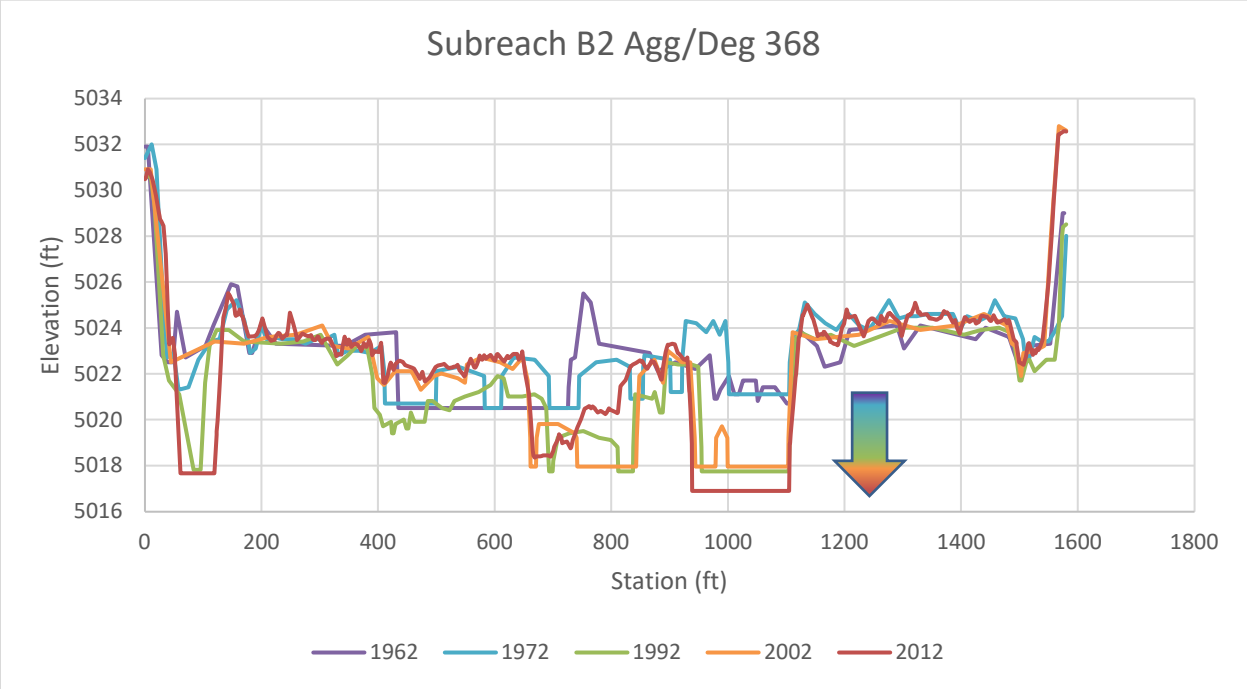

Figure 3-11 Subreach B2: Channel evolution of representative cross section Agg/Deg 368. Significant channel degradation and narrowing occurred between 1972 and 2012. Note: it appears that the side channel thalweg at station 100 ft was missed in the 2002 survey.

Figure 3-12 shows the evolution of the channel in Subreach B3 using a representative cross section at Agg/Deg 418 for the evaluated years.

In Subreach B3, the channel aggraded by 2 feet between 1962 and 1972 at Agg/Deg 368. The 1962 cross-section shows a more clearly defined low flow channel that is approximately 60 feet wide and 2 foot deep. In contrast, the 1972 cross-section shows no clearly defined low flow channel. Between 1972 and 1992, the channel degraded by 3 feet and became more clearly distinguishable from the floodplain. The channel and floodplain remain relatively static between 1992 and 2002, with approximately 1 foot of aggradation at the mid-channel island between stations 700 ft and 800 ft. Between 2002 and 2012, 1 foot of aggradation has occurred in the channel. This is due to construction of the ABCWUA Adjustable Height Dam in 2005, which is located approximately 2,000 feet downstream of Agg/Deg 418 at Agg/Deg 422. While approximately 2-3 feet of net degradation has occurred in this reach over the last 40 years, the channel width has not been impacted as significantly as the channel in Subreaches B1 and B2.

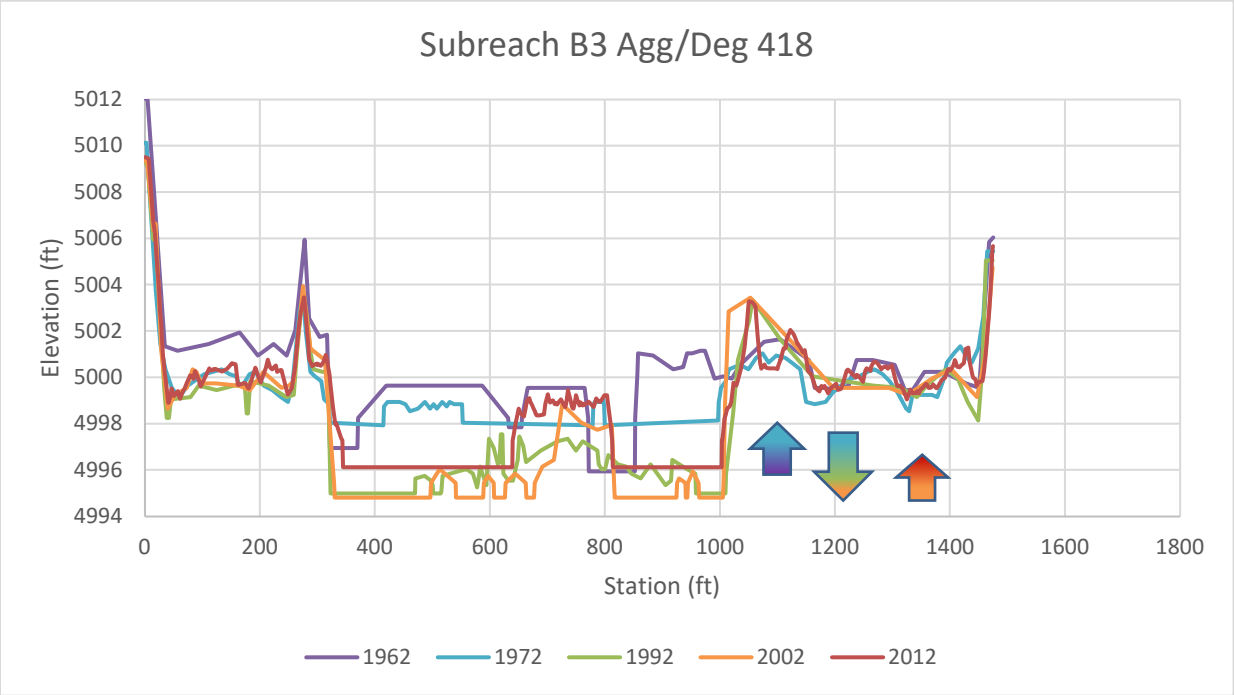

Figure 3-12 Subreach B3: Channel evolution of representative cross section Agg/Deg 418. Note less degradation and narrowing than seen in Subreaches B1 and B2.

Figure 3-13 shows the evolution of the channel in Subreach B4 using a representative cross section at Agg/Deg 442 for the evaluated years.

In Subreach B4, the channel aggraded between 1962 and 1972. The 1962 cross-section shows a more clearly defined low flow channel that is approximately 100 feet wide and 2 feet deep. In contrast, the 1972 cross-section shows a much wider channel with no clearly defined low flow channel. Between 1972 and 1992, the channel degraded by 2 feet and formed a deeper main channel (right) and side channel (left). Roughly 0.5 feet of degradation occurred between 1992 and 2002. Between 2002 and 2012 the channel did not degrade at Agg/Deg 442, but the left side channel, previously 100 feet wide in 2002, aggrades and becomes incorporated into the floodplain in 2012. Overall, a total of 3 feet of degradation occurred in the 40 years between 1972 and 2012.

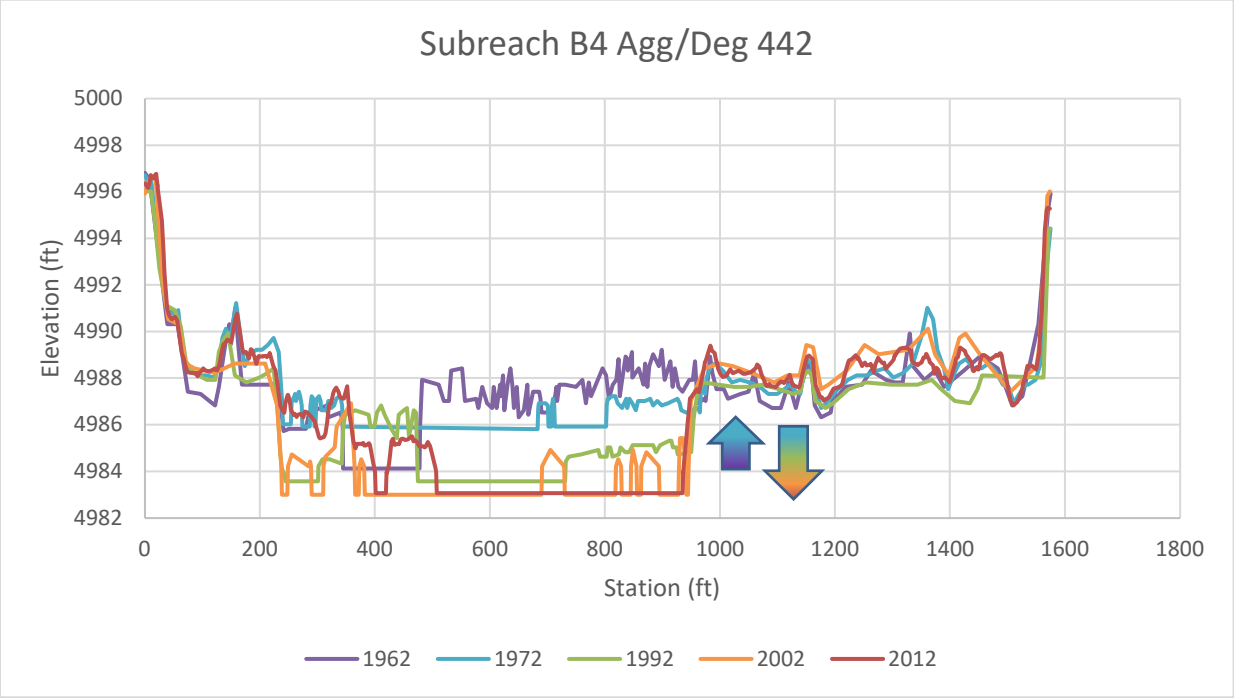

Figure 3-13 Subreach B4: Channel evolution of representative cross section Agg/Deg 442.

3.3 Bed Material

Bed material samples were collected at various location in the river reach denoted by Agg/Deg locations. There are bed material samples available for analysis of the Bernalillo Reach from the years 1990 to 2020. **Figure 3-14** shows the median grain diameter of each sample versus Agg/Deg location downstream of the Highway 550 Bridge (i.e., the start of the Bernalillo Reach).

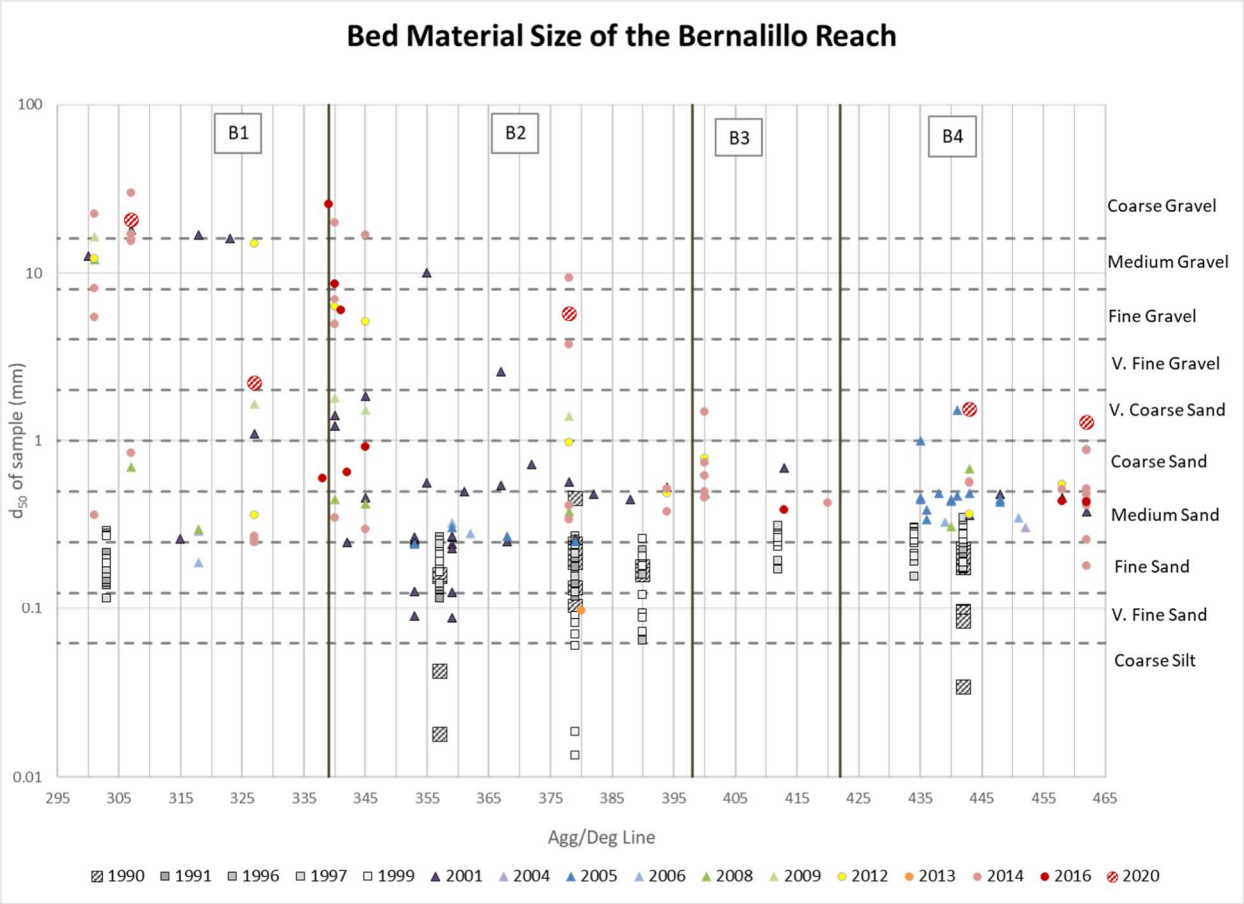

Figure 3-14 Median grain diameter size of samples taken throughout the Bernalillo Reach

Throughout the reach, the median diameter size of the samples typically varies between 0.0625 millimeter and 2 millimeters for the years in which data were collected. However, larger grain sizes, up to coarse gravel, were found in the upstream stream subreaches, B1 and B2, particularly in more recent years. **Figure 3-15** shows how the average bed material has changed over time in each subreach. In general, the has been a trend of the bed material coarsening over time. However, for a majority of the Bernalillo Reach, the grain size diameters correspond with classifications of fine sand to fine gravel, emphasizing the majority of Bernalillo Reach is a sand-bed river with some coarse silt and some gravels.

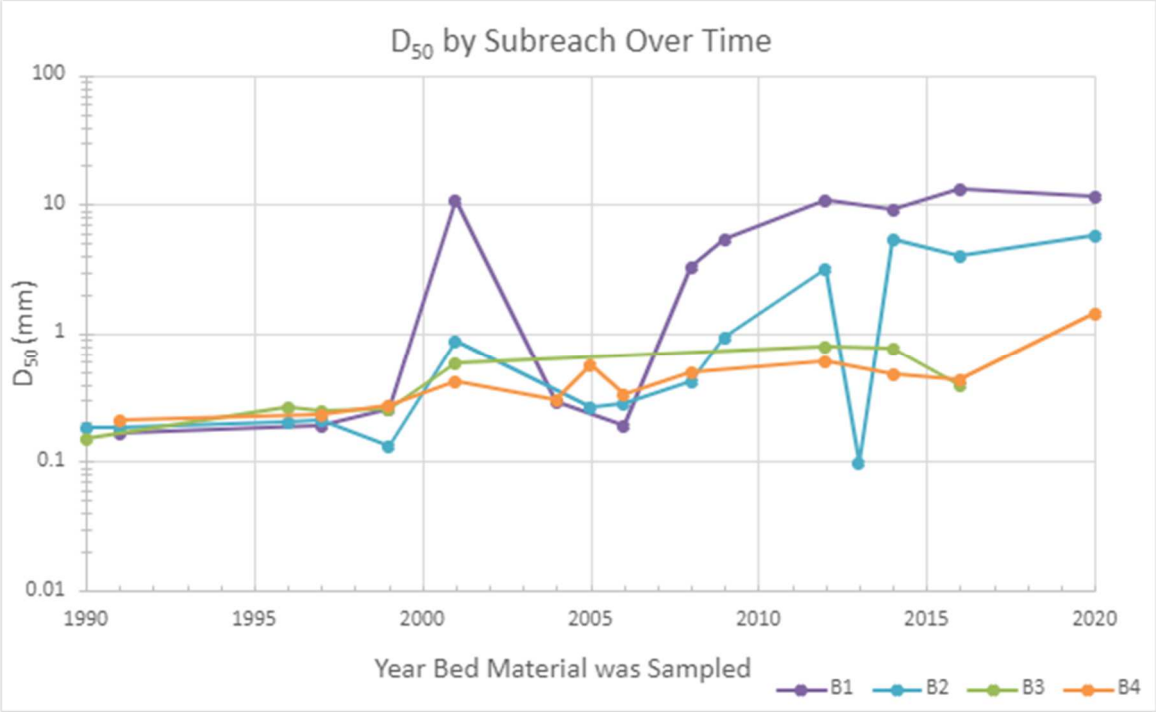

Figure 3-15 D50 change over time by subreach

3.4 Hydraulic Geometry

Flow depth, velocity, width, wetted perimeter of the main channel, and bed slope are obtained using HEC-RAS 6.2.0 with a discharge of 3,000 cfs and 5,000 cfs. 3,000 cfs was selected because it is the approximate bankfull condition of previously studied reaches on the Middle Rio Grande. 5,000 cfs was selected because it is the discharge that most likely represents bankfull conditions in the Bernalillo and Montaño reaches. Bankfull conditions are the maximum discharges with limited likelihood of overbanking (LaForge et al., 2019 and Yang et al., 2019). It is important to note that, for certain years analyzed, 3,000 cfs and 5,000 cfs does activate the flood plain and is not bankfull discharge. This can be seen in Habitat Maps found in **Appendix E**. A discharge of 3,000 cfs has a daily exceedance of around 9.9%. A 5,000 cfs discharge has a daily exceedance of 3.3%. A 1,000 cfs, has a daily exceedance probability around 33.8%. Since the 1,000 cfs flow is a more common flow in the subreach, it was also included in the hydraulic geometry analysis. For the plots of the hydraulic geometry variables, the values were averaged by subreach for each year analyzed.

The HEC-RAS results shown in **Figure 3-16** show a general trend that matches the trend seen in **Sections 3.1 and 1.1**. For all flows, there is generally an increase in wetted top width from 1962 to 1972, except in subreach B4 at 3,000 cfs and 5,000 cfs. From 1972 to 1992, there is a large decrease in wetted top width. From 1992 to 2012, there is generally a decrease in top width, except at 5,000 cfs. The fluctuation between 1962 to 1972 and 1972 to 2012 are a result of the aggradation and degradation trends that the Bernalillo Reach experienced during those time periods. The aggradation was most likely a result of large sediment discharge events between 1962 and 1972, as seen in **Section 2.3**.

Because top width and hydraulic depth are typically inversely related for the same discharge, it is expected that the change in hydraulic depth results over time will have the opposite trend that the change in wetted top width results showed from subreach to subreach. **Figure 3-17** shows the HEC-RAS calculated hydraulic depths (area over top width) at discharges of 1,000 cfs, 3,000 cfs, and 5,000 cfs. In general, the HEC-RAS

calculated results are similar to what is expected at 1,000 cfs. However, at 3,000 cfs and 5,000 cfs, the hydraulic depth in B1 should be higher in 1962 than in 1972 because the river is wider in 1972 than 1962.

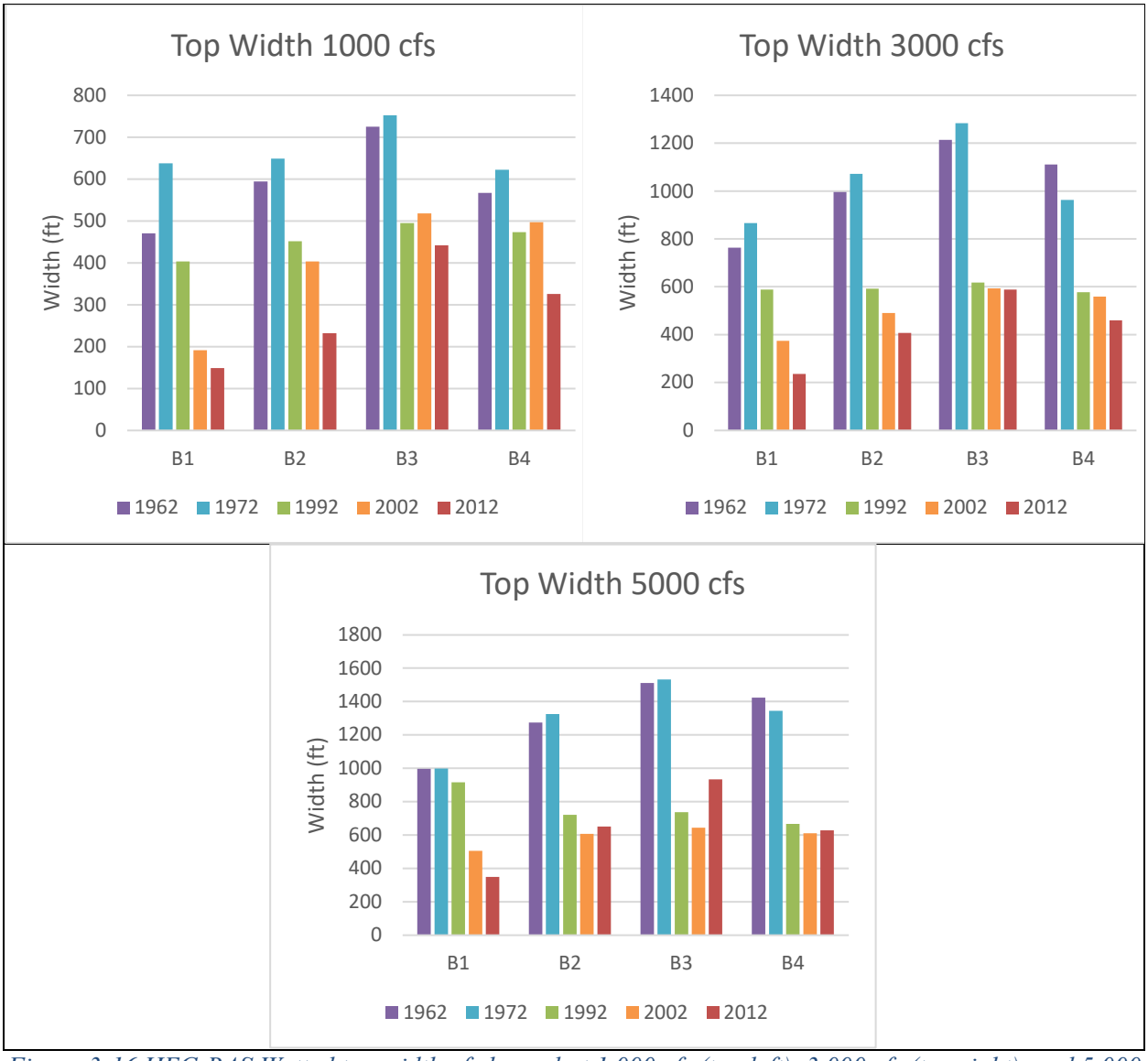

Figure 3-16 HEC-RAS Wetted top width of channel at 1,000 cfs (top left), 3,000 cfs (top right), and 5,000 cfs (bottom middle)

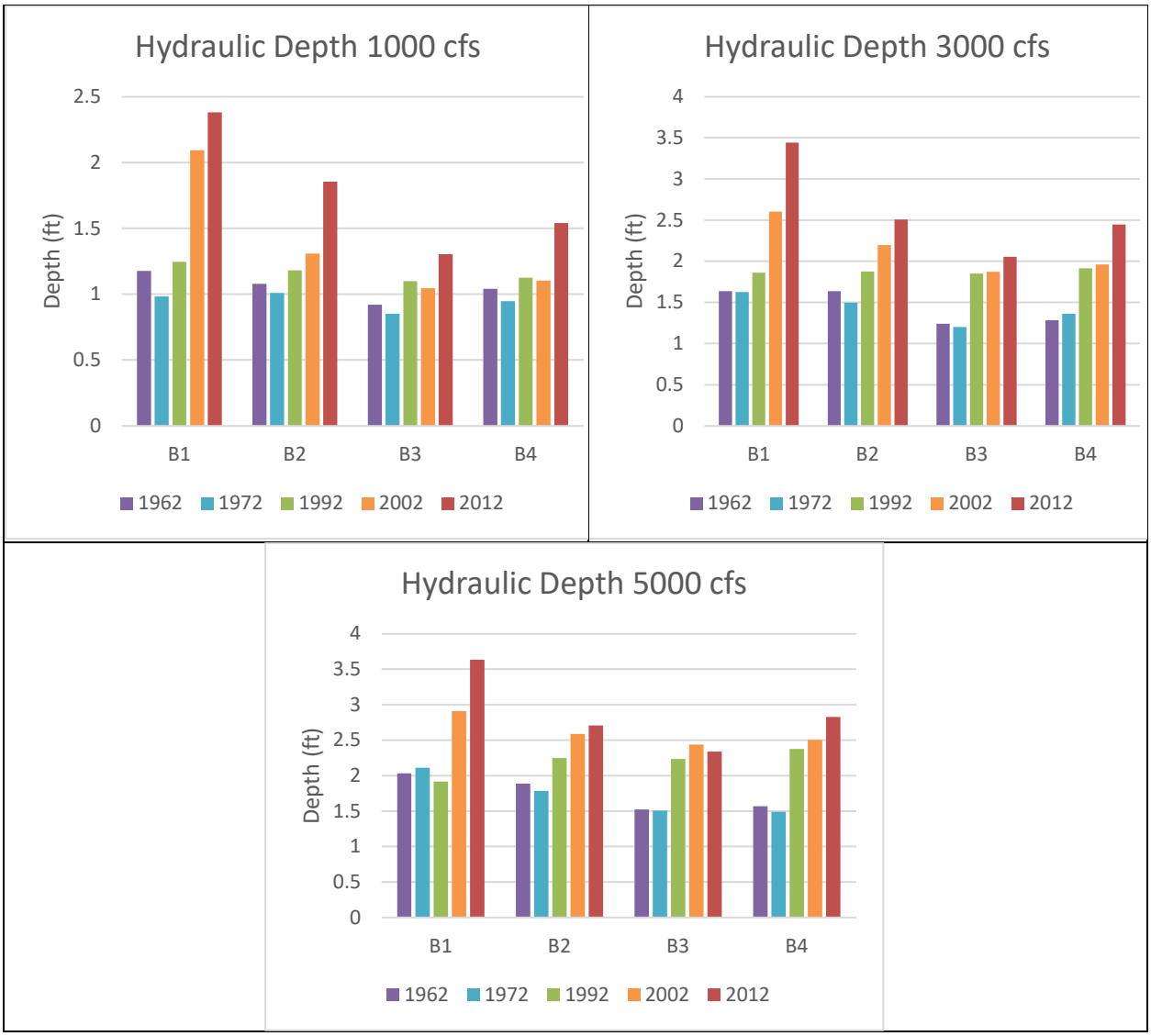

Figure 3-17 HEC-RAS Hydraulic depth at 1,000 cfs (top left), 3,000 cfs (top right), and 5,000 cfs(bottom)

The results for the wetted perimeter of the main channel were obtained by using HEC-RAS and is represented by **Figure 3-18.** Generally, the main channel wetted perimeter follows a similar trend to the top width. All of the subreaches generally show a steady decline in main channel wetted perimeter throughout the time interval analyzed. There are exceptions in some of the subreaches where the is an increase in wetted perimeter from 1962 to 1972, following by a decrease for the remaining periods. This matches the trends seen for the wetted top widths in **Section 3.1** and is due to the aggradation and degradation trends shown in **Section 3.2**. It is important to note that the wetted perimeter is confined to the main channel and shows how the main channel has changed over time.

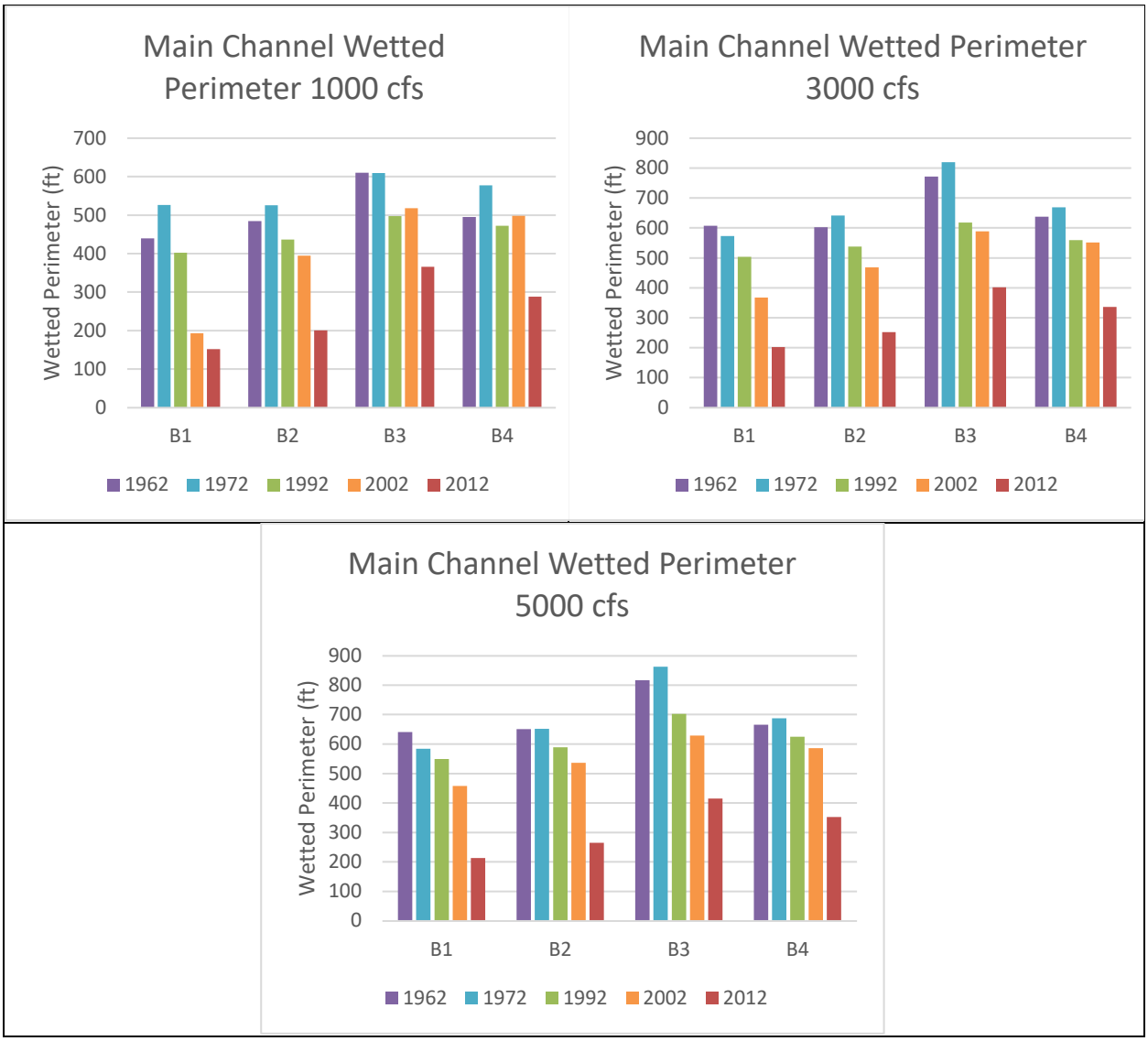

Figure 3-18 HEC-RAS Main Channel Wetted Perimeter at 1,000 cfs (top left), 3,000 cfs (top right), and 5,000 cfs (bottom middle).

The bed slope was calculated by taking the slope of a linear fitted line for each subreach. The bed slope of the linear fitted line is shown in in **Section 0** and **Figure 3-19** below. The left bar chart in **Figure 3-19** shows a water surface slope calculated off of the water surface profile at 500 cfs for each subreach, while the right bar chart in **Figure 3-19** shows the bed slope for each subreach. This slope has fluctuated but has stayed relatively stable, with a bed slope of around 0.0008 over the time interval of 1962 to 2012. Subreach B1 ultimately both dropped in bed slope from around 0.0009 to 0.00075 between 1992 and 2002. In 2005, the ABCWUA Adjustable Height Dam was constructed at the end of the B3 reach. Due to the aggradation and degradation that occurred upstream and downstream of the dam, respectively, the bed slopes between 2002 and 2012 decreased in B2, B3, and B4.

Changes in flow depth and slope often have an inverse relationship. In general, as slope decreases the flow depth increases. This trend can be seen in the Bernalillo Reach, through all subreaches. As seen in **Figure 3-17,** the hydraulic depth increases significantly from 1992 to 2012. The inverse trend in seen below in **Figure 3-19**, where the slope has decreased from 1992 to 2012. It is importat to note that these subreaches

each have there own characteristics and trends where between 1962 and 2012. Those trends are further discussed in **Section 3.2** and **Section 0**.

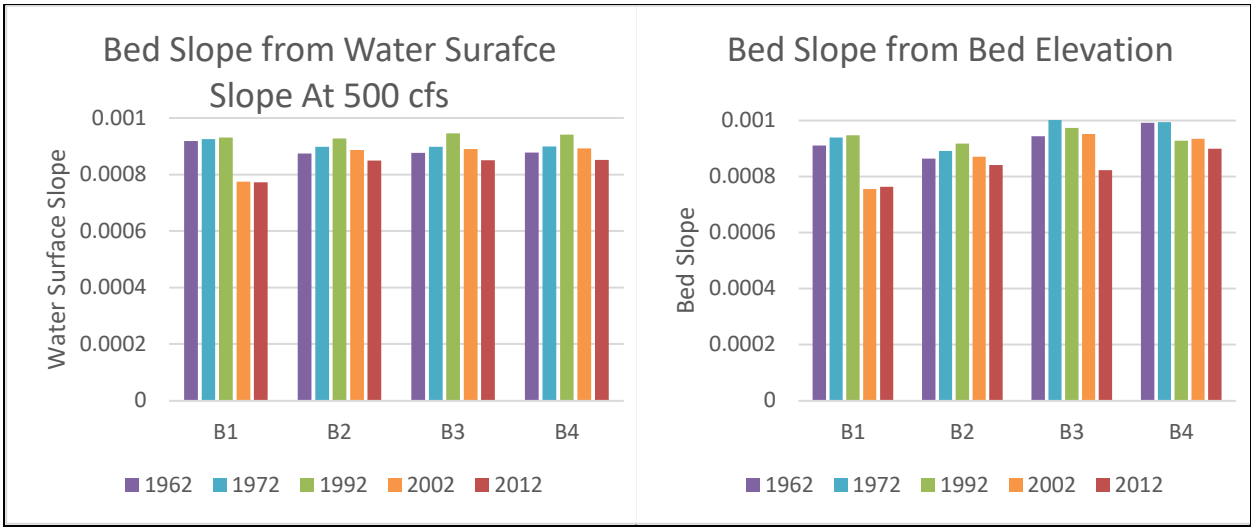

Figure 3-19 Water surface slope at 500 cfs (left) and channel bed slope (right).

3.5 Channel Response Models

The Julien and Wargadalam (JW) equations were used to predict the downstream hydraulic geometry of rivers (Julien and Wargadalam, 1995). These equations were based on empirical analysis of over 700 single-threaded rivers and channels, and predicted the width and depth likely to result from a given discharge, grain size and slope:

$$h = 0.2Q^{\frac{2}{6m+5}}D_s^{\frac{6m}{6m+5}}S^{\frac{-1}{6m+5}}$$

$$W = 1.33Q^{\frac{4m+2}{6m+5}}D_s^{\frac{-4m}{6m+5}}S^{\frac{-1-2m}{6m+5}}$$

Where $m = 1/\left[2.3\log\left(\frac{2h}{D_s}\right)\right]$, h is the flow depth, W is the channel width, Q is the flow discharge, D_s is the median grain size, and S is the slope. A discharge of 3,000 cfs, the same discharge as in the previous HEC-RAS analysis, was used. The values for slope and grain size were obtained from **Section 3.4/0** and **Section 3.3**, respectively. Due to missing grain size data for every year, the median D_{50} with a (*) symbol indicates data that was that does not match the specified year in **Table 3-2**. If data was unavailable for the specific year presented in Table 1 it was attempted to keep the data used for the median D_{50} of 1992 within the 1990s, median D_{50} of 2001 within the 2000s, and median D_{50} of 2012 within the 2010s. The results are compared to the observed active channel widths (from the GIS analysis of the digitized planforms) in **Table 3-2** and plotted in **Figure 3-20**. The percent difference was calculated as:

$$\text{Percent Difference} = 100 * \left(\frac{\text{predicted width} - \text{observed width}}{\text{observed width}}\right)$$

Table 3-2 Julien-Wargadalam channel width prediction

Year	Subreach	Ds (mm)	Slope	Predicted Width (ft)	Observed Width (ft)	Precent Difference
1992	B1	0.168*	0.0010	255	493	-48%
	B2	0.182*	0.0009	257	578	-56%
	B3	0.149*	0.0010	254	668	-62%
	B4	0.211*	0.0009	257	579	-56%
2002	B1	10.830*	0.0008	284	379	-25%
	B2	0.869*	0.0009	264	356	-26%
	B3	0.590*	0.0010	258	473	-45%
	B4	0.420*	0.0009	258	489	-47%
2012	B1	10.822	0.0008	283	342	-17%
	B2	3.206	0.0008	271	329	-18%
	B3	0.789	0.0008	267	439	-39%
	B4	0.602	0.0009	261	448	-42%

*See Table B-1 in Appendix B for specific years used for Ds values.

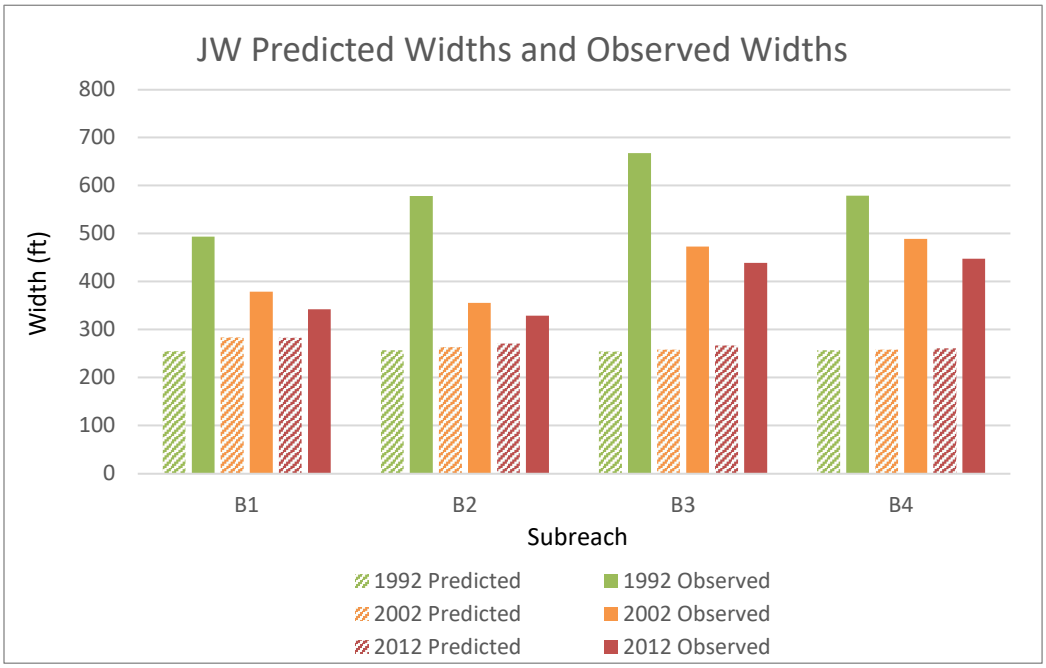

Figure 3-20 Julien and Wargadalam predicted widths and observed widths of the channel

The predicted JW widths are narrower than the observed widths for all subreaches in the Bernalillo Reach. The JW equations predict that the channel width for all subreaches should be narrower, 250 to 285 feet, than observed. When calculating the predicted width, the bankfull discharge was used, when in reality varying discharges would be occurring in the river. This could lead to the greater variability in the observed width values. It is important to note that the JW equations represent a river whose morphodynamics are in equilibrium. The morphodynamic equilibrium is assuming there would be no aggradation nor degradation occurring. The Bernalillo Reach has been going through cycles of aggradation and degradation showing that the river is not in equilibrium and is continuously changing.

4 HEC-RAS Modeling for Silvery Minnow Habitat

The Rio Grande Silvery Minnow (RGSM or silvery minnow) is an endangered fish species that is native to the Middle Rio Grande. Currently, it occupies only about seven percent of its historical range (U.S. Fish and Wildlife Service, 2010). It was listed on the Endangered Species List by the US Fish and Wildlife Service in 1994.

One of the most important aspects of silvery minnow habitat is the connection of the main channel to the floodplain. Spawning is stimulated by peak flows in late April to early June. These flows should create shallow water conditions on the floodplains, which is ideal nursery habitat for the silvery minnow (Mortensen et al., 2019). Silvery minnows require specific velocity and depth ranges depending on the life stage that the fish is in. **Table 4-1** outlines these velocity and depth guidelines. Fish population counts are available prior to 1993 to the present. Therefore, analysis of silvery minnow habitat will not begin prior to 1992.

Table 4-1 Rio Grande Silvery Minnow habitat velocity and depth range requirements (from Mortensen et al., 2019)

	Velocity (cm/s)	Velocity (ft/s)	Depth (cm)	Depth (ft)
Adult Habitat	<40	<1.31	>5 and <60	>0.16 and <1.97
Juvenile Habitat	<30	<0.98	>1 and <50	>0.03 and <1.64
Larvae Habitat	<5	<0.16	<15	<0.49

4.1 Modeling Data and Background

The data available to develop these models varies year by year. Cross section geometry was available for the years 1962, 1972, 1992, 2002, and 2012. In 2012, additional LiDAR data of the floodplain was available, which allowed the development of a terrain for RAS-Mapper. Therefore, RAS-Mapper was used in 2012 only, while comparisons across years are done using 1-D techniques.

4.1.1 Levee and Ineffective Flow Analysis

HEC-RAS distributes water within the channel by filling each available cross section from the lowest elevation upwards. Much of the MRG is either perched or has been altered with levees, so this can lead to inaccurate predictions of the flow distribution within the cross sections (overpredicting water in the floodplains), therefore, overpredicting hydraulically suitable habitat.

Initial analysis of the years 1962 – 2012 showed that the years 1962, 1972, and 2012 were most likely overpredicting the amount of floodplain inundation in the two upstream subreaches. The initial no levee HEC-RAS top width results were compared with the width defined by vegetation from **Section 1.1** and cross checked with aerial imagery to determine that some areas of disconnected flow would not naturally occur due to bridge crossings, tributary outlets, levees, etc. Computational levees were used in HEC-RAS geometries for 1962 and 1972 to keep the water contained in the channel until bankfull is reached. Most of the levee adjustments occurred along the right floodplain in the B1 and B2 subreaches where the floodplain is wide. At this location, the newly constructed Highway 550 and a new ditch connection to the river effectively cut off a large, wide side channel along the right bank. Without levee placement, this resulted in unrealistic predictions of wide, shallow flow and model results that were likely not representative of actual conditions at the site. The computational levees were either placed at the high points along the bank closest to the channel or at an elevation of a high point in the cross section upstream where there isn't a flow path connecting the two in the aerials.

By 2012, the channel had narrowed and deepened, which disconnected many of the side channels at lower flood events. However, since a 1-D HEC-RAS model fills from the bottom up, sections of the side channels were beginning to fill at lower flood events despite not being connected to the main channel upstream or downstream. To resolve this, ineffective flow areas were added along the floodplains. The elevations of ineffective areas were generally set at elevations that allowed for flow conveyance when flow was connected but prevented flow conveyance at lower flow events when these areas were not connected upstream to downstream.

4.2 Width Slices Methodology

Without a terrain for 1962-2002, additional methods had to be considered to determine a metric of fish habitat in area per distance and in length of river. HEC-RAS has the capability to perform a flow distribution analysis to calculate the laterally varying velocities, discharges, and depths throughout a cross section as described in chapter 4 of the HEC-RAS Hydraulic Reference Manual (US Army Corps of Engineers, 2016). HEC-RAS allows each cross-section to be divided into 45 slices. Although other reaches of the RGSM relies heavily on floodplains for habitat (due to higher velocities and depths in the main channel), the Bernalillo Reach main channel contains more variability than the floodplains contain, so 10 width slices were assigned in each floodplain and 25 width slices were assigned in the main channel. An example of the flow distribution in a cross-section is shown in **Figure 4-1**. The velocity and depth of each slice were analyzed to determine the total width at each agg/deg line that meets the RGSM larval, juvenile, and adult criteria. Because the agg/deg lines are spaced approximately 500 feet apart, the hydraulically suitable widths were multiplied by 500 feet to obtain an area of hydraulically suitable habitat per length of river.

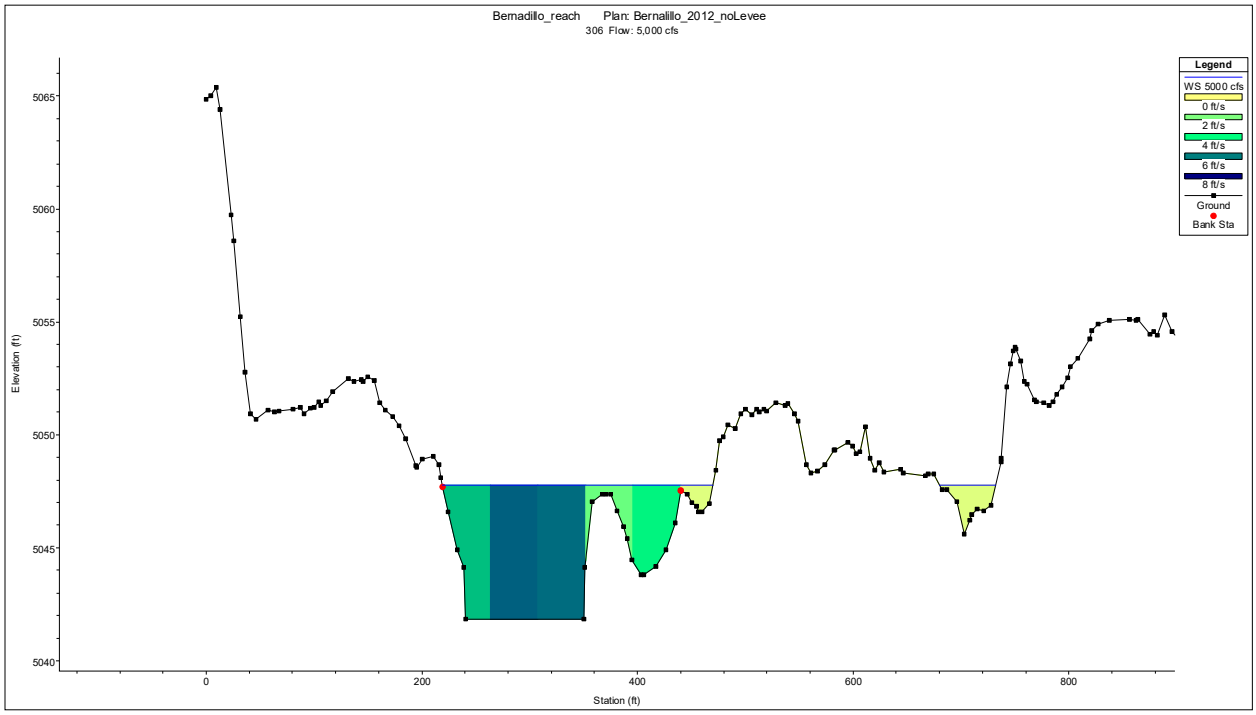

Figure 4-1 Cross-section with flow distribution from HEC-RAS with 20 vertical slices in the floodplains and 25 vertical slices in the main channel. The yellow and green slices are small enough that the discrete color changes look more like a gradient.

4.3 Width Slices Habitat Results

The width slices method was first used to analyze the habitat availability throughout the Bernalillo Reach at a reach scale for the years of 1962, 1972, 1992, 2002, and 2012. For the discharges at which the water is contained in the main channel, there is less habitat availability. In general, when the discharge increases and the water can spill out onto the floodplains, there is suddenly an increase in area where the depth and velocity criteria are met, as shown in **Figure 4-2 to Figure 4-4** below. For the years 1992 – 2012, increased flow in the channel resulted in an increase in habitat availability. For the earlier years, there is a steady increase in habitat availability with flow until 8,000 cfs, then the availability decreases as the depths and velocity exceed the Rio Grande Silvery Minnow habitat velocity and depth range requirements.

Throughout the Bernalillo Reach, the results follow a similar trend for larvae, juvenile, and adult stage habitat. There was more habitat availability during the years of 1962 and 1972. There is a dramatic decrease in habitat between 1972 and 1992, which corresponds to the degradation and the decrease in active top width that the reach experiences during that time frame. See **Section 3** for more information on the change in channel characteristics between time periods. There is limited available larvae habitat in comparison to the juvenile and adult available habitats, although it slightly increases as the flow increases through the channel and more of the floodplain is activated. The Bernalillo Reach generally shows less overall habitat availability compared with other reaches of the MRG. As a basis for comparison, the Bosque reach shows roughly 2-4 times more larval habitat and 4-6 times more juvenile and adult habitat at flows between 2,500 cfs and 5,000 cfs than the Bernalillo Reach in 2012 (Scheid et al. 2022). For the Bernalillo Reach, the main channel provides more opportunities for habitat than previously studied reaches (Sperry 2022 and Scheid et al. 2022). This could be due to the relatively consistent main channel hydraulic depths seen throughout the subreaches, as well as a larger number of mid-channel bars that provide habitat as they are inundated. As seen in **Figure 3-17** in **Section 3.4**, as flow increases, the hydraulic depths do not change by a large amount, so the there is more consistent habitat available.

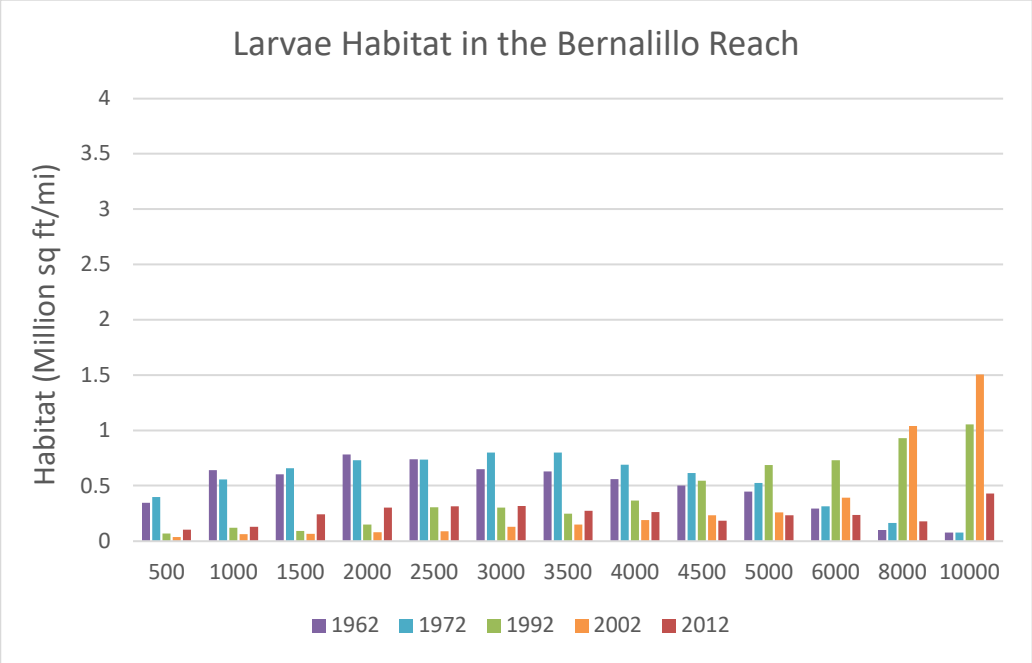

Figure 4-2 Larval RGSM habitat availability throughout the Bernalillo Reach

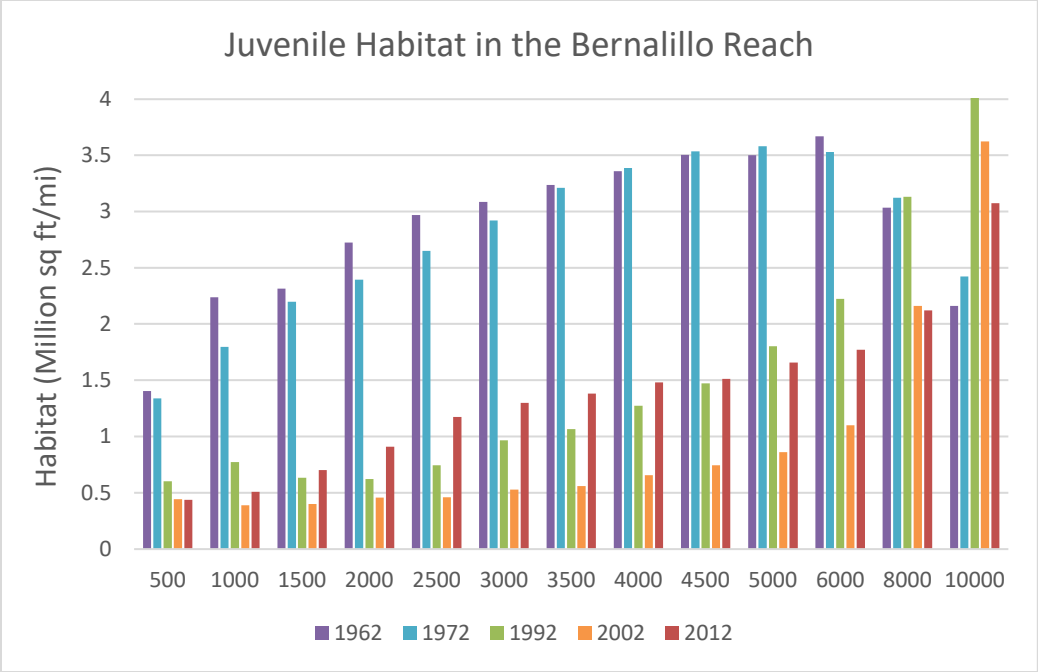

Figure 4-3 Juvenile RGSM habitat availability throughout the Bernalillo Reach

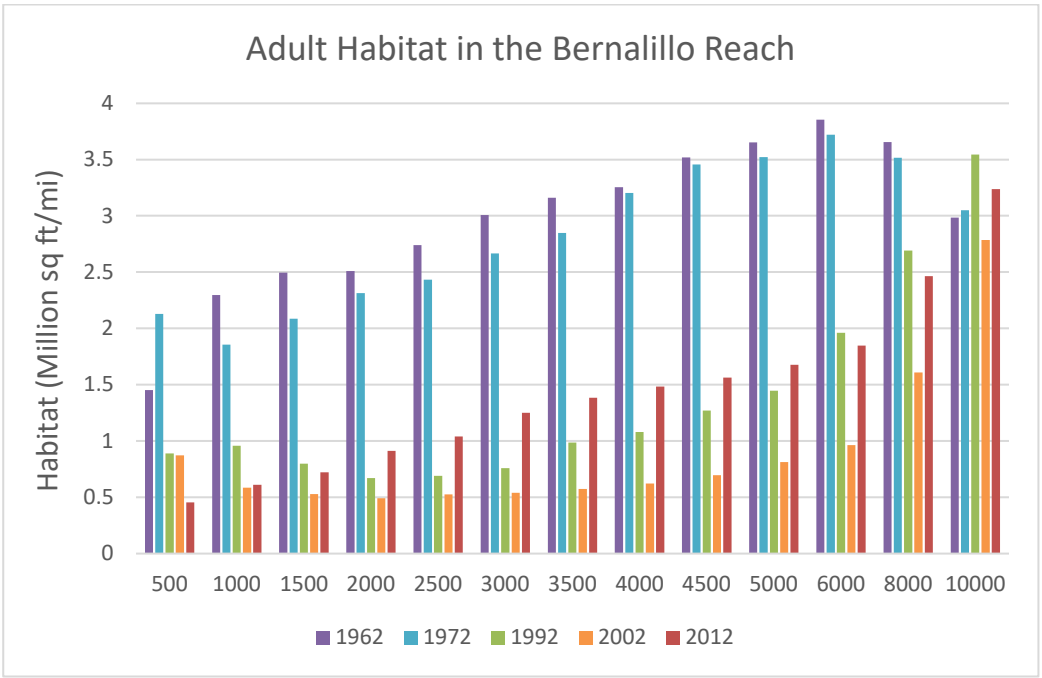

Figure 4-4 Adult RGSM habitat availability throughout the Bernalillo Reach

The width slices method was also used to analyze the habitat availability throughout the Bernalillo Reach at a subreach level. Stacked habitat bar charts were created to portray the spatial variation of hydraulically suitable habitat of the RGSM throughout the Bernalillo Reach. The bar charts display the width of habitat at different discharges for 2012. To convert the hydraulically suitable habitat to an area, these values would

be multiplied by 500 ft, which is approximate the distance between each agg/deg line. **Figure 4-5** shows the 2012 habitat availability from 500 cfs to 10,000 cfs for Subreaches B1 through B4.

Based on this method, applied to the 2012 data, Subreach B3 consistently had the most hydraulic suitable habitat for larvae, juvenile, and adult life stages at the discharges lower than 1500 cfs. Above 1500cfs, Subreaches B2 and B3 had the most juvenile and adult hydraulic suitable habitat and had similar magnitudes while B1 and B2 offered more larva habitat during those flows. At 10,000 cfs, B4 had a similar magnitude as B2 and B3 for the juvenile and adult life stages. For the larvae, B1 spiked to the highest magnitude at 10,000 cfs.

The channel form of B2 and B3 may be more efficient at reaching the RGSM's habitat criteria of velocity and flow depth for the juvenile and adult life stages, while B1 and B2 may be for efficient for the larvae. As seen in **Section 0**, B1 and B2 generally have wider floodplains, so this indicates that the floodplains are most suitable for the larvae while the channels might be more suitable for the juveniles and adults. Additional bar charts for all subreaches and life stages are located in **Appendix D**.

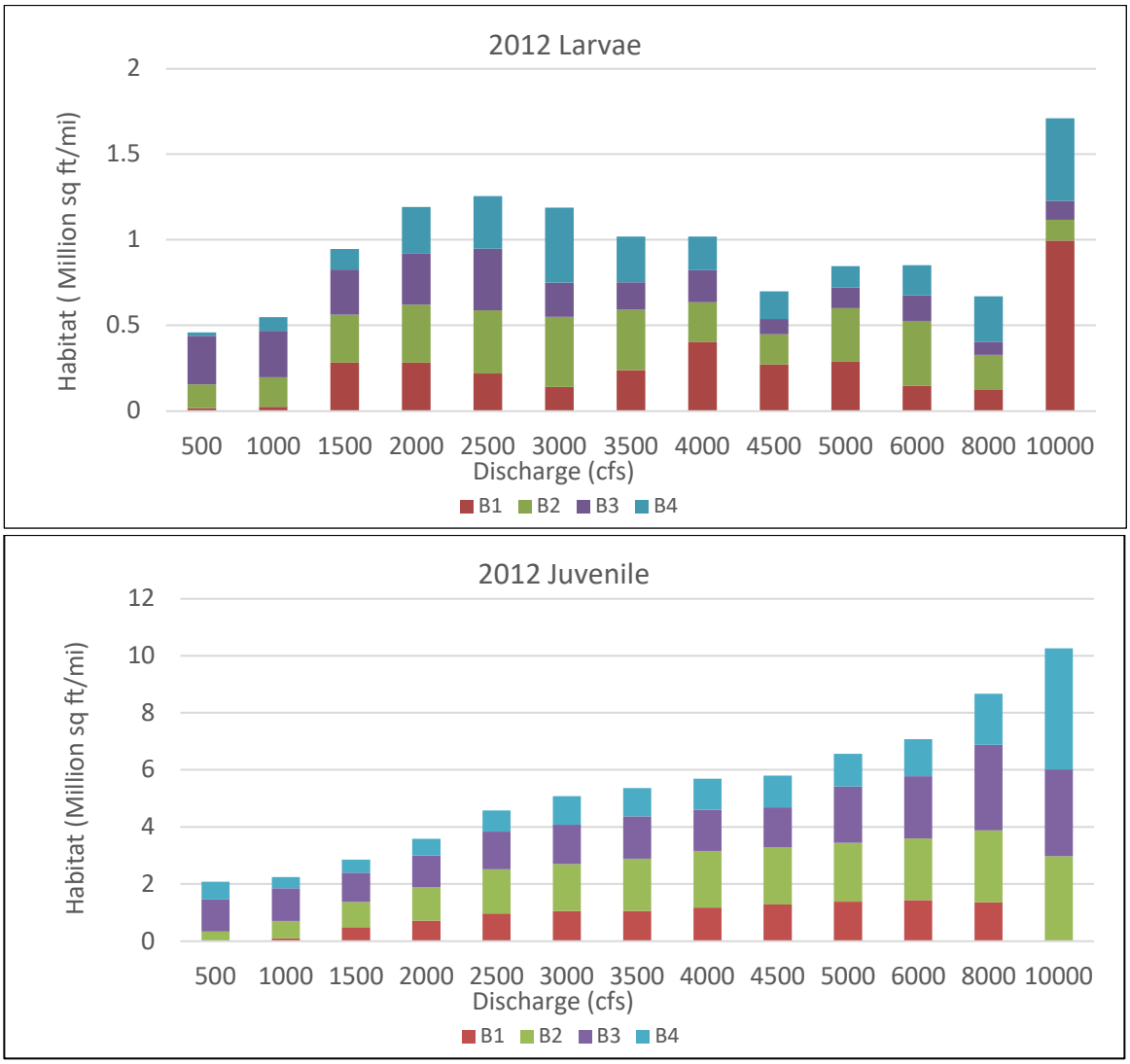

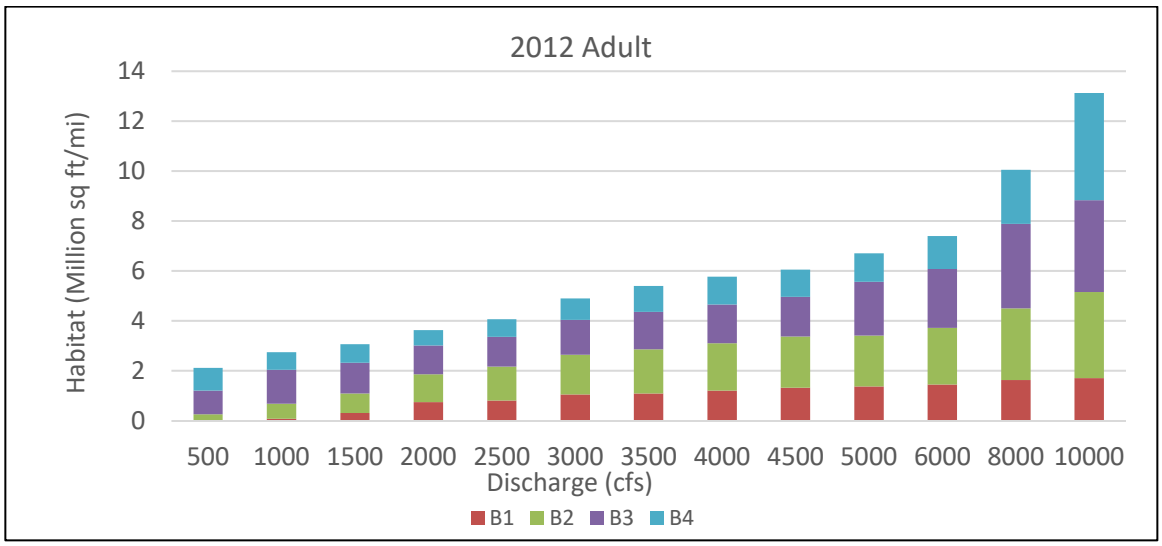

Figure 4-5 Stacked habitat charts at different scales to display spatial variations of habitat throughout the Bernalillo Reach in 2012

4.4 RAS-Mapper Methodology

By using RAS-Mapper, the goal was to transform the 1-D habitat estimates into pseudo two-dimensional (2-D) results. RAS-Mapper overlays the water onto a prescribed terrain and interpolates the water surface elevation to create an estimate of the location of water inundation, which can then be used to predict locations of hydraulically suitable habitat for the Rio Grande Silvery Minnow (RGSM).

The HEC-RAS geometry data that was necessary for the RAS-Mapper analysis (geo-referenced cross-sections and a LiDAR surface to generate a terrain) was available only for the year 2012. Therefore, only 2012 results were processed in RAS-Mapper. The original 2012 LiDAR data was used to develop a raster on ArcGIS Pro software (intellectual property of ESRI), which could be imported as a terrain from RAS-Mapper. The RAS-Mapper application distributes the water throughout the terrain, interpolating between the cross-sections, which results in a more thorough understanding of where water is present in a channel.

RAS-Mapper will also predict the flow depth and velocity at a given discharge. It should be noted that while the cross-sectional data has a low-flow channel stamped into each cross section, the LiDAR surface used for mapping does not include channel data below the water surface. As a result, the water depth in the channel generated from RAS-Mapper underestimates the flow depth by around 2 feet throughout the entire reach and will not show accurate habitat mapping within the main channel. Given that suitable habitat is generally found in the floodplain, this was not as great of a concern. Additionally, the habitat graphs discussed in **Sections 4.2** and **4.3** account for the low flow channel and are therefore not subject to this same error.

ArcGIS Pro was used to combine the RAS-Mapper generated raster datasets for velocity and depth so that RGSM depth and velocity criteria could be applied to identify the areas of potential suitable habitat. The results were used to create maps that show the areas of hydraulically suitable habitat for each life stage of the RGSM throughout the Bernalillo Reach.

4.5 RAS-Mapper Habitat Results in 2012

While the width slice method quantitatively determined areas with increased potential for habitat, RAS-Mapper was used to spatially depict the areas of potential RGSM habitat throughout the Bernalillo Reach

of the MRG and display the results on a map of the river. The hydraulically suitable habitat for each life stage was mapped at discharges of 1,500 cfs, 3,000 cfs, and 5,000 cfs, which have post-dam daily exceedance probabilities of around 20.2%, 9.9%, and 3.3%, respectively (**Figure 2-17**). The habitat maps for each reach at these discharges are available in Appendix E.

The hydraulically suitable habitat is primarily seen in the side channels where velocities are slower and channel depths are smaller. According to the RAS-Mapper results and the habitat graphs (**Figure 4-5**), there is more hydraulically suitable habitat for all life stages in Subreaches B2 and B3 than there are in Subreaches B1 and B4. B1 shows the least amount of suitable habitat for juveniles and adults at the more frequent 1,500 cfs magnitude flood events, although it does show more potential for larvae habitat along the side channels. The 2,000 cfs to 3,000 cfs range of flood events show the most potential for larvae habitat among the four subreaches, while suitable larvae habitat is generally reduced as flow depth increases within the side channels at higher magnitude flood events. Conversely, suitable habitat for juveniles and adults generally increases with increased flood magnitude.

Figure 4-6, **Figure 4-7**, and **Figure 4-8** show an example of potentially suitable habitat at the downstream section of Subreach B2 at flow rates of 1,500 cfs, 3,000 cfs, and 5,000 cfs, respectively. At this location, the greatest degree of larvae suitable habitat occurs at 1,500 cfs, and generally begins to disappear as flow rate increases. A greater amount of juvenile and adult habitat can be found along the side channels at 3,000 cfs as these channels become more activated. At 5,000 cfs, suitable habitat begins to shift from the side channels to the islands, which become submerged at the higher flow rate. This results in an overall increase in juvenile and adult habitat at 5,000 cfs.

All habitat mapping for the Bernalillo Reach of the MRG can be found in **Appendix E**.

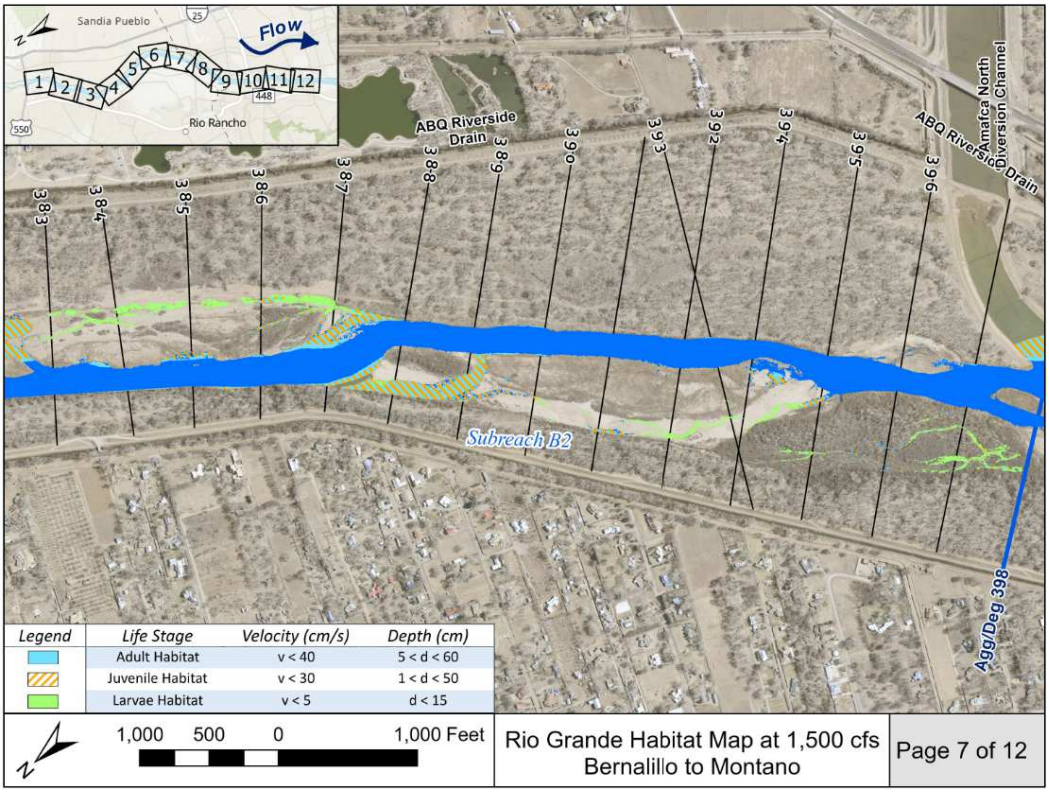

Figure 4-6 Suitable habitat in 2012 for each life stage at 1,500 cfs at the downstream section of B2. Dark blue inundation area is not suitable for habitat at any life stage. (Based on 1D HEC-RAS results)

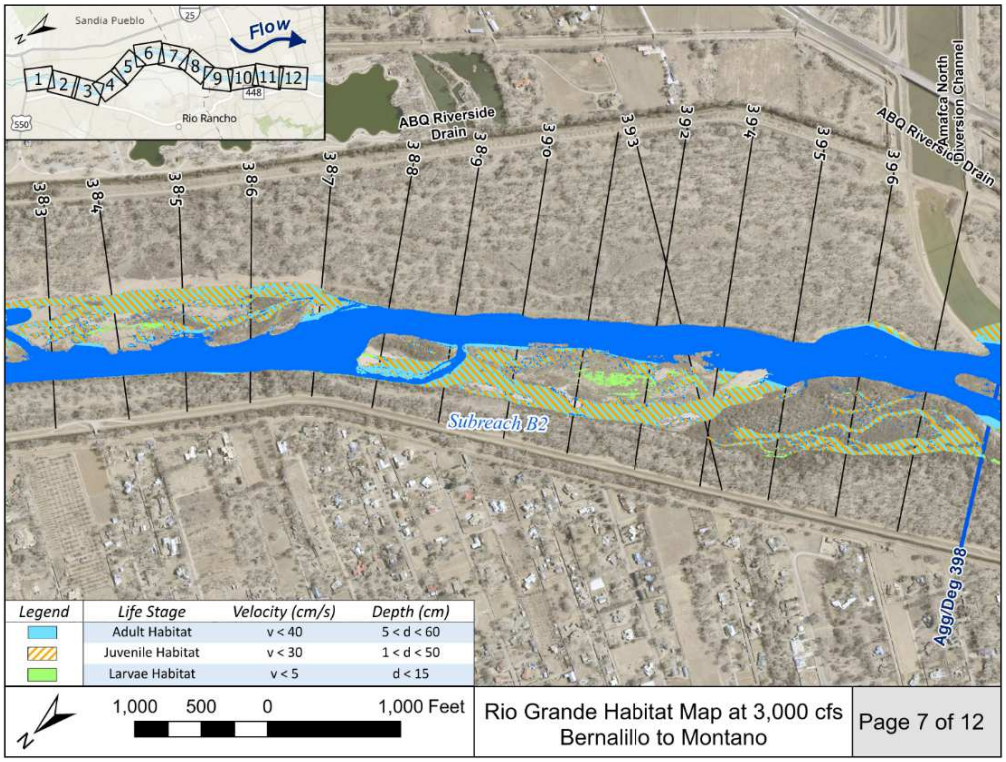

Figure 4-7 Suitable habitat in 2012 for each life stage at 3,000 cfs at the downstream section of B2. Dark blue inundation area is not suitable for habitat at any life stage. (Based on 1D HEC-RAS results)

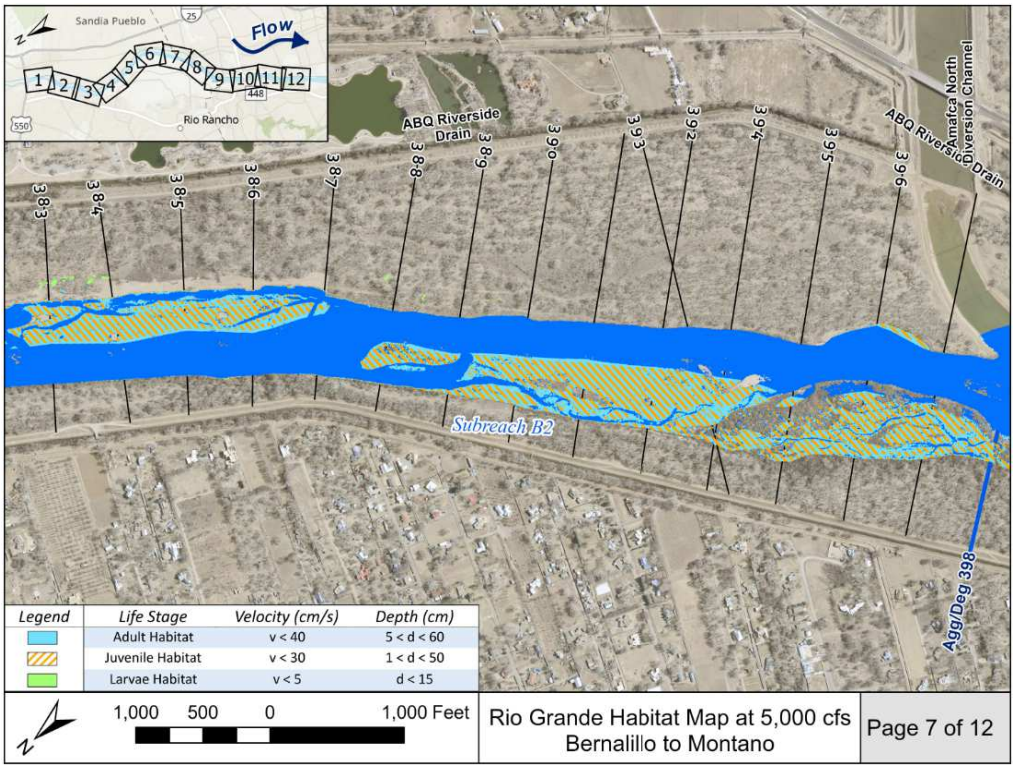

Figure 4-8 Suitable habitat in 2012 for each life stage at 5,000 cfs at the downstream section of B2. Dark blue inundation area is not suitable for habitat at any life stage. (Based on 1D HEC-RAS results)

4.6 Disconnected Areas

RAS-Mapper provides the opportunity to identify areas that likely meet the velocity and depth requirements of the RGSM at specified discharges. RAS-Mapper may also be beneficial for identifying areas throughout the reach than may contain water but are not connected to the main channel. These may be possible areas of focus for restoration efforts to increase habitat potential.

By connecting several of these disconnected areas, the RGSM may gain a great amount of possible habitat. **Figure 4-9** shows one instance of a disconnected area in Subreach B2. The disconnected area is emphasized by the red rectangles. These low-laying areas appear to contain side channels that historically became inundated at lower magnitude flood events, but over time have become disconnected from the main channel due to aggradation. The disconnected areas could identify problem areas for the RGSM by indicating that there are areas where fish may become stranded in months when the river contains less water and disconnected areas form. Conversely, these areas could become possible restoration sites leading to an increase in hydraulically suitable RGSM habitat.

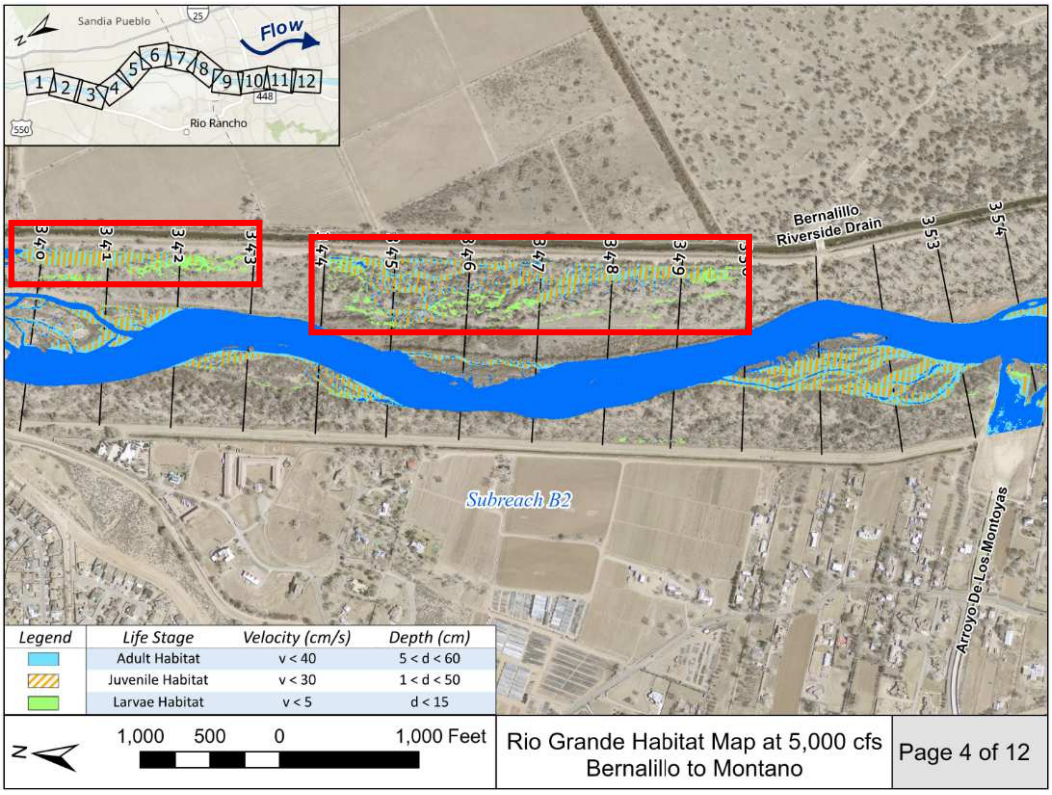

Figure 4-9 Disconnected low-laying areas that are no longer connected to the main channel at 5,000 cfs in Subreach B2. (Based on 1D HEC-RAS results)

Figure 4-10 shows another example of a disconnected area in Subreach B3. If this area were to be reconnected to the floodplain through restoration efforts, it may be particularly beneficial in increasing suitable larvae habitat at this location.

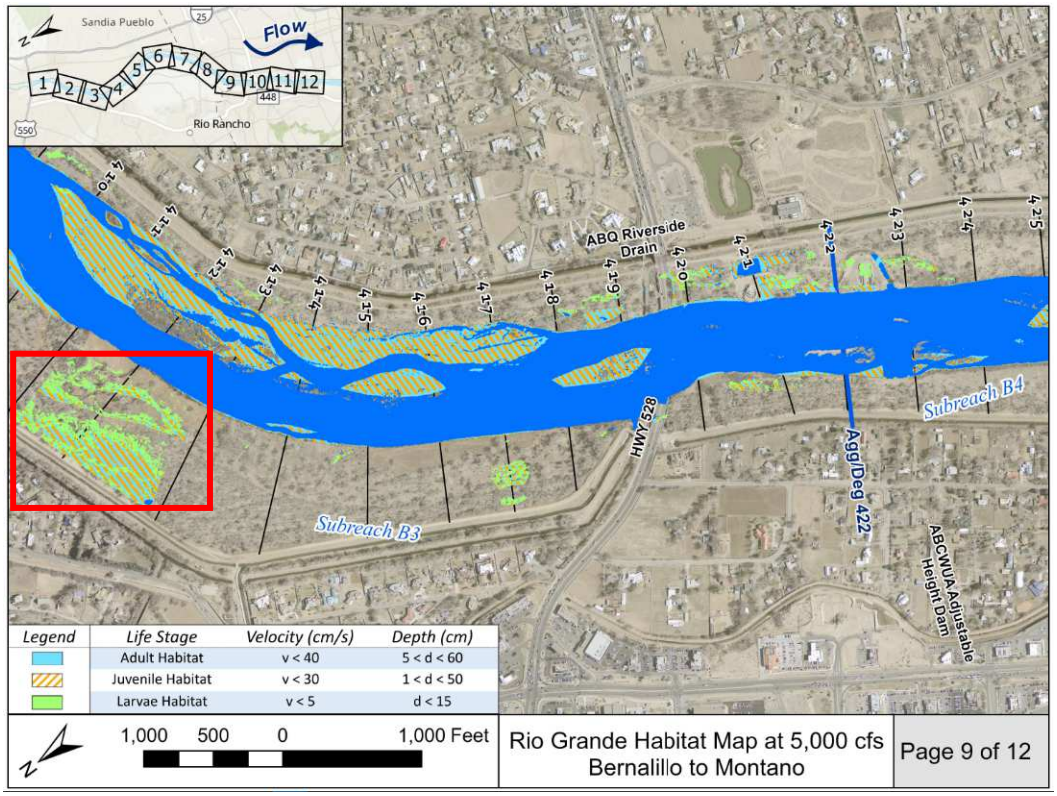

Figure 4-10 Disconnected low-laying areas that are no longer connected to the main channel at 5,000 cfs in Subreach B3. (Based on 1D HEC-RAS results)

5 1D and 2D Hydraulic Modeling Comparison

5.1 Purpose of Comparison

The Bernalillo Reach has many instances of split flow around the number mid-channel bars and islands. As discussed in previous sections, assumptions regarding ineffective flow areas and levees were made to complete the 1D HEC-RAS analysis. The 2012 HEC-RAS results were then mapped using RAS-Mapper, where the calculated water surface is overlayed onto the 2012 Lidar terrain files and interpolated between sections. This creates a pseudo 2D result.

The purpose of this comparison study is to compare the outputs of a true 2D hydraulic model to the pseudo 2D results that the 1D HEC-RAS model created. To eliminate long model run times, this additional study focuses on the two most downstream reaches, B3 and B4. These two reaches were chosen for this study because there are many instances of split flow due to in-channel islands and bars, which could play an important role in quantifying Silvery Minnow habitat availability. Subreaches B3 and B4 combined are approximately 7.5 miles. The flows that were used in the analysis were 1,500 cfs, 3,000 cfs, and 5,000 cfs.

Understanding the differences between the results of the 1D model compared to a 2D model would be beneficial in understanding how accurate the assumptions regarding split flow were in the basic 1D model. The 2D model that was used in this study is SRH2D using SMS.

5.2 Summary of 1D HEC-RAS Model Development

The 1D HEC-RAS Model provided by USBR was created from a 2012 LiDAR survey. To account for flow in the river during the LiDAR data collection, the bottom of the river was lowered approximately 1ft to 1.5 ft and showed a flat bottom. Within HEC-RAS, the model is georeferenced. It is the only model used in the Bernalillo Reach study that is georeferenced. The cross sections are located every 500 ft throughout the Bernalillo reach. The bank locations were also set by USBR prior the model being provided to CSU.

5.2.1 Manning's n Values

For consistency with previous MRG Reach studies, the manning's n values were set based on bank station locations. The reach is mostly sand and the manning's n value used for the active channel was 0.025. For the overbanks/floodplains, which is mostly vegetated, a manning's n value used is 0.10. It is important to note that most of the mid-channel islands has the lower, active channel manning's n value, even though they are vegetated.

5.2.2 Split Flow Assumptions

Many of the side channels and floodplains were disconnected from the MRG River in the 2012 LiDAR because the channel has been in a cycle of narrowing and deepening over time. However, HEC-RAS fills from the bottom in each section, so the side channels can convey water even though they are disconnected from the main channel. To account for the mid-channel islands and the instances of split flow, ineffective flow areas were added along the floodplains. The elevations of the ineffective flow areas were set at elevations that allowed for flow conveyance during higher flows when the side channel would be active but prevent flow conveyance at lower flows when the side channel is disconnected upstream. **Figure 5-1** below shows an example cross section that shows the ineffective flow areas in green.

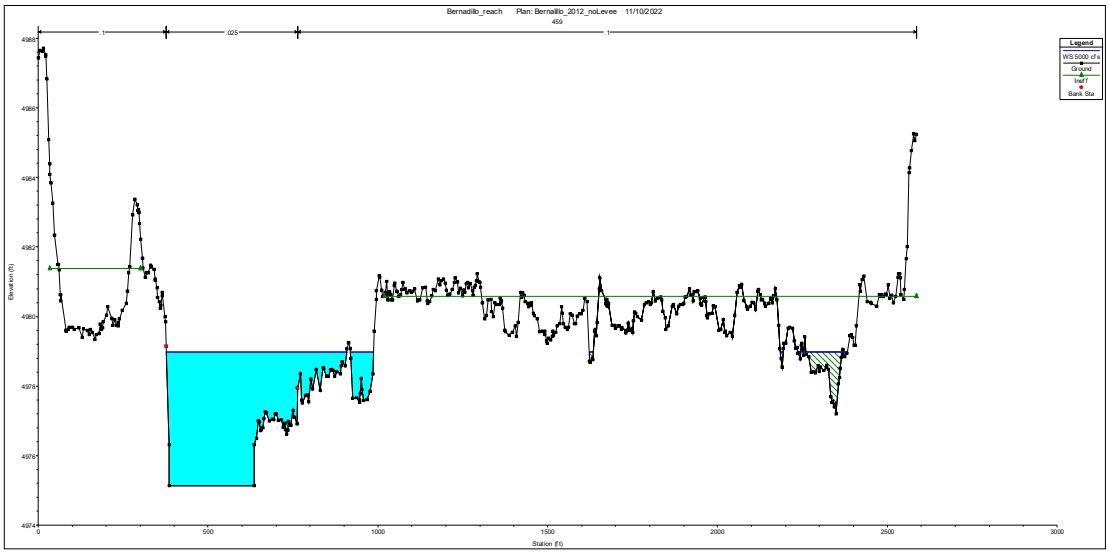

Figure 5-1: Example 1D cross section showing ineffective flow areas.

5.2.3 Boundary Conditions

The upstream boundary condition is flow. The flows that were chosen for the silvery minnow habitat analysis are 1,500 cfs, 3,000 cfs, and 5,000 cfs which are approximately the 20%, 10%, and 3% daily exceedances probabilities, respectively.

The downstream boundary condition of the Bernalillo reach model is normal depth with a slope = 0.0007, which corresponds to the energy grade line at the end of the Bernalillo reach in the full Middle Rio Grande River 1D model.

5.2.4 RAS-Mapper Processing

The 1D HEC-RAS results are post-processed using RAS-Mapper within the HEC-RAS application. RAS-Mapper overlays the water onto the 2012 LiDAR data. It interpolates the water surface elevation to create a "pseudo" 2D results that estimate of the location of water inundation, flow depth, and velocity across the terrain. It important noted that while the cross-sectional data has a low-flow channel stamped into each cross section, the LiDAR surface used for mapping does not include channel data below the water surface. As a result, the water depth in the channel generated from RAS-Mapper underestimates the flow depth by around 1.5 feet throughout the entire reach and will not show accurate habitat mapping within the main channel. Given that suitable habitat is generally found in the floodplain, this was not as great of a concern. RAS-Mapper creates a raster file that can be brought into other post-processing programs such as SMS or ArcMap. These "pseudo" 2D raster results will be used for comparison to a true 2D model in this study.

5.3 2D SRH-2D Model Development

The 2D model was setup using SMS version 13.1 and ran with SRH-2D.

5.3.1 Terrain and Grid Development

The LiDAR terrain file was manipulated in AutoCAD Civil3D 2021 to incorporate a lower channel to represent the river channel bathymetry and match the cross sections use in the 1D HEC-RAS model. In the figures below, this surface is denoted as Lidar+Bathy. See **Figure 5-2** below of the terrain file used in the 2D model. For additional comparison, the 2D model was also ran with just the LiDAR terrain without the

channel bottom adjustment to see how it compared to the RAS-Mapper results produced from the 1D hydraulic model. In the figures below, this surface is denoted as LidarOnly. The computational grid for the active channel was rectangular grids that were 15ft across the channel and 30ft long in profile. On the floodplains, the computational grid was triangulated.

5.3.2 Manning's n Values

To simplify the changing variables for the comparison, the same manning's n values from the 1D model were used for the 2D model. The bank lines were exported from RAS-Mapper and used to create the material polygons in SMS. **Figure 5-2** below shows the manning's n mapping. Green represents the floodplain at n = 0.1 and purple represents the active channel at n = 0.25. Similar to the 1D, there are vegetated islands within the active channel that are not represented accurately.

Figure 5-2: Bernalillo Reaches B3 and B4 terrain and manning's n mapping.

5.3.3 Boundary Conditions and Model Controls

The boundary conditions are consistent between the 2D and the 1D model. The three flow rates are 1,500 cfs, 3,000 cfs, and 5,000 cfs. The downstream boundary condition is a stage discharge curve that was an output for HEC-RAS at the downstream boundary of the 1D model.

5.4 Hydraulics Comparison

The figures in the main body of this study focus on a sub-portion of the B3 and B4 reaches in order to clearly show the differences at an adequate scale. **Figure 5-3** shows the region circled. This region also has many mid-channel islands, where the HEC-RAS model might not be accurately representing the hydraulics.

As seen in the **Figure 5-4**, **Figure 5-5**, and **Figure 5-6** below, the HEC-RAS "pseudo" 2D velocity results are generally faster than the SRH-2D models. The amount of overbank inundation is greater in the SRH-2D models compared to the HEC-RAS "pseudo" 2D model results. In the models where the LiDAR was not adjusted, the amount of overbank inundation is generally greater than the other models. The same pattern occurs for all of the flow rates analyzed.

Figure 5-7, **Figure 5-8**, and **Figure 5-9** show the depth results comparison for the different flow rates. The depths are generally deeper in the SRH-2D models compared to the "pseudo" 2D HEC-RAS results. The depths were deeper in the model where the LiDAR was modified to account for the water surface during

the survey, which makes sense since the velocities are faster, the ground is higher, but the flow is the same. Conservation of mass, where Q = VA, explains the depth difference.

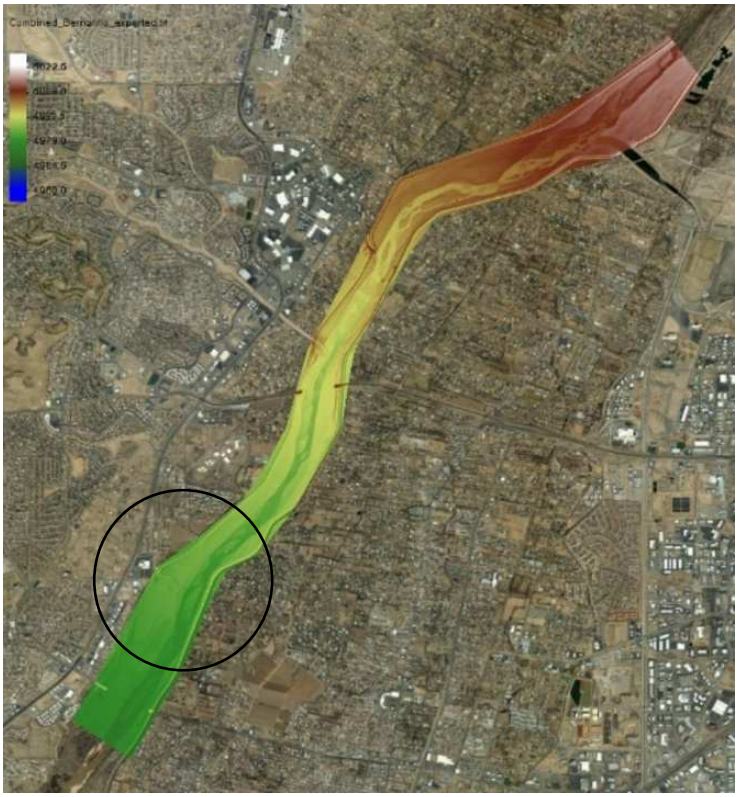

Figure 5-3: Focus area of presented hydraulic results.

5.4.1 Velocity Results

Figure 5-4: 1,500 cfs Velocity Results (scale 0-6ft/s)

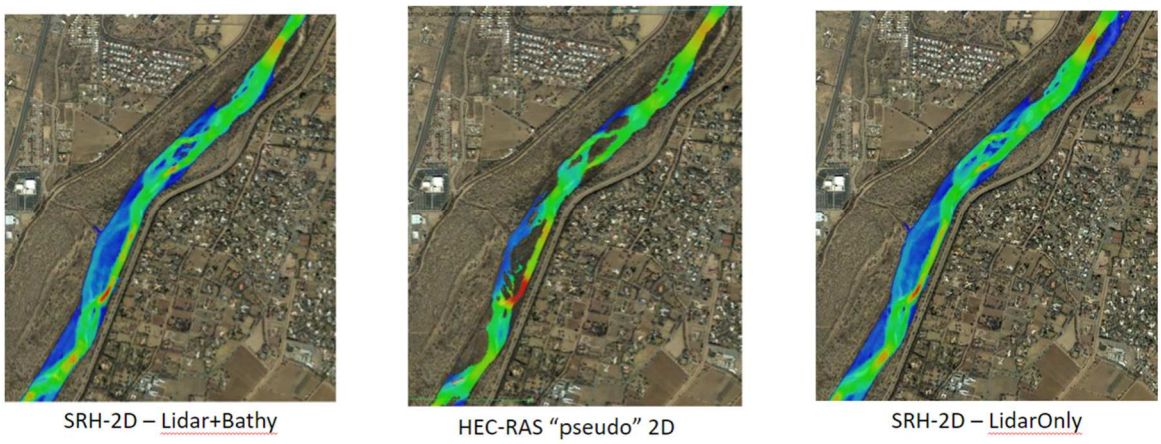

Figure 5-5: 3,000 cfs Velocity Results (scale 0-6ft/s)

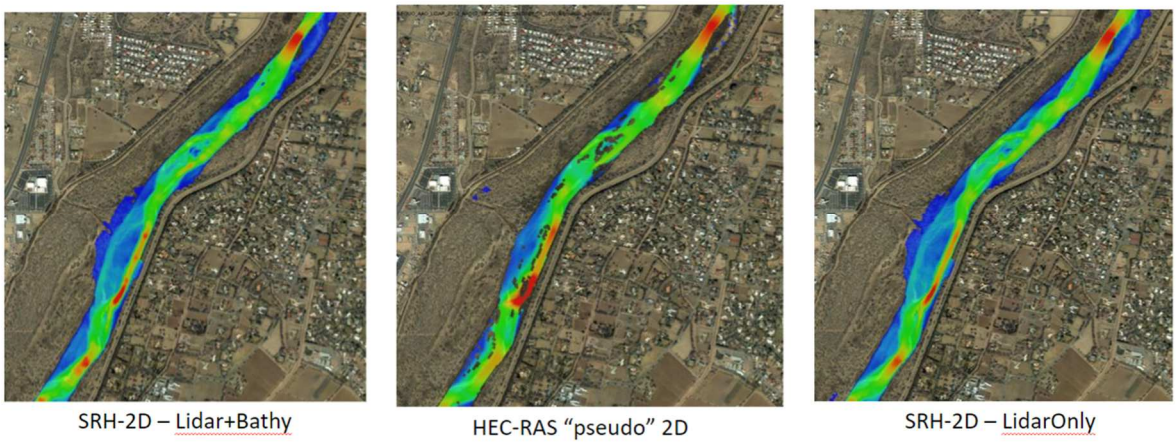

Figure 5-6: 5,000 cfs Velocity Results (scale 0-6ft/s)

5.4.2 Depth Results

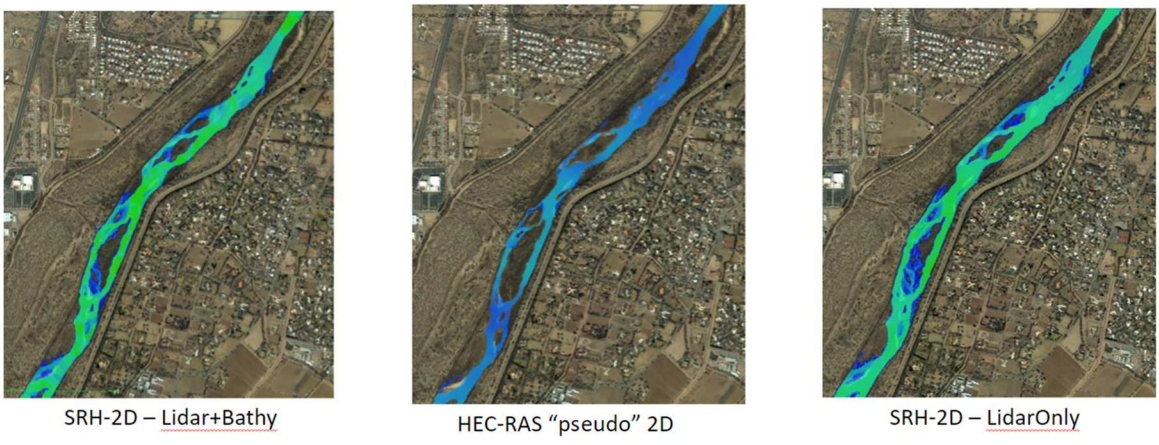

Figure 5-7: 1,500 cfs Depth Results (scale 0-6ft)

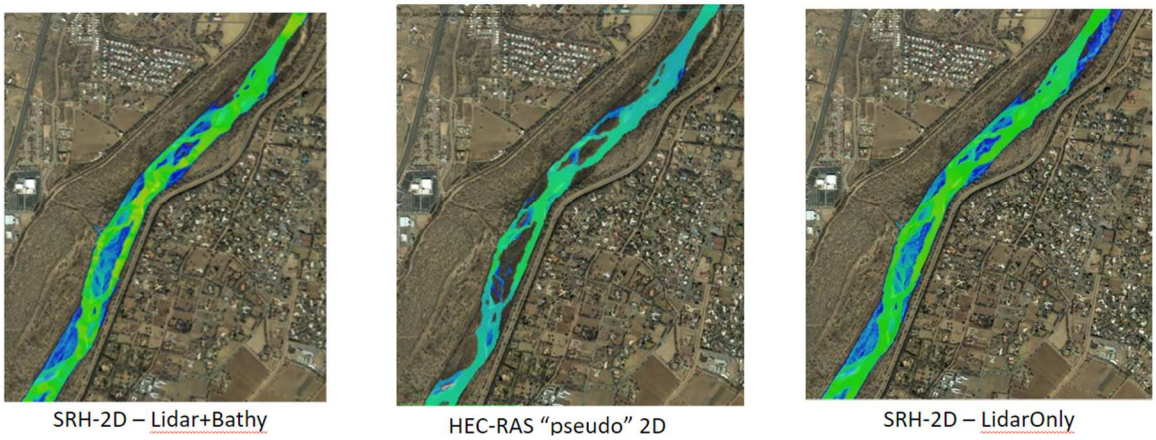

Figure 5-8 : 3,000 cfs Depth Results (scale 0-6ft)

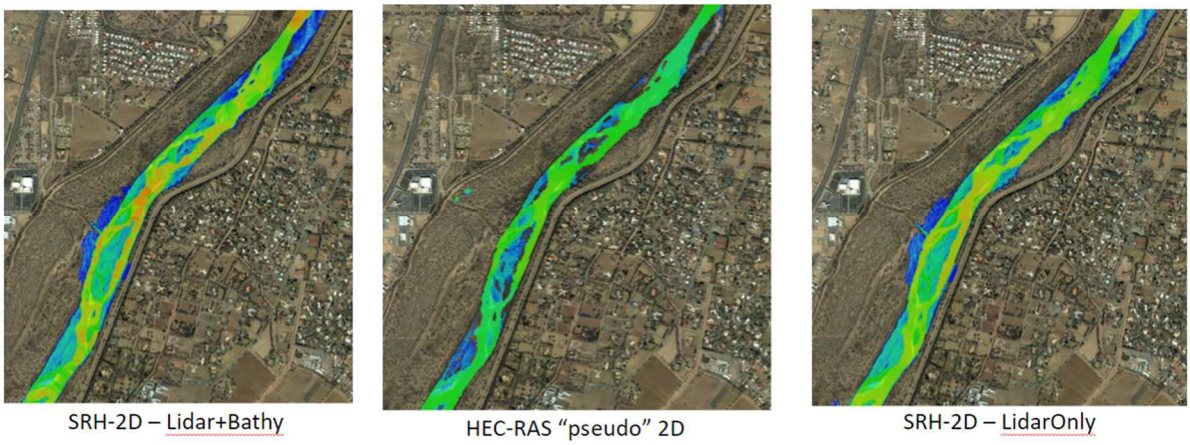

Figure 5-9: 5,000 cfs Depth Results (scale 0-6ft)

5.5 Habitat Availability Comparison

To calculate the habitat availability, the Zonal Classification function within SMS was performed on the results for each model results. Using the criteria shown in **Table 4-1**, area outputs of appropriate habitat for each stage of the Silver Minnow's life cycles, which are adult, juvenile, and larvae. **Table 5-1** below shows the area outputs, while **Figure 5-10** shows the acreage of habitat availability quantitatively.

For all flows, the HEC-RAS "pseudo" 2D results had the least amount of available habitat at all stages. When the LiDAR terrain was not adjusted for the water surface, it provided the most amount of habitat at all life stages. It seems that the SRH-2D Model with the adjusted terrain most likely represents the true amount of habitat availability given the assumptions made regarding channel bottom and roughness.

Although the different models showed different quantities of available silvery minnow habitat, it is important to note that the locations of the most habitat were the same between the different models. These generalized locations of habitat availability could help river managers and biologists identify locations of future river restoration efforts.

Table 5-1: Silvery Minnow Habitat Availability Quantities

1,500 cfs			
	SRH2D-Lidary+Bathy Area	**HEC Pseudo 2D Area**	**SRH2D-LidarOnly Area**
Adult	93 acre	52 acre	176 acre
Juvenile	69 acre	45 acre	152 acre
Larvae	25 acre	1 acre	57 acre
3,000 cfs			
	SRH2D-Lidary+Bathy Area	**HEC Pseudo 2D Area**	**SRH2D-LidarOnly Area**
Adult	141 acre	77 acre	187 acre
Juvenile	126 acre	56 acre	184 acre
Larvae	41 acre	10 acre	183 acre
5,000 cfs			
	SRH2D-Lidary+Bathy Area	**HEC Pseudo 2D Area**	**SRH2D-LidarOnly Area**
Adult	226 acre	144 acre	334 acre
Juvenile	210 acre	132 acre	291 acre
Larvae	56 acre	24 acre	67 acre

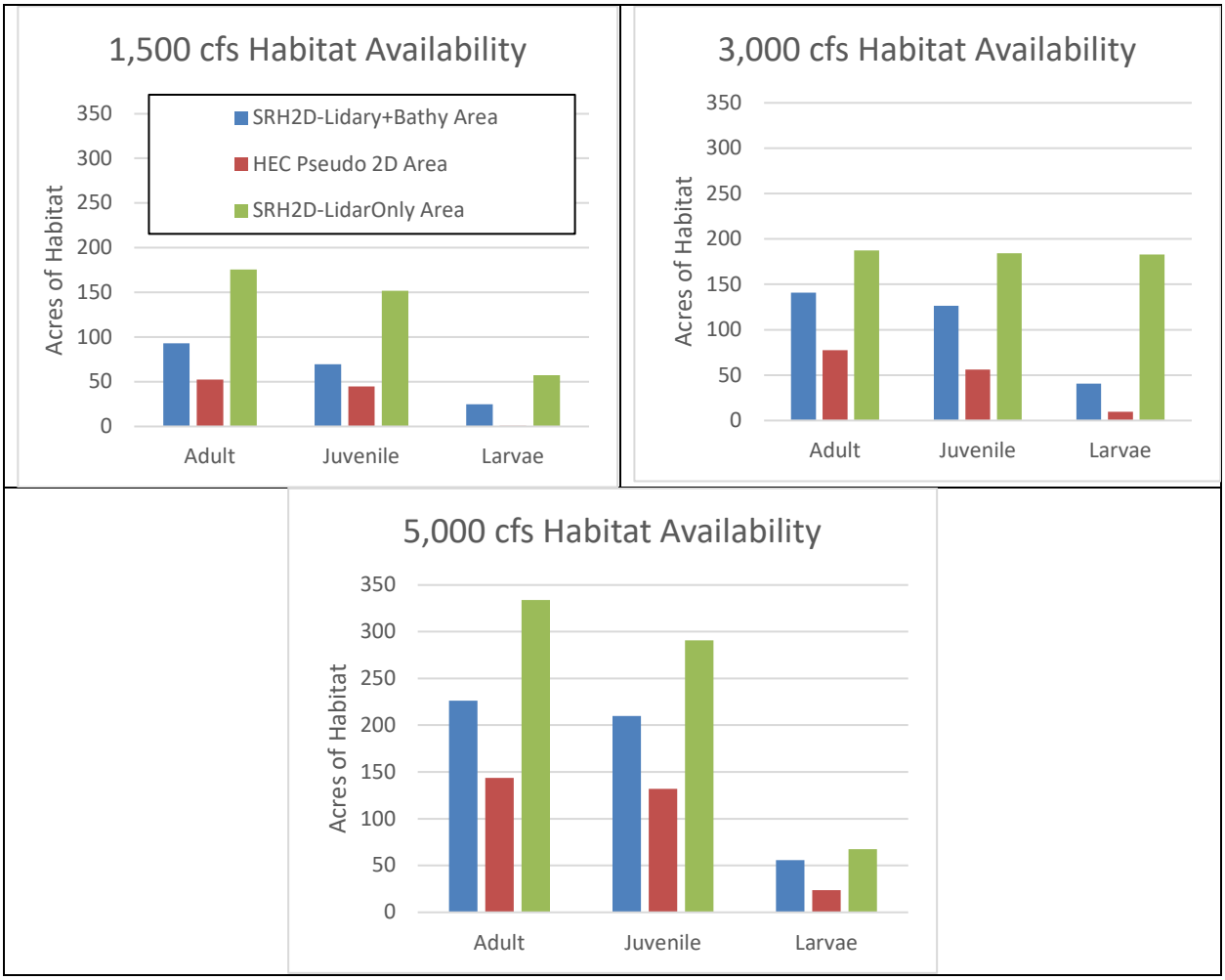

Figure 5-10: Habitat Availability Comparison

5.6 1D to 2D Hydraulic Modeling Conclusion

In this additional study, 1D HEC-RAS hydraulic results were compared to a 2D SRH-2D model. In general, velocities were slower and depths were deeper in the 2D hydraulic model than in the 1D model. The 1D model mapped as "pseudo" 2D results also showed less floodplain connectivity than the 2D SRH-2D model, although generally the active channel flow paths remained the same between the two models. This indicates that the ineffective flow areas that were used in the model did help with some of the flow splits, but also might have blocked some of the floodplain connectivity from occurring.

Since there was a larger amount of habitat availability in the higher flows than in the lower flows, it could indicate that the increased floodplain connectivity is related to the habitat availability. This confirms what was assumed to be true in the 1D hydraulic model. The general trend of increasing amount of habitat as flows increase was consistent between all models whether modeled in 2D or 1D.

When quantifying the silvery minnow habitat availability, the 1D HEC-RAS model resulted in an underestimation of the habitat availability for all life stages. This could be related to the increased floodplain connectivity that the 2D model had compared to the 1D model. For some life stages and flows, the HEC-RAS model produced less than half of the amount that the 2D model showed. However, the relative increases followed similar trends within the life stages. The general zones of habitat availability also followed similar trends between the 1D and 2D models. This could indicate that the 1D HEC-RAS model and it's RAS Mapper "pseudo" results, along with the assumptions that were made for the 1D hydraulic model, are sufficient for identifying potential areas of increased habitat availability and future river restoration efforts. However, it is not sufficient at quantifying the amount of habitat.

6

6 Bernalillo Reach Conclusion

The Bernalillo Reach extends from the Hwy 550 bridge crossing in Bernalillo and ends at the Montaño bridge crossing in Albuquerque, New Mexico. The goal of this reach report is to evaluate the spatial and temporal changes in morpho-dynamic processes in the Bernalillo Reach and to utilize hydraulic modeling to identify areas of habitat availability for the different life stages of the RGSM. This was done by delineating the Bernalillo Reach into four subreaches based on geomorphic characteristics, analyzing trends of precipitation and flow and sediment discharge through the Bernalillo Reach, analyzing trends in geomorphic change from 1962 to 2012 using a detailed 1D HEC-RAS model provided by USBR, and characterizing available RGSM habitat using the 1D hydraulic model. Due to the assumptions made in the 1D hydraulic model and the presence of flow splits around midchannel islands bars, the results from the 1D HEC-RAS model were compared to the results generated from a 2D hydraulic model using SRH2D.

The major findings of this study are listed below:

- The hydrograph of the Bernalillo Reach was impacted by the construction of Cochiti Dam. Prior to the dam completion, there was a greater frequency and magnitude of large flood events. Spring snowmelt typically supplies the greatest water and sediment discharge volumes. Some occasional monsoonal thunderstorms transport the greatest concentrations of suspended sediment, but only for short periods of time. The sediment flux into the river seems to be primarily driven by snowmelt that drains into the ephemeral tributaries and nearby arroyos to wash sediment into the MRG. The Jemez River contributes a large portion of sediment to the MRG.
- Between 1962 and 1972, the Bernalillo Reach was in the process of aggrading, with the greatest degree of aggradation occurring in Subreaches B1 and B2 (~1 to 2 feet). This aggradation led to an increase in bed elevation and steepening in channel slope during this decade. Following the completion of the Cochiti dam in 1973 the channel began to incise, with the most significant channel bed degradation occurring in Subreach B1 and B2 (~3 to 8 feet). In 2005, the ABCWUA Adjustable Height Dam was constructed at the end of the B3 reach. The adjustable height dam raised the bed elevation and caused aggradation to occur immediately upstream and degradation to occur immediately downstream.
- The Subreaches B2 and B3 may be more efficient at reaching the Rio Grande Silvery Minnow's habitat criteria of velocity and flow depth for the juvenile and adult life stages, while B1 and B2 may be for efficient for the larvae.
- When quantifying the silvery minnow habitat availability, the pseudo 2D mapping created by the 1D HEC-RAS model resulted in an underestimation of the habitat availability for all life stages. However, the relative increases and general locations of availably habitat followed similar trends between the 1D and 2D models for all of the life stages and these generalized locations could help river managers and biologists identify locations of future river restoration efforts.

7 Bibliography

Radobenko, C, Corsi, B, Anderson, T and Julien, P.Y. (2022). Draft Report. "Middle Rio Grande Bernalillo Reach Report: Morpho-dynamic Processes and Silvery Minnow Habitat from Hwy 550 Bridge to Montaño Road Bridge," Submitted to the U.S. Bureau of Reclamation, Albuquerque, New Mexico.

Anderson, T, Radobenko, C, Corsi, B and Julien, P.Y. (2022). Draft Report. "Middle Rio Grande Montaño Reach Report: Morpho-dynamic Processes and Silvery Minnow Habitat from the Montaño Road Bridge Crossing to the Isleta Diversion Dam," Submitted to the U.S. Bureau of Reclamation, Albuquerque, New Mexico.

Beckwith, T and Julien, P.Y. (2020) "Middle Rio Grande Escondida Reach Report: Morpho-dynamic Processes and Silvery Minnow Habitat from Escondida Bridge to US-380 Bridge (1918-2018.)" Colorado State University, Fort Collins, CO.

Bovee, K.D., Waddle, T.J., and Spears, J.M. (2008). "Streamflow and endangered species habitat in the lower Isleta reach of the middle Rio Grande." *U.S. Geological Survey Open-File Report 2008-1323*.

Fogarty, C and Julien, P.Y. (2020). *Linking Morphodynamic Processes and Silvery Minnow Habitat Conditions in the Middle Rio Grande – Isleta Reach, New Mexico.* Colorado State University, Fort Collins, CO.

Doidge, S and Julien, P.Y. (2019). Draft Report. *Middle Rio Grande San Acacia Reach: Morphodynamic Processes and Silvery Minnow Habitat from San Acacia Diversion Dam to Escondida Bridge*, Colorado State University, Fort Collins, CO.

Fitzner, A. (2018). Draft Report "Reclamation Managing Water in the West." *Bureau of Reclamation Draft Lower Reach Plan*, Albuquerque Area Office, Albuquerque, NM, 36 p.

Greimann B., and Holste N. (2018). "Analysis and Design Recommendations of Rio Grande Width", T*echnical Service Center, Sedimentation and River Hydraulic Group, U.S. Bureau of Reclamation, Denver, CO*

Holste, N. (2020) "One-Dimensional Numerical Modeling of Perched Channels." *U.S. Bureau of Reclamation, Denver, CO.*

Julien, P.Y. (2002). *River Mechanics,* Cambridge University Press, New York

Julien, P. Y., and Wargadalam, J. (1995). "Alluvial channel geometry: theory and applications." *Journal of Hydraulic Engineering*, American Society of Civil Engineers, 121(4), 312–325.

Klein, M., Herrington, C., AuBuchon, J., and Lampert, T. (2018a). *Isleta to San Acacia Geomorphic Analysis*, U.S. Bureau of Reclamation, Reclamation River Analysis Group, Albuquerque, New Mexico.

Klein, M., Herrington, C., AuBuchon, J., and Lampert, T. (2018b). *Isleta to San Acacia Hydraulic Modeling Report*, U.S. Bureau of Reclamation, Reclamation River Analysis Group, Albuquerque, New Mexico.

LaForge, K., Yang, C.Y., Julien, P.Y., and Doidge, S. (2019). Draft Report. *Rio Puerco Reach: Hydraulic Modeling and Silvery Minnow Habitat Analysis*, Colorado State University, Fort Collins, CO.

Larsen, A. (2007). *Hydraulic modeling Analysis of the Middle Rio Grande-Escondida Reach, New Mexico*. M.S thesis, Civil Engineering Department, Colorado State University, Fort Collins, CO.

Makar, P. (2006). "Channel Widths Changes Along the Middle Rio Grande, NM." *Proceedings of the Eith Federal Interagency Sedimentation Conference*, Bureau Of Reclamation, Denver, CO. 943 p.

Makar, P., Massong, T., and Bauer, T. (2006). "Channel Widths Change Along the Middle Rio Grande, NM." *Joint 8th Federal Interagency Sedimentation Conference, Reno, NV, April 2 -April6, 2006.*

Massong, T., Paula, M., and Bauer, T. (2010). "Planform Evolution Model for the Middle Rio Grande, NM." *2nd Joint Federal Interagency Conference, Las Vegas, NV, June 27 - July 1, 2010*.

MEI. (2002). *Geomorphic and Sedimentologic Investigations of the Middle Rio Grande between Cochiti Dam and Elephant Butte Reservoir*, Mussetter Engineering, Inc., Fort Collins, CO, 220 p.

Mortensen, J.G., Dudley, R.K., Platania, S.P., and Turner, T.F. (2019). Draft report. *Rio Grande Silvery Minnow Habitat Synthesis,* University of New Mexico with American Southwest Ichthyological Researchers, Albuquerque, NM.

Mortensen, J.G., Dudley, R.K., Platania, S.P., White, G.C., and Turner, T.F., Julien, P.Y., Doidge, S, Beckwith, T., Fogarty, C. (2020). Draft Report. *Linking Morpho-Dynamics and Bio-Habitat Conditions on the Middle Rio Grande: Linkage Report 1- Isleta Reach Analyses*. Submitted to the U.S. Bureau of Reclamation, Albuquerque, New Mexico.

Owen, T. E., Anderson, K., and Julien, P. (2011). *Elephant Butte Reach: South boundary of Bosque del Apache NWR to Elephant Butte Reservoir hydraulic modeling analysis, 1962- 2010.* Colorado State University, Fort Collins, CO.

Owen, T. E., (2012). *Geomorphic Analysis Of the Middle Rio Grande - Elephant Butte Reach, New Mexico.* Colorado State University, Fort Collins, CO.

Pinson, A.O., Scissons, S.K., Brown, S.W., Walther, D.E. (2014). Post Flood Report: Record Rainfall and Flooding Events during September 2013 in New Mexico, Southeastern Colorado and Far West Texas, U.S. Army Corps of Engineers, Albuquerque, New Mexico.

Pinson, A.O., Scissons, S.K., Brown, S.W., Walther, D.E. (2014). *Post Flood Report: Record Rainfall and Flooding Events during September 2013 in New Mexico, Southeastern Colorado and Far West Texas,* U.S. Army Corps of Engineers, Albuquerque, New Mexico

Posner, A. J. (2017). Draft report. *Channel conditions and dynamics of the Middle Rio Grande River,* U.S. Bureau of Reclamation, Albuquerque, New Mexico.

Scurlock, D. (1998). "From the Rio to the Sierra: an environmental history of the Middle Rio Grande Basin." *General Technical Report RMRS-GTR-5. Fort Collins, CO: US Department of Agriculture, Forest Service, Rocky Mountain Research Station, 440 p.*

Shah-Fairbank, S. C., Julien, P. Y., and Baird, D. C. (2011). "Total sediment load from SEMEP using depth-integrated concentration measurements." Journal of Hydraulic Engineering, 137(12), 1606–1614.

Schied, A., Sperry, D. J., and Julien, P.Y. (2022). *Middle Rio Grande Bosque Reach Report: Morpho-dynamic Processes and Silvery Minnow Habitat from US-380 Bridge to Southern Boundary of Bosque Del Apache National Wildlife Refuge (BDANWR)*. Final report prepared for the United States Bureau of Reclamation. Colorado State University, Fort Collins, CO.

Shrimpton, C. P, (2012). *Analysis of Sediment Plug Hypotheses Middle Rio Grande, NM.* Colorado State University, Fort Collins, CO.

Sperry, D.J., Scheid, A., and Julien, P.Y. (2022). *Middle Rio Grande Elephant Butte Reach Report: Morpho-dynamic Processes and Silvery Minnow Habitat from the Southern Boundary of the Bosque Del Apache National Wildlife Refuge to Elephant Butte Reservoir.* Final report prepared for the United States Bureau of Reclamation. Colorado State University, Fort Collins, CO.

Towne, L. (2007). "Infrastructure and Management of the Middle Rio Grande." *The Middle Rio Grande Today, Burequ of Reclamation,* 17 p.

U.S. Bureau of Reclamation. (2012). "Middle Rio Grande River Maintenance Program - Comprehensive Plan and Guide." Albuquerque Area Office, Albuquerque, New Mexico, 202p.

U.S. Bureau of Reclamation. (2021). “Water Operations: Historical Data.” Online Resource. https://www.usbr.gov/rsvrWater/HistoricalApp.html

U.S. Fish and Wildlife Service. (2007). “Rio Grande Silvery Minnow (Hybognathus amarus).” Draft Revised Recovery Plan, Albuquerque, New Mexico, 174 p.

Varyu, D. (2013). *Aggradation / Degradation Volume Calculations: 2002-2012*. U.S. Department of the Interior, Bureau of Reclamation, Technical Services Center, Sedimentation and River Hydraulics Group. Denver, CO.

Varyu, D. (2016). *SRH-1D Numerical Model for the Middle Rio Grande: Isleta Diversion Dam to San Acacia Diversion Dam*. U.S. Department of the Interior, Bureau of Reclamation, Technical Services Center, Sedimentation and River Hydraulics Group. Denver, CO.

Yang, C.Y. (2019). *The Sediment Yield of South Korean Rivers*, Colorado State University, Fort Collins, CO.

Yang, C.Y. and Julien, P.Y. (2019). “The ratio of measured to total sediment discharge.” *International Journal of Sediment Research*, 34(3), pp.262-269.

Yang, C.Y., LaForge, K., Julien, P.Y., and Doidge, S. (2019). Draft Report. *Isleta Reach: Hydraulic Modeling and Silvery Minnow Habitat Analysis*, Colorado State University, Fort Collins, CO.

Appendix A

Cumulative Plots used in the Subreach Delineation, Aerial Imagery with Agg/deg Line Labels

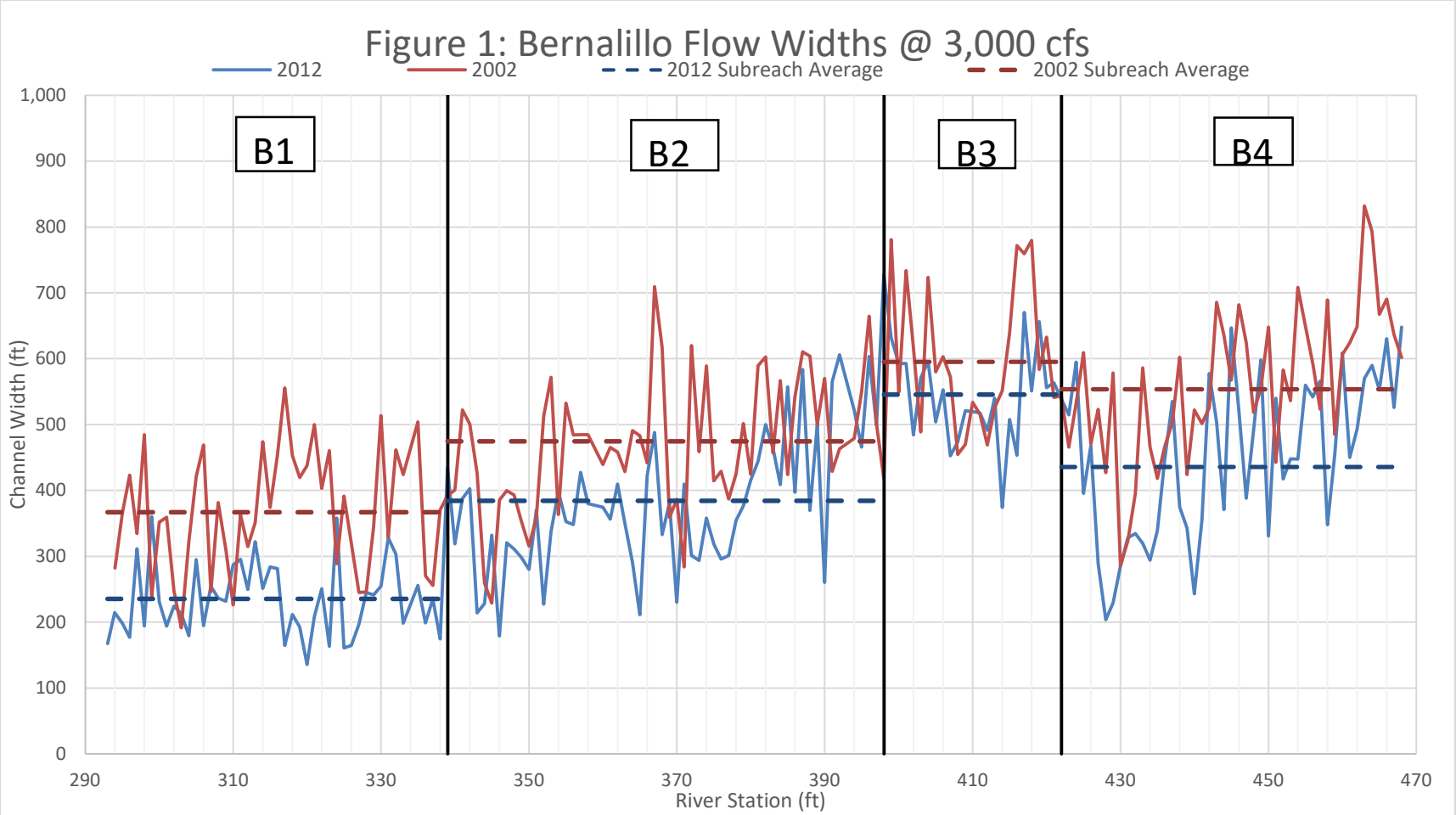

2002		
Subreach	**Average Flow Width, ft**	**Standard Deviation**
B1	367.0	90.9
B2	474.9	105.2
B3	595.4	104.1
B4	553.7	111.9

2012		
Subreach	**Average Flow Width, ft**	**Standard Deviation**
B1	235.5	54.3
B2	384.3	109.2
B3	545.6	74.9
B4	435.8	114.9


Figure 2: Cumulative Bernalillo Flow Widths @ 3,000 cfs
2012
2002
B1
B2
B3
B4
Width (ft)
90,000
80,000
70,000
60,000
50,000
40,000
30,000
20,000
10,000
0
290
310
330
350
370
390
410
430
450
470
River Station (ft)

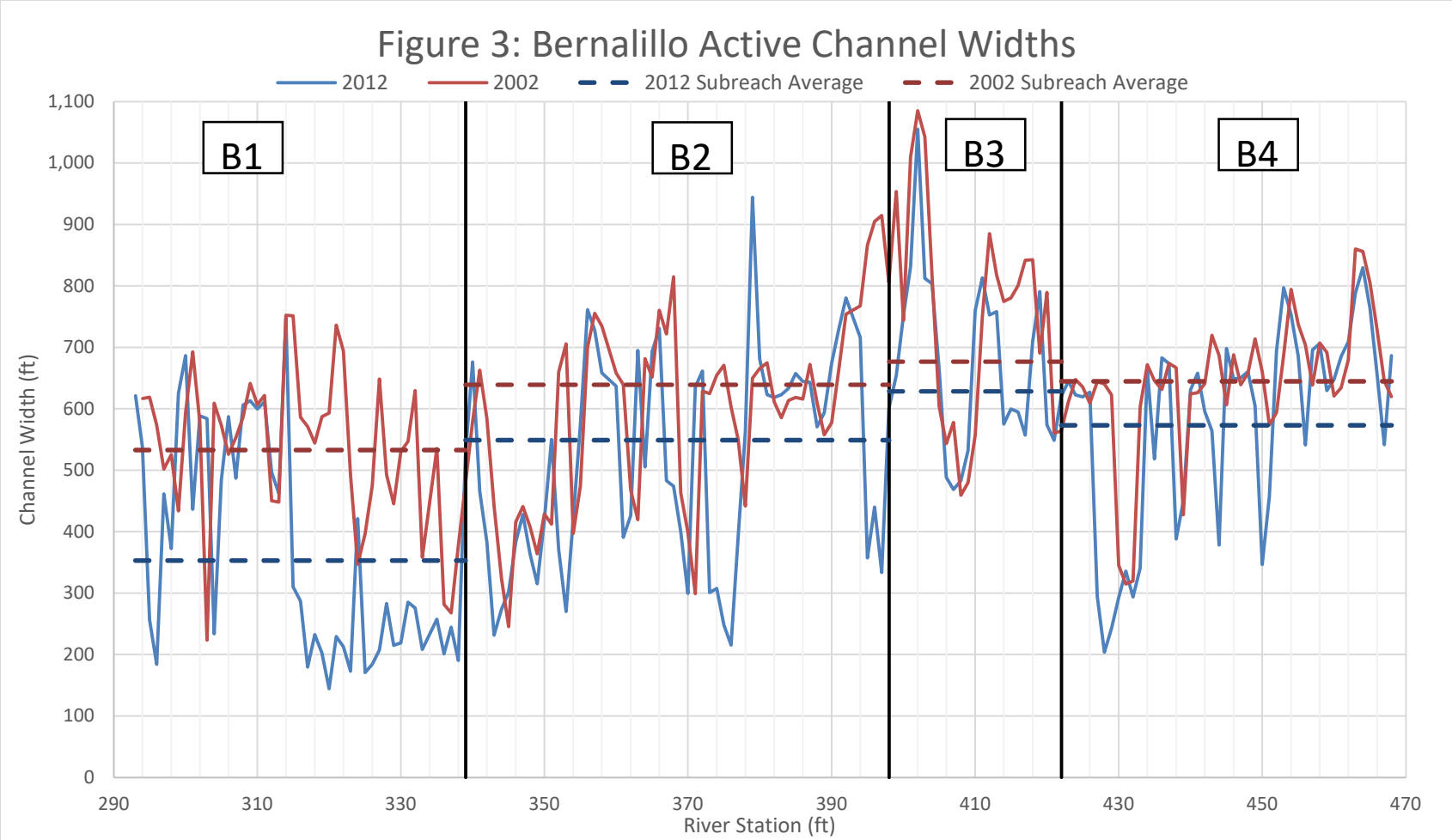

2012		
Subreach	**Average Active Channel Width, ft**	**Standard Deviation**
B1	353.1	172.0
B2	549.0	185.7
B3	628.5	124.8
B4	573.3	167.3

2002		
Subreach	**Average Active Channel Width, ft**	**Standard Deviation**
B1	533.0	120.3
B2	639.1	180.5
B3	676.8	120.9
B4	644.9	114.5

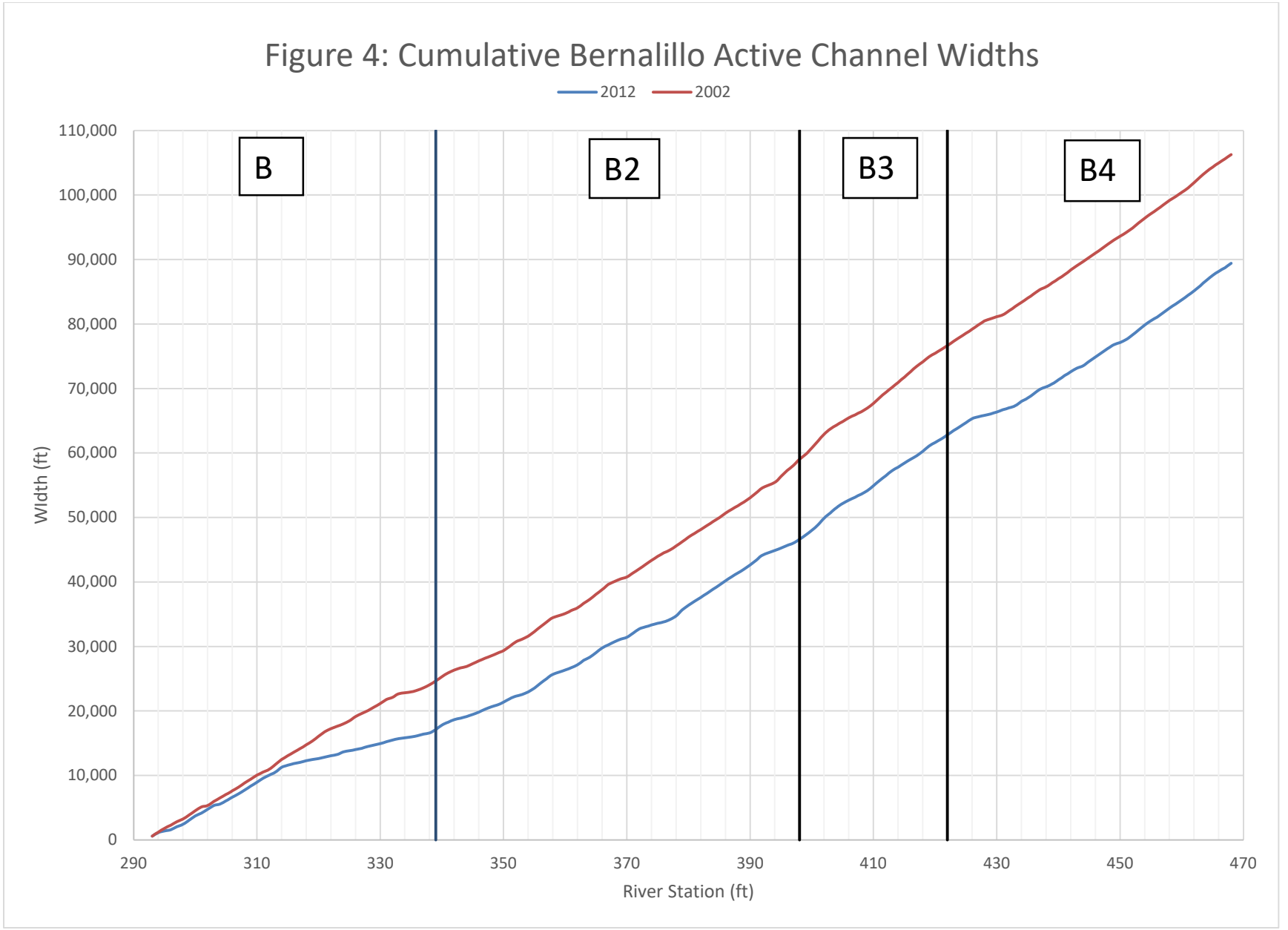
Figure 4: Cumulative Bernalillo Active Channel Widths
2012
2002
B
B2
B3
B4
Width (ft)
110,000
100,000
90,000
80,000
70,000
60,000
50,000
40,000
30,000
20,000
10,000
0
290
310
330
350
370
390
410
430
450
470
River Station (ft)

Figure 5: Longitudinal Profile of Bernalillo Reach

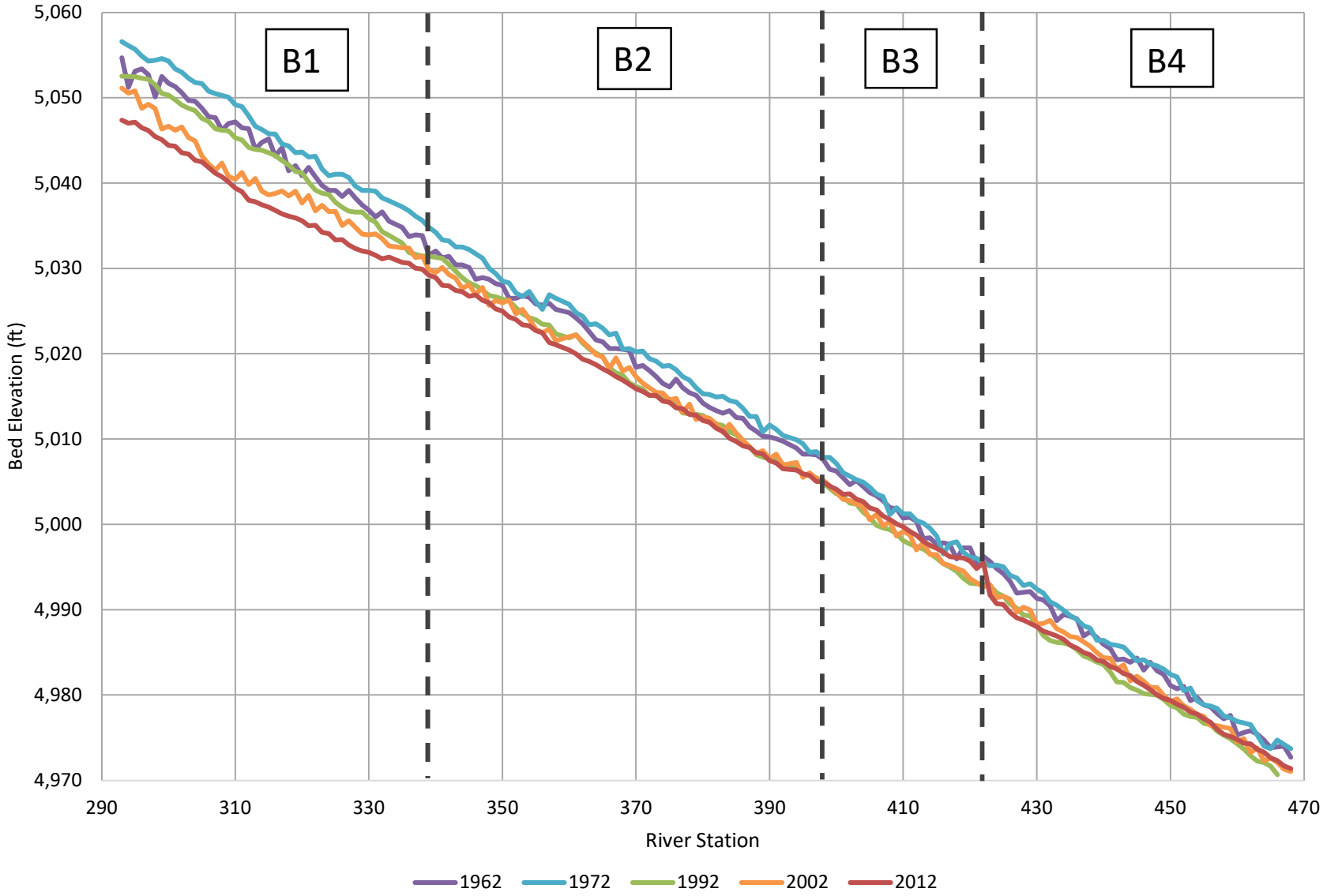

Figure 6: 2012 Bed Material Size of the Bernalillo Reach

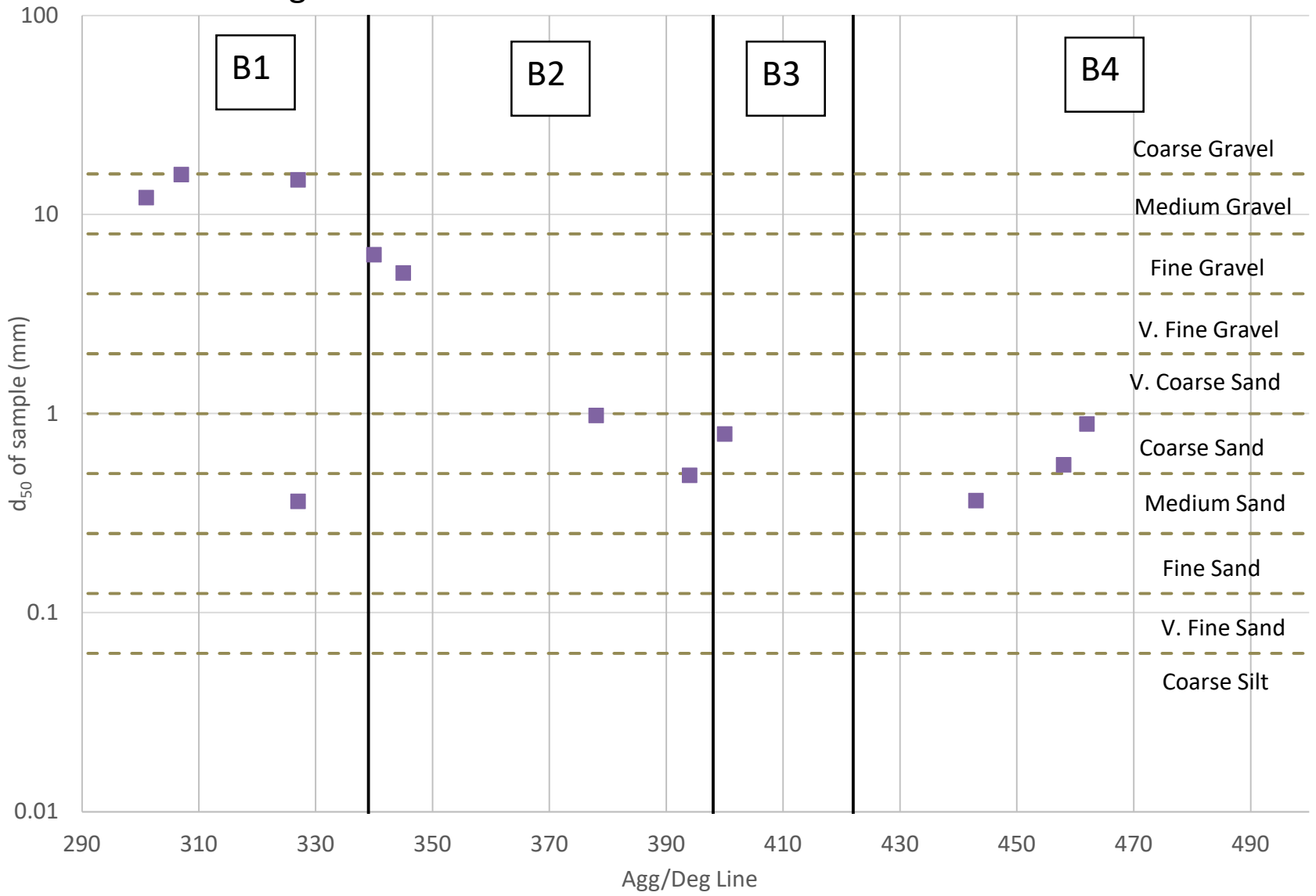

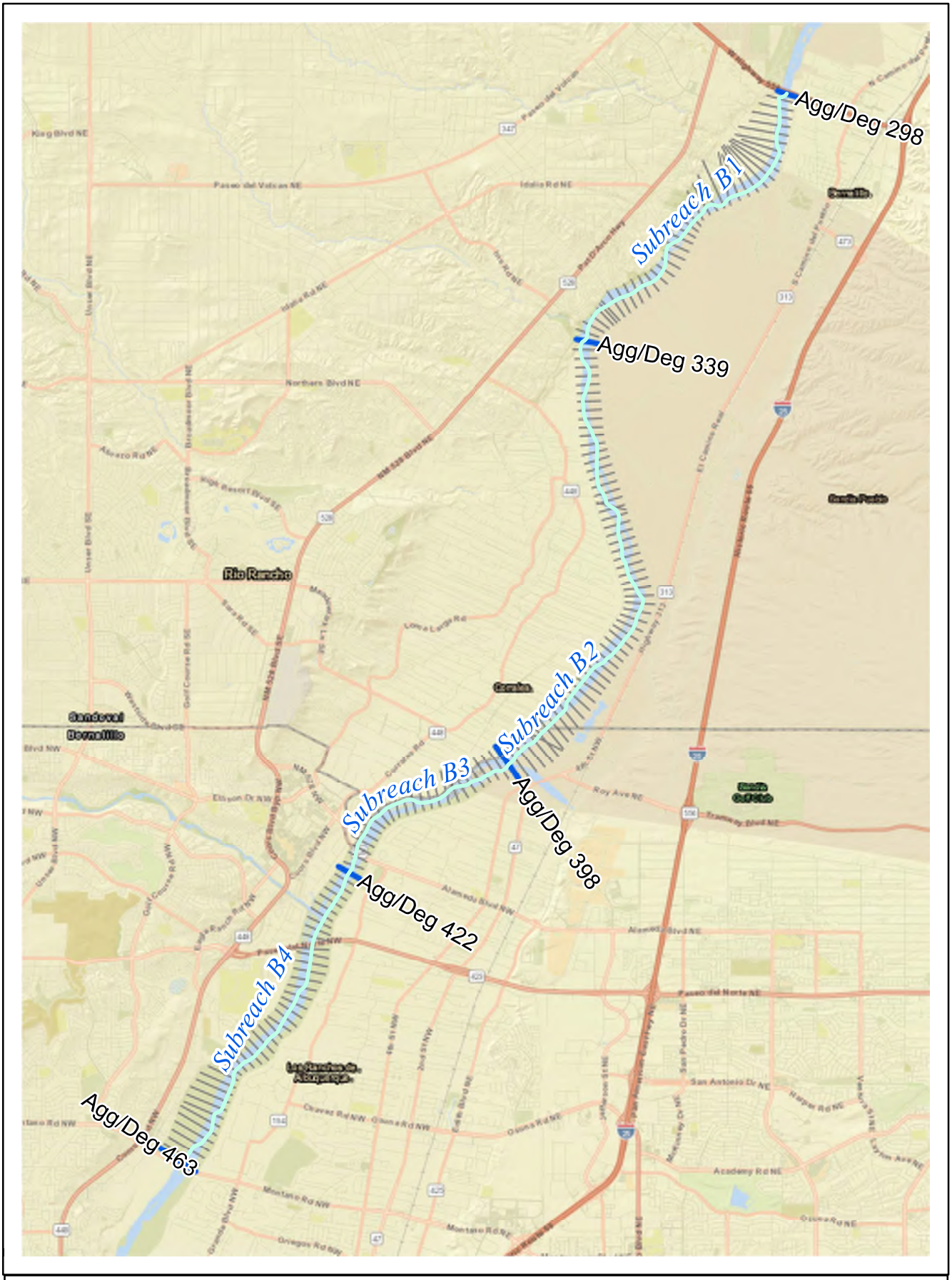

Bernalillo Subreach
Overview Map

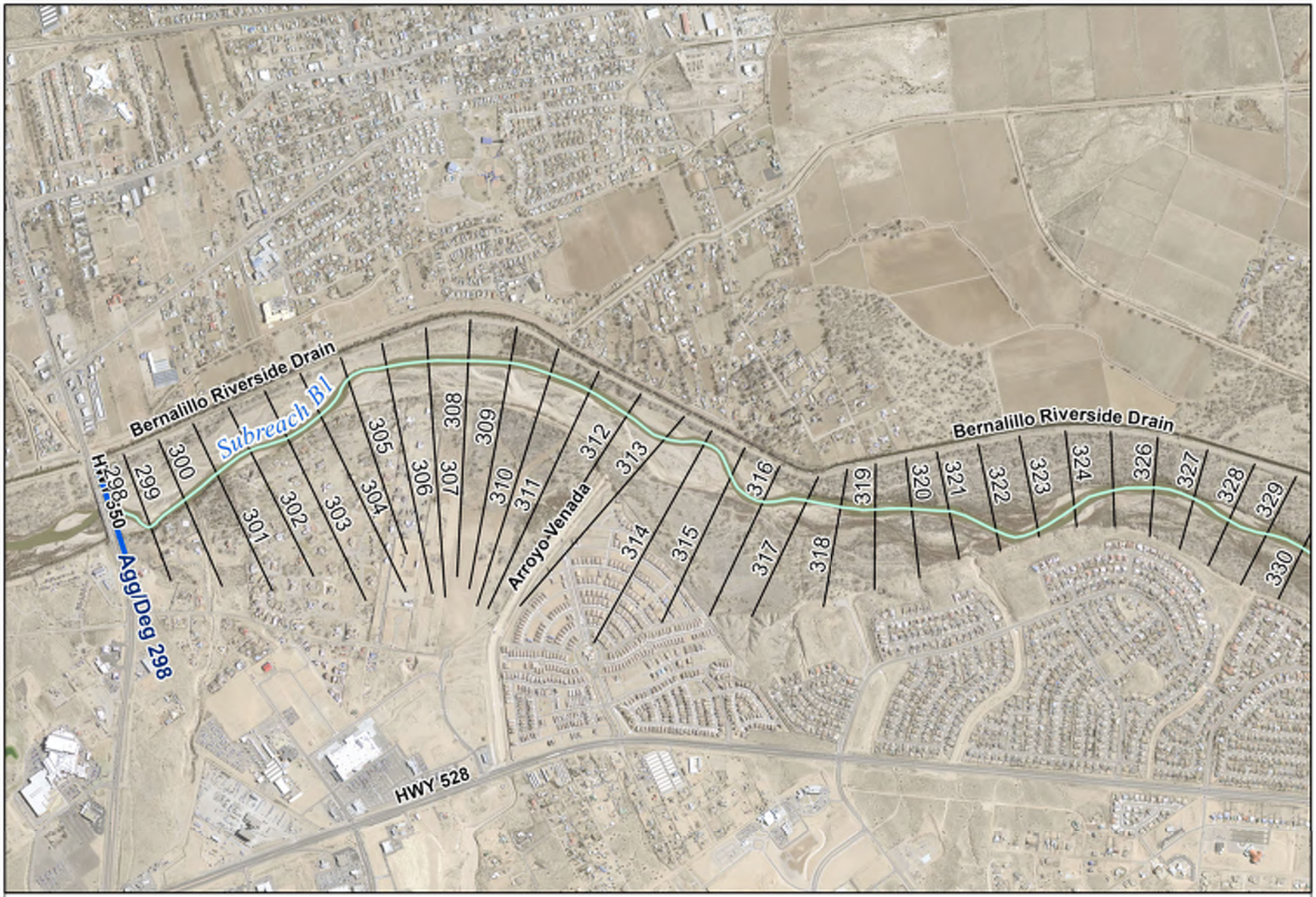

Rio Grande Subreach Map
Bernalillo to Montano

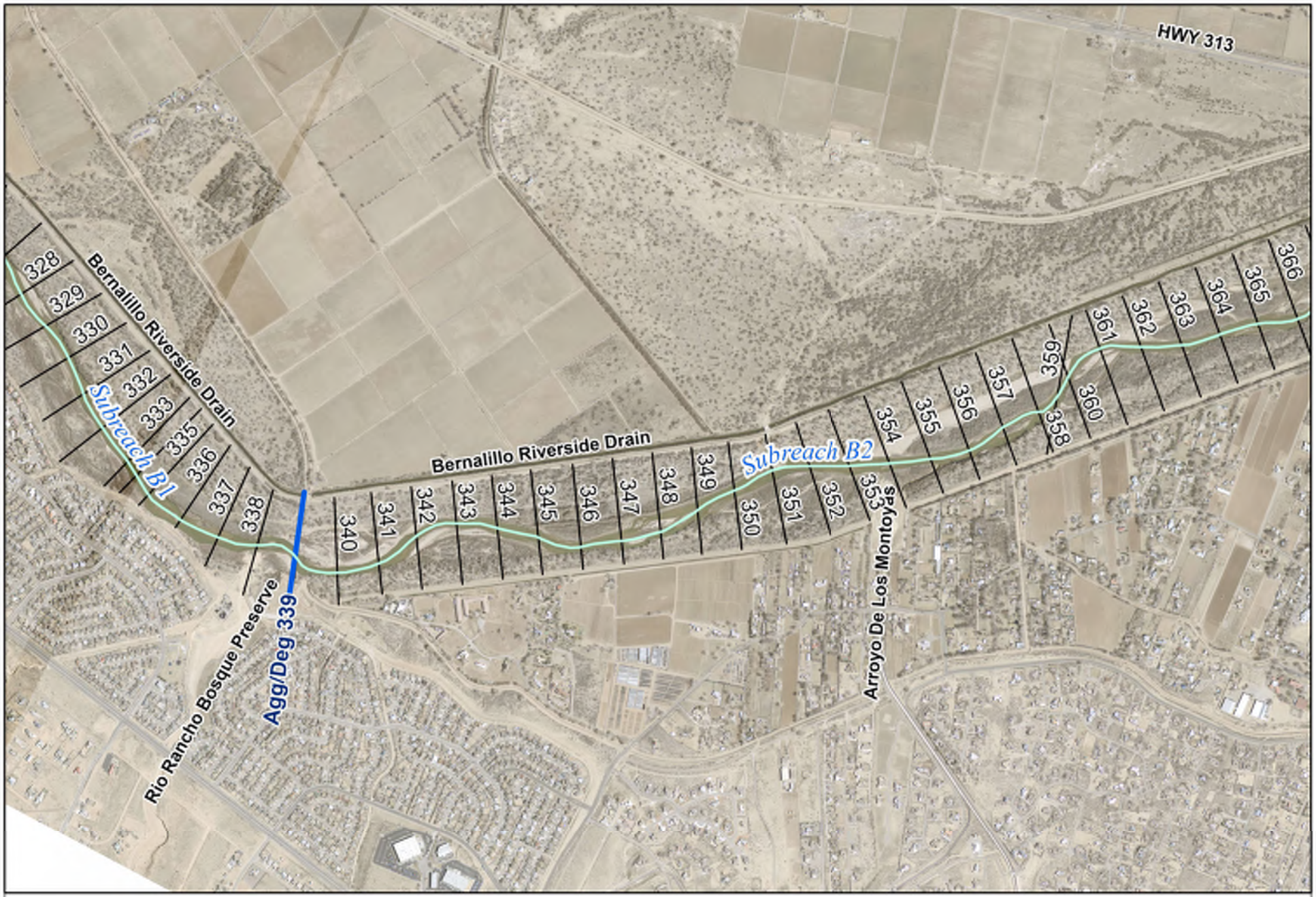

Rio Grande Subreach Map
Bernalillo to Montano

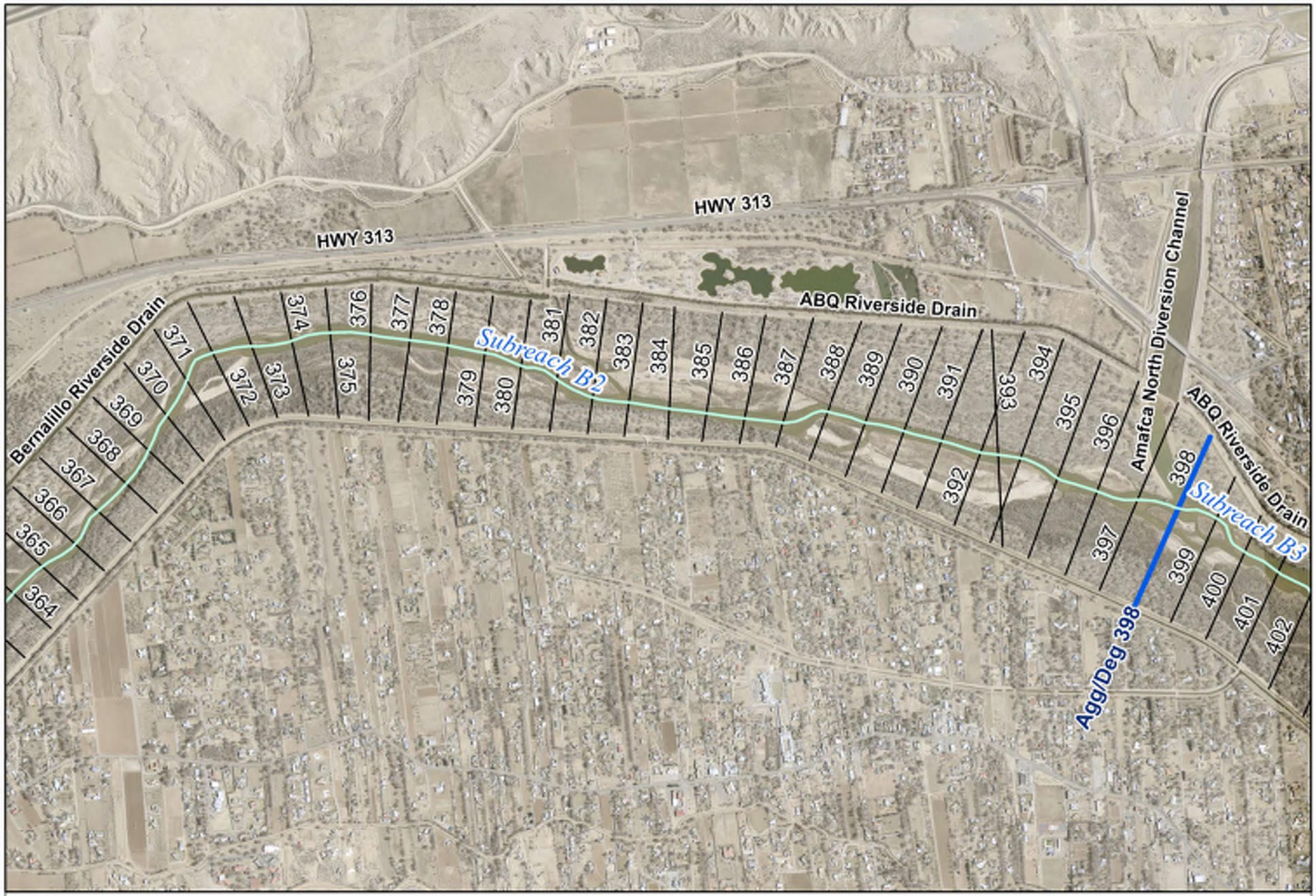

Rio Grande Subreach Map
Bernalillo to Montano

Rio Grande Subreach Map
Bernalillo to Montano

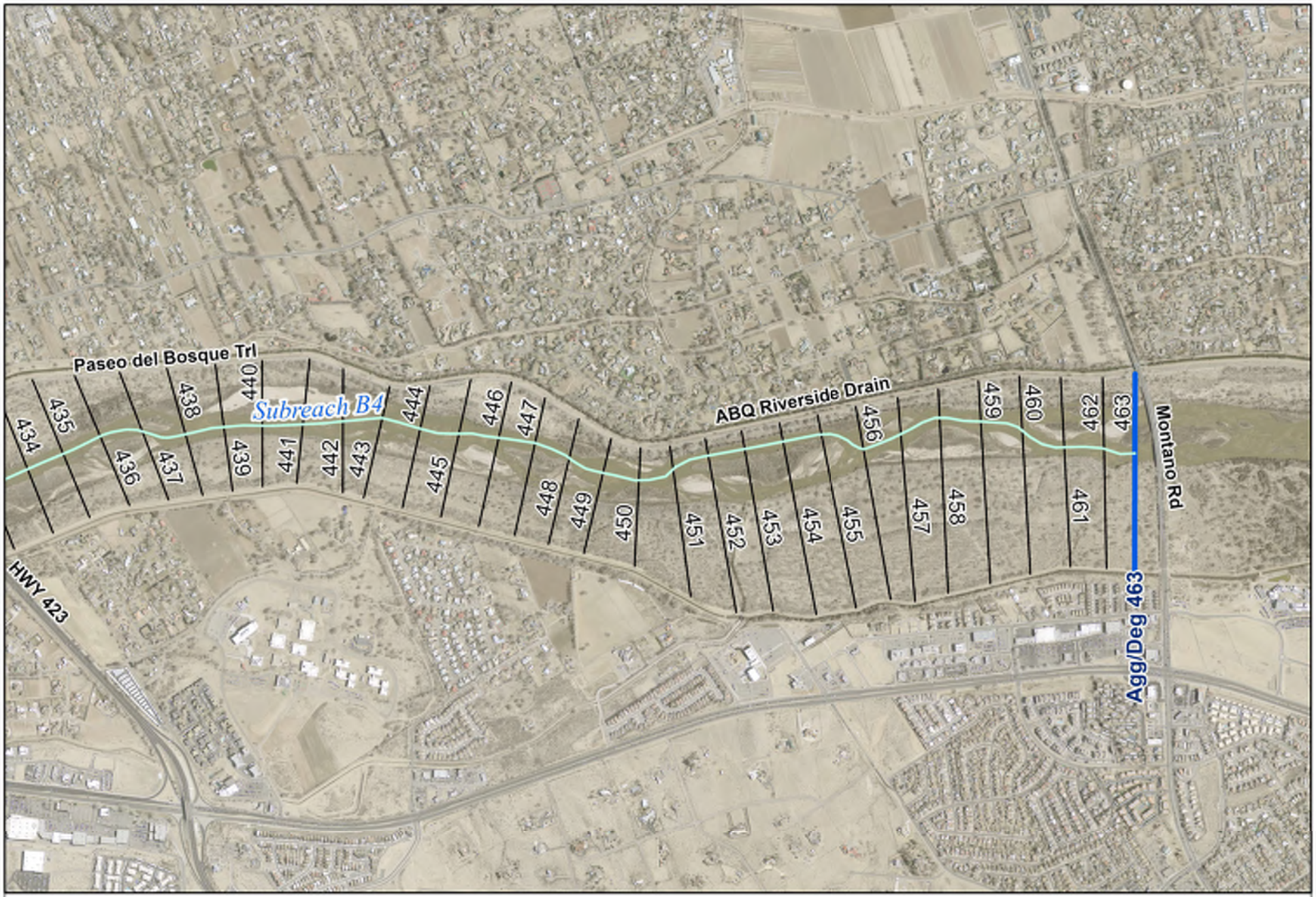

2,500 1,250 0 2,500 Feet

Rio Grande Subreach Map
Bernalillo to Montano

Appendix B

Years used in JW Calculations for D50

Table B-1 Years used in JW Calculations for D50

Year Analyzed	Subreach	Year Used
1992	B1	1991
	B2	1991
	B3	1990
	B4	1991
2002	B1	2001
	B2	2001
	B3	2001
	B4	2001
2012	B1	2012
	B2	2012
	B3	2012
	B4	2012

Appendix C

Additional Figures from Geomorphology Analyses

(Sediment Rating Curve/Alpha Method Example)

Wetted Top Width Plots

In Section 3.1, the cross-section moving averaged top width was plotted for all agg/deg lines in the Bernalillo Reach. Figures C-1, C-2, and C-3 show each cross-section top width plotted against the agg/deg lines rather than the moving average at discharges of 1,000 cfs, 3,000 cfs, and 5,000 cfs.

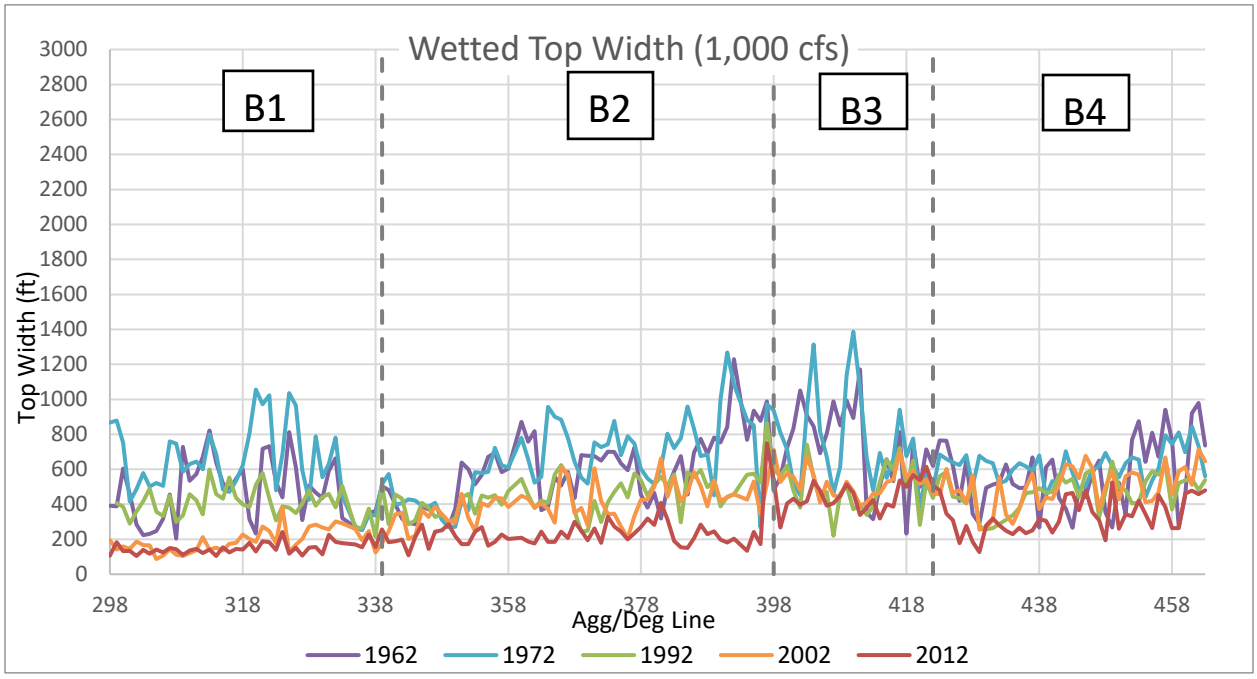

Figure C-1 Wetted top width at each agg/deg line in the Bernalillo Reach at a discharge of 1,000 cfs

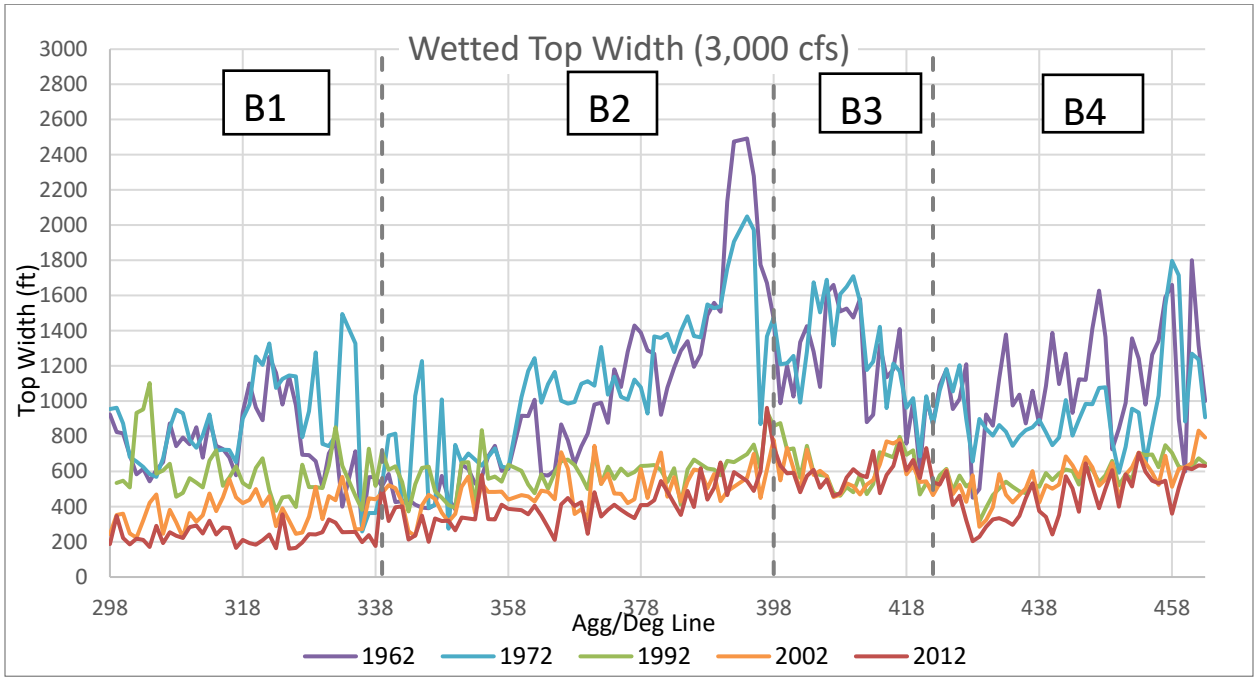

Figure C-2 Wetted top width at each agg/deg line in the Bernalillo Reach at a discharge of 3,000 cfs

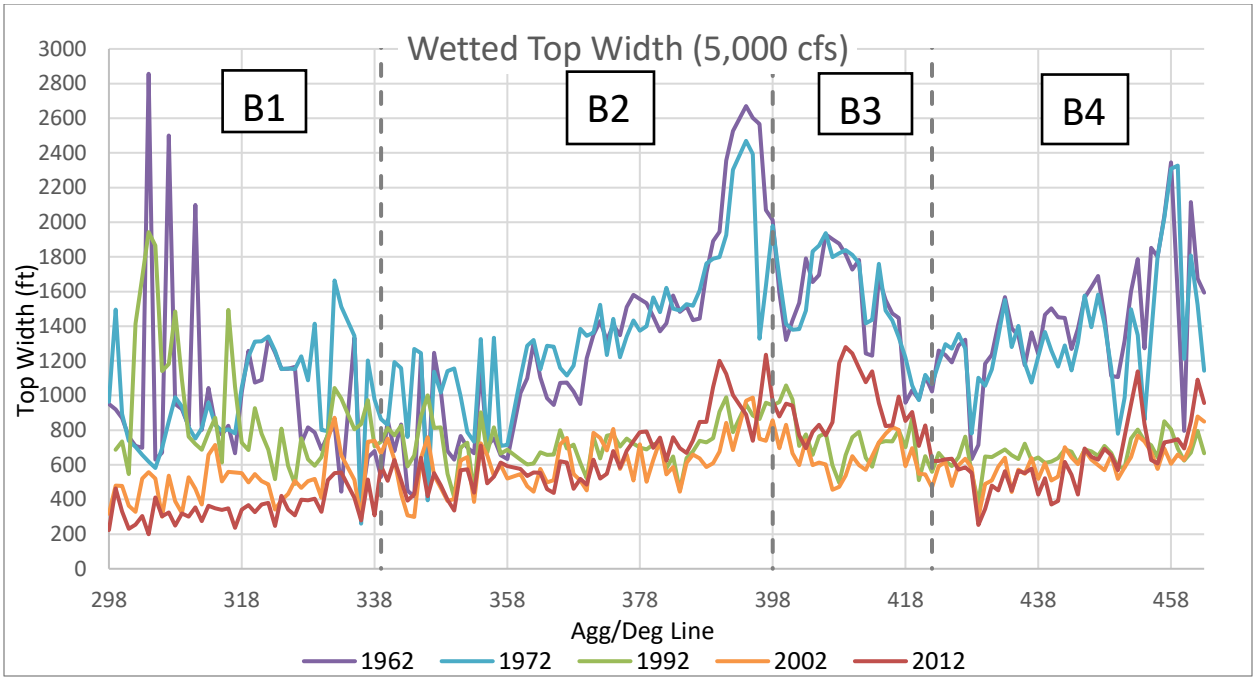

Figure C-3 Wetted top width at each agg/deg line in the Bernalillo Reach at a discharge of 5,000 cfs

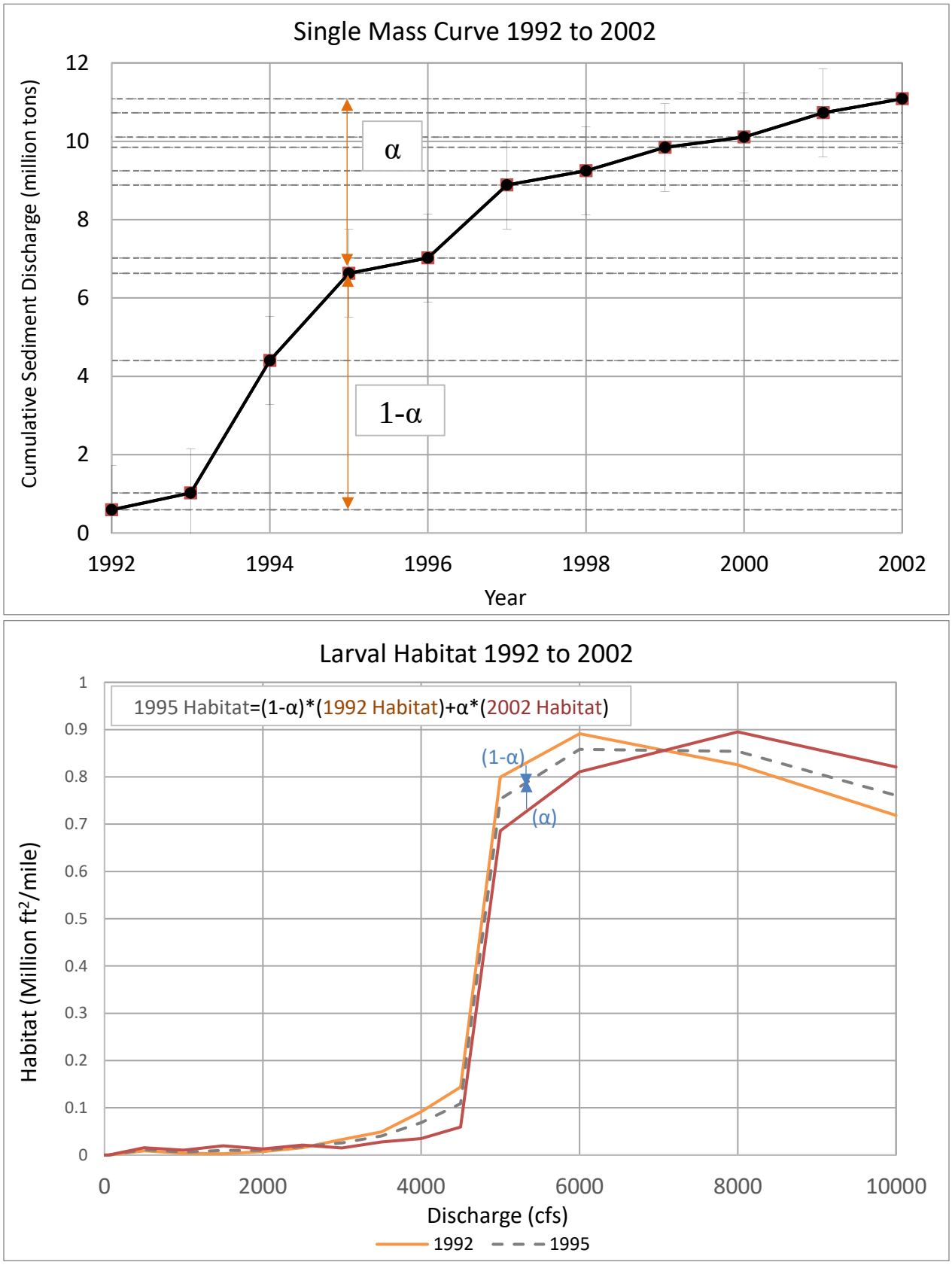

Figure C-4 Example of annual habitat interpolating using the sediment rating curve and alpha technique

Appendix D

Additional Figures from Habitat Analyses

(Habitat Charts by Subreach, Spatially Varying Habitat Charts, Habitat Curves)

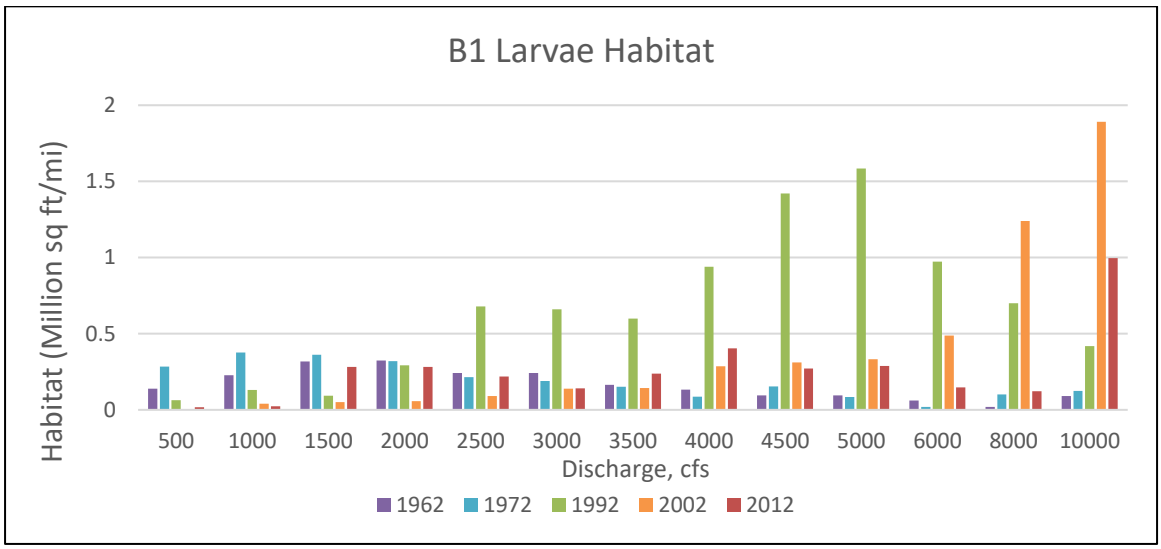

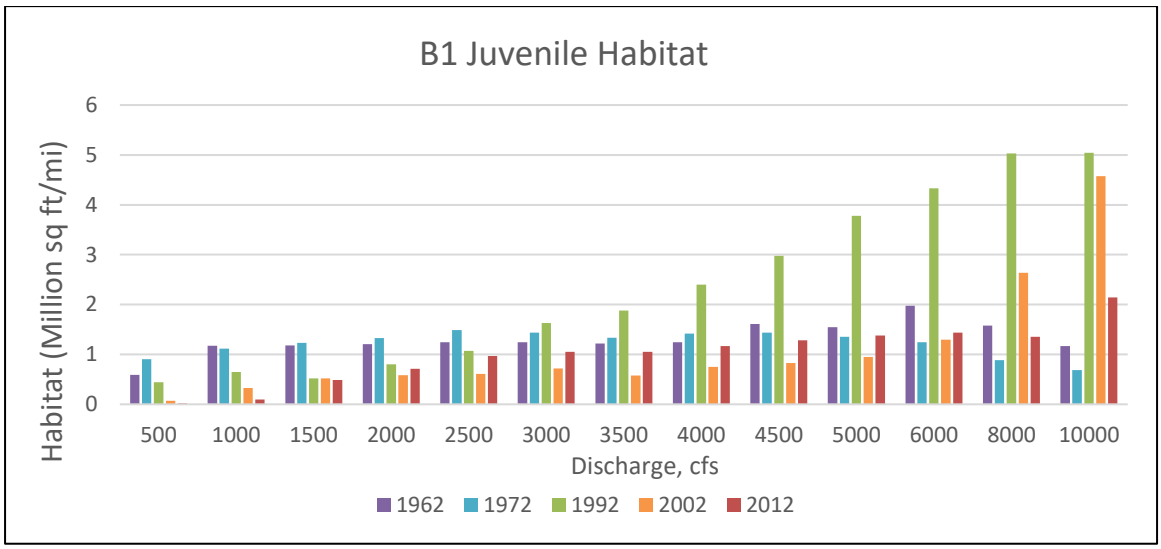

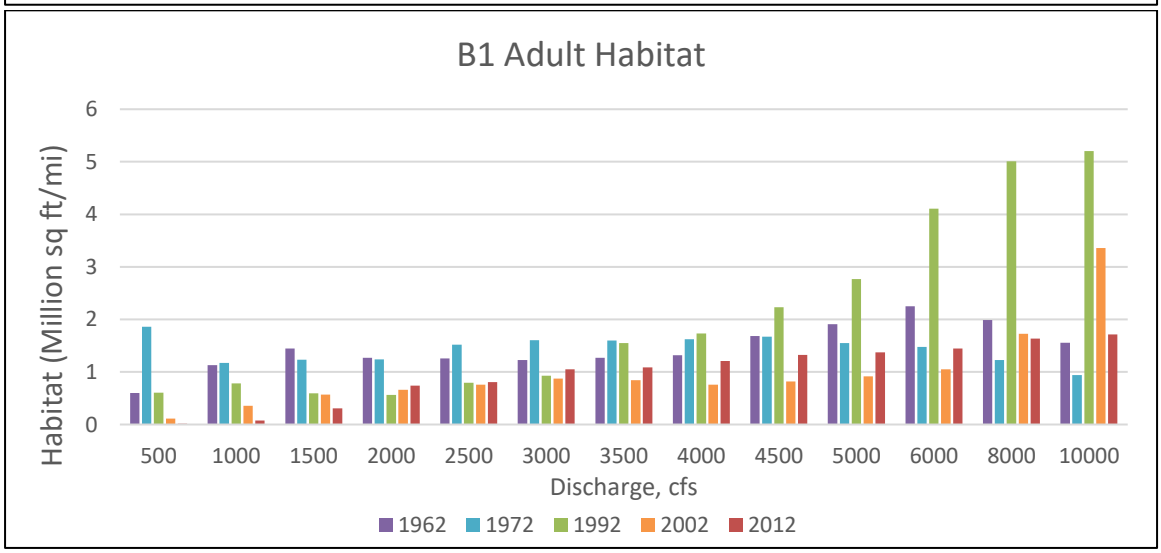

Figure D-1 RGSM habitat availability in Bernalillo Subreach, B1

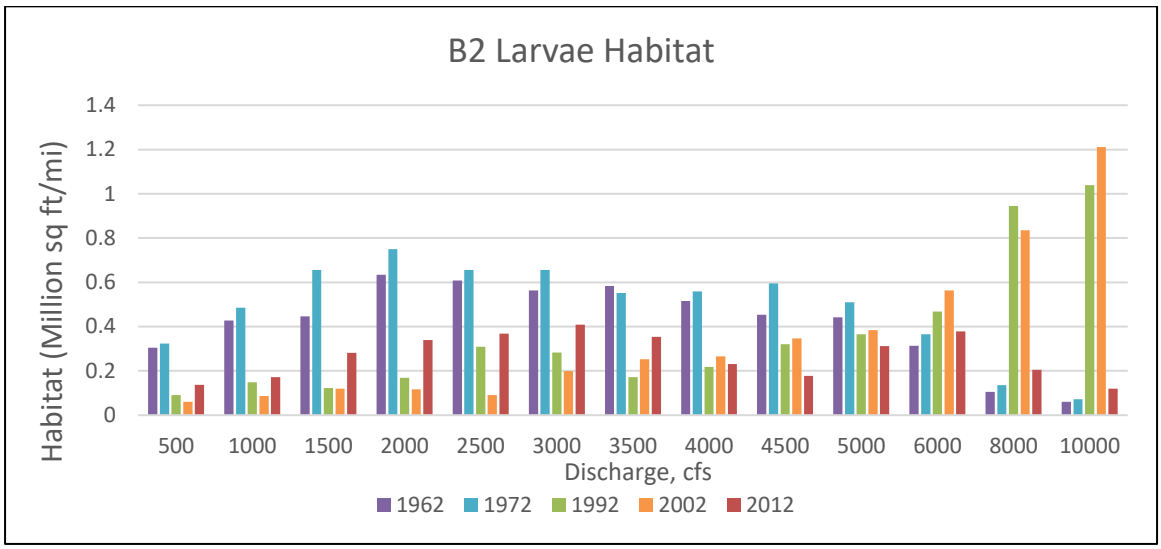

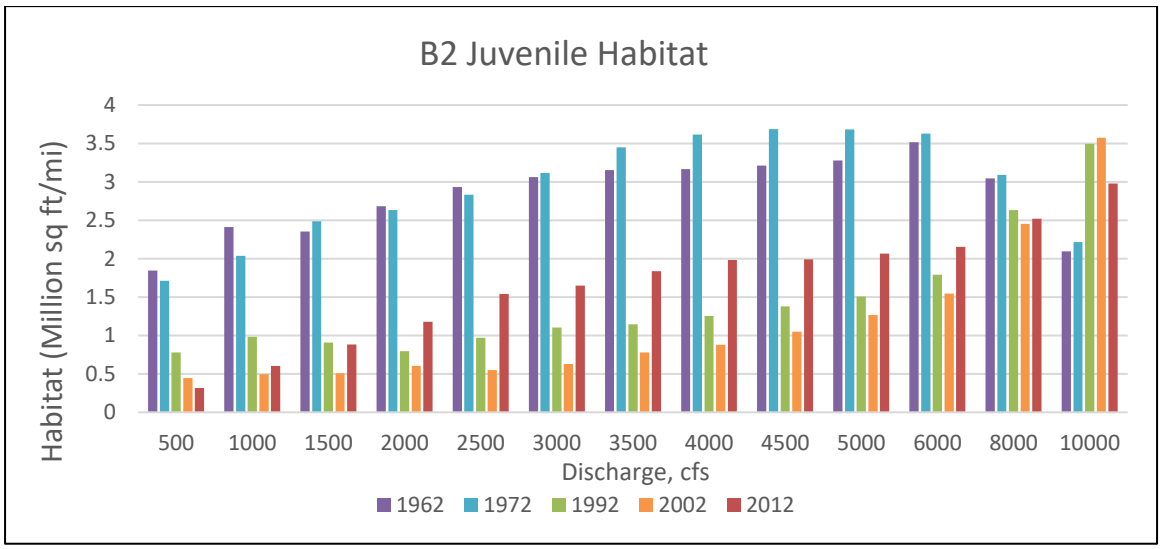

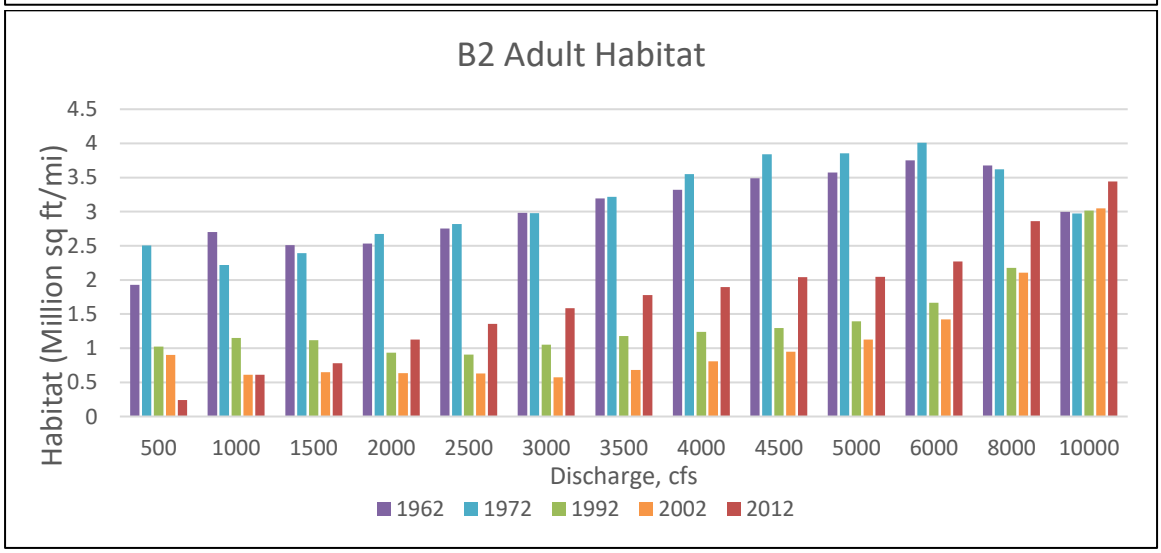

Figure D-2 RGSM habitat availability in Bernalillo Subreach, B2

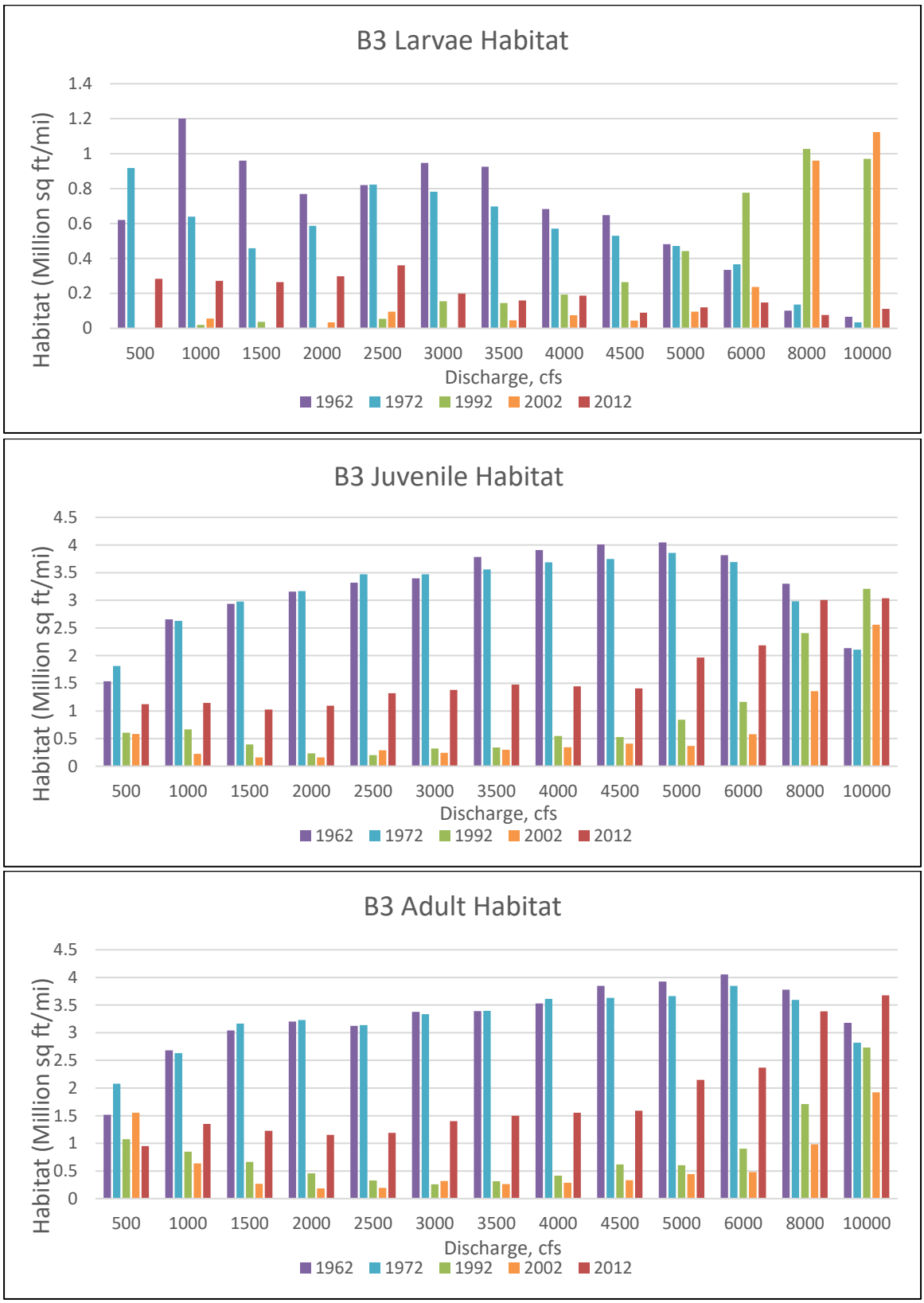

Figure D-3 RGSM habitat availability in Bernalillo Subreach, B3

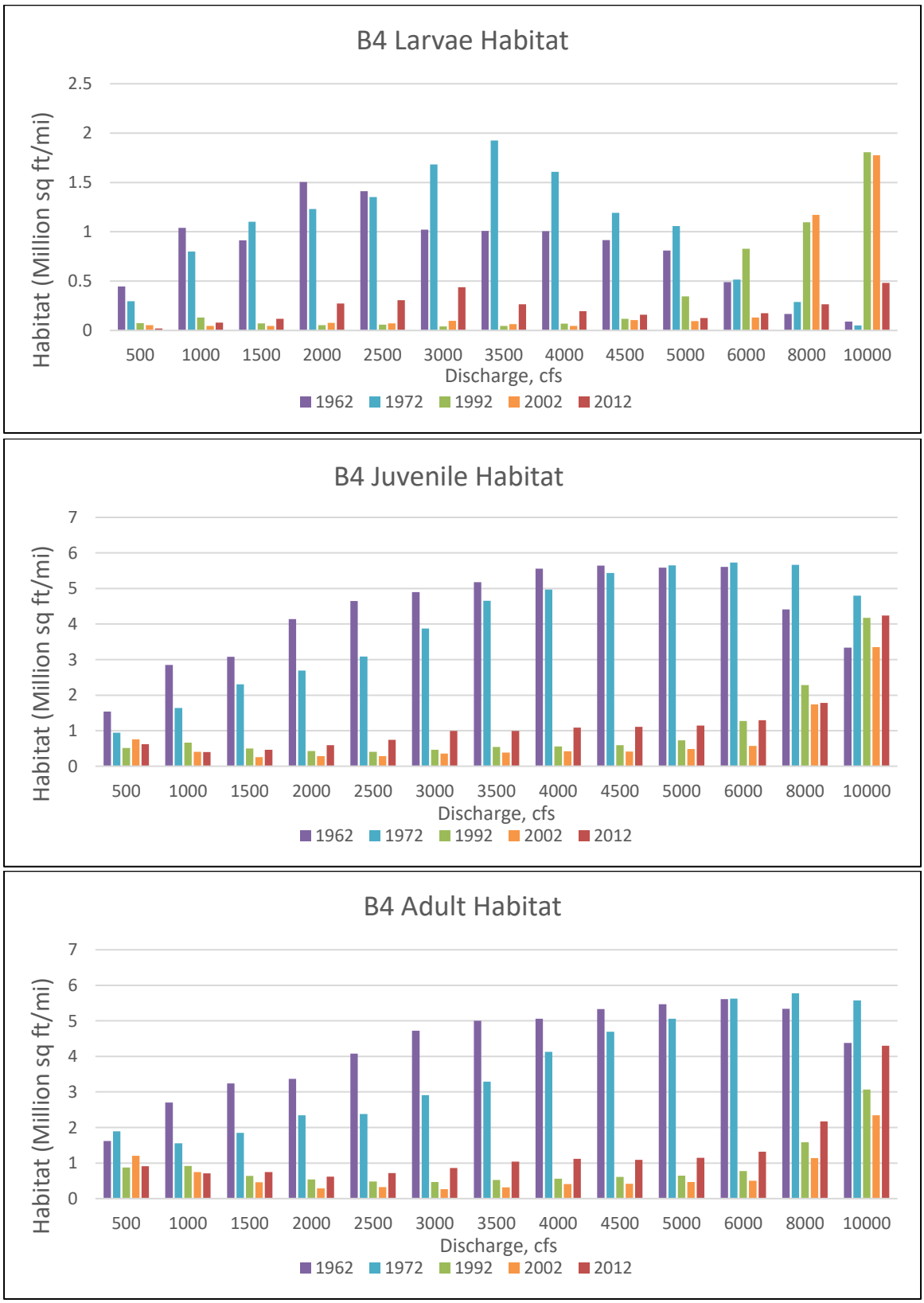

Figure D-4 RGSM habitat availability in Bernalillo Subreach, B4

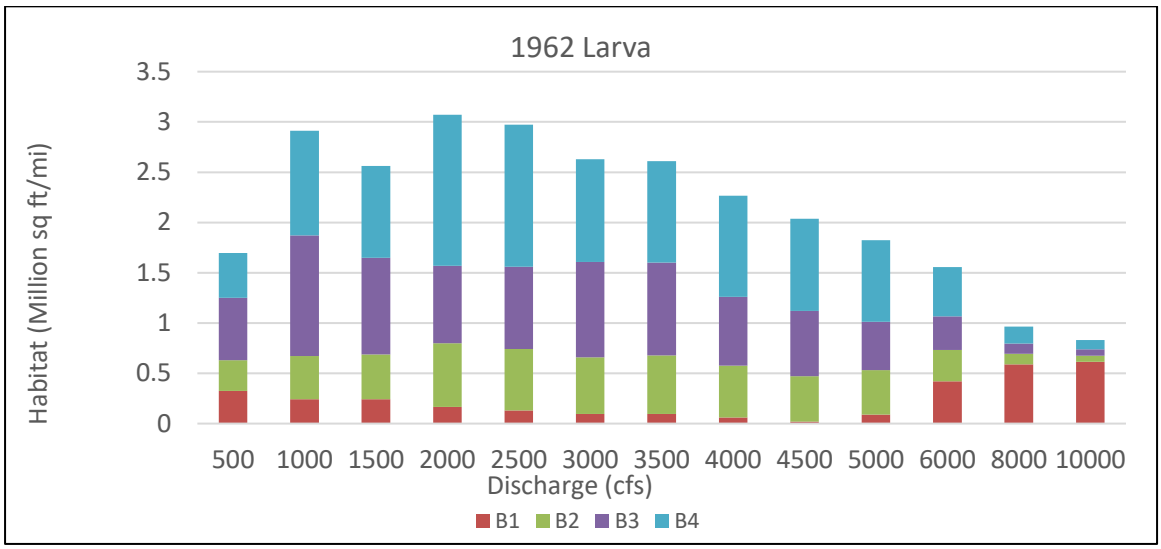

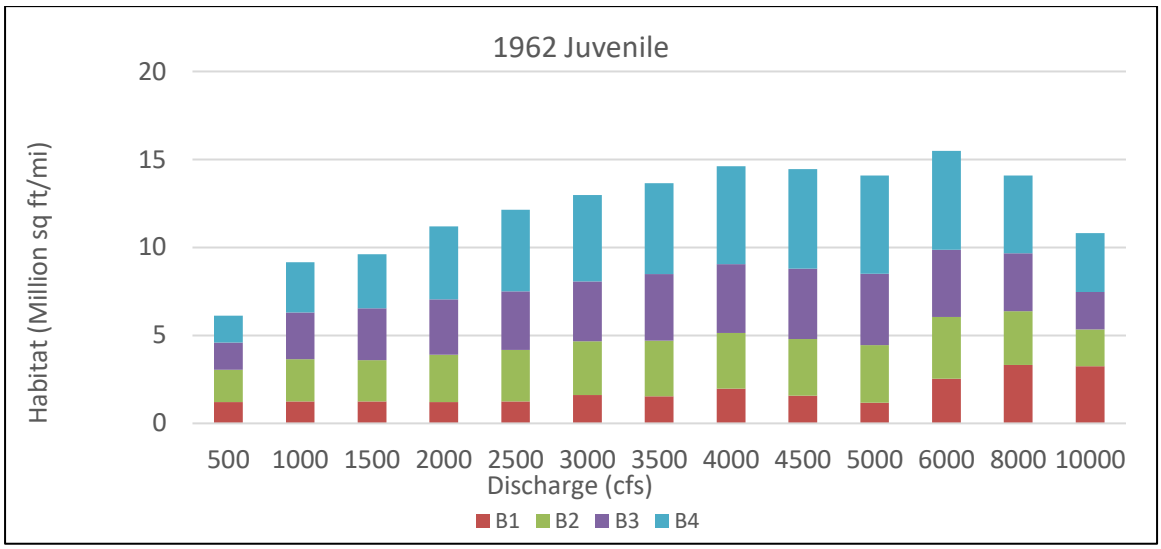

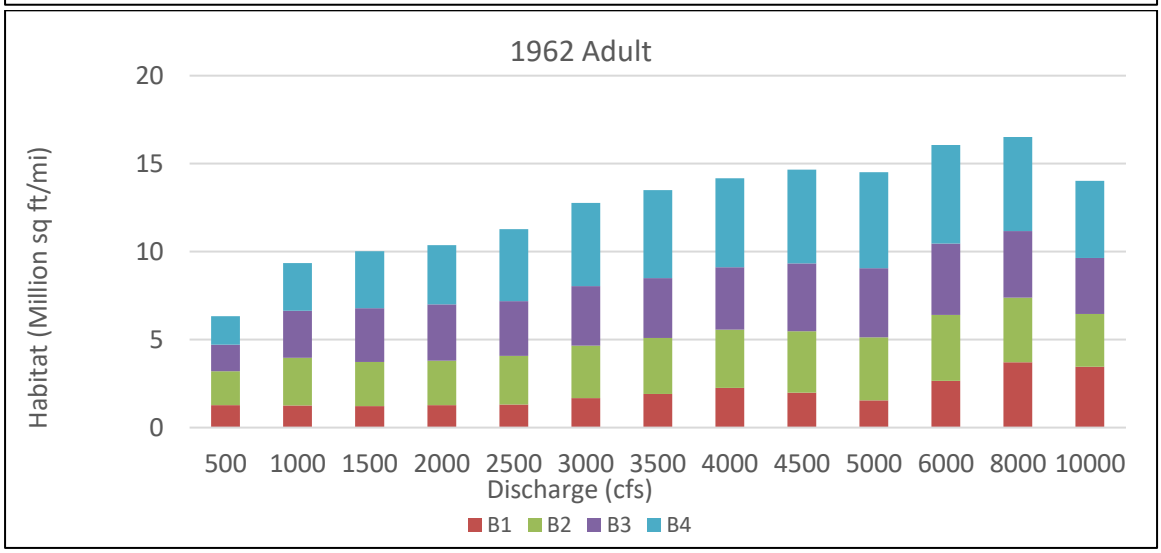

Figure D-5 Stacked habitat charts at different scales to display spatial variations of habitat throughout the Bernalillo reach in 1962

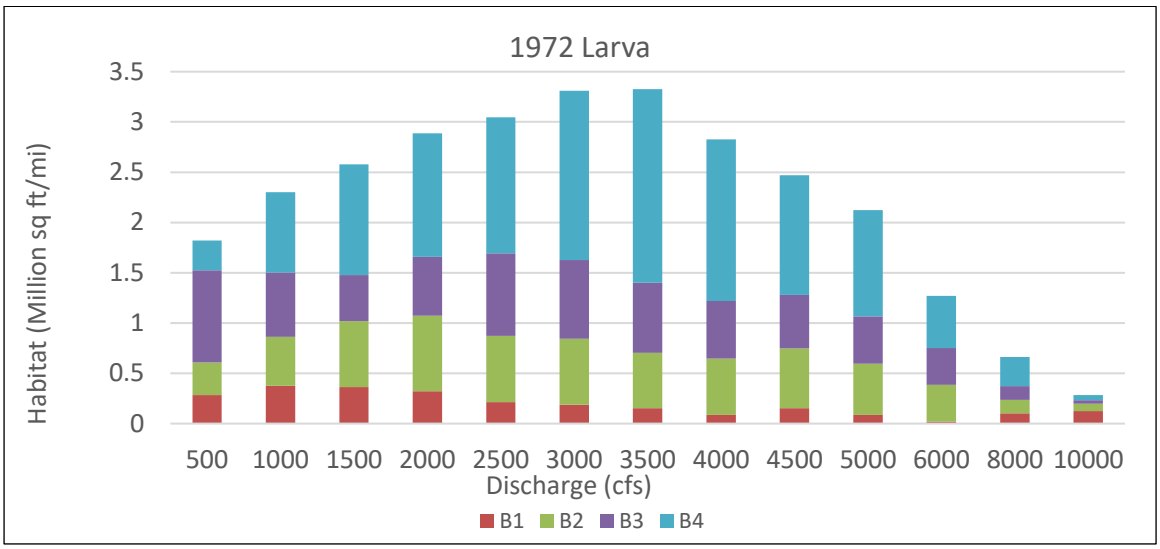

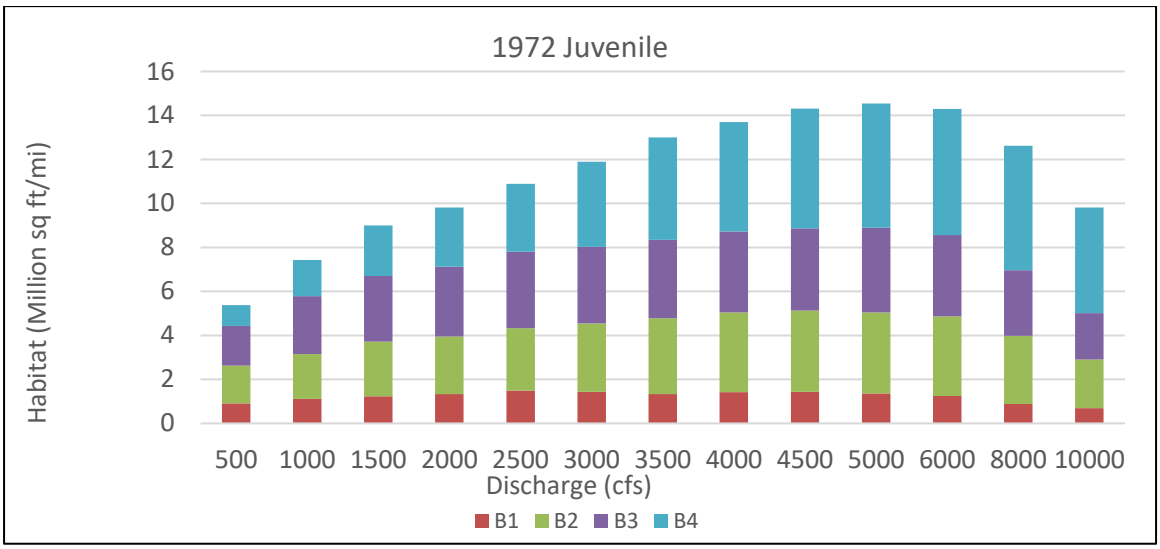

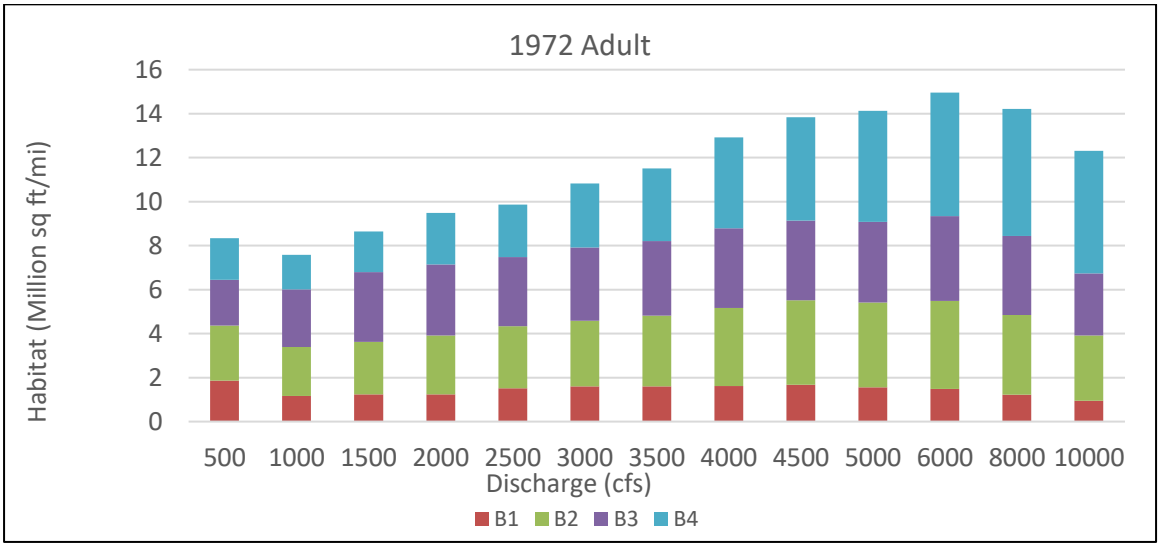

Figure D-6 Stacked habitat charts at different scales to display spatial variations of habitat throughout the Bernalillo reach in 1972

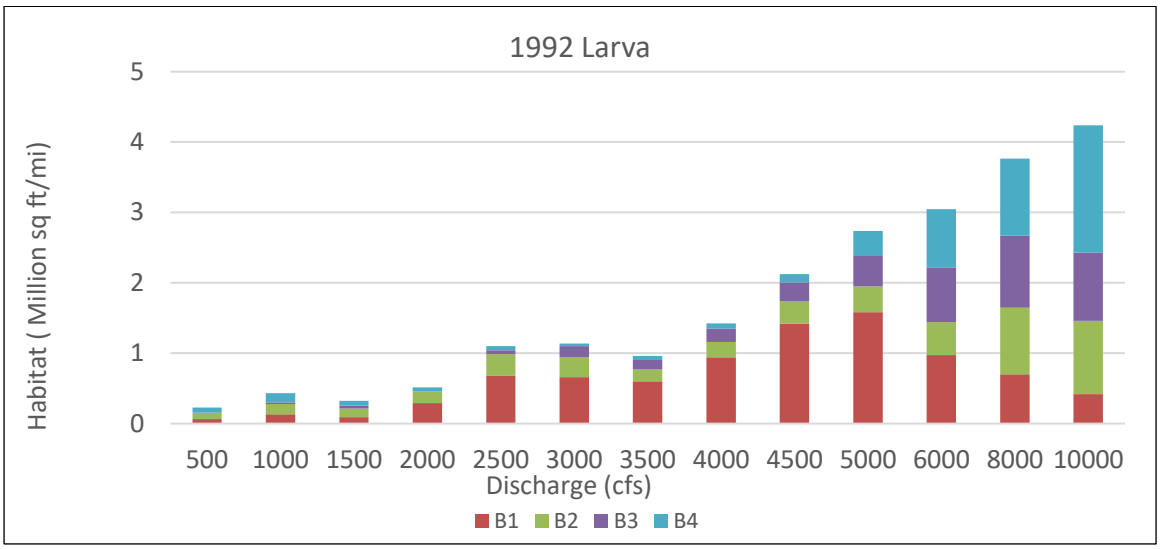

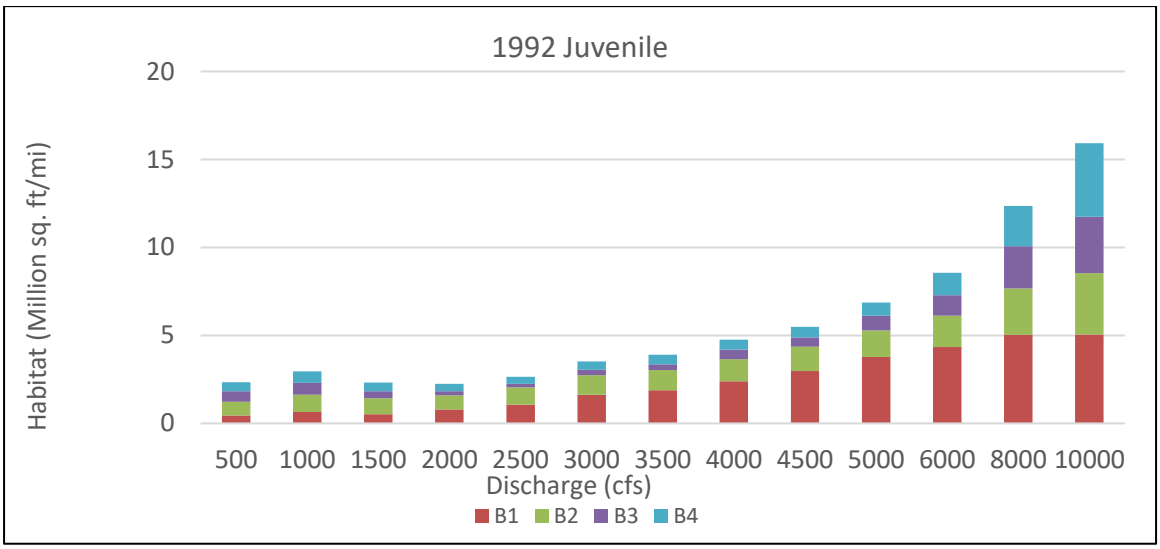

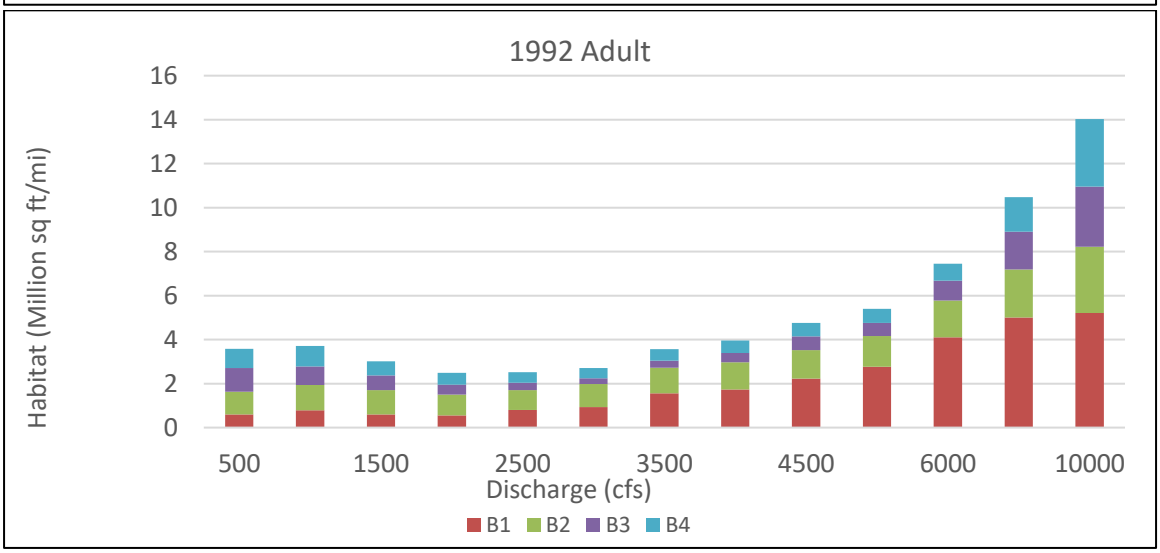

Figure D-7 Stacked habitat charts at different scales to display spatial variations of habitat throughout the Bernalillo reach in 1992

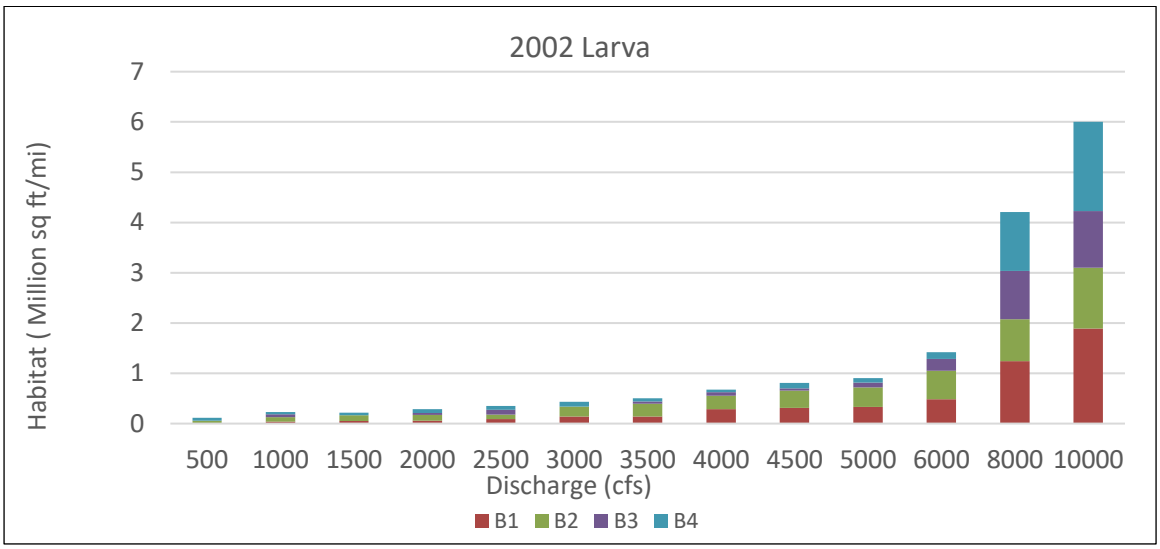

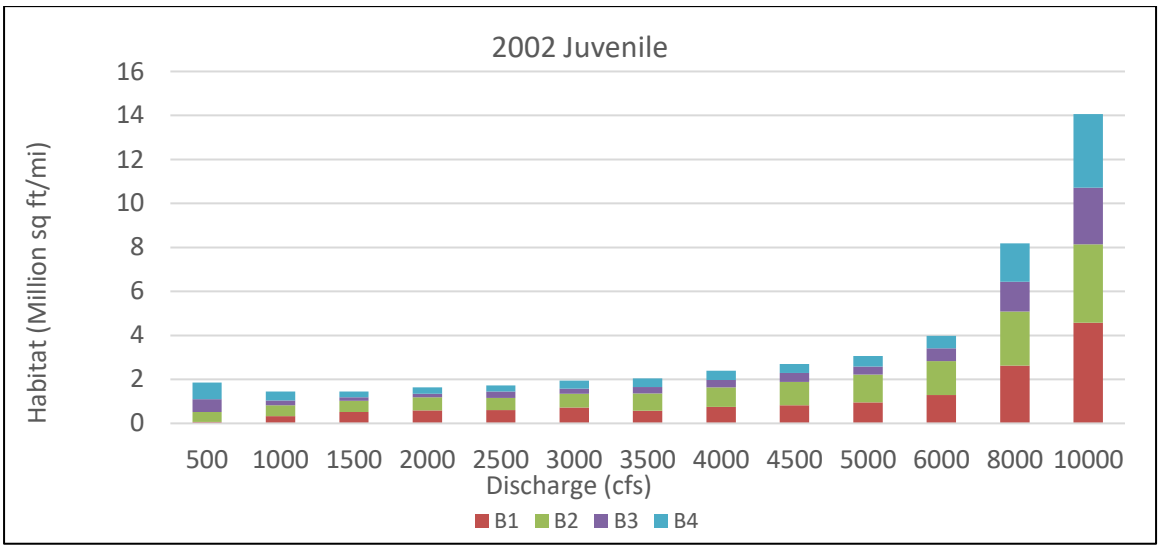

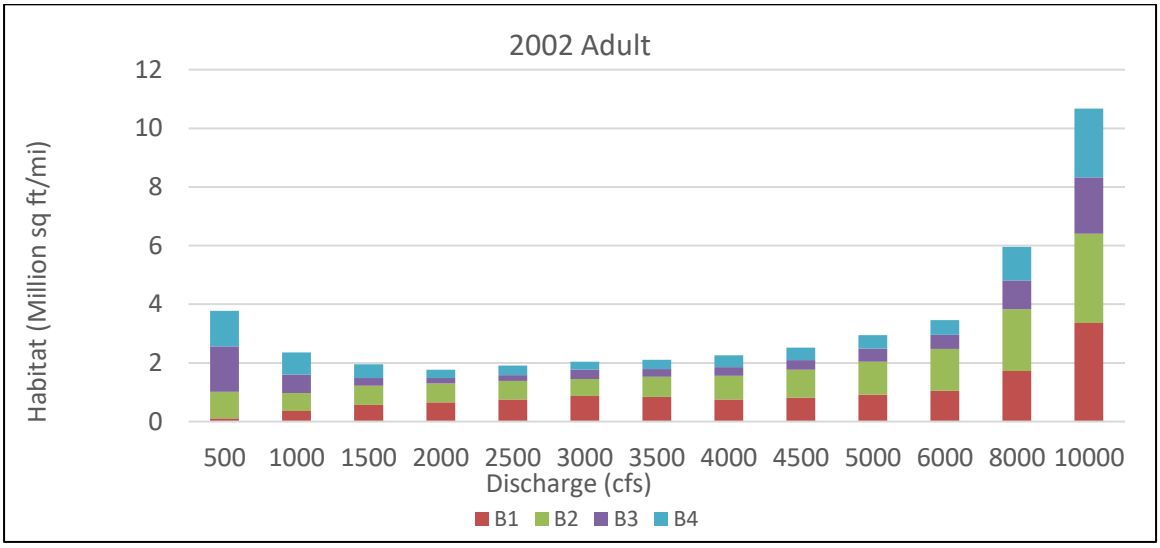

Figure D-8 Stacked habitat charts at different scales to display spatial variations of habitat throughout the Bernalillo reach in 2002

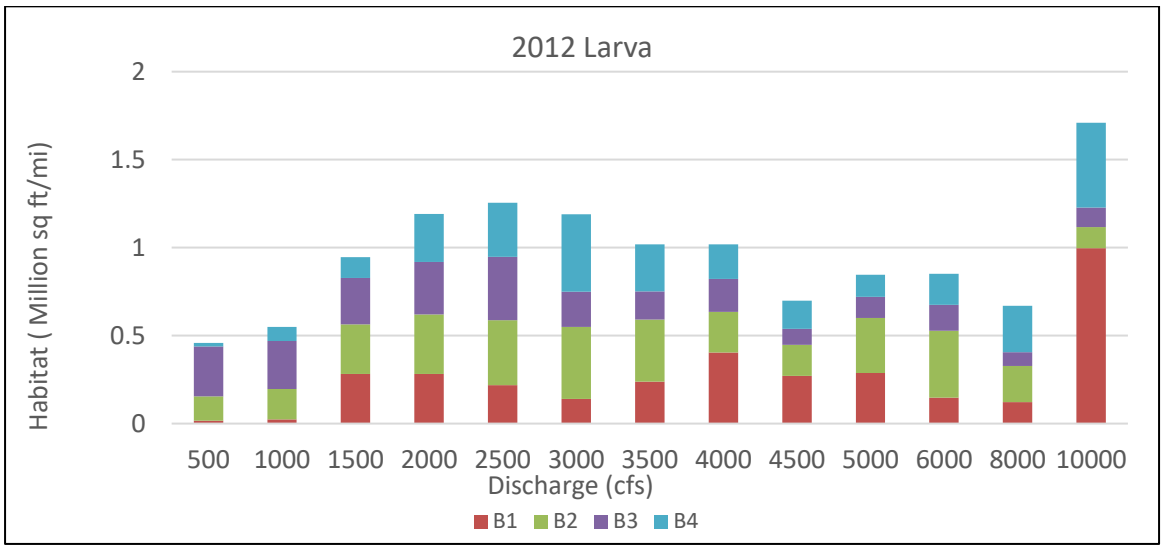

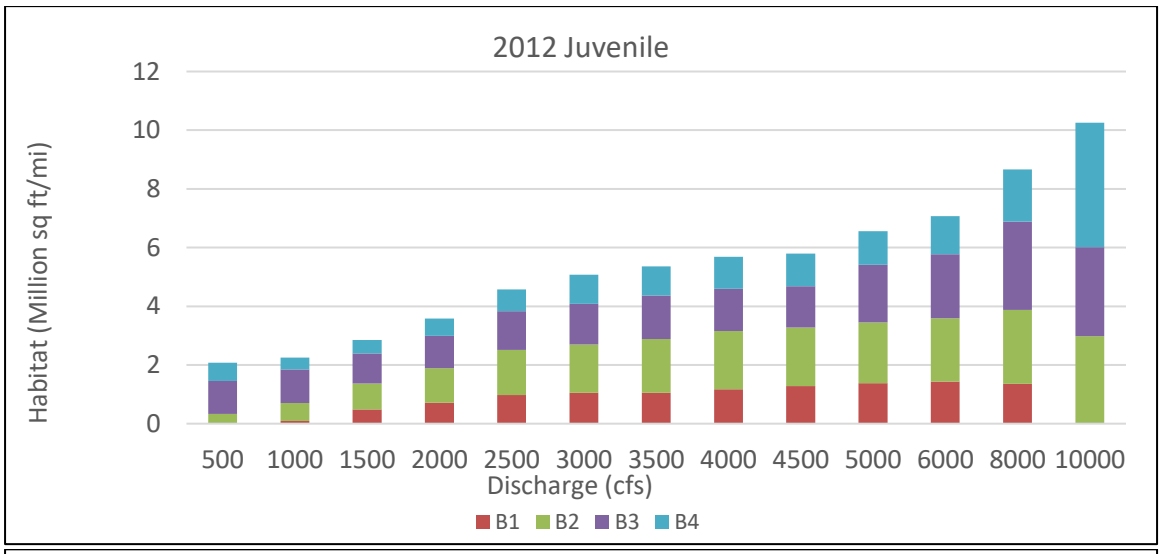

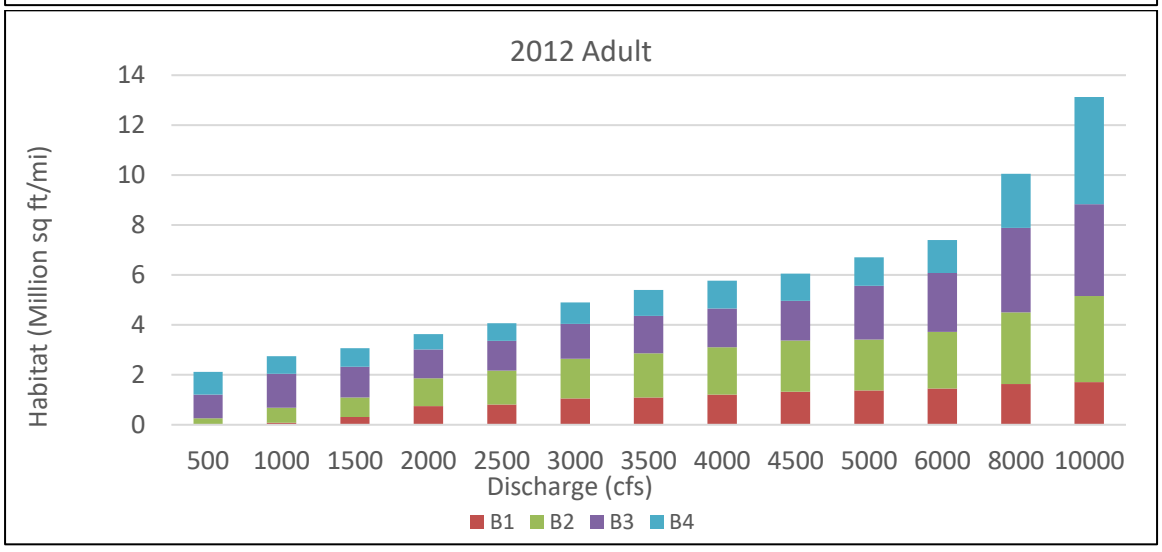

Figure D-9 Stacked habitat charts at different scales to display spatial variations of habitat throughout the Bernalillo reach in 2012

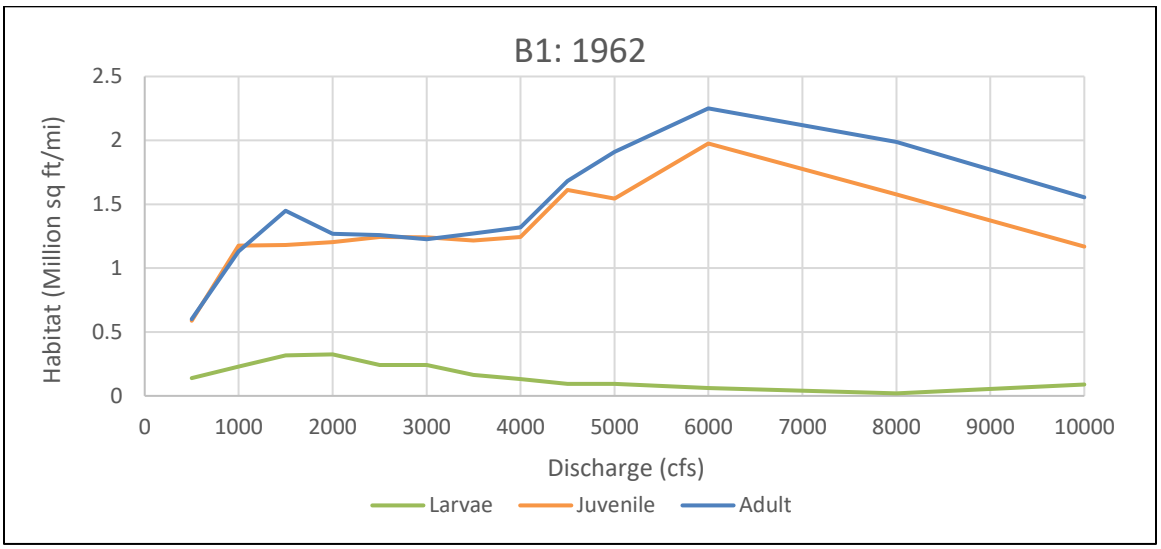
B1: 1962
Habitat (Million sq ft/mi)
2.5
2
1.5
1
0.5
0
0
1000
2000
3000
4000
5000
6000
7000
8000
9000
10000
Discharge (cfs)
Larvae
Juvenile
Adult

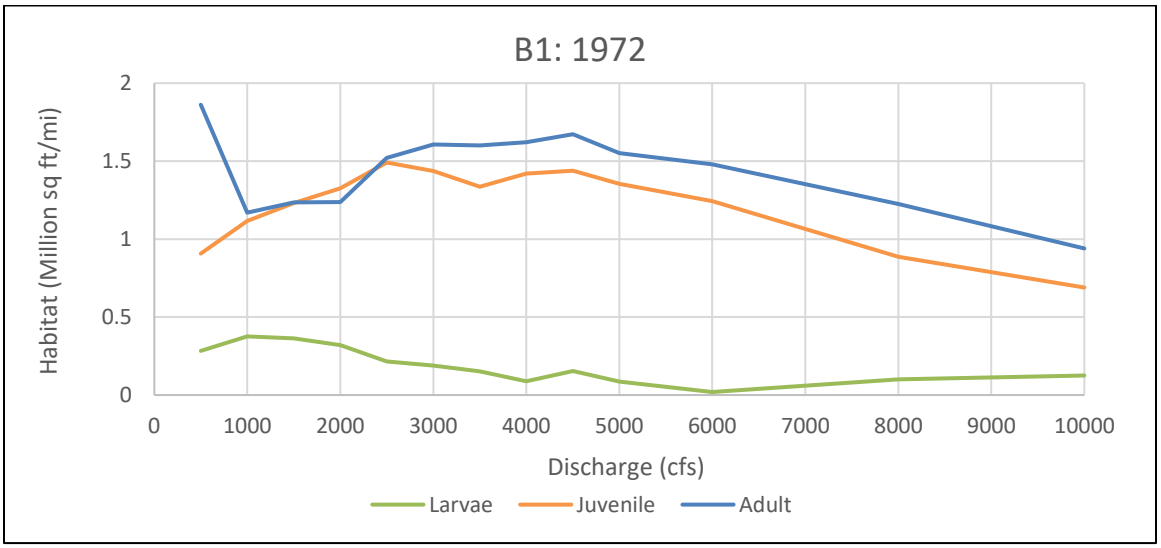
B1: 1972
Habitat (Million sq ft/mi)
2
1.5
1
0.5
0
0
1000
2000
3000
4000
5000
6000
7000
8000
9000
10000
Discharge (cfs)
Larvae
Juvenile
Adult

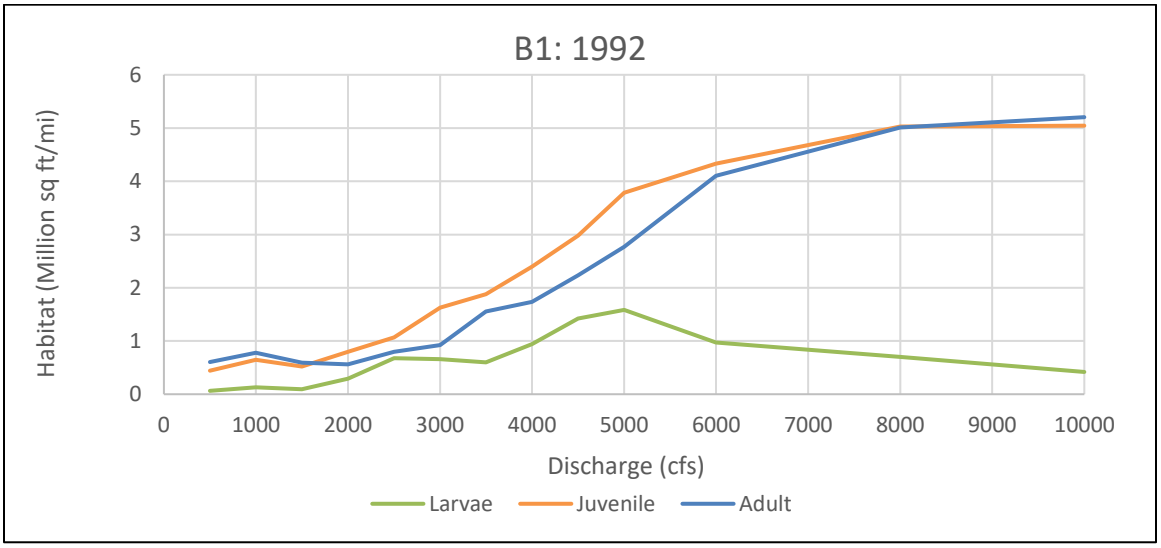
B1: 1992
Habitat (Million sq ft/mi)
6
5
4
3
2
1
0
0
1000
2000
3000
4000
5000
6000
7000
8000
9000
10000
Discharge (cfs)
Larvae
Juvenile
Adult

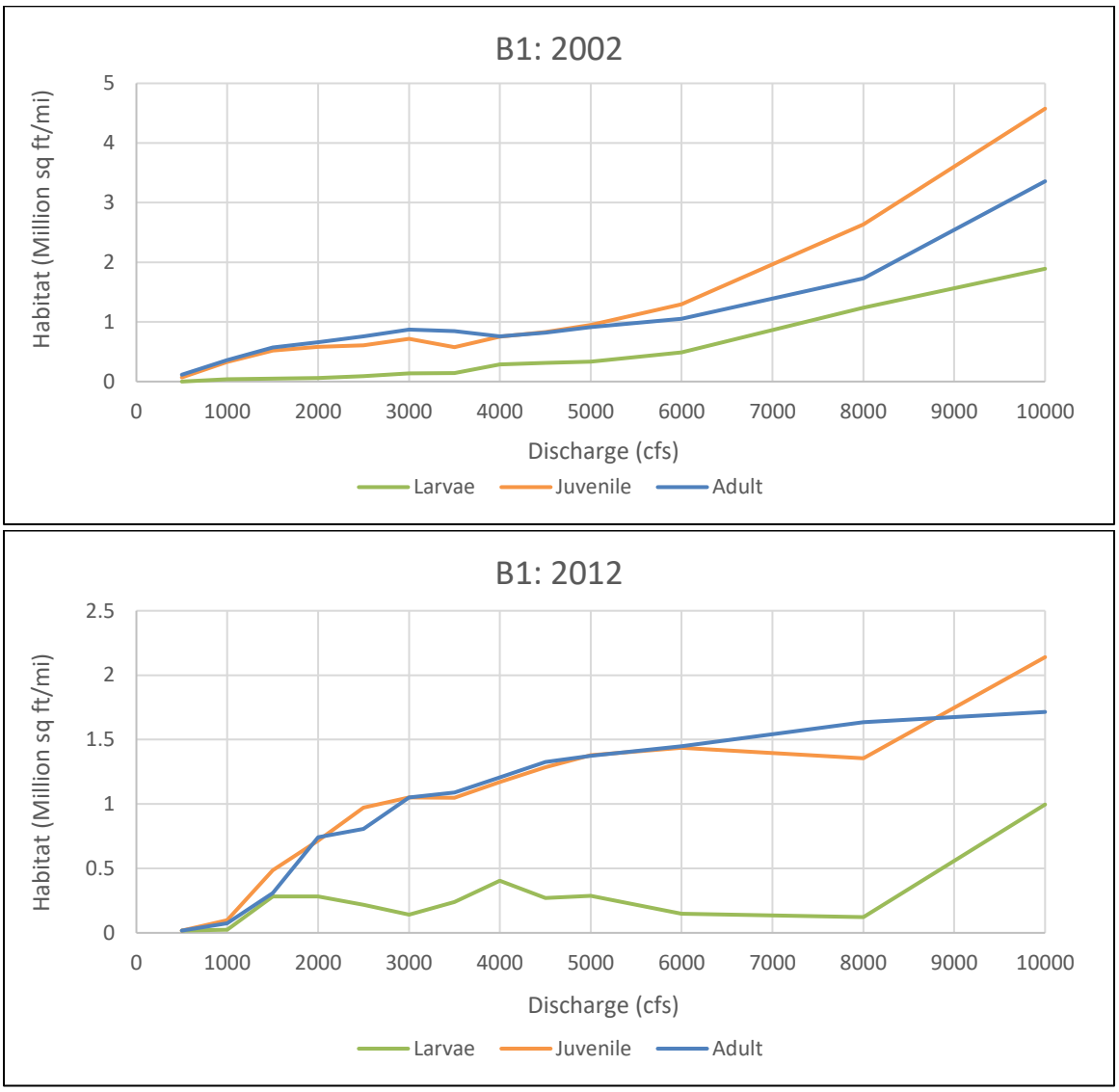

Figure D-10 Life stage habitat curves for Bernalillo Subreach B1 for the years 1962 to 2012.

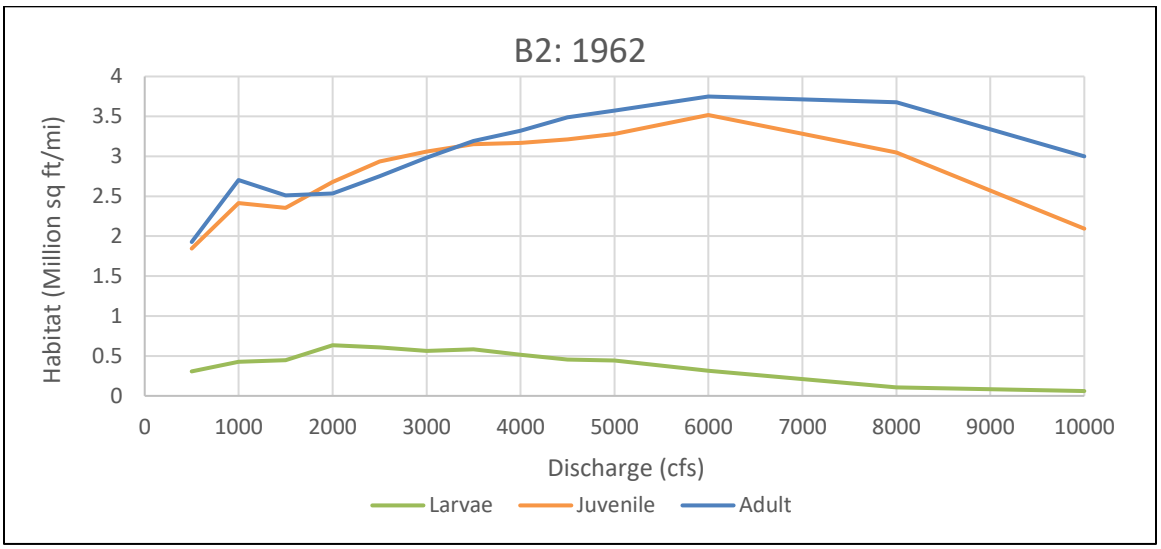
B2: 1962
Habitat (Million sq ft/mi)
4
3.5
3
2.5
2
1.5
1
0.5
0
0
1000
2000
3000
4000
5000
6000
7000
8000
9000
10000
Discharge (cfs)
Larvae
Juvenile
Adult

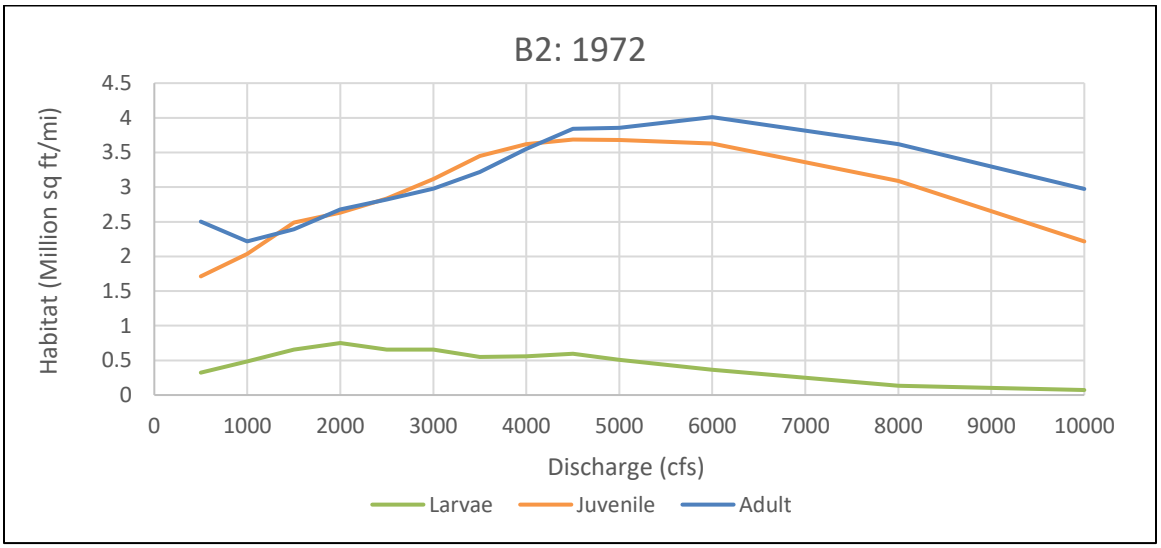
B2: 1972
Habitat (Million sq ft/mi)
4.5
4
3.5
3
2.5
2
1.5
1
0.5
0
0
1000
2000
3000
4000
5000
6000
7000
8000
9000
10000
Discharge (cfs)
Larvae
Juvenile
Adult

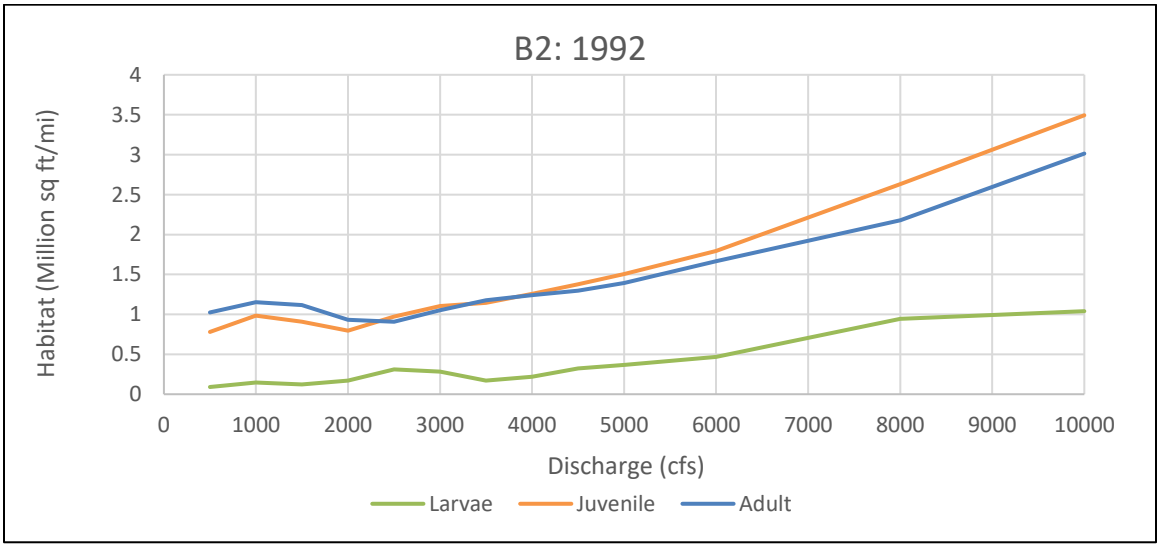
B2: 1992
Habitat (Million sq ft/mi)
4
3.5
3
2.5
2
1.5
1
0.5
0
0
1000
2000
3000
4000
5000
6000
7000
8000
9000
10000
Discharge (cfs)
Larvae
Juvenile
Adult

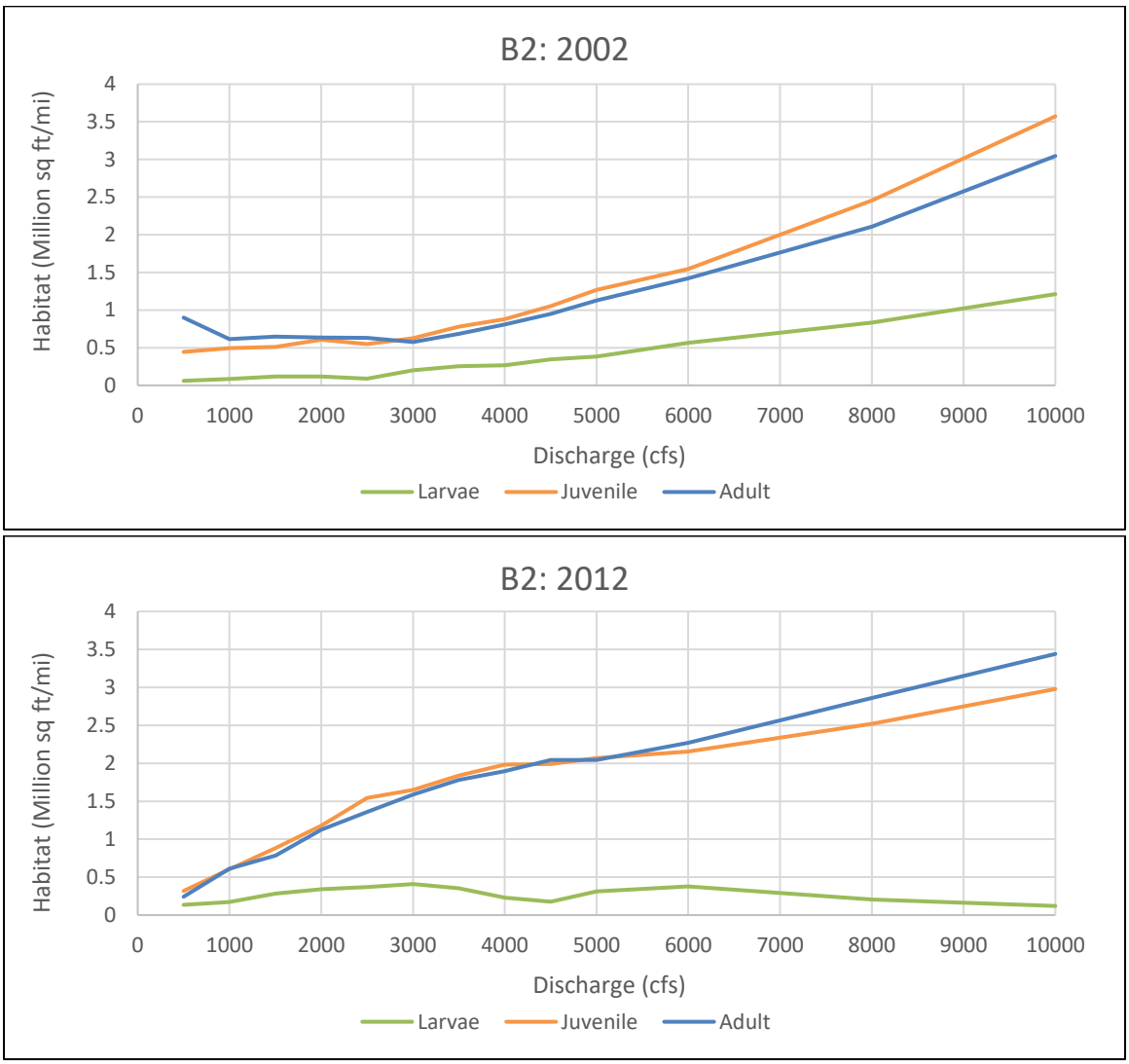

Figure D-11 Life stage habitat curves for Bernalillo Subreach B2 for the years 1962 to 2012.

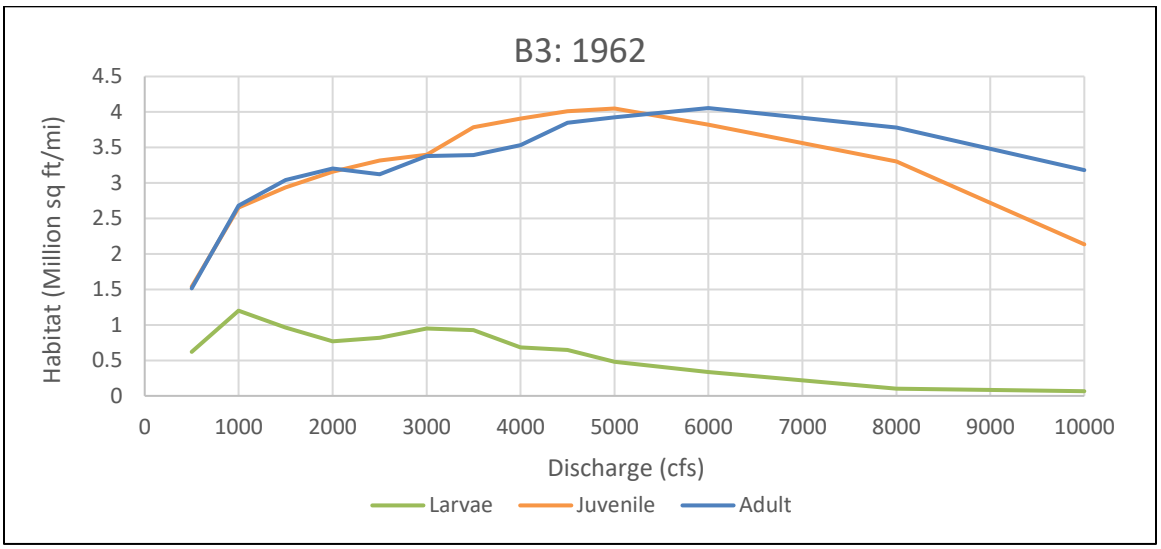
B3: 1962
Habitat (Million sq ft/mi)
4.5
4
3.5
3
2.5
2
1.5
1
0.5
0
0
1000
2000
3000
4000
5000
6000
7000
8000
9000
10000
Discharge (cfs)
Larvae
Juvenile
Adult

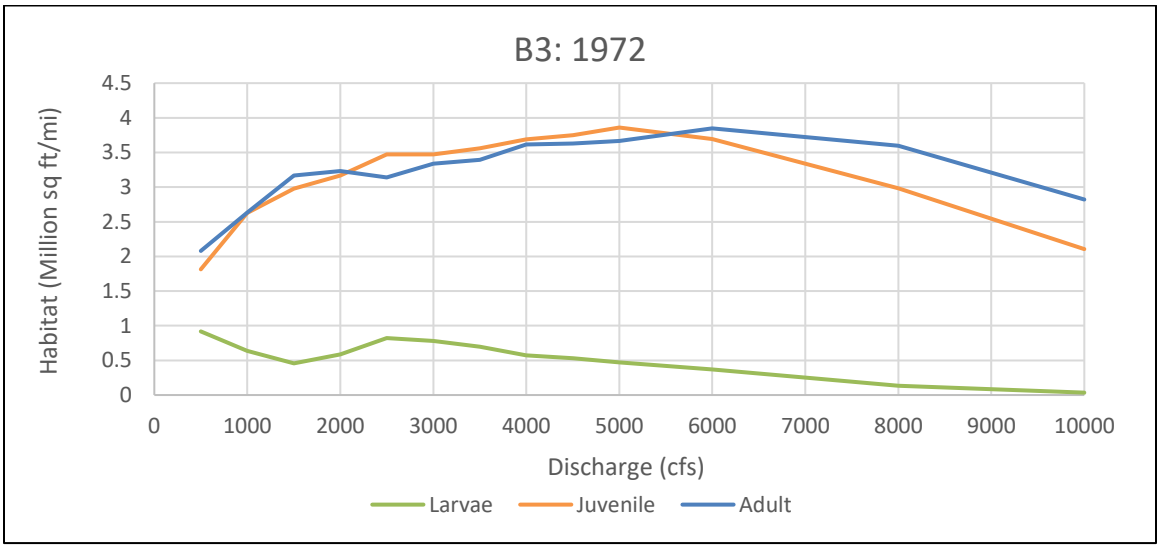
B3: 1972
Habitat (Million sq ft/mi)
4.5
4
3.5
3
2.5
2
1.5
1
0.5
0
0
1000
2000
3000
4000
5000
6000
7000
8000
9000
10000
Discharge (cfs)
Larvae
Juvenile
Adult

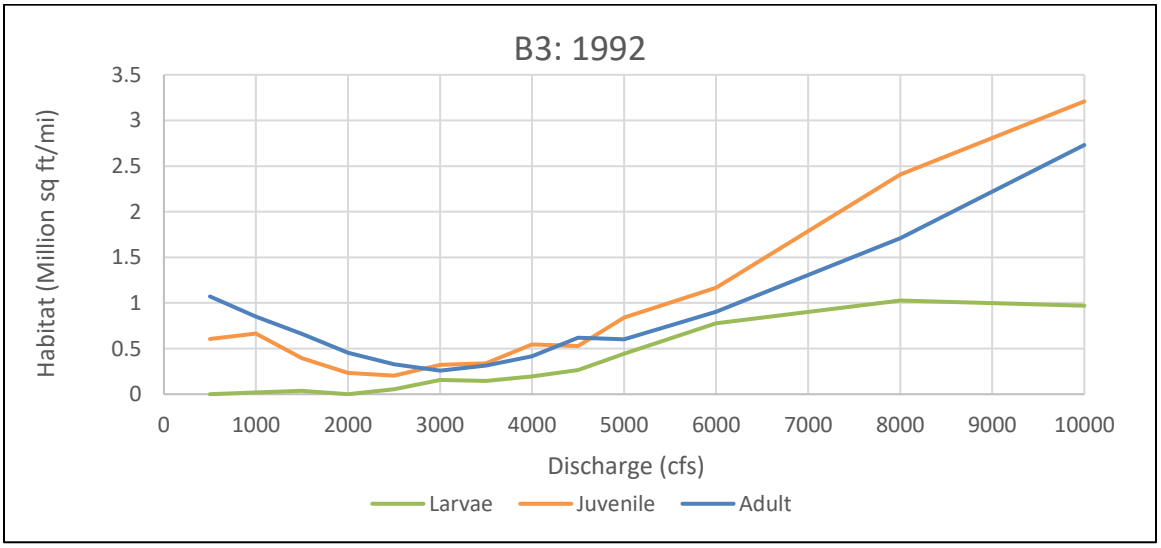
B3: 1992
Habitat (Million sq ft/mi)
3.5
3
2.5
2
1.5
1
0.5
0
0
1000
2000
3000
4000
5000
6000
7000
8000
9000
10000
Discharge (cfs)
Larvae
Juvenile
Adult

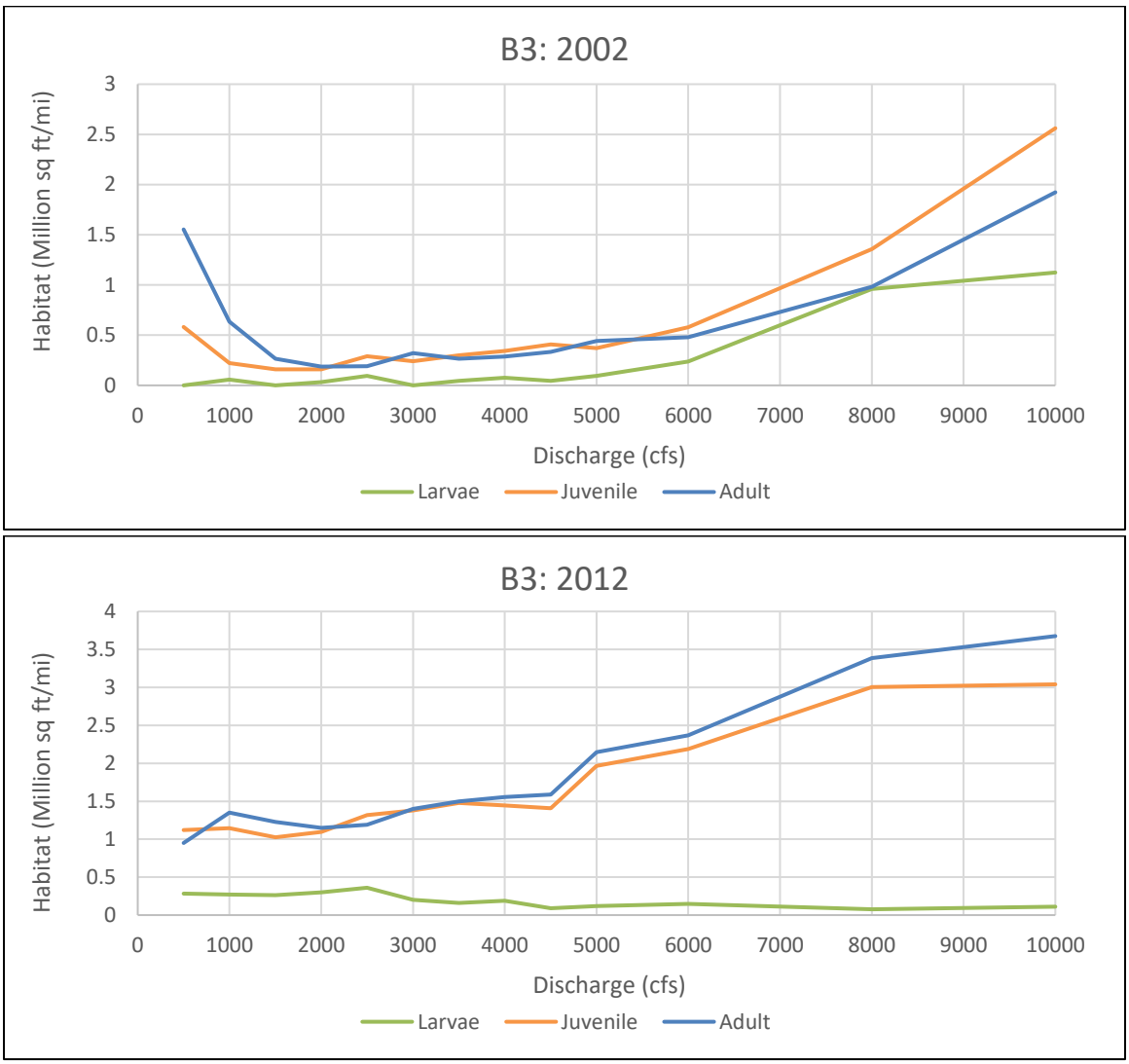

Figure D-12 Life stage habitat curves for Bernalillo Subreach B3 for the years 1962 to 2012.

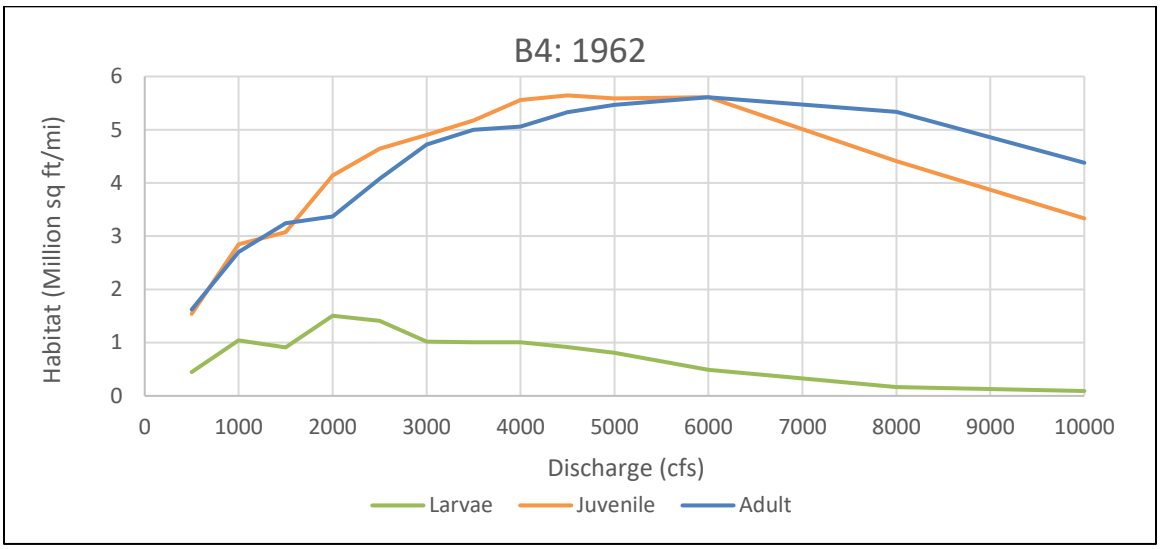
B4: 1962
Habitat (Million sq ft/mi)
0
1
2
3
4
5
6
0
1000
2000
3000
4000
5000
6000
7000
8000
9000
10000
Discharge (cfs)
Larvae
Juvenile
Adult

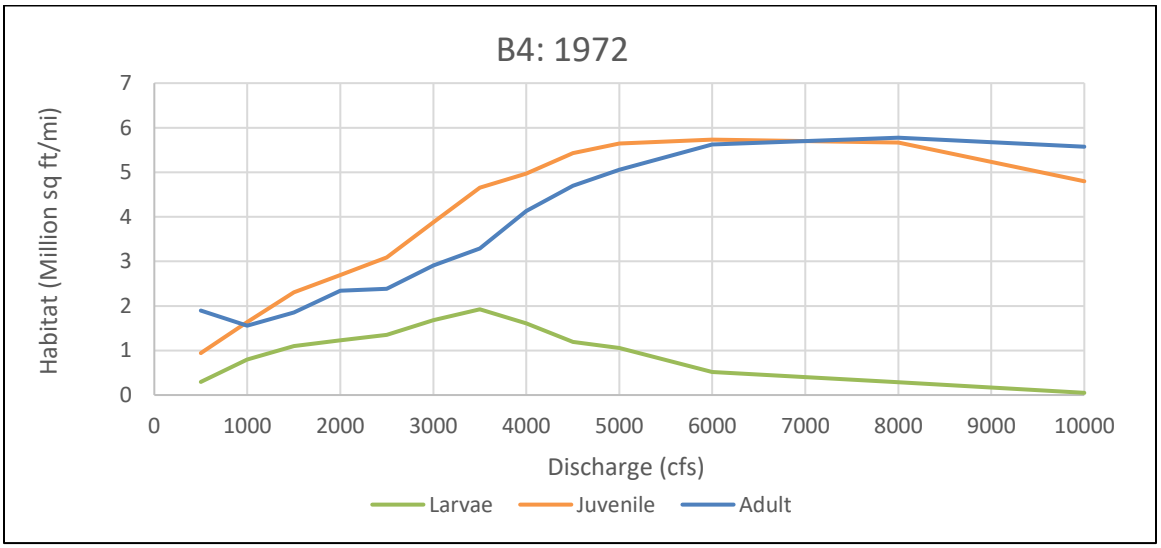
B4: 1972
Habitat (Million sq ft/mi)
0
1
2
3
4
5
6
7
0
1000
2000
3000
4000
5000
6000
7000
8000
9000
10000
Discharge (cfs)
Larvae
Juvenile
Adult

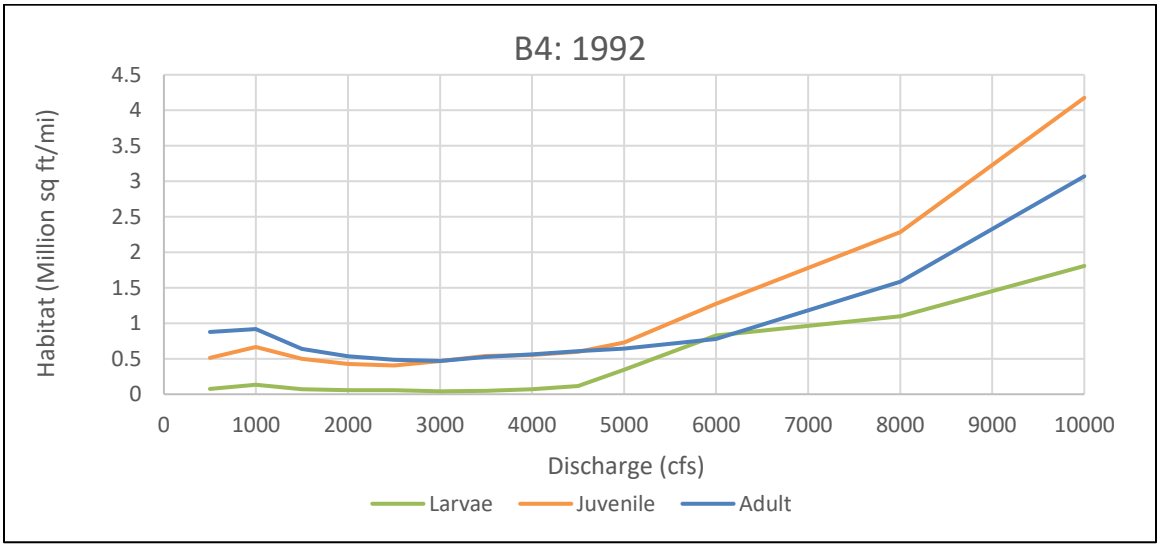
B4: 1992
Habitat (Million sq ft/mi)
0
0.5
1
1.5
2
2.5
3
3.5
4
4.5
0
1000
2000
3000
4000
5000
6000
7000
8000
9000
10000
Discharge (cfs)
Larvae
Juvenile
Adult

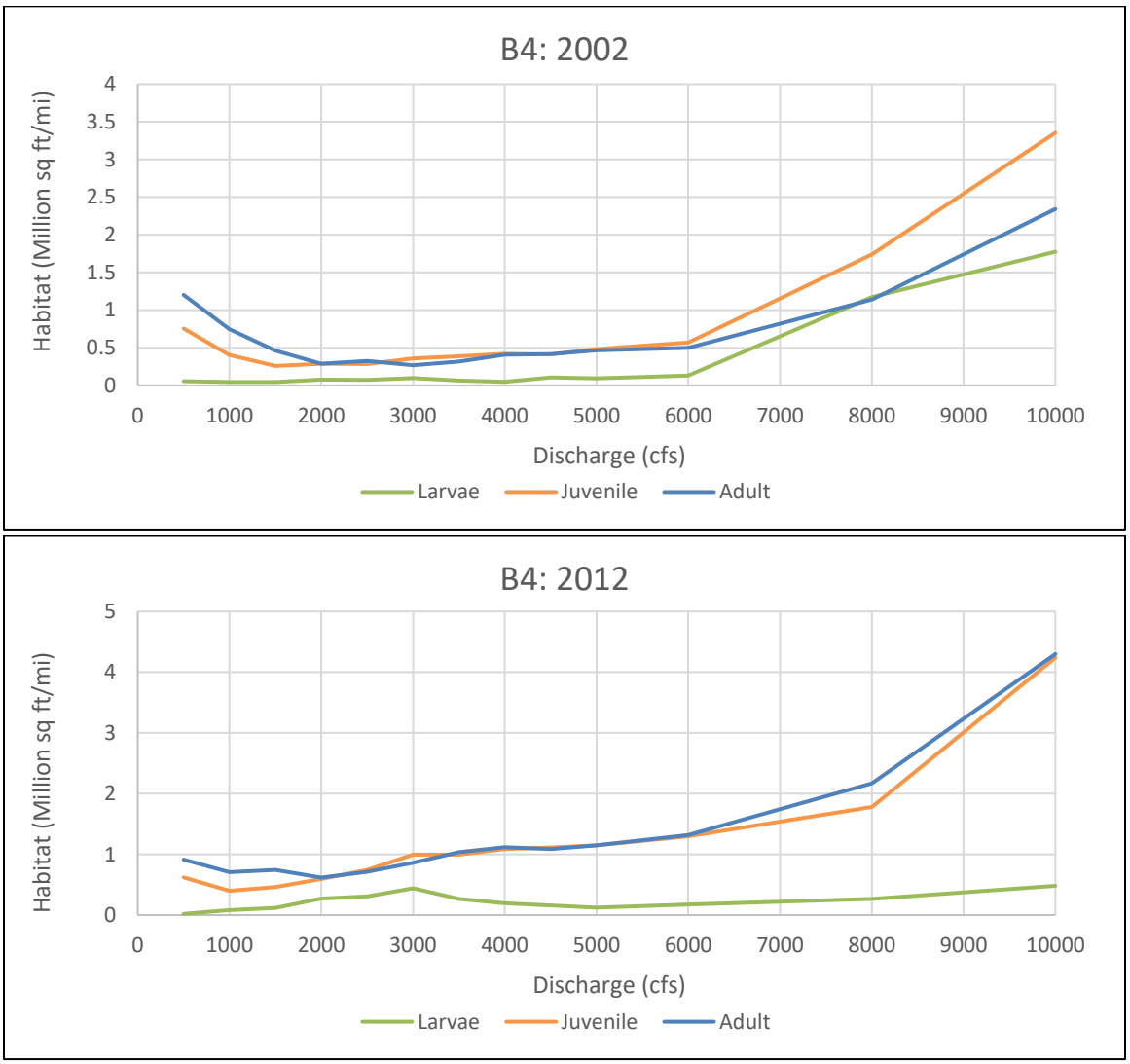

Figure D-13 Life stage habitat curves for Bernalillo Subreach B4 for the years 1962 to 2012.

Appendix E

Maps of Hydraulically Suitable Habitat for the Rio Grande Silvery Minnow

(1,500 cfs, 3,000 cfs, and 5,000 cfs Flow Events)

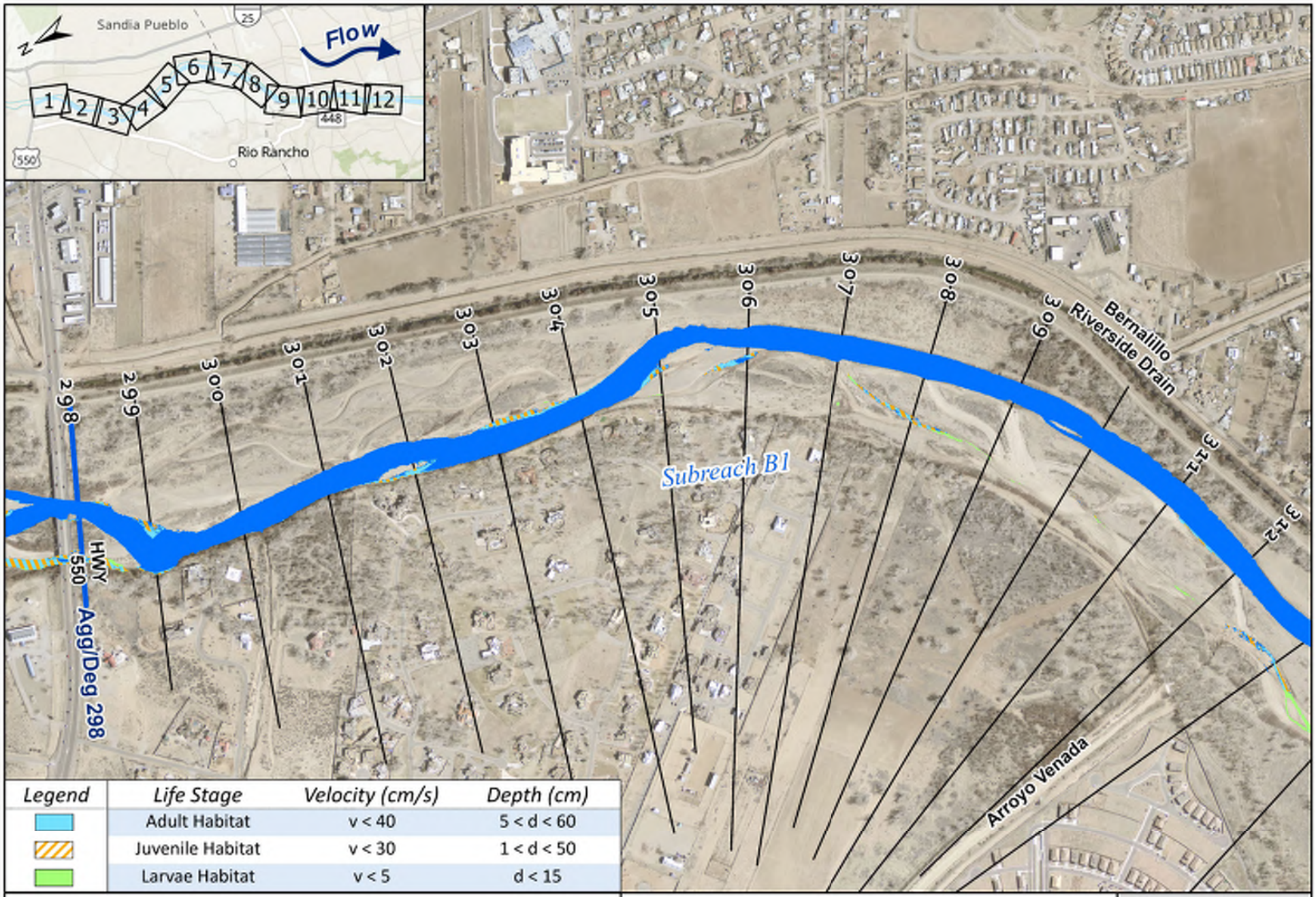

Legend	Life Stage	Velocity (cm/s)	Depth (cm)
	Adult Habitat	v < 40	5 < d < 60
	Juvenile Habitat	v < 30	1 < d < 50
	Larvae Habitat	v < 5	d < 15

1,000 500 0 1,000 Feet

Rio Grande Habitat Map at 1,500 cfs
Bernalillo to Montano

Rio Grande Habitat Map at 1,500 cfs
Bernalillo to Montano

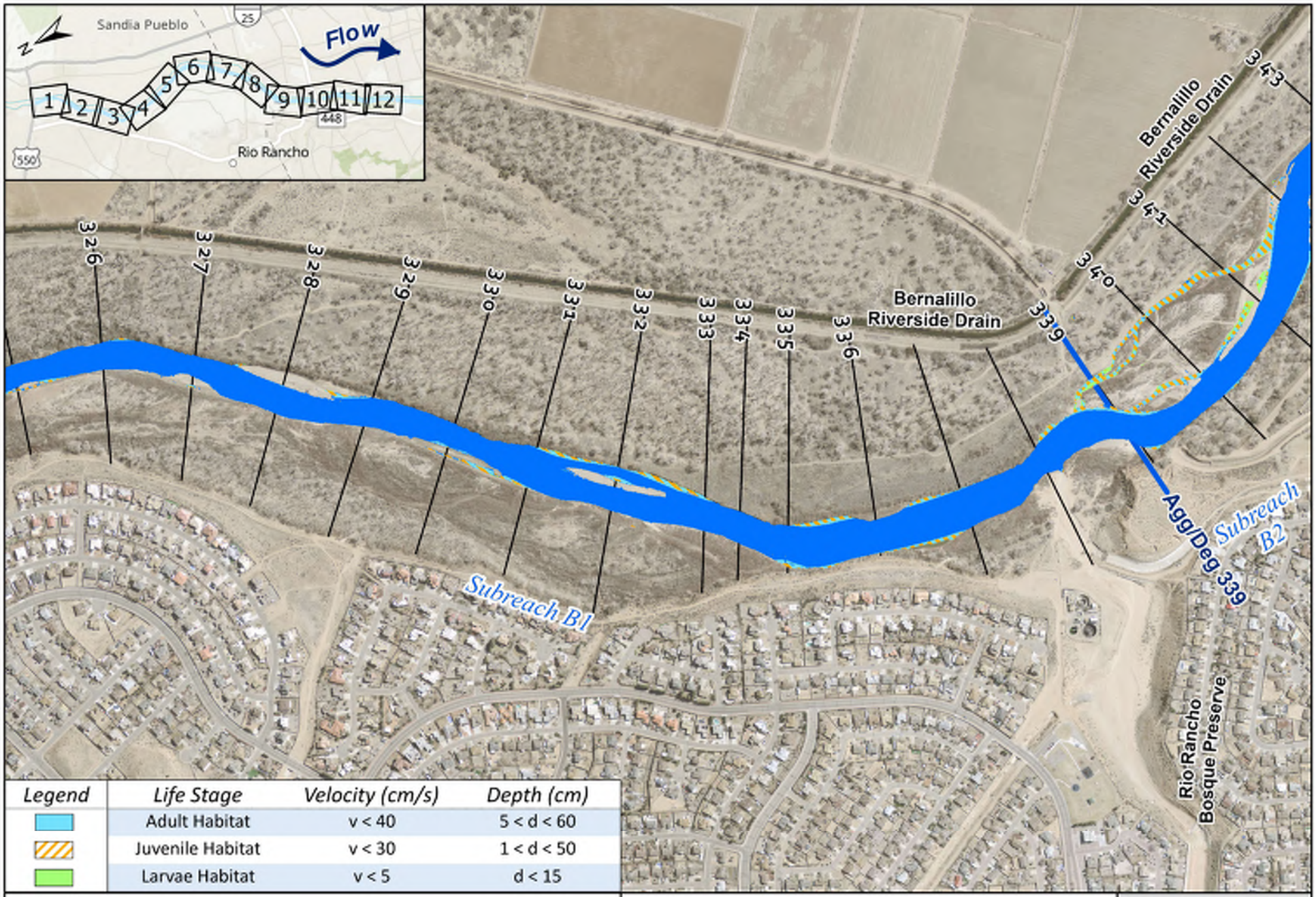

Legend	Life Stage	Velocity (cm/s)	Depth (cm)
	Adult Habitat	v < 40	5 < d < 60
	Juvenile Habitat	v < 30	1 < d < 50
	Larvae Habitat	v < 5	d < 15

1,000 500 0 1,000 Feet

Rio Grande Habitat Map at 1,500 cfs
Bernalillo to Montano

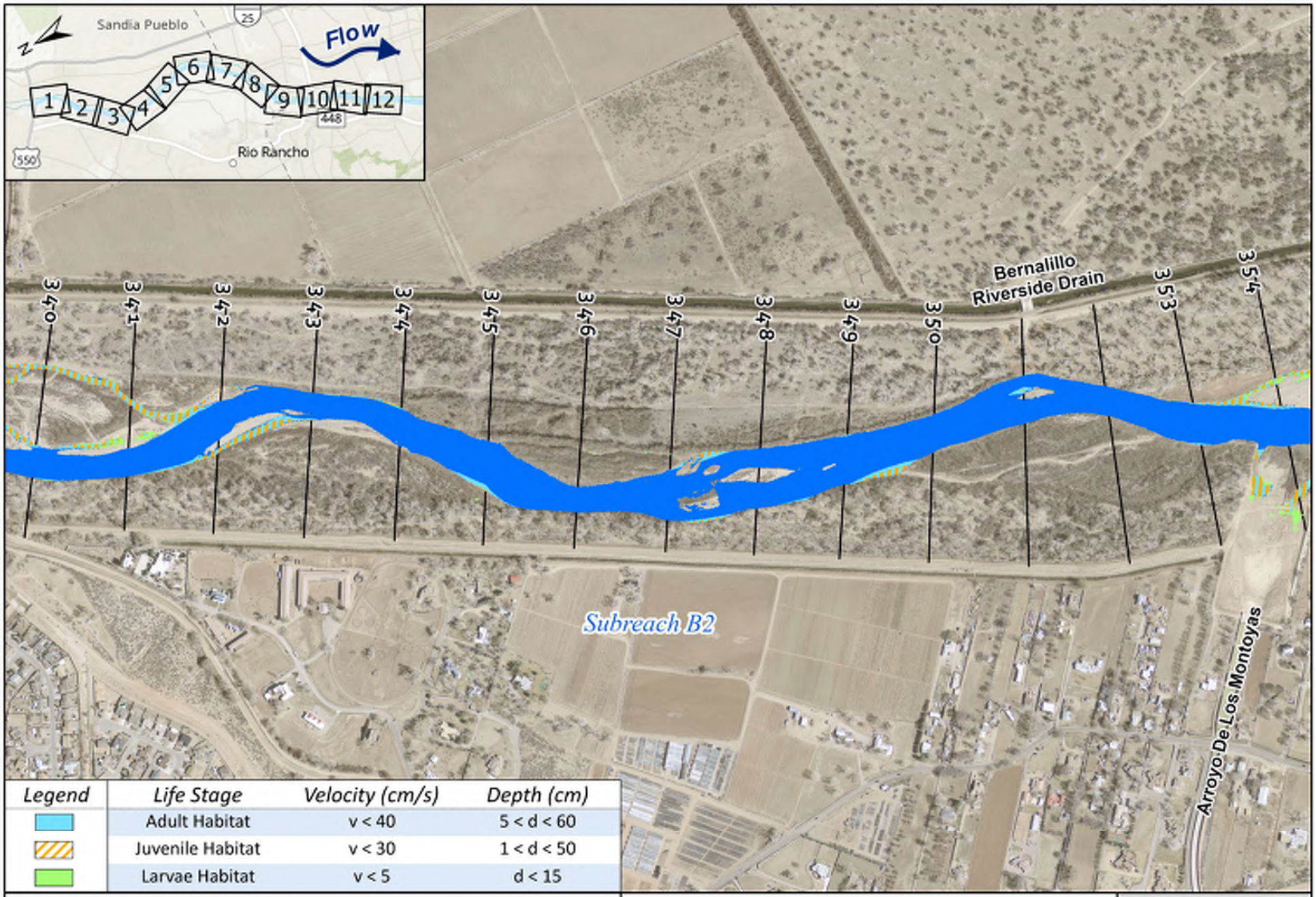

Legend	Life Stage	Velocity (cm/s)	Depth (cm)
	Adult Habitat	v < 40	5 < d < 60
	Juvenile Habitat	v < 30	1 < d < 50
	Larvae Habitat	v < 5	d < 15

N

1,000 500 0 1,000 Feet

Rio Grande Habitat Map at 1,500 cfs
Bernalillo to Montano

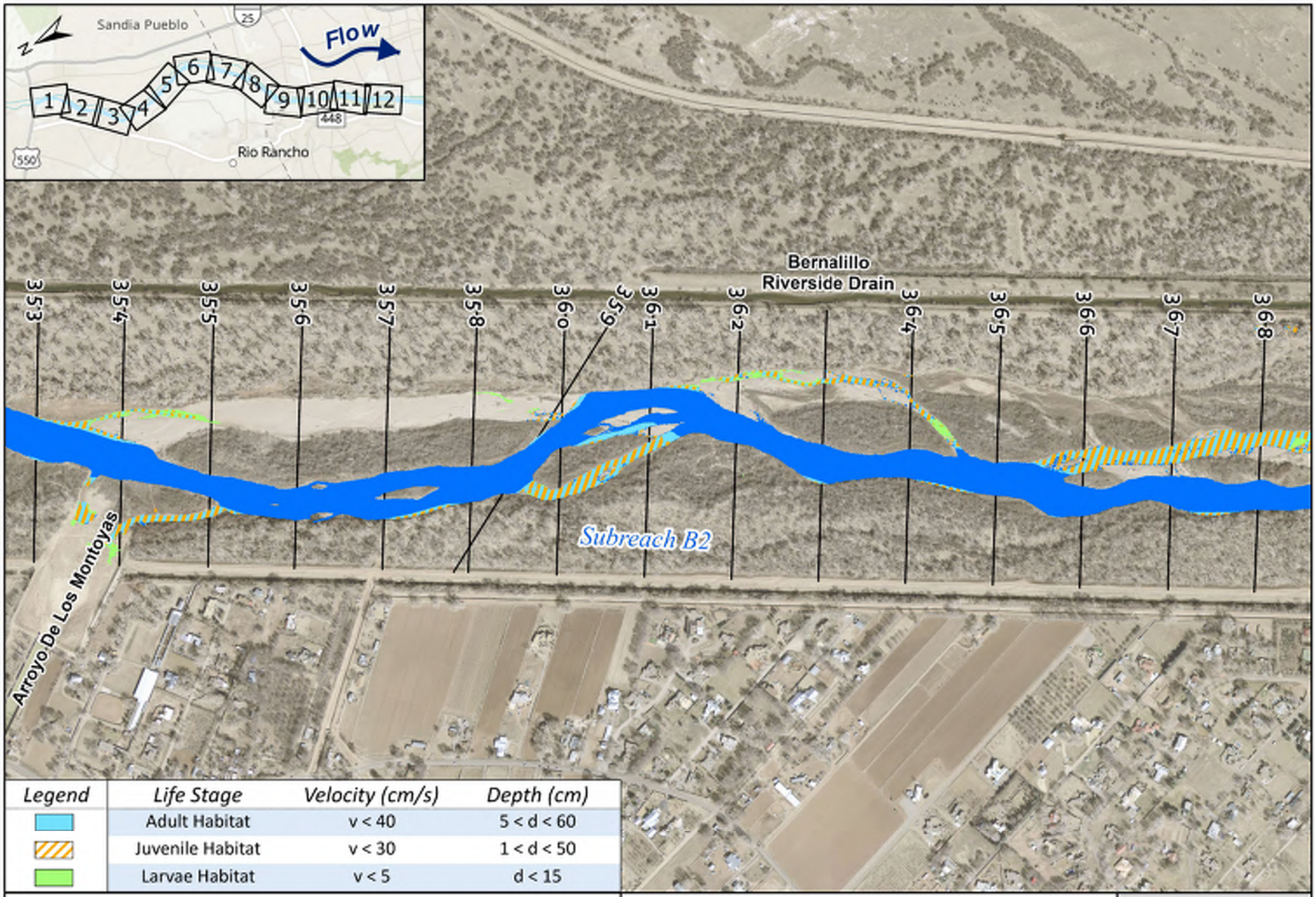

Legend	Life Stage	Velocity (cm/s)	Depth (cm)
	Adult Habitat	v < 40	5 < d < 60
	Juvenile Habitat	v < 30	1 < d < 50
	Larvae Habitat	v < 5	d < 15

N

1,000 500 0 1,000 Feet

Rio Grande Habitat Map at 1,500 cfs
Bernalillo to Montano

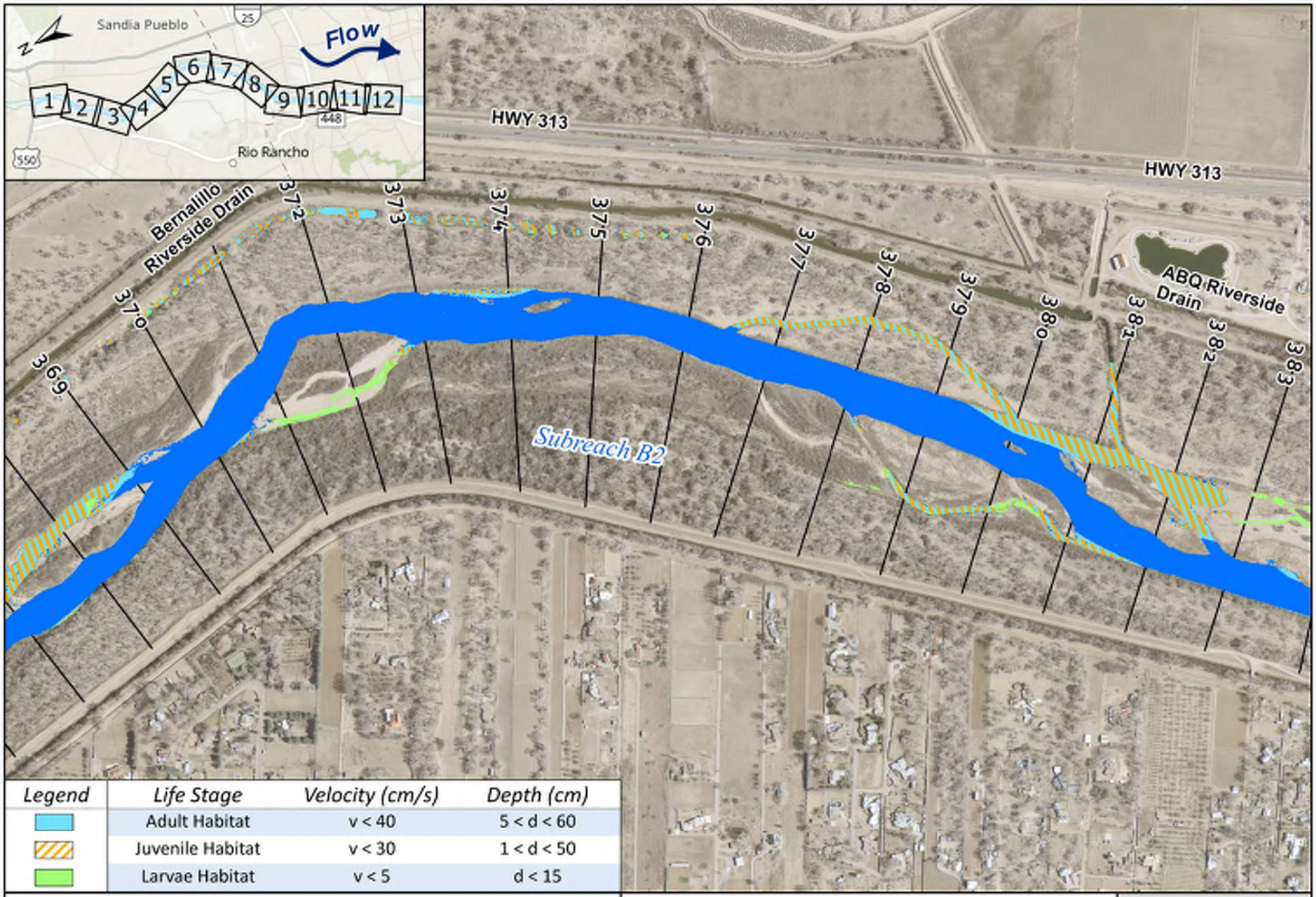

Legend	Life Stage	Velocity (cm/s)	Depth (cm)
	Adult Habitat	v < 40	5 < d < 60
	Juvenile Habitat	v < 30	1 < d < 50
	Larvae Habitat	v < 5	d < 15

1,000 500 0 1,000 Feet

Rio Grande Habitat Map at 1,500 cfs
Bernalillo to Montano

Rio Grande Habitat Map at 1,500 cfs
Bernalillo to Montano

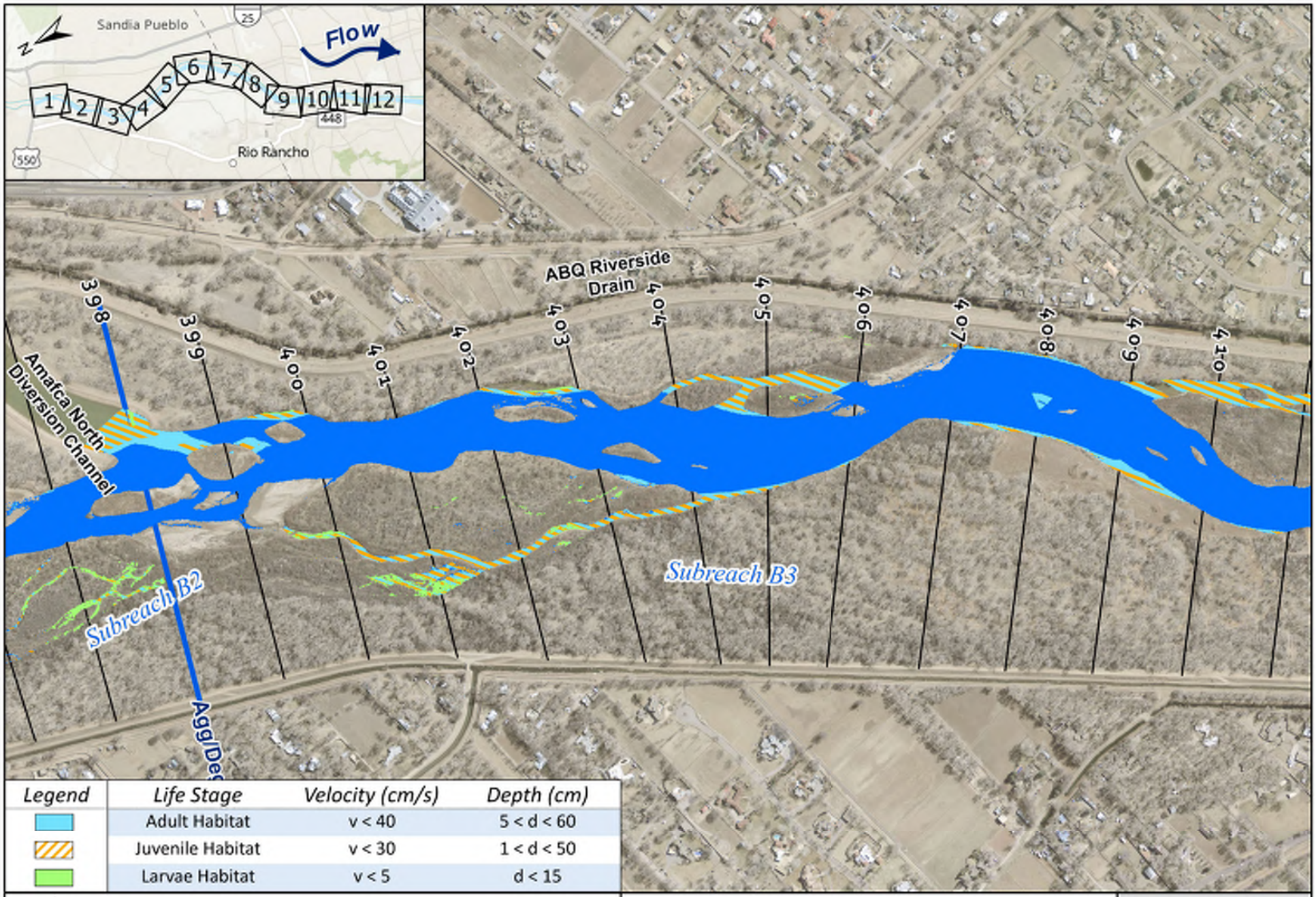

Rio Grande Habitat Map at 1,500 cfs
Bernalillo to Montano

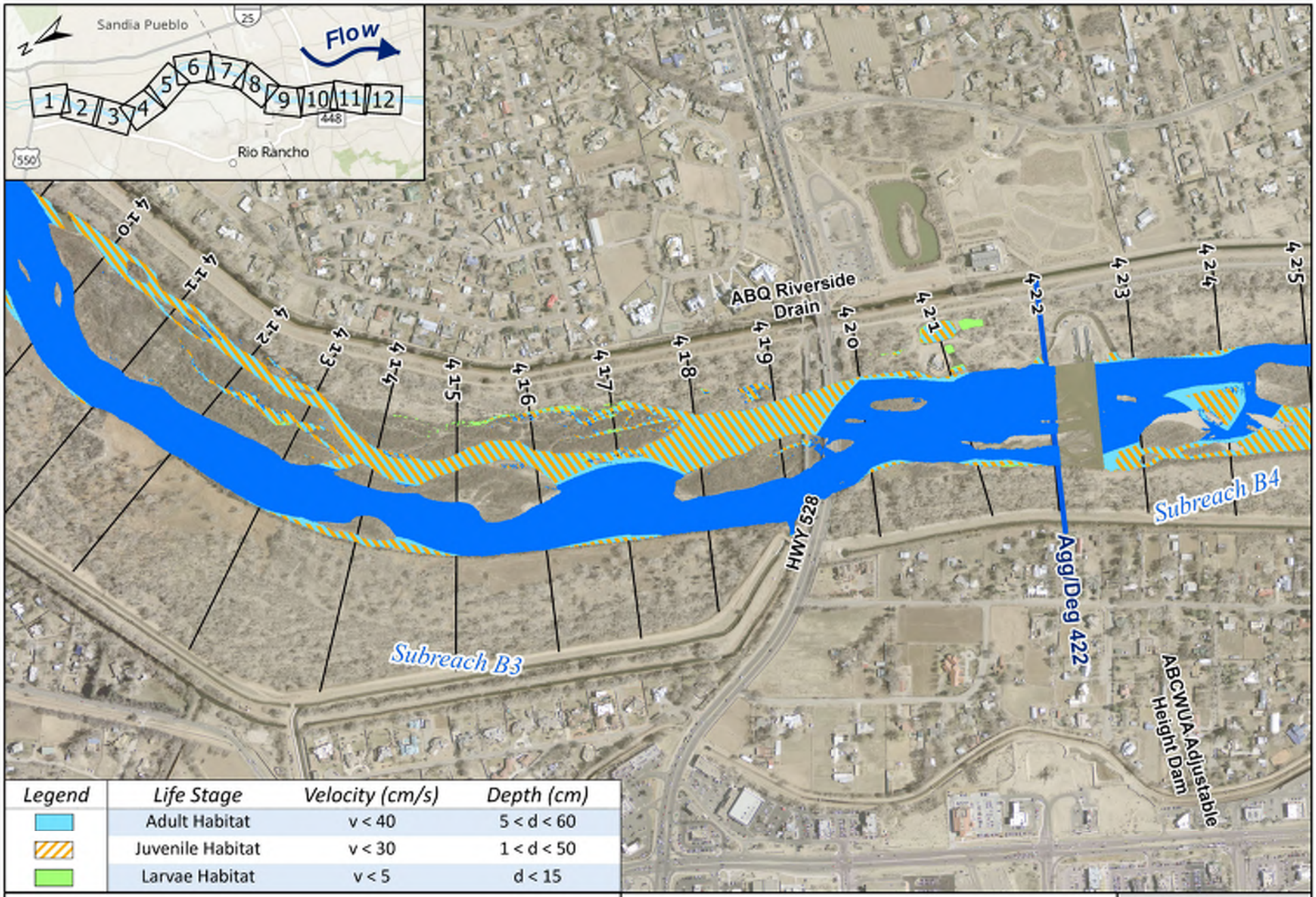

Legend	Life Stage	Velocity (cm/s)	Depth (cm)
	Adult Habitat	v < 40	5 < d < 60
	Juvenile Habitat	v < 30	1 < d < 50
	Larvae Habitat	v < 5	d < 15

1,000 500 0 1,000 Feet

Rio Grande Habitat Map at 1,500 cfs
Bernalillo to Montano

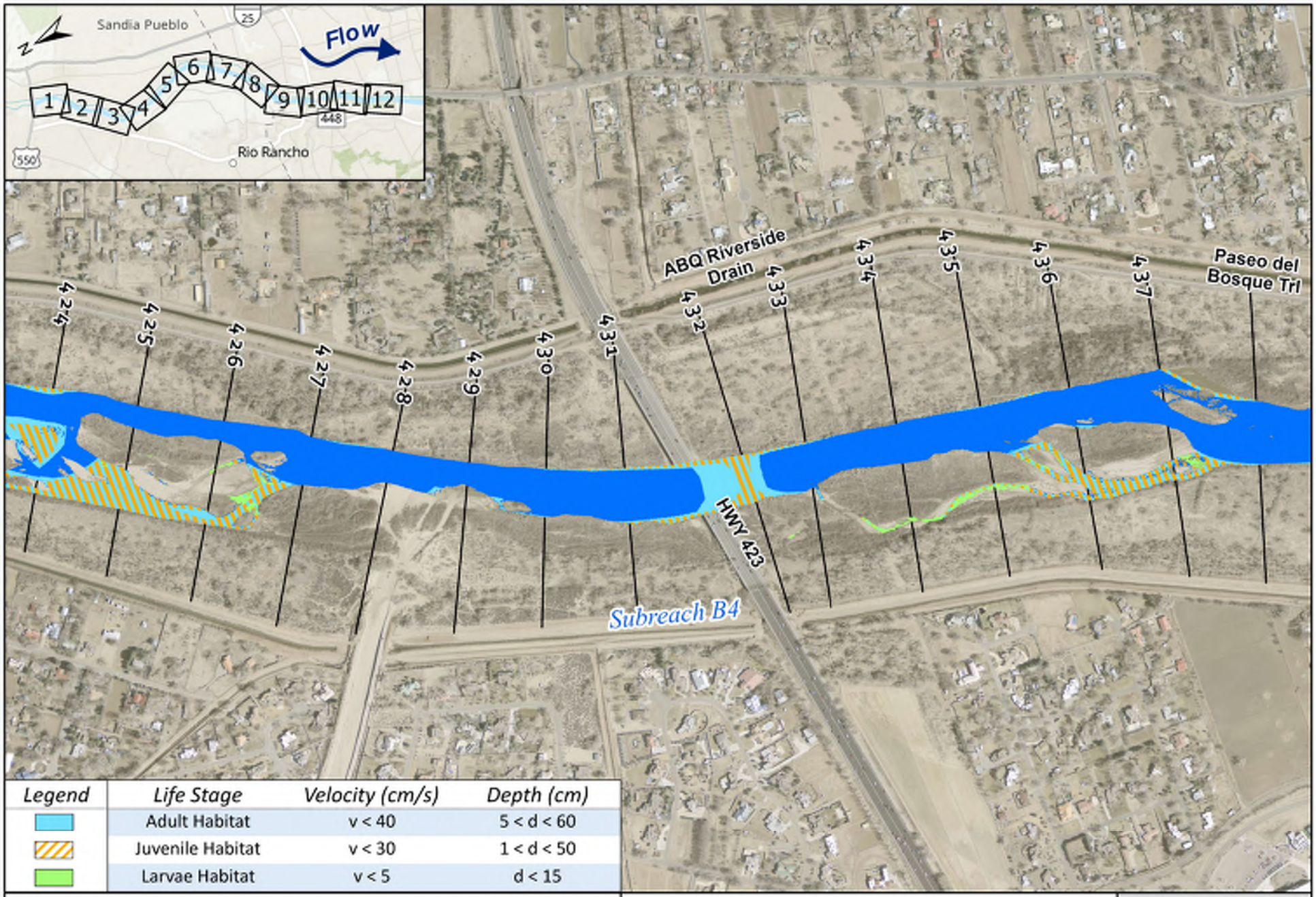

Legend	Life Stage	Velocity (cm/s)	Depth (cm)
	Adult Habitat	v < 40	5 < d < 60
	Juvenile Habitat	v < 30	1 < d < 50
	Larvae Habitat	v < 5	d < 15

1,000 500 0 1,000 Feet

Rio Grande Habitat Map at 1,500 cfs
Bernalillo to Montano

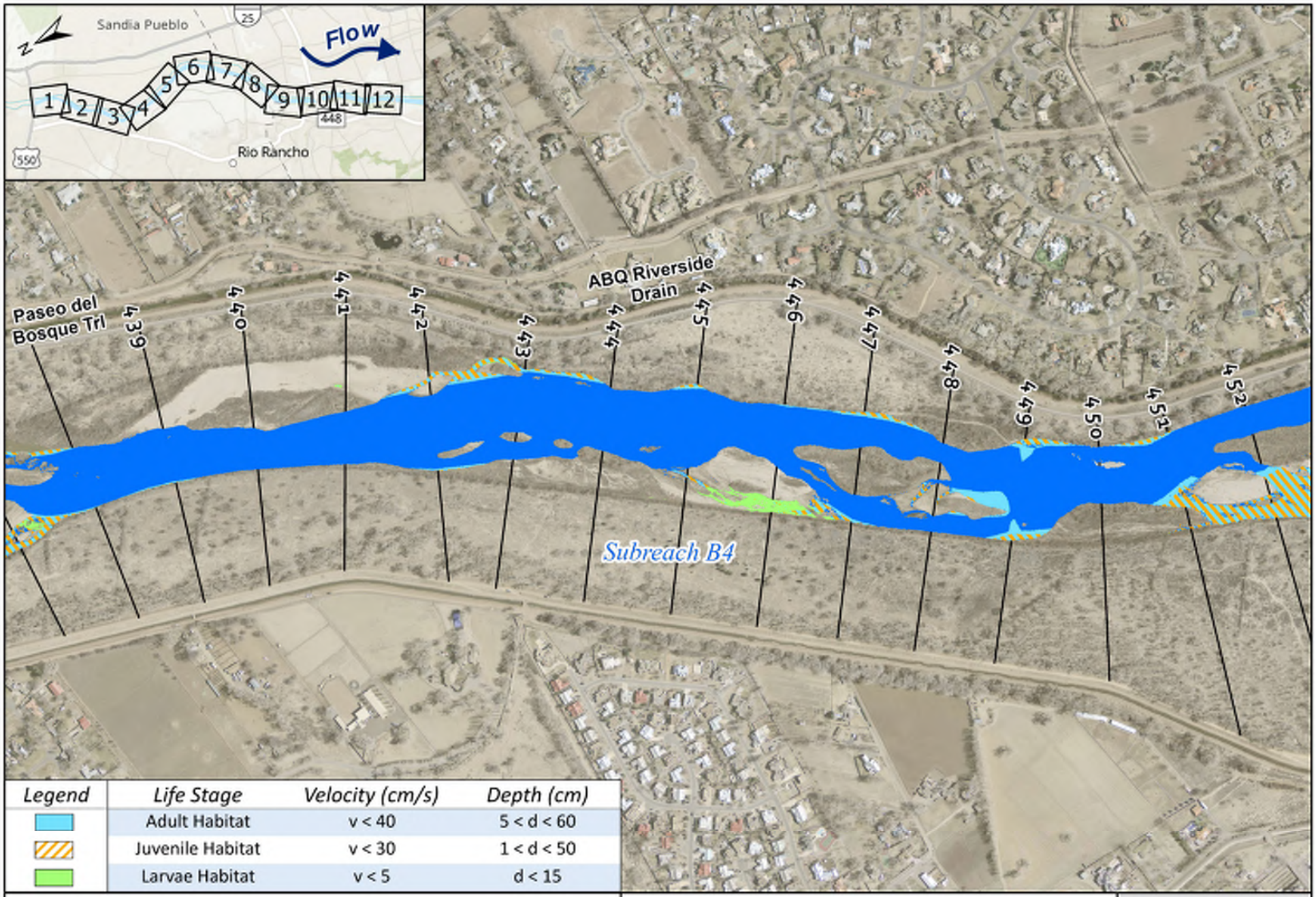

Legend	Life Stage	Velocity (cm/s)	Depth (cm)
	Adult Habitat	v < 40	5 < d < 60
	Juvenile Habitat	v < 30	1 < d < 50
	Larvae Habitat	v < 5	d < 15

1,000 500 0 1,000 Feet

Rio Grande Habitat Map at 1,500 cfs
Bernalillo to Montano

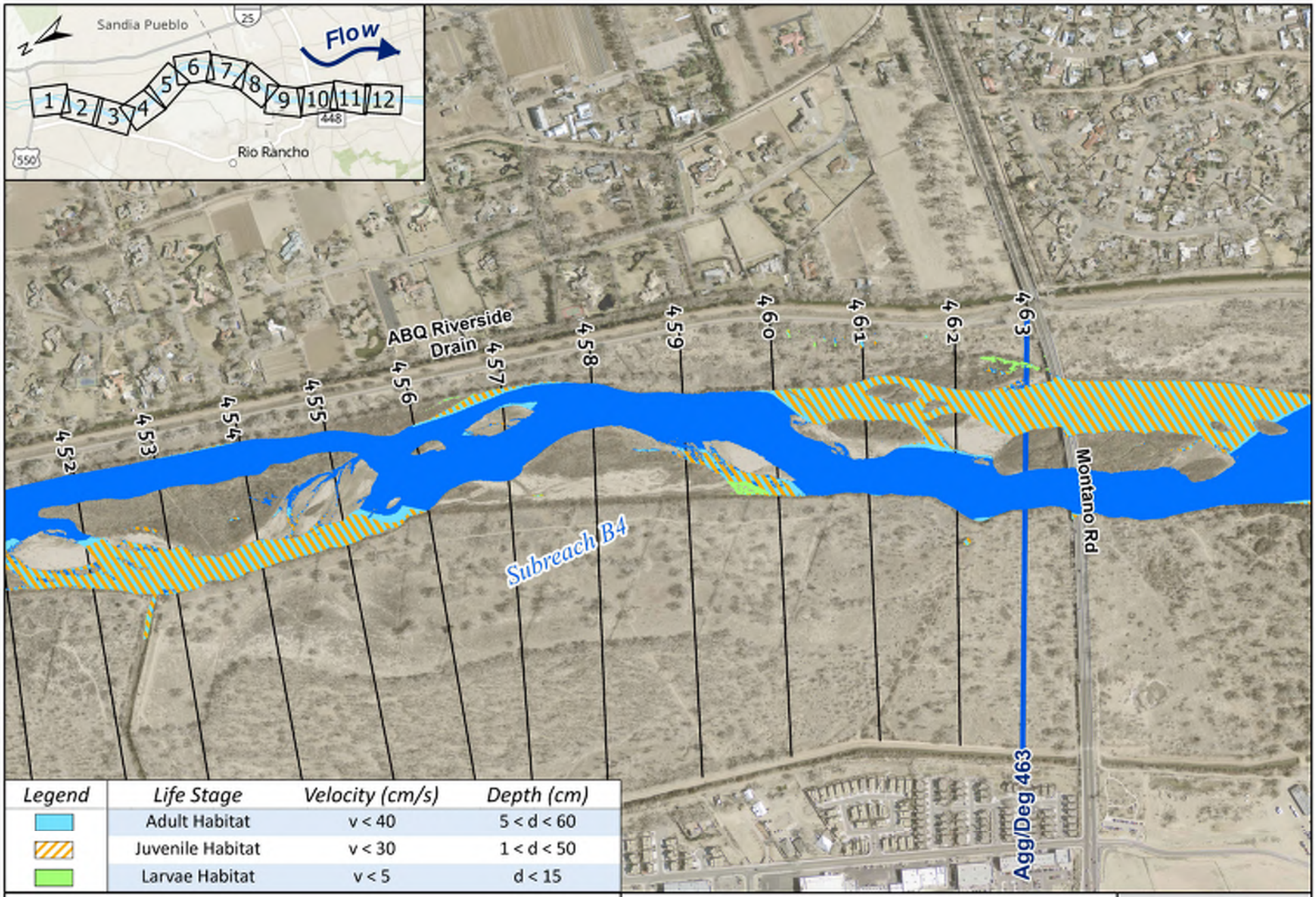

Rio Grande Habitat Map at 1,500 cfs
Bernalillo to Montano

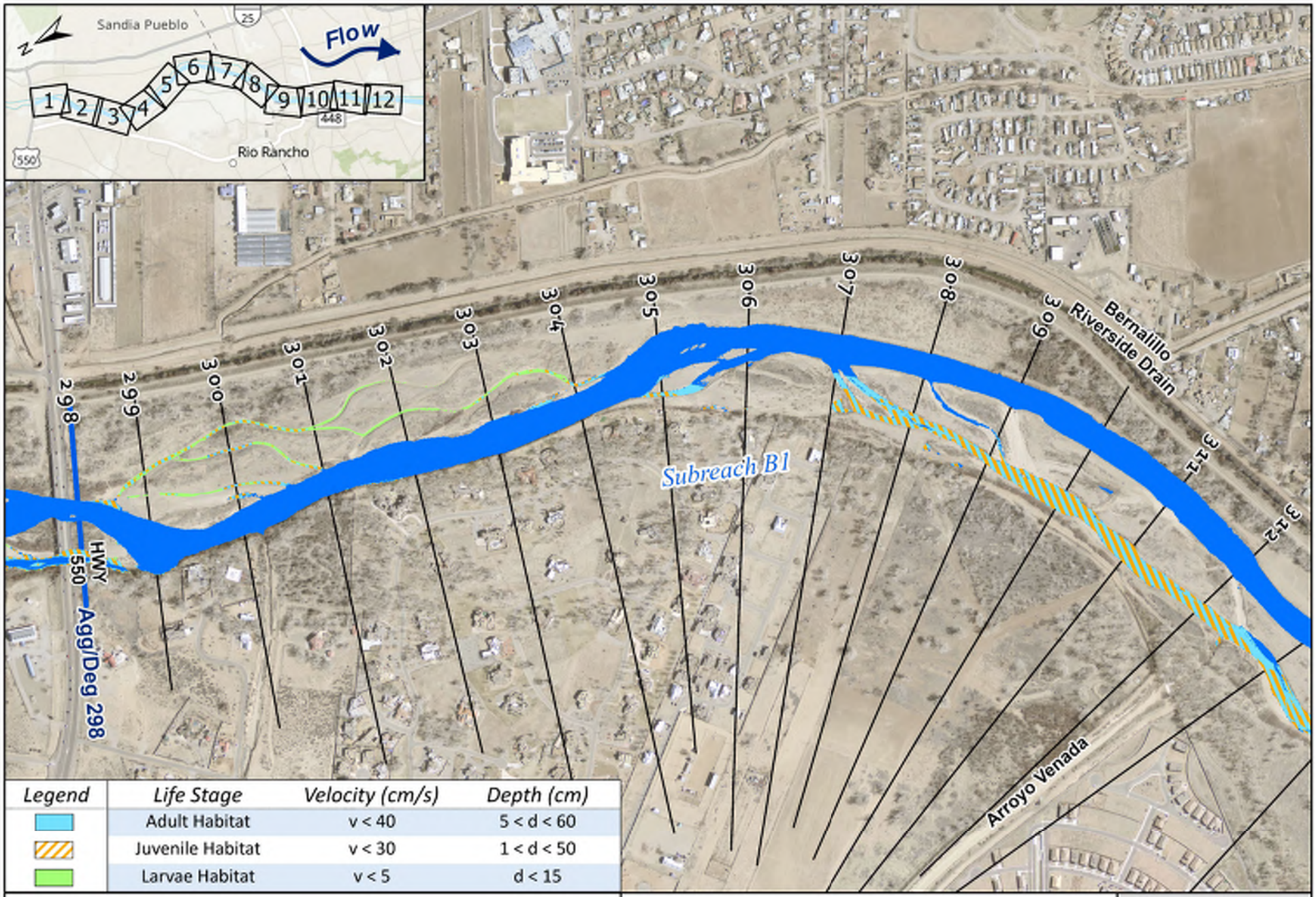

Legend	Life Stage	Velocity (cm/s)	Depth (cm)
	Adult Habitat	v < 40	5 < d < 60
	Juvenile Habitat	v < 30	1 < d < 50
	Larvae Habitat	v < 5	d < 15

1,000 500 0 1,000 Feet

Rio Grande Habitat Map at 3,000 cfs
Bernalillo to Montano

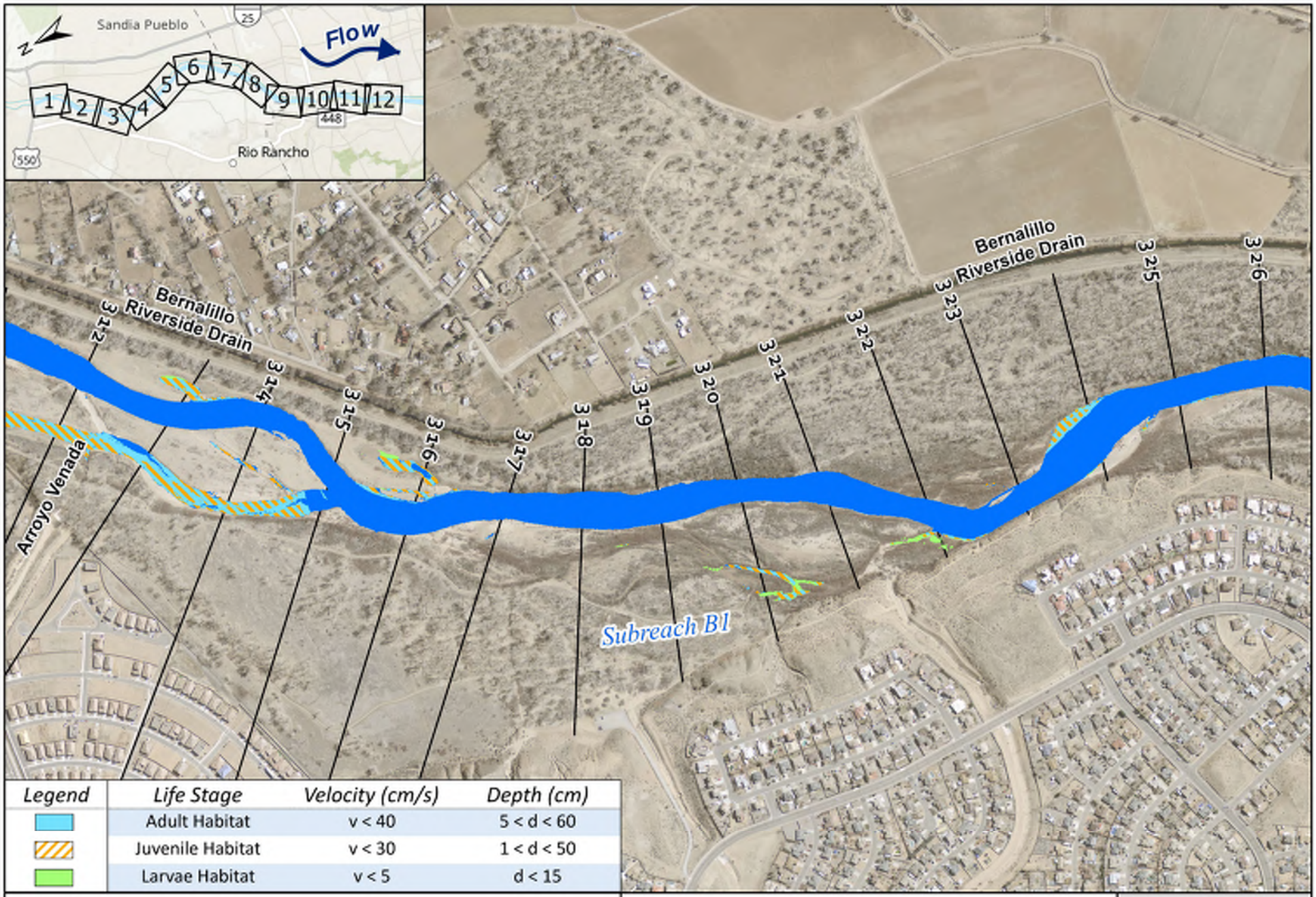

Legend	Life Stage	Velocity (cm/s)	Depth (cm)
	Adult Habitat	v < 40	5 < d < 60
	Juvenile Habitat	v < 30	1 < d < 50
	Larvae Habitat	v < 5	d < 15

1,000 500 0 1,000 Feet

Rio Grande Habitat Map at 3,000 cfs
Bernalillo to Montano

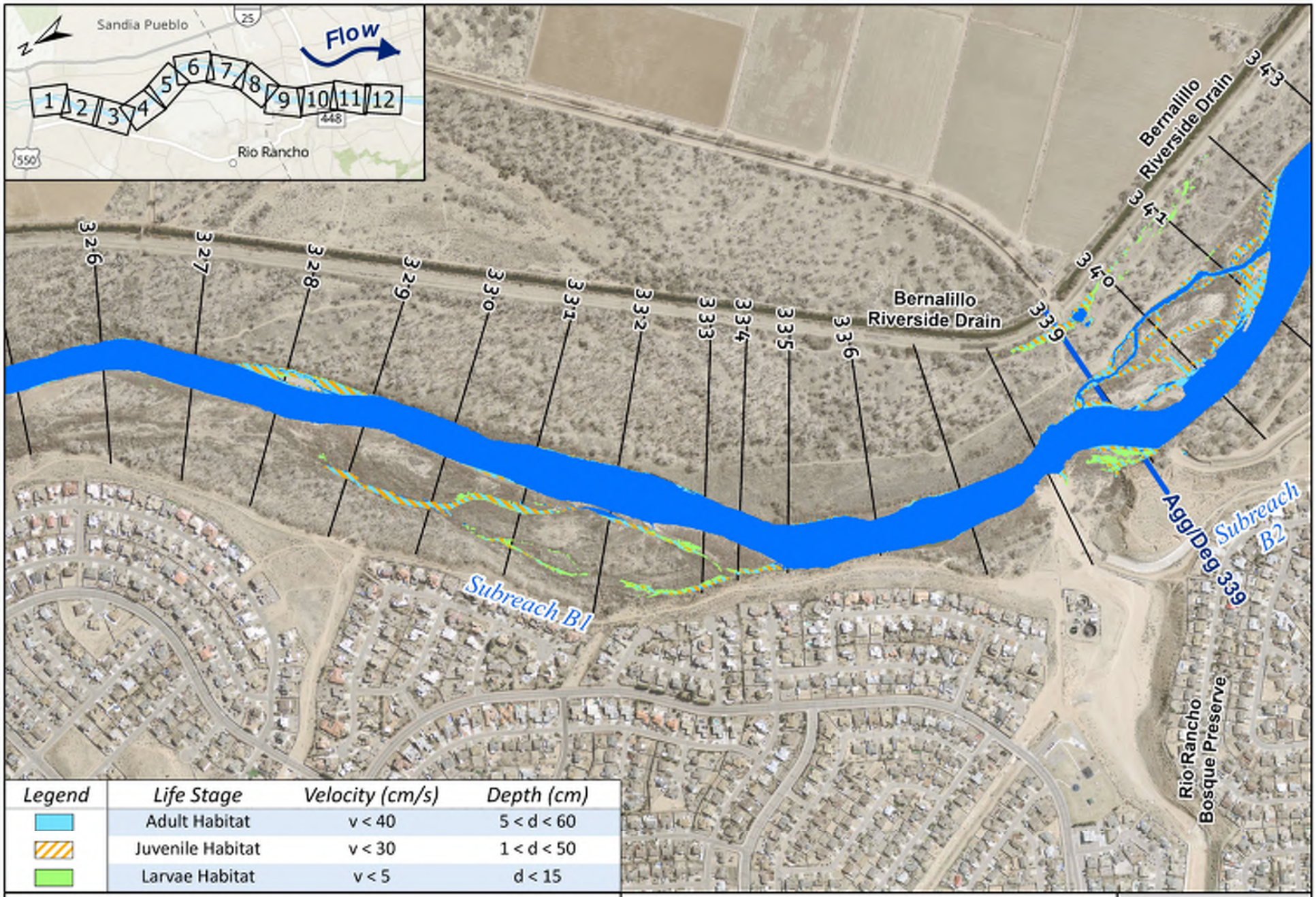

Legend	Life Stage	Velocity (cm/s)	Depth (cm)
	Adult Habitat	v < 40	5 < d < 60
	Juvenile Habitat	v < 30	1 < d < 50
	Larvae Habitat	v < 5	d < 15

1,000 500 0 1,000 Feet

Rio Grande Habitat Map at 3,000 cfs
Bernalillo to Montano

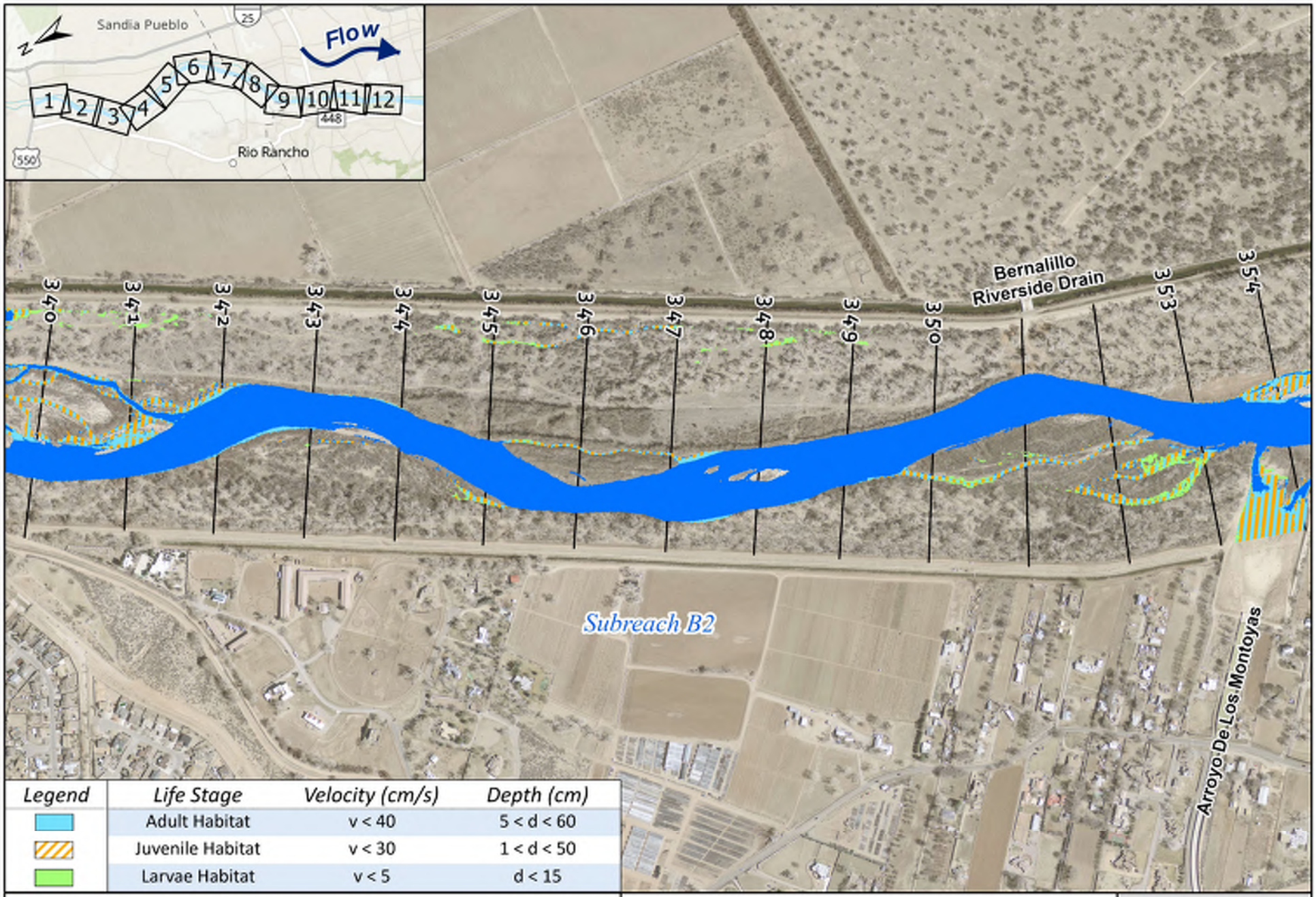

Legend	Life Stage	Velocity (cm/s)	Depth (cm)
	Adult Habitat	v < 40	5 < d < 60
	Juvenile Habitat	v < 30	1 < d < 50
	Larvae Habitat	v < 5	d < 15

1,000 500 0 1,000 Feet

Rio Grande Habitat Map at 3,000 cfs
Bernalillo to Montano

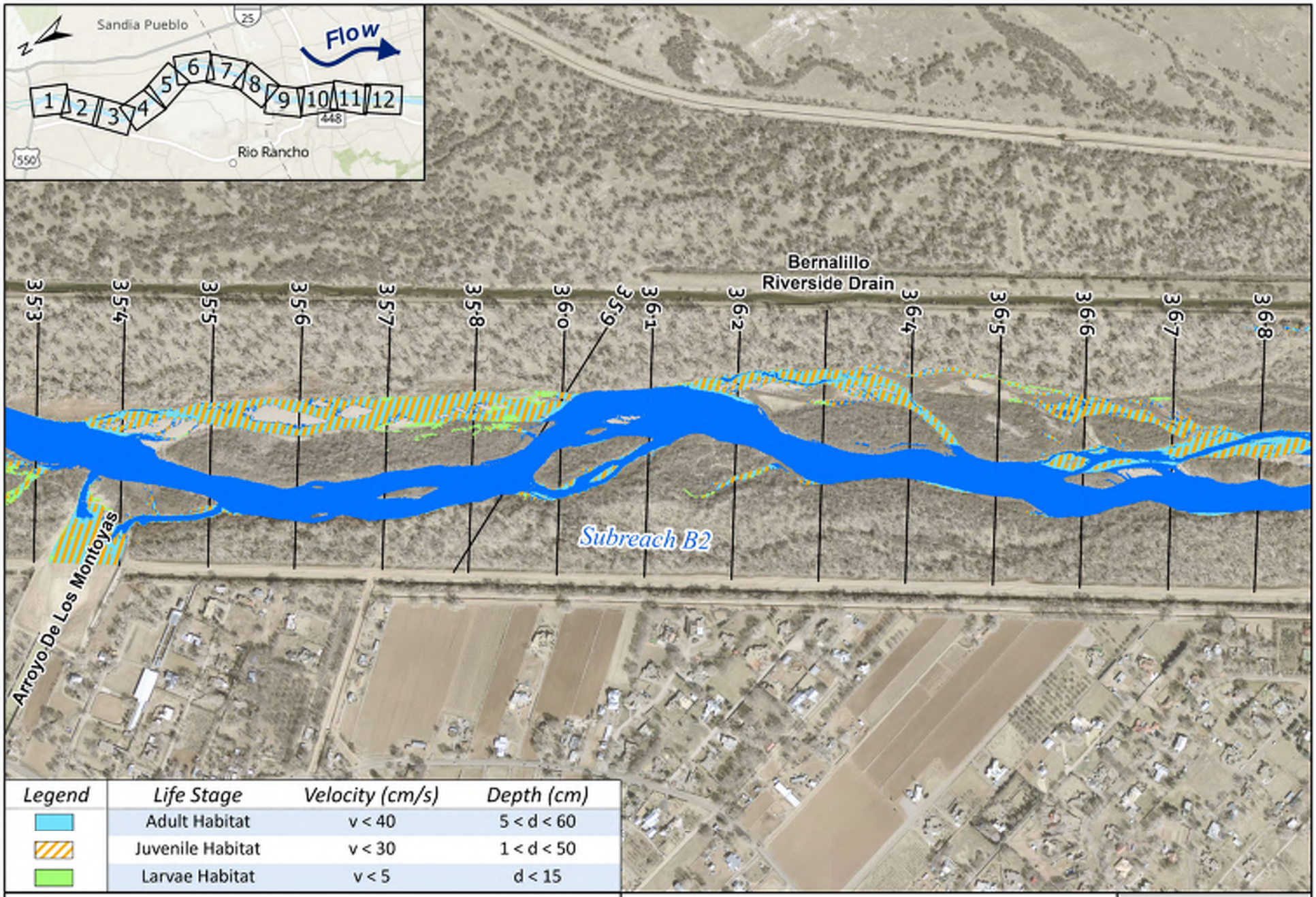

Legend	Life Stage	Velocity (cm/s)	Depth (cm)
	Adult Habitat	v < 40	5 < d < 60
	Juvenile Habitat	v < 30	1 < d < 50
	Larvae Habitat	v < 5	d < 15

N

1,000 500 0 1,000 Feet

Rio Grande Habitat Map at 3,000 cfs
Bernalillo to Montano

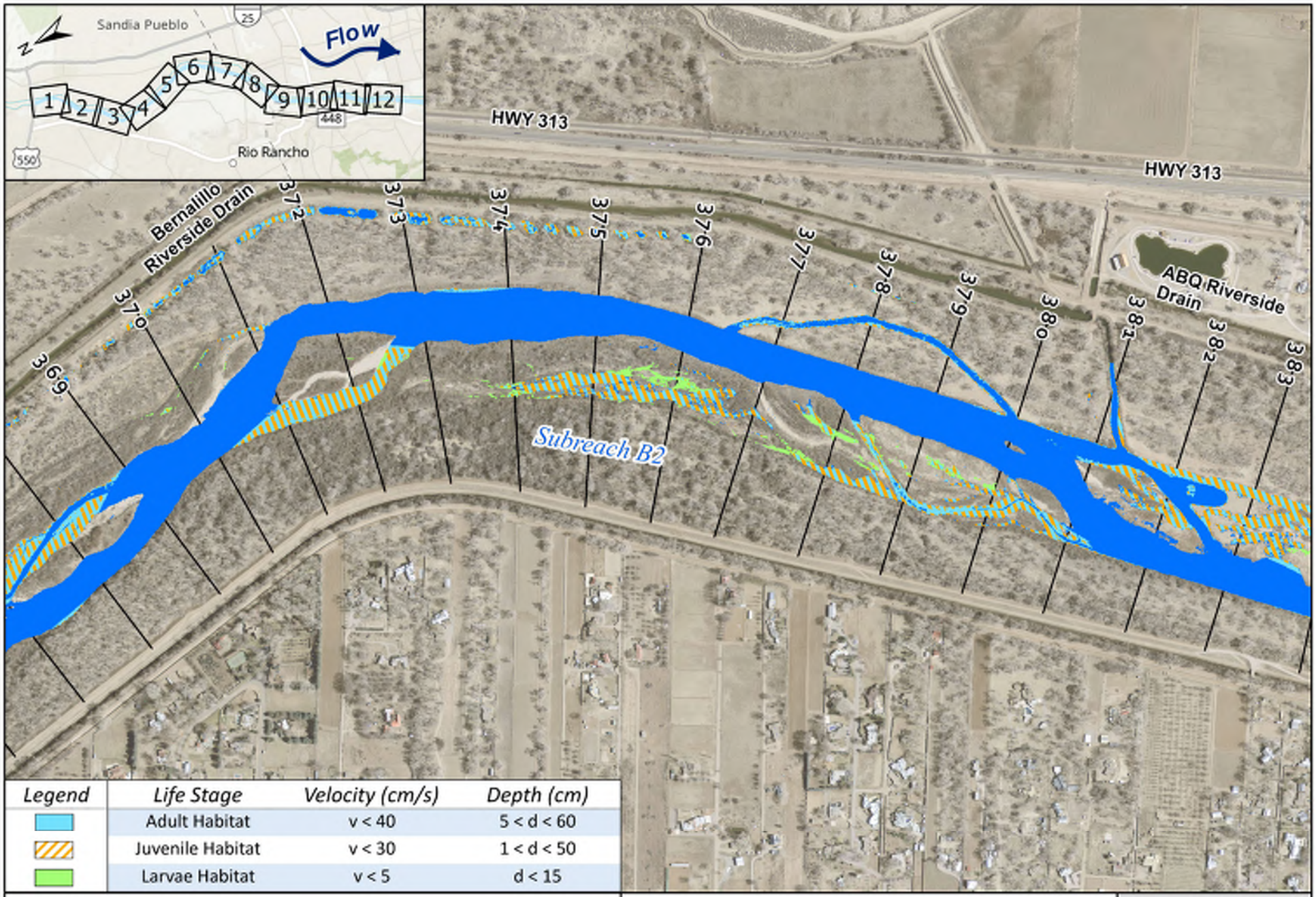

Legend	Life Stage	Velocity (cm/s)	Depth (cm)
	Adult Habitat	v < 40	5 < d < 60
	Juvenile Habitat	v < 30	1 < d < 50
	Larvae Habitat	v < 5	d < 15

1,000 500 0 1,000 Feet

Rio Grande Habitat Map at 3,000 cfs
Bernalillo to Montano

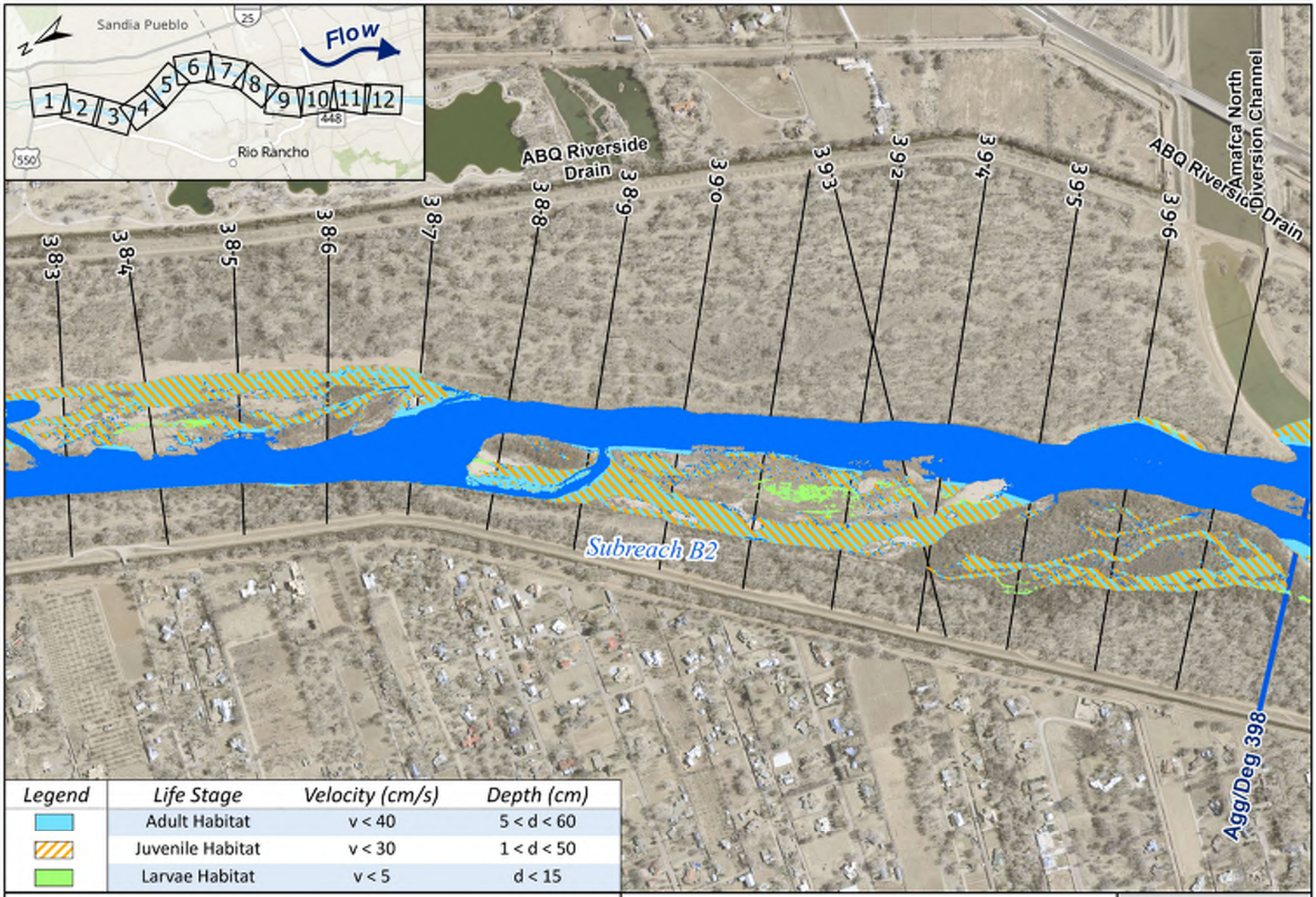

Rio Grande Habitat Map at 3,000 cfs
Bernalillo to Montano

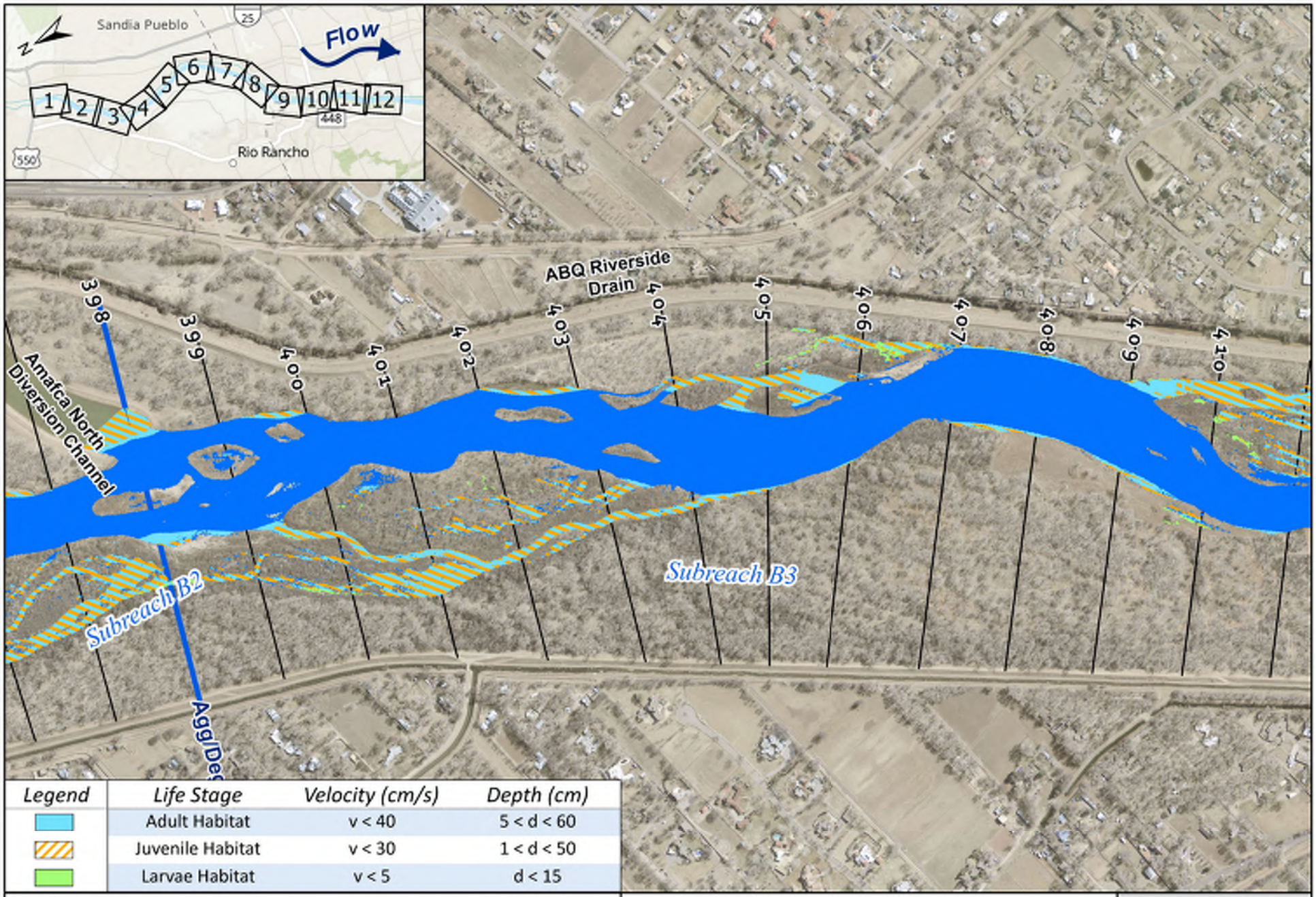

Legend	Life Stage	Velocity (cm/s)	Depth (cm)
	Adult Habitat	v < 40	5 < d < 60
	Juvenile Habitat	v < 30	1 < d < 50
	Larvae Habitat	v < 5	d < 15

N

1,000 500 0 1,000 Feet

Rio Grande Habitat Map at 3,000 cfs
Bernalillo to Montano

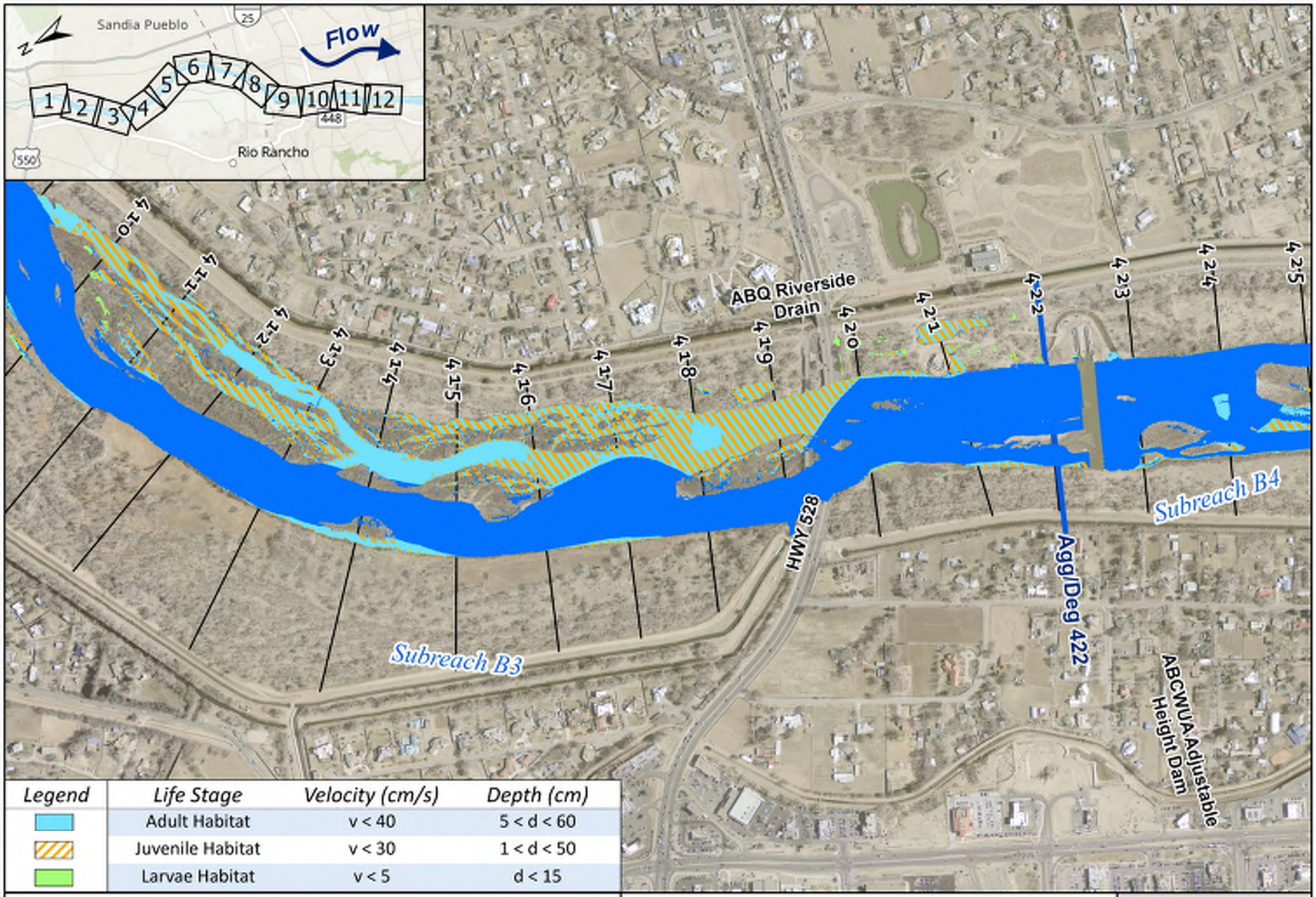

Legend	Life Stage	Velocity (cm/s)	Depth (cm)
	Adult Habitat	v < 40	5 < d < 60
	Juvenile Habitat	v < 30	1 < d < 50
	Larvae Habitat	v < 5	d < 15

1,000 500 0 1,000 Feet

Rio Grande Habitat Map at 3,000 cfs
Bernalillo to Montano

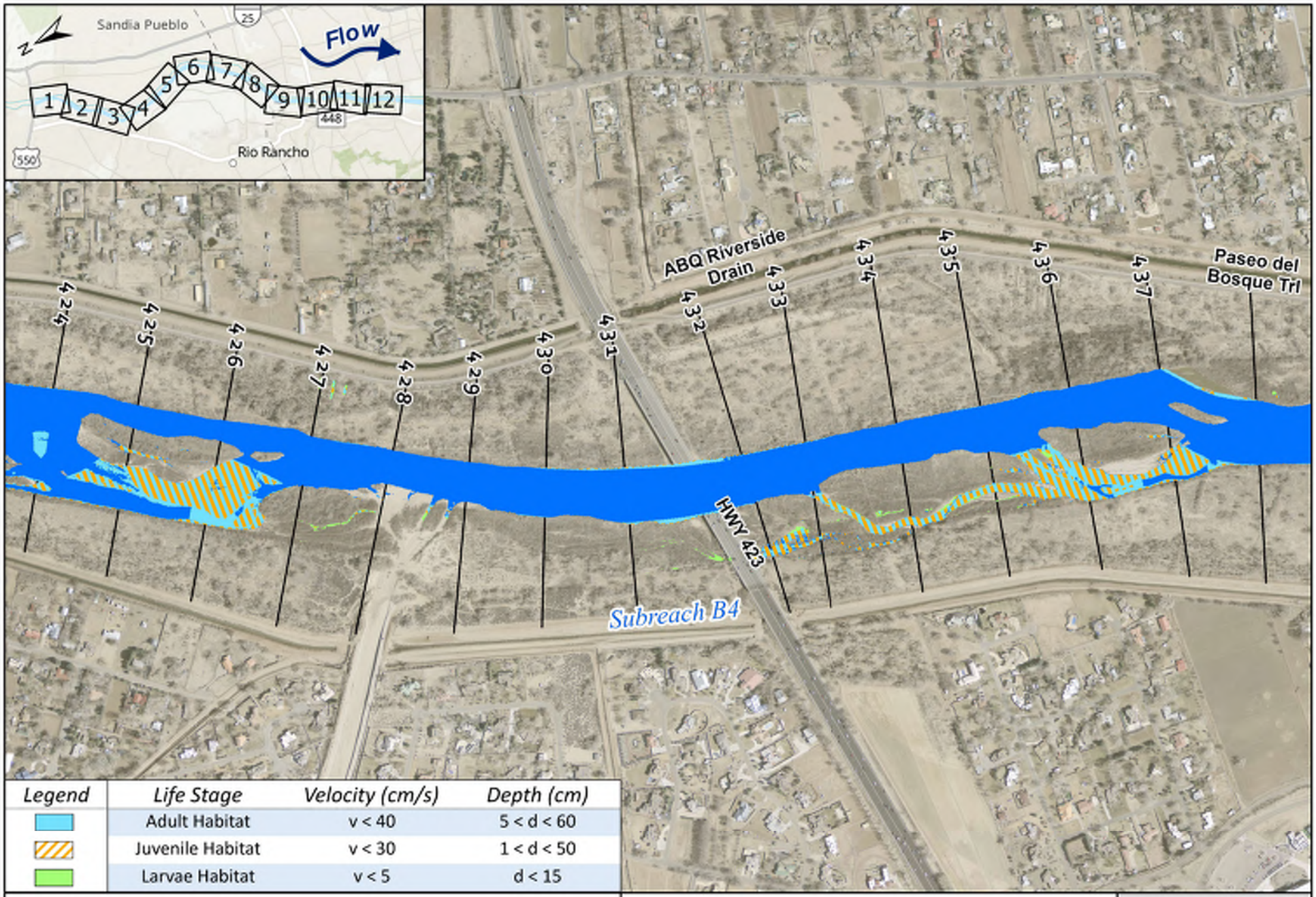

Legend	Life Stage	Velocity (cm/s)	Depth (cm)
	Adult Habitat	v < 40	5 < d < 60
	Juvenile Habitat	v < 30	1 < d < 50
	Larvae Habitat	v < 5	d < 15

1,000 500 0 1,000 Feet

Rio Grande Habitat Map at 3,000 cfs
Bernalillo to Montano

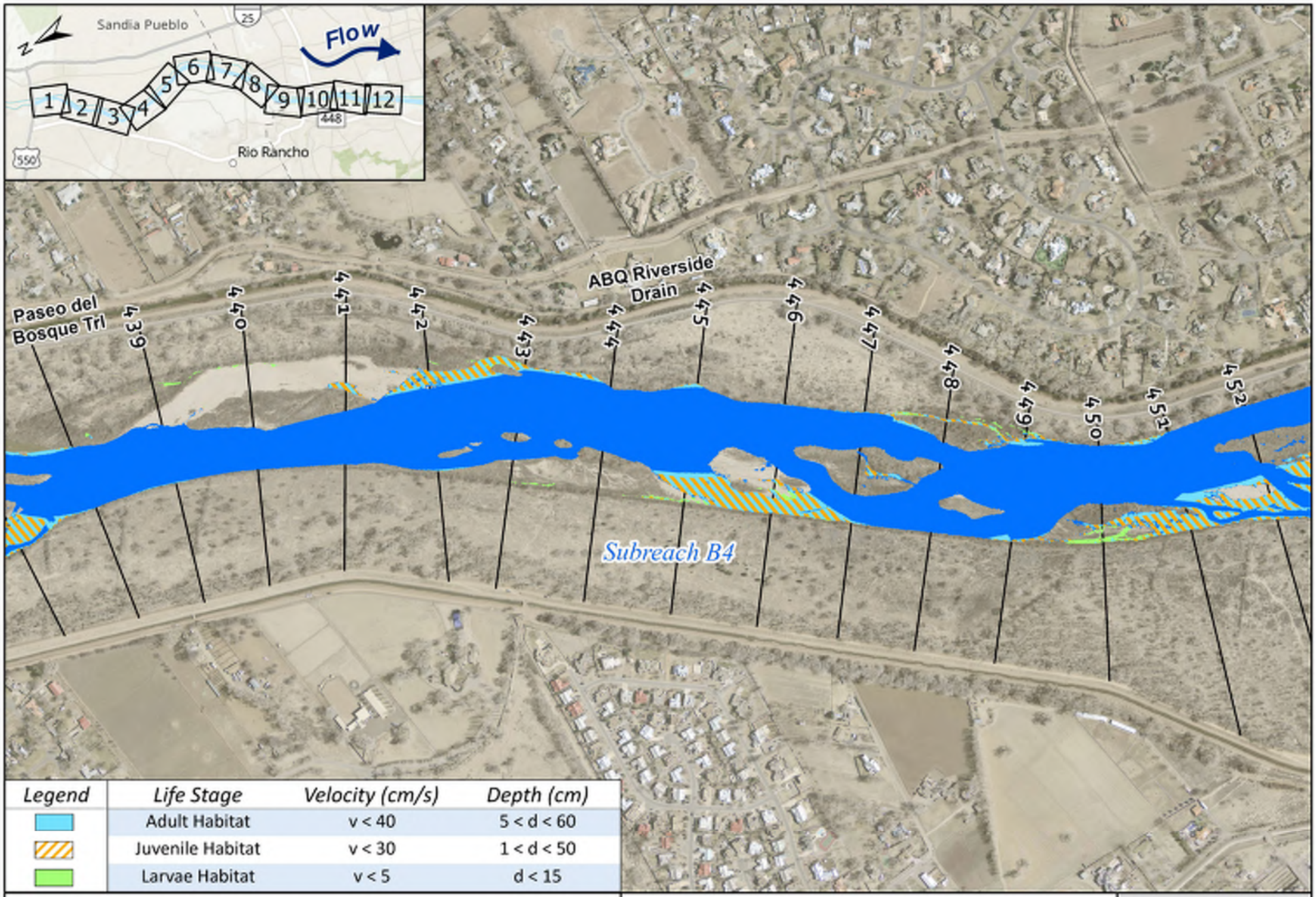

Legend	Life Stage	Velocity (cm/s)	Depth (cm)
	Adult Habitat	v < 40	5 < d < 60
	Juvenile Habitat	v < 30	1 < d < 50
	Larvae Habitat	v < 5	d < 15

1,000 500 0 1,000 Feet

Rio Grande Habitat Map at 3,000 cfs
Bernalillo to Montano

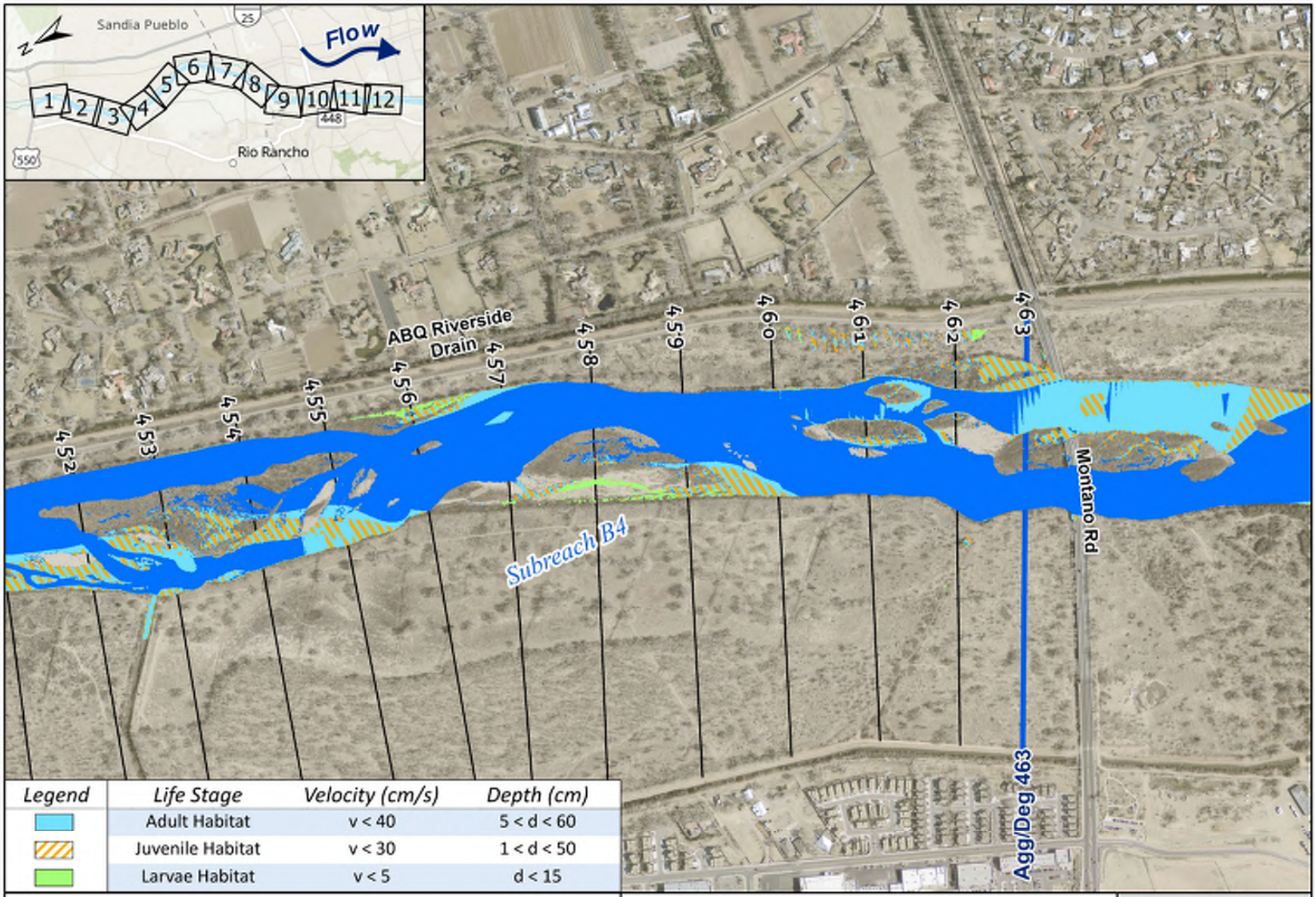

Rio Grande Habitat Map at 3,000 cfs
Bernalillo to Montano

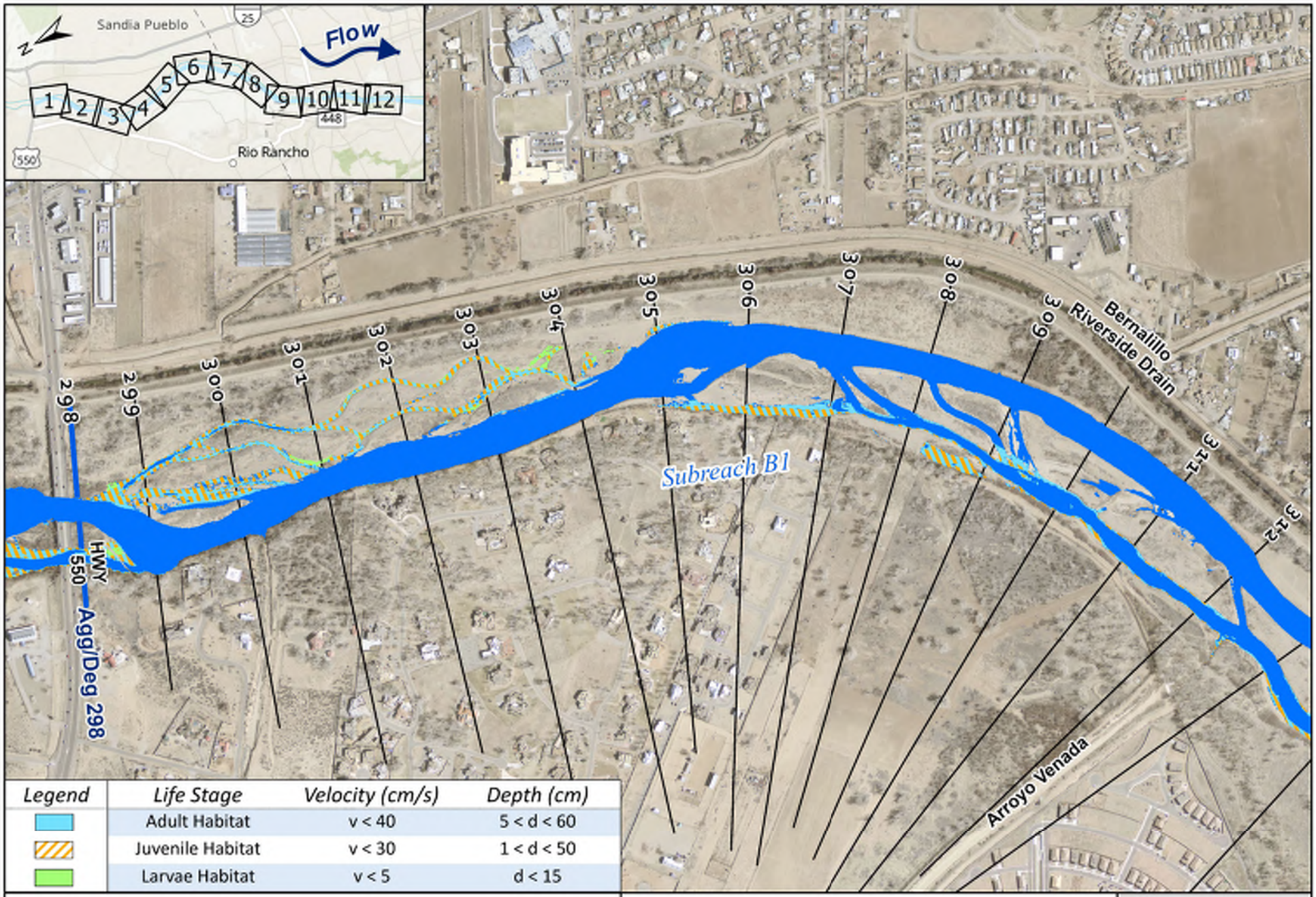

Rio Grande Habitat Map at 5,000 cfs
Bernalillo to Montano

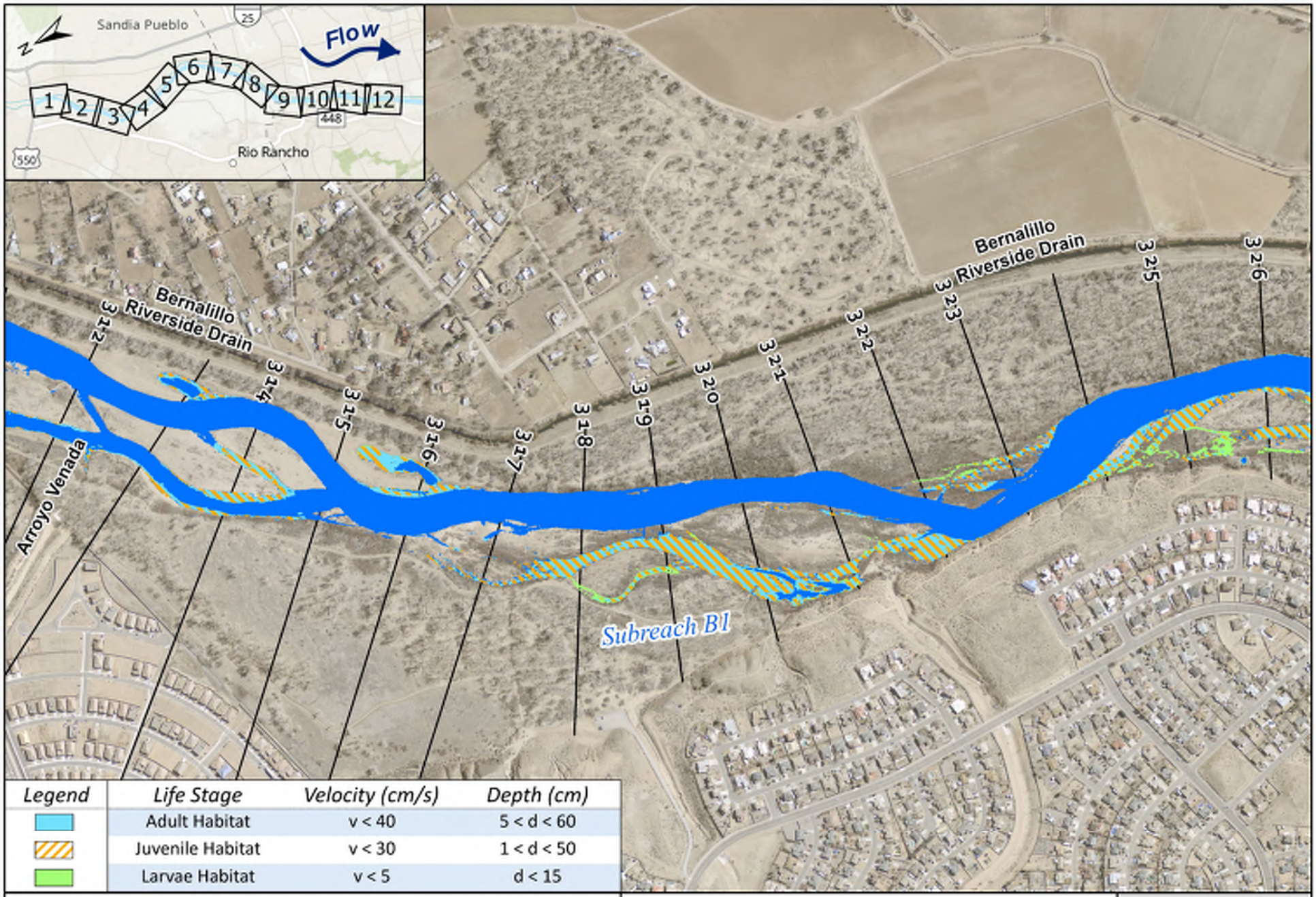

Legend	Life Stage	Velocity (cm/s)	Depth (cm)
	Adult Habitat	v < 40	5 < d < 60
	Juvenile Habitat	v < 30	1 < d < 50
	Larvae Habitat	v < 5	d < 15

1,000 500 0 1,000 Feet

Rio Grande Habitat Map at 5,000 cfs
Bernalillo to Montano

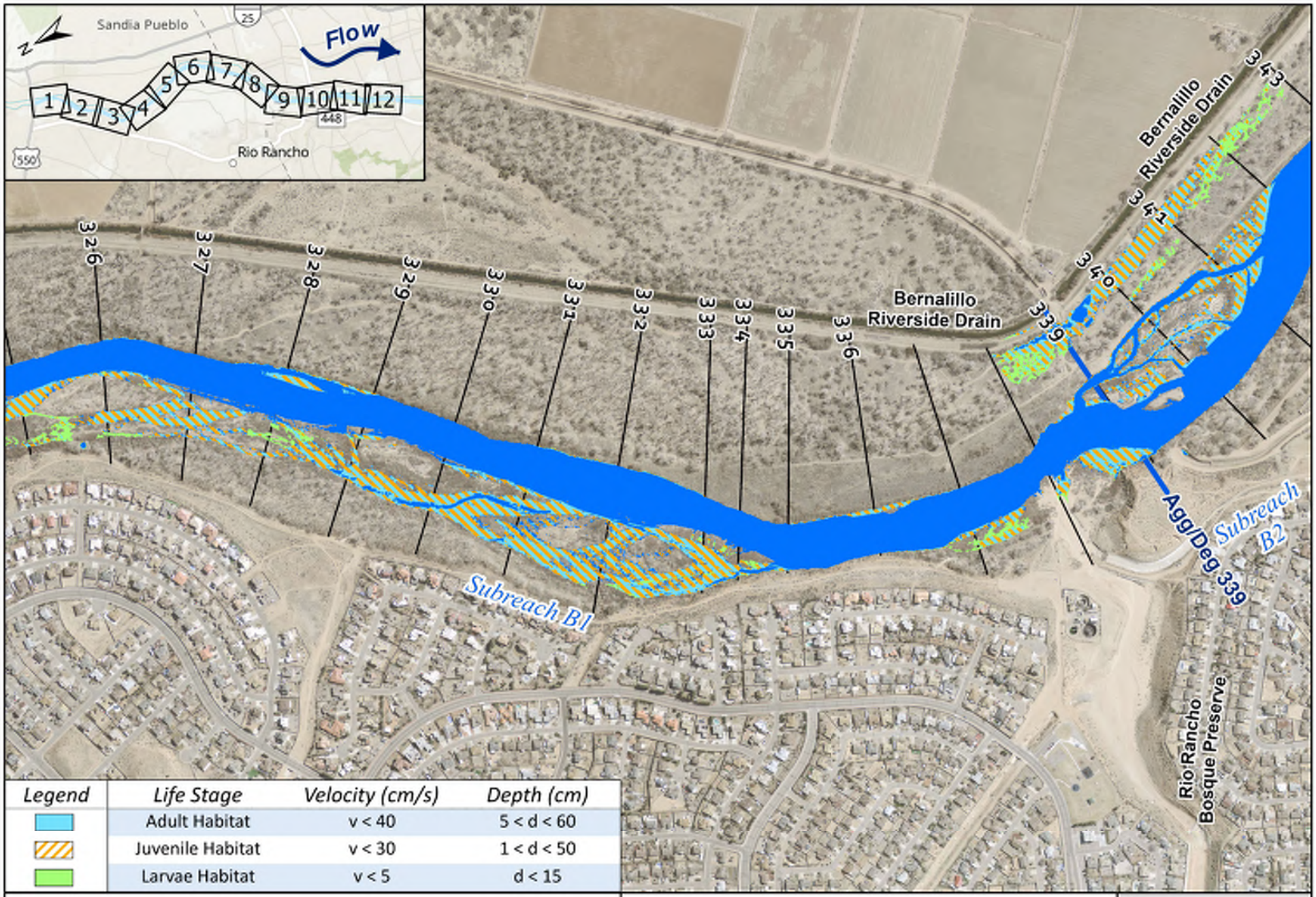

Legend	Life Stage	Velocity (cm/s)	Depth (cm)
	Adult Habitat	v < 40	5 < d < 60
	Juvenile Habitat	v < 30	1 < d < 50
	Larvae Habitat	v < 5	d < 15

1,000 500 0 1,000 Feet

Rio Grande Habitat Map at 5,000 cfs
Bernalillo to Montano

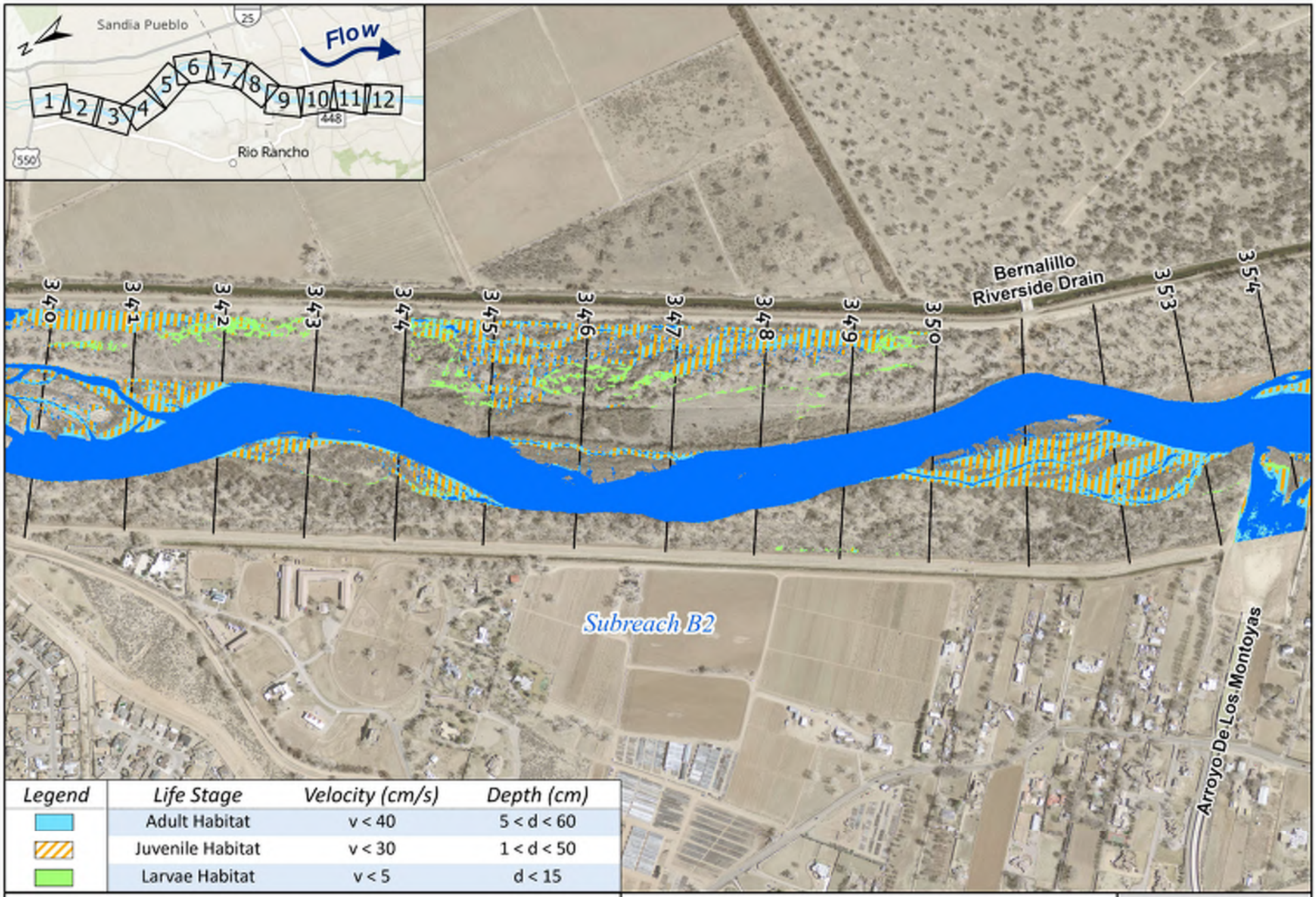

Legend	Life Stage	Velocity (cm/s)	Depth (cm)
	Adult Habitat	v < 40	5 < d < 60
	Juvenile Habitat	v < 30	1 < d < 50
	Larvae Habitat	v < 5	d < 15

N

1,000 500 0 1,000 Feet

Rio Grande Habitat Map at 5,000 cfs
Bernalillo to Montano

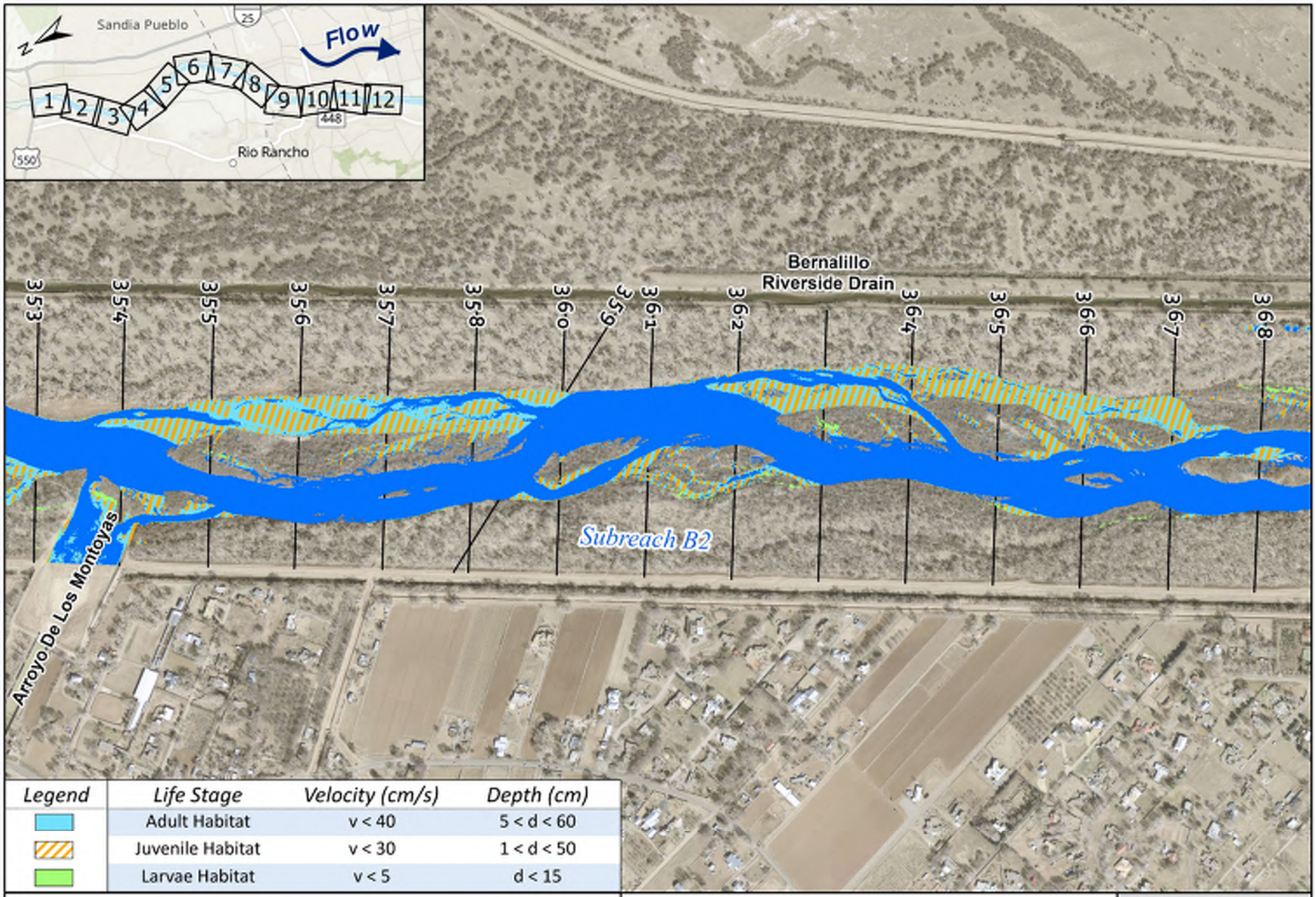

Legend	Life Stage	Velocity (cm/s)	Depth (cm)
	Adult Habitat	v < 40	5 < d < 60
	Juvenile Habitat	v < 30	1 < d < 50
	Larvae Habitat	v < 5	d < 15

N

1,000 500 0 1,000 Feet

Rio Grande Habitat Map at 5,000 cfs
Bernalillo to Montano

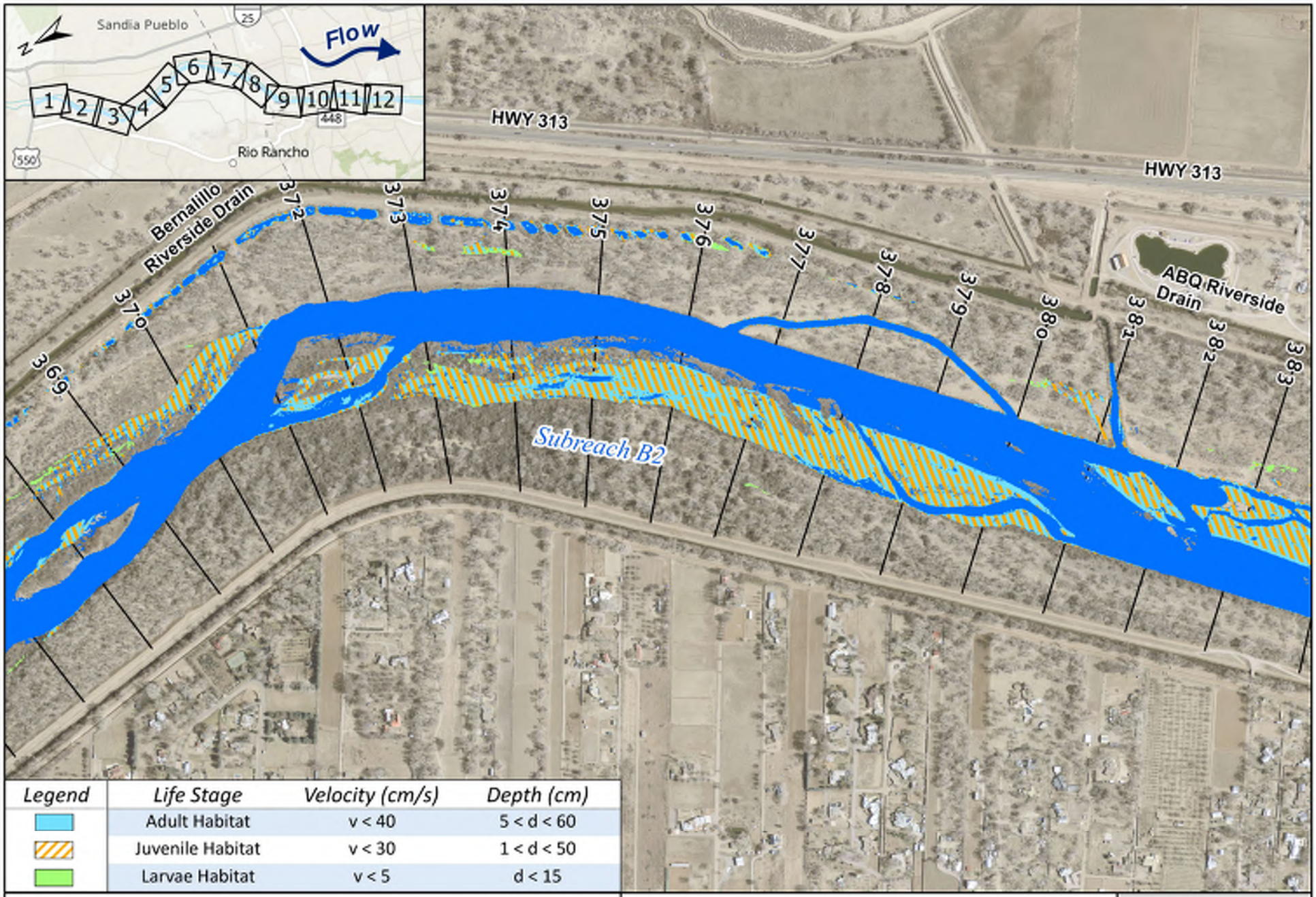

Legend	Life Stage	Velocity (cm/s)	Depth (cm)
	Adult Habitat	v < 40	5 < d < 60
	Juvenile Habitat	v < 30	1 < d < 50
	Larvae Habitat	v < 5	d < 15

1,000 500 0 1,000 Feet

Rio Grande Habitat Map at 5,000 cfs
Bernalillo to Montano

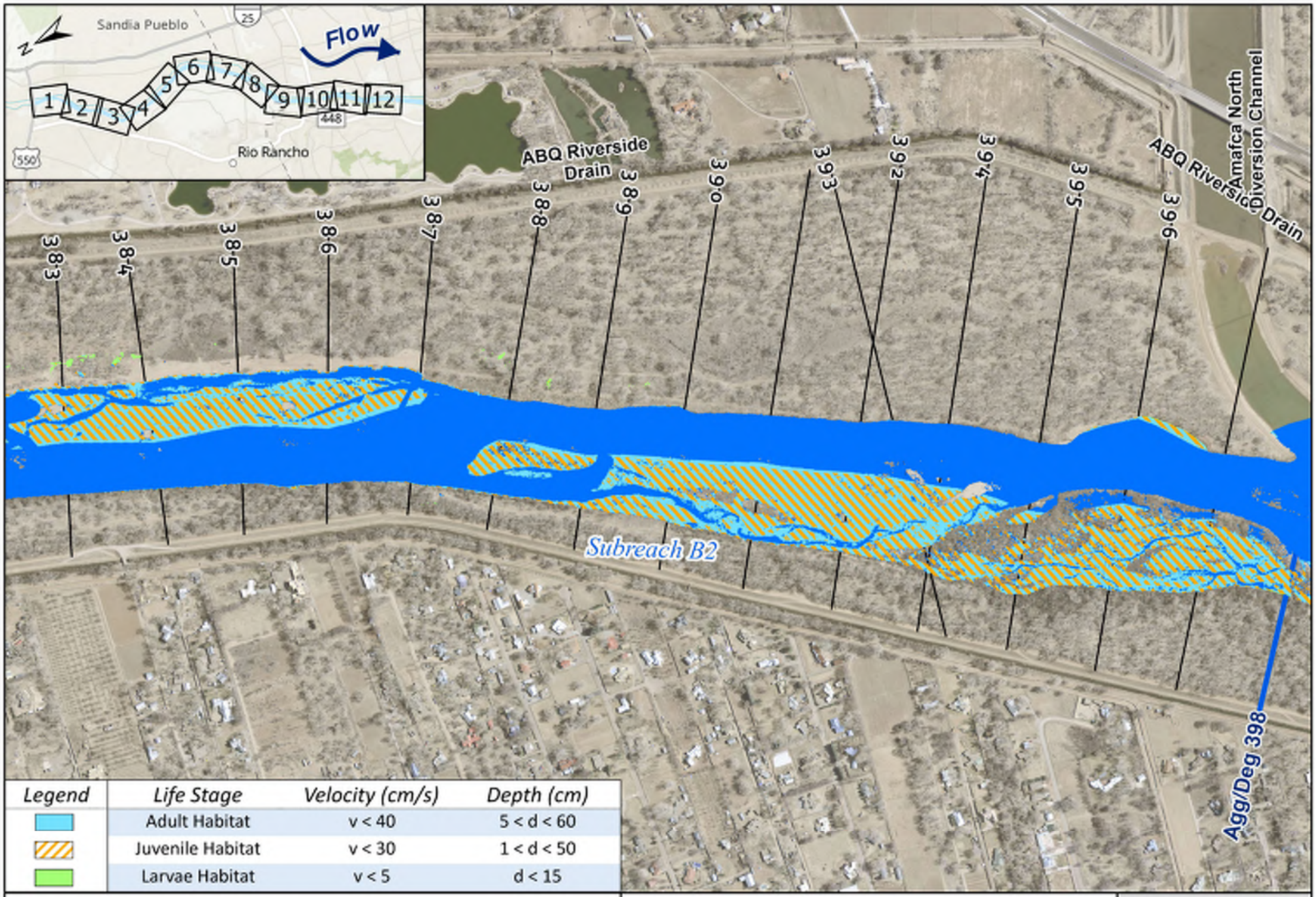

Rio Grande Habitat Map at 5,000 cfs
Bernalillo to Montano

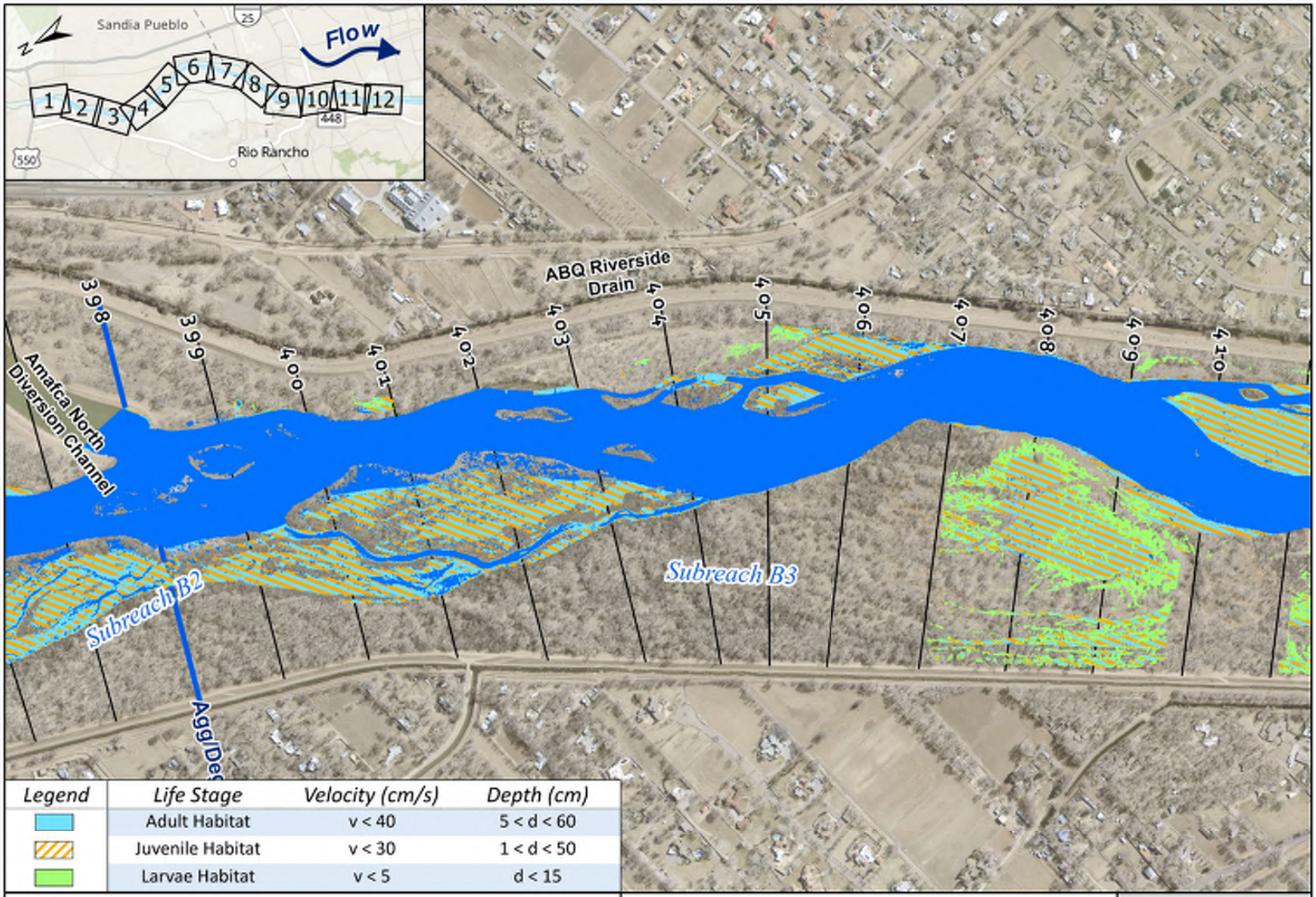

Legend	Life Stage	Velocity (cm/s)	Depth (cm)
	Adult Habitat	v < 40	5 < d < 60
	Juvenile Habitat	v < 30	1 < d < 50
	Larvae Habitat	v < 5	d < 15

N

1,000 500 0 1,000 Feet

Rio Grande Habitat Map at 5,000 cfs
Bernalillo to Montano

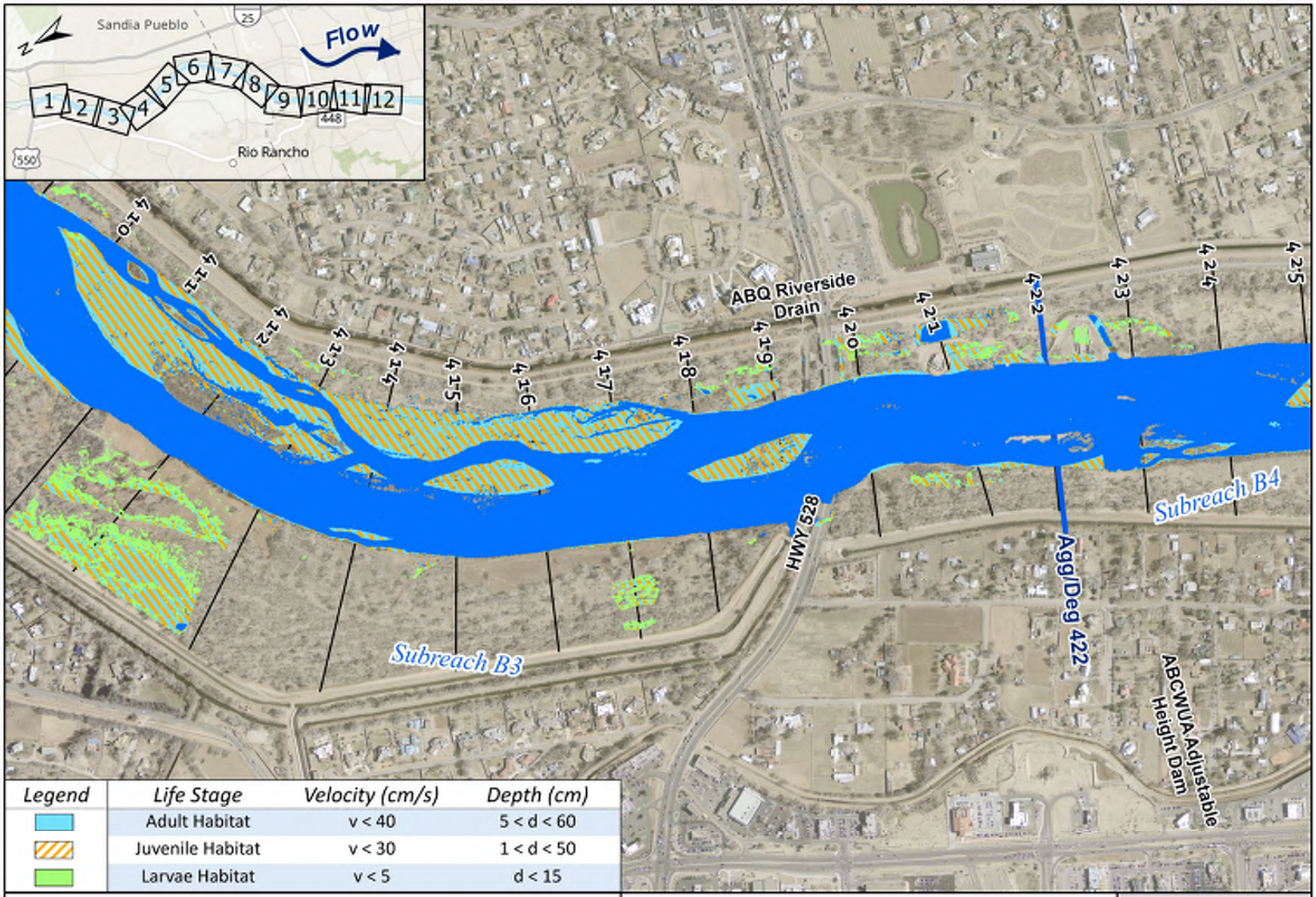

Legend	Life Stage	Velocity (cm/s)	Depth (cm)
	Adult Habitat	v < 40	5 < d < 60
	Juvenile Habitat	v < 30	1 < d < 50
	Larvae Habitat	v < 5	d < 15

1,000 500 0 1,000 Feet

Rio Grande Habitat Map at 5,000 cfs
Bernalillo to Montano

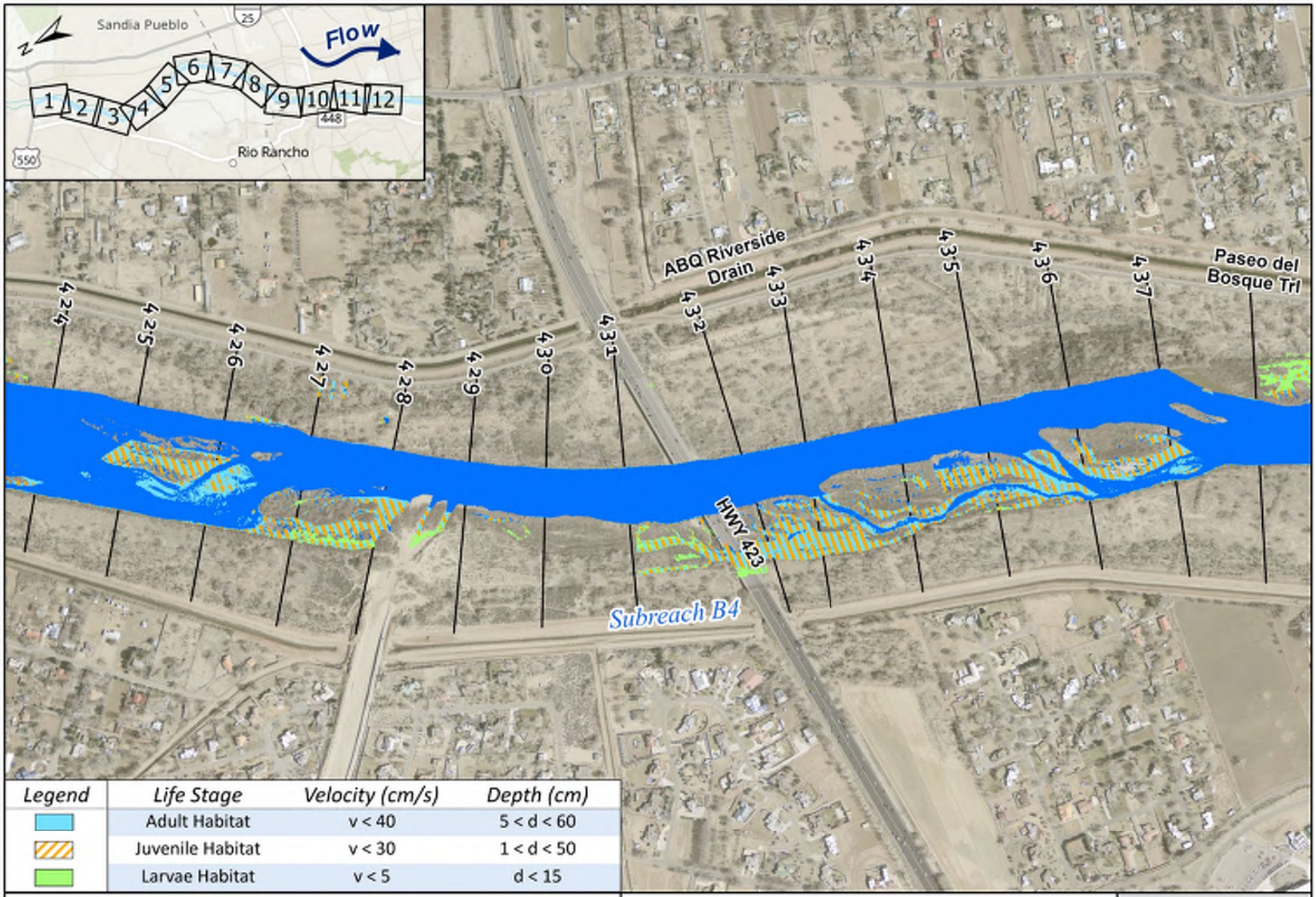

Legend	Life Stage	Velocity (cm/s)	Depth (cm)
	Adult Habitat	v < 40	5 < d < 60
	Juvenile Habitat	v < 30	1 < d < 50
	Larvae Habitat	v < 5	d < 15

1,000 500 0 1,000 Feet

Rio Grande Habitat Map at 5,000 cfs
Bernalillo to Montano

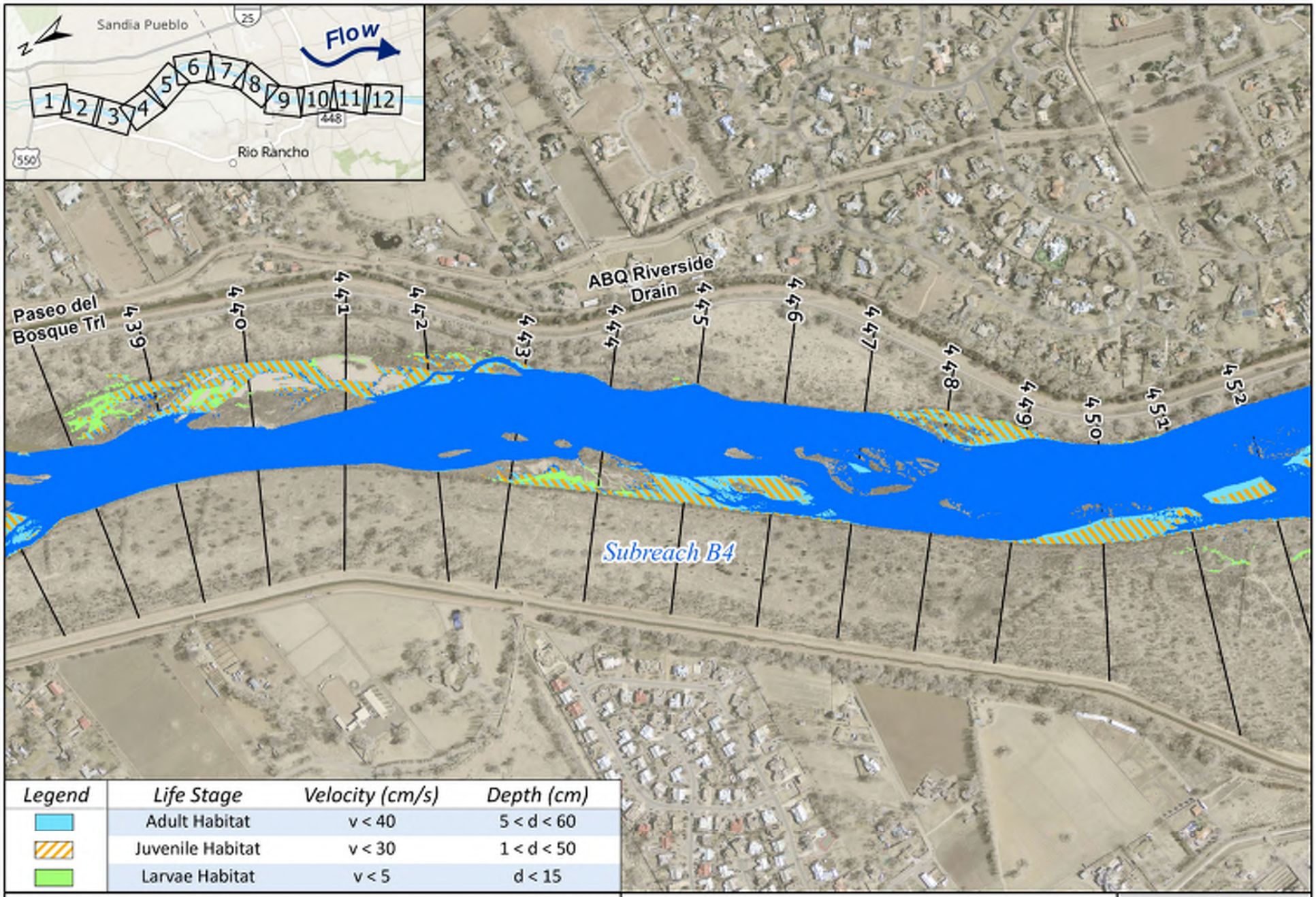

Legend	Life Stage	Velocity (cm/s)	Depth (cm)
	Adult Habitat	v < 40	5 < d < 60
	Juvenile Habitat	v < 30	1 < d < 50
	Larvae Habitat	v < 5	d < 15

1,000 500 0 1,000 Feet

Rio Grande Habitat Map at 5,000 cfs
Bernalillo to Montano

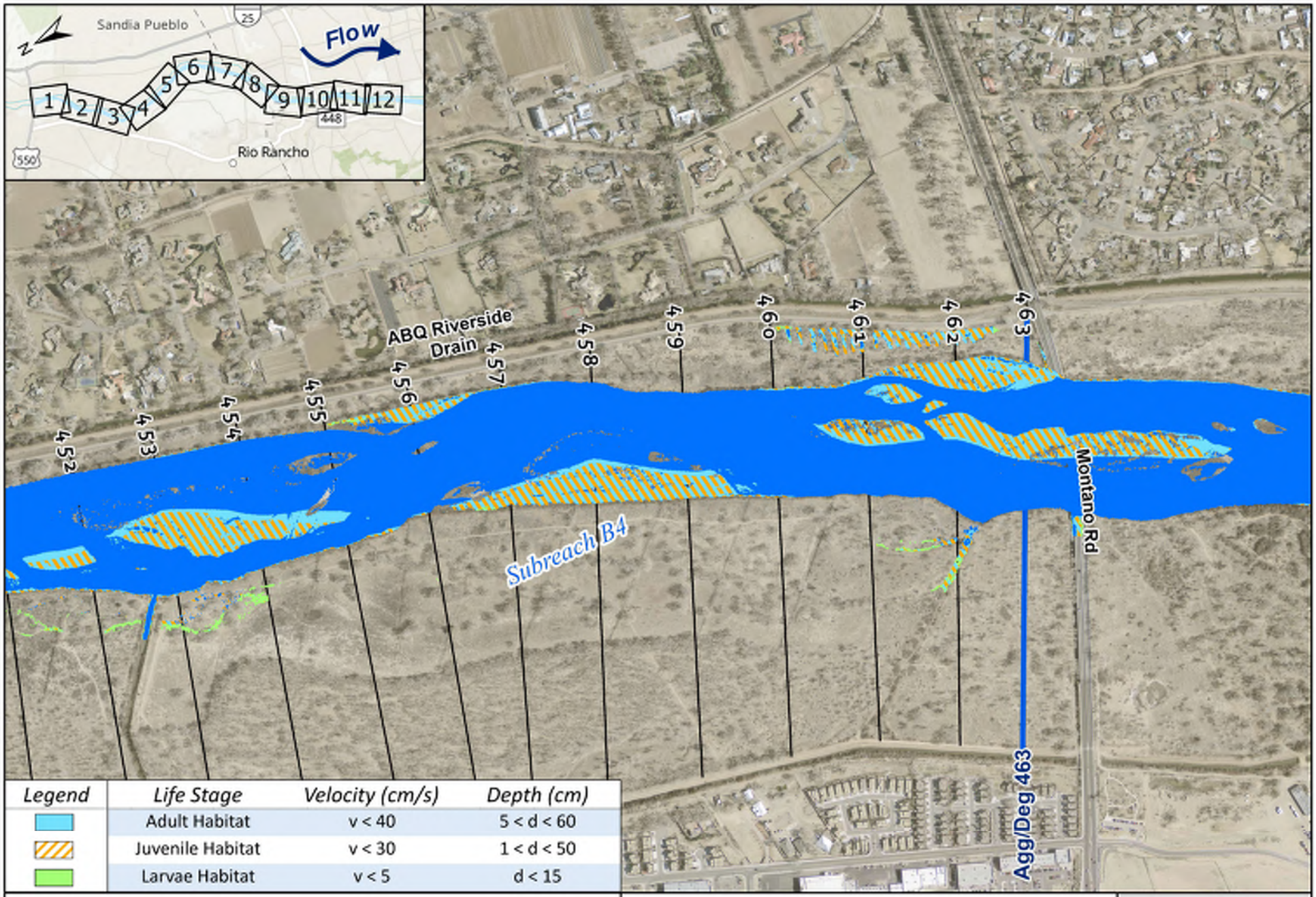

Legend	Life Stage	Velocity (cm/s)	Depth (cm)
	Adult Habitat	v < 40	5 < d < 60
	Juvenile Habitat	v < 30	1 < d < 50
	Larvae Habitat	v < 5	d < 15

1,000 500 0 1,000 Feet

Rio Grande Habitat Map at 5,000 cfs
Bernalillo to Montano

Appendix F

HEC-RAS Model File Log

The HEC-RAS model files used for the analyses are shown in **Table F-1**. Most of the files for a given type (geometry, flow, etc.) contain identical conditions. For conciseness, these commonalities are:

- All **Flow files** contain thirteen discharge (cfs) profiles: 500, 1000, 1500, 2000, 2500, 3000, 3500, 4000, 4500, 5000, 6000, 8000, and 10000.
- **Downstream (DS) normal depth boundary conditions** were found from modeling the entire MRG at the specified discharges (DS normal depth boundary condition: 0.0007). The energy grade line slope at 5 cross sections DS of the Bernalillo DS boundary at each discharge became the DS boundary condition for the Bernalillo reach flow files. The boundary conditions range from 0.0007 to 0.0009 depending on the discharge.
- The **Manning's roughness** is n = 0.025 in the main channel and n = 0.01 elsewhere.
- **Flow distribution locations** were set at 10/25/10 for the LOB, Channel, and ROB for plans used to quantify habitat availability.
- **Geometry files** contain 5 cross-sections upstream and 5 cross-sections downstream of the Bernalillo Boundaries

See **Table F-2** for the full list of HEC-RAS files.

Table F-1 HEC-RAS files used during analyses

Project Name		
Extension	***Name***	***Description***
.prj	Bernalillo_reach	Surveyed cross sections in years: 1962,1972, 1992, and 2002. LiDAR in 2012 along the Bernalillo reach of the MRG.
Geometry Files		
Extension	***Name***	***Description***
.g14	1962_modlevee	Existing conditions with some levees in B1 and B2.
.g13	1972_modllevee	Existing conditions with some levees in B1 and B2.
.g11	1992_nolevee	Existing conditions with no flow constraints.
.g12	2002_nolevee	Existing conditions with no flow constraints.
.g08	2012_nolevee	Existing conditions with ineffective flow constraints.
Steady Flow Files		
Extension	***Name***	***Description***
.f02	Bernalillo_2012	DS Boundary condition: Normal Depth 0.0007-0.0009
.f03	Bernalillo_1962-2002	
Steady Plan Files		
Extension	***Name***	***Description (geometry file & flow file)***
.p13	Bernalillo_1972_modLevee	.g14 and .f03
.p12	Bernalillo_1972_modLevee	.g13 and .f03
.p10	Bernalillo_1992_noLevee	.g11 and .f03
.p11	Bernalillo_2002_noLevee	.g12 and .f03
.p08	Bernalillo_2012_noLevee	.g08 and .f02

Table F-2 Full list of HEC-RAS files

Project Name		
Extension	***Name***	***Description***
.prj	Bernalillo_reach	Surveyed cross sections in years: 1962,1972, 1992, and 2002. LiDAR in 2012 along the Bernalillo reach of the MRG.
Geometry Files		
Extension	***Name***	***Description***
.g01	1962	1962 unmodified Bernalillo reach survey cross sections, as received
.g03	1972	1972 unmodified Bernalillo reach survey cross sections, as received
.g04	1992	1992 unmodified Bernalillo reach survey cross sections, as received
.g05	2002	2002 unmodified Bernalillo reach survey cross sections, as received
.g06	2012	2012 unmodified Bernalillo reach survey cross sections, as received
.g07	Full_2012	Entire MRG 2012 geometry (Agg/Deg: 17 – EB 63), as received
.g08	2012_nolevee	2012 Bernalillo reach survey cross section with original levees removed and ineffective flow areas added
.g09	1962_nolevee	1962 Bernalillo reach survey cross section with original levees removed
.g10	1972_nolevee	1972 Bernalillo reach survey cross section with original levees removed
.g11	1992_nolevee	1992 Bernalillo reach survey cross section with original levees removed
.g12	2002_nolevee	2002 Bernalillo reach survey cross section with original levees removed
.g13	1972_modlevee	1972 Bernalillo reach survey cross section with original levees removed and new levees placed in B1 and B2
.g14	1962_modlevee	1962 Bernalillo reach survey cross section with original levees removed and new levees placed in B1 and B2
Steady Flow Files		
Extension	***Name***	***Description***
.f01	Full_Flows	DS Boundary condition: Normal Depth 0.0007
.f02	Bernalillo_2012	DS Boundary condition: Normal Depth 0.0007-0.0009
.f03	Bernalillo_1962-2002	DS Boundary condition: Normal Depth 0.0007-0.0009

Steady Plan Files		
Extension	***Name***	***Description (geometry & flow)***
.p01	Full_River	.g07 and .f01
.p02	Bernalillo_2012	.g06 and .f02
.p03	Bernalillo_2002	.g05 and .f03
.p04	Bernalillo_1992	.g04 and .f03
.p05	Bernalillo_1972	.g03 and .f03
.p06	Bernalillo_1962	.g01 and .f03
.p07	Bernalillo_1962_noLevee	.g09 and .f03
.p08	Bernalillo_2012_noLevee	.g08 and .f02
.p09	Bernalillo_1972_noLevee	.g10 and .f03
.p10	Bernalillo_1992_noLevee	.g11 and .f03
.p11	Bernalillo_2002_noLevee	.g11 and .f03
.p12	Bernalillo_1972_modLevee	.g13 and .f03
.p13	Bernalillo_1962_modLevee	.g14 and .f03